

**PHYTOCHEMICAL STUDIES AND THE BIOACTIVITIES OF
COMPOUNDS FROM *OCHROSIA OPPOSITIFOLIA*,
RAUVOLFIA REFLEXA AND *ACTINODAPHNE*
*MACHROPHYLLA***

MEHRAN FADAEINASAB

**FACULTY OF SCIENCE
UNIVERSITY OF MALAYA
KUALA LUMPUR**

2014

**PHYTOCHEMICAL STUDIES AND THE BIOACTIVITIES OF
COMPOUNDS FROM *OCHROSIA OPPOSITIFOLIA*,
RAUVOLFIA REFLEXA AND *ACTINODAPHNE*
*MACHROPHYLLA***

MEHRAN FADAEINASAB

**THESIS SUBMITTED IN FULFILMENT
OF THE REQUIREMENTS FOR THE DEGREE
OF DOCTOR OF PHILOSOPHY**

**DEPARTMENT OF CHEMISTRY
FACULTY OF SCIENCE
UNIVERSITY OF MALAYA
KUALA LUMPUR**

2014

ABSTRACT

The chemical constituents of *Ochrosia oppositifolia*, *Rauvolfia reflexa* (Apocynacea) and *Actinodaphne machrophylla* (Lauracea) have been studied. The compounds were extracted from the bark and leaves of the plants using *n*-hexane, dichloromethane and methanol as solvents. The crudes were subjected to extensive chromatographic techniques such as column chromatography (CC), preparative thin layer chromatography (PTLC), and high performance liquid chromatography (HPLC). Structural elucidation was established through several spectroscopic methods, such as 1D-NMR (¹H, ¹³C, DEPT, NOE), 2D-NMR (COSY, NOESY, HMQC, and HMBC), UV, IR, and MS (GCMS, LCMS and HREIMS) and comparison with the published data.

In this study, a total of twenty eight known and new compounds were isolated. Three known indole alkaloids namely isoreserpiline (**120**), neisosposinine (**121**) and reserpiline (**122**) were isolated from the bark of *Ochrosia oppositifolia*. Ten indole alkaloids and one β - carboline alkaloid were obtained from the bark of *Rauvolfia reflexa*, these are rauvolfine B (**123**), rauvolfine C (**124**) vinorine (**125**), rescinnamine (**126**), cantleyine (**127**), akuammilan-17-oic acid, 1,2-dihydro-3-hydroxy-1-methyl-, methyl ester (**128**), undulifoline (**129**), macusine B (**130**), isoreserpiline (**120**), akuammilan-17-oic acid, 12-hydroxy-, methyl ester (**131**) among these rauvolfine B (**123**) and rauvolfine C (**124**) appeared to be new. In addition, six known phenolic compounds and one new β - carboline alkaloid were isolated from the leaves of *Rauvolfia reflexa* namely 17-methoxy-carbonyl-14- heptadecaenyl- 4-hydroxy-3-methoxy cinnamate (**132**), 3-methyl-10,11-dimethoxyl-6-methoxycarbonyl- β - carboline (**133**), (*E*)-methyl 3-(4-hydroxy-3,5-dimethoxyphenyl) acrylate (**134**), 1,2,3,4- tetrahydro -1- oxo- β - carboline (**135**), 3-hydroxy- β -carboline (**136**), (*E*)-3-(3,4,5-trimethoxyphenyl) acrylic acid (**137**) and benzenepropanoic acid, 3- methoxy

(**138**). 17-methoxy-carbonyl-14- heptadecaenyl- 4-hydroxy-3-methoxy cinnamate (**132**), and 3- methyl-10, 11-dimethoxyl-6- methoxycarbonyl- β - carboline (**133**) were the new compounds isolated from the leaves of *Rauvolfia reflexa*.

The bark of *Actinodaphne macrophylla* has afforded eight known isoquinoline alkaloids, cycleanine (**139**), (-) -10-demethylxylopinine (**140**), reticuline (**141**), (+) - laurotetanine (**142**), (+) - bicuculine (**143**), (-) α - hydrastine (**144**), (+) - parafumine (**145**) and (+) - anolobine (**146**).

Six samples from the bark and leaves of *ochrosia oppositifolia* including three crude extracts and three indole alkaloids and eight isoquinoline alkaloids from the bark of *Actinodaphne macrophylla* have been tested for their *in-vitro* inhibitory activity against *P. falciparum* 3D7. Among the crude extracts of *Ochrosia oppositifolia* dichloromethane crude extract of bark showed the most potent inhibitory activity, with the IC₅₀ value of 0.05051 μ g/mL, the other crude extracts and compounds showed weak or no inhibitory activity against *P. falsiparum* as compare as standard which is chloroquine.

Three indole alkaloids isolated from the bark of *Ochrosia oppositifolia* and eight isoquinoline alkaloids isolated from the bark of *Actinodaphne macrophylla* showed moderate *in vitro* antiplasmodial activities against *Plasmodium falciparum* 3D7 with the IC₅₀ of 0.29 μ M, 0.75 μ M and 1.13 μ M for isoreserpiline (**120**), neisosposinine (**121**), reserpiline (**122**) and 0.08 μ M, 1.18 μ M, 3.11 μ M, 0.65 μ M, 0.26 μ M, 3.99 μ M and 1.38 μ M for cycleanine (**139**), (-) -10-Demethylxylopinine (**140**), reticuline (**141**), (+) - laurotetanine (**142**), (+) – bicuculine (**143**), (-) - a- hydrastine (**144**), (+) - parfumine (**145**) and (+) - anolobine (**146**) respectively which are comparable with standard chloroquine. Antialzheimer activity of crude extracts and pure compounds isolated from the leaves and the bark of *Rauvolfia reflexa* was carried out. The dichloromethane and ethanol crude

extracts of the leaves and methanol crude extract of the bark exhibited good inhibitory activity against both enzymes, while the methanol crude extract of the leaves showed moderate inhibitory activity against acetylcholinesterase (AChE).

Cytotoxic effects of rauwolfine B (**123**), macusine B (**130**) and isoreserpiline (**120**) against different cancer and normal cell lines were determined. At the tested concentrations (1.5 – 250 μ M), macusine B (**130**) and isoreserpiline (**120**) did not effectively suppress the cell proliferations of cancer cells. Rauwolfine B (**123**) revealed moderate cytotoxic effects against two breast cancer cells (MCF-7 and MDA-MB-231) and colon cancer cells (HT-29). However, test on colon cancer cells (HCT-116), rauwolfine B (**123**) elicited the strongest cytotoxic effect with IC_{50} value of 46.86, 39.93 and 33.38 μ M after 24, 48 and 72 h of treatment respectively. Rauwolfine B (**123**) was selected for further study on the possible mechanism as it shown potential activity activity against HCT-116 cell line. Morphological changes in the treated HCT-116 cells with rauwolfine B (**123**) were observed under fluorescent microscope. After 24 h, apparent marks of apoptosis, such as membrane blebbing and cytoplasmic shrinkage were noted at IC_{50} dose of rauwolfine B (**123**).

ABSTRAK

Kajian terhadap sebatian kimia *Ochrosia oppositifolia*, *Rauvolfia reflexa* (Apocynacea) dan *Actinodaphne machrophylla* (Lauracea) telah dijalankan. Kesemua sebatian tersebut diekstrak daripada kulit batang pokok dan daun menggunakan larutan seperti n-hexane, dikhlorometana dan metanol. Ekstrak mentah kemudian dipisahkan menggunakan pelbagai kaedah kromatografi seperti kromatografi turus (CC), kromatografi persiapan lapisan nipis (PTLC) dan kromatografi cecair prestasi tinggi (HPLC). Seterusnya, sebatian-sebatian tersebut dielusidasi dengan menggunakan teknik spektroskopik seperti 1D-NMR (^1H , ^{13}C , DEPT dan NOE), 2D-NMR (COSY, NOESY, HMQC dan HMBC), UV, IR dan MS (GC-MS, LC-MS dan HREIMS) serta kaedah perbandingan literatur.

Dalam kajian ini, dua puluh lapan sebatian lama dan baru telah dipisahkan. Sebatian-sebatian tersebut ialah tiga sebatian lama alkaloid indol dipisahkan daripada kulit batang pokok *Ochrosia oppositifolia*, iaitu isoreserpiline (**120**), neisosposinine (**121**) and reserpiline (**122**). Manakala, sepuluh sebatian lama telah dijumpai daripada kulit batang pokok *Rauvolfia reflexa* adalah rauvolfine B (**123**), rauvolfine C (**124**) vinorine (**125**), rescinnamine (**126**), cantleyine (**127**), akuammilan-17-oic acid, 1,2-dihydro-3-hydroxy-1-methyl-, methyl ester (**128**), undulifoline (**129**), macusine B (**130**), isoreserpiline (**120**), akuammilan-17-oic acid, 12-hydroxy-, methyl ester (**131**). Di samping itu, tujuh sebatian lama fenolik daripada daun *Rauvolfia reflexa* juga telah dipisahkan iaitu 17-methoxy-carbonyl-14-heptadecaenyl-4-hydroxy-3-methoxy cinnamate (**132**), 3-methyl-10,11-dimethoxyl-6-methoxycarbonyl- β -carboline (**133**), (*E*)-methyl 3-(4-hydroxy-3,5-dimethoxyphenyl) acrylate (**134**), 1,2,3,4-tetrahydro-1-oxo- β -carboline (**135**), 3-hydroxy- β -carboline (**136**), (*E*)-3-(3,4,5-trimethoxyphenyl) acrylic acid (**137**) and benzenepropanoic acid, 3-methoxy (**138**). Lapan sebatian lama alkaloid isoquinolin telah

dipisahkan daripada kulit batang pokok *Actinodaphne macrophylla* adalah cycleanine (**139**), (-) - 10-demethylxylopinine (**140**), reticuline (**141**), (+) - laurotetanine (**142**), (+) - bicuculine (**143**), (-) α -hydrastine (**144**), (+) - parafumine (**145**) and (+) -anolobine (**146**). Manakala, alkaloid indol daripada kulit batang pokok of *Rauvolfia reflexa*, rauvolfine B (**123**) and rauvolfine C (**124**) telah dipisahkan kali pertama untuk species ini. 17-methoxy-carbonyl-14-heptadecaenyl-4-hydroxy-3-methoxy cinnamate (**132**) dan 3-metil-10,11-dimeoxil-6-metoxikarbonil- β -karbolin (**113**) adalah sebatian baru β -karbolin alkaloid yang telah dipisahkan daripada daun *Rauvolfia reflexa*.

Enam sampel daripada kulit batang pokok dan daun *Ochrosia oppositifolia* termasuk tiga ekstrak mentah dan tiga indol alkaloid dan lapan isoquinolin alkaloid daripada kulit batang pokok *Actinodaphne macrophylla* telah dikaji untuk perencatan aktiviti *in-vitro* terhadap *P.falciparum* 3D7. Di antara ekstrak mentah *Ochrosia oppositifolia*, kulit batang pokok ekstrak mentah diklorometana menunjukkan perencatan aktiviti yang paling berkesan iaitu dengan nilai IC_{50} ialah 0.05051 $\mu\text{g/mL}$ manakala ekstrak mentah yang lain dan sebatian-sebatian yang lain menunjukkan perencatan aktiviti yang lemah atau tiada perencatan aktiviti terhadap *P. falciparum* dibandingkan dengan standard khloroquin.

Tiga indol alkaloid yang telah dipisahkan daripada kulit batang pokok *Ochrosia oppositifolia* dan lapan isoquinolin alkaloid dipisahkan daripada kulit batang pokok *Actinodaphne macrophylla* menunjukkan antiplasmodial aktiviti yang sederhana terhadap *Plasmodium falciparum* 3D7 dengan IC_{50} ialah 0.29 μM , 0.75 μM dan 1.13 μM untuk isoreserpilin (**120**), neisosposinin (**121**), reserpinin (**122**), dan 0.08 μM , 1.18 μM , 3.11 μM , 0.65 μM , 0.26 μM , 3.99 μM dan 1.38 μM untuk ciclenin (**139**), (-) -10 demetilxilopinin (**140**), reticulin (**141**), (+) - laurotetanin (**142**), (+) - bicuculin (**143**), (-)-

α -hidrastin (**144**), (+) - parfumin (**145**) dan (+) - anolobin (**146**) jika dibandingkan dengan standard khloroquin.

Aktiviti anti-alzheimer telah dijalankan terhadap ekstrak mentah dan sebatian lama yang telah dipisahkan daripada daun dan kulit batang pokok *Rauvolfia reflexa*. Ekstrak mentah diklorometana dan etanol daripada daun serta ekstrak mentah metanol daripada kulit batang pokok menunjukkan aktiviti perencatan yang baik untuk kedua-dua enzim manakala ekstrak mentah metanol daripada daun menunjukkan aktiviti perencatan yang sederhana terhadap asetilklolinesteras (AChE).

Sebatian rauwolfina B (**123**), macusina B (**130**) dan isoreserpilin (**120**) menunjukkan kesan sitotoksik terhadap sel kanser dan sel normal telah dikaji. Ujian kepekatan (1.5 -250 μ M), macusina B (**130**) dan isoreserpilin (**120**) tidak memberi kesan penyekatan kepada sel proliferasi oleh sel kanser. Manakala, rauwolfina B (**123**) menunjukkan kesan yang sederhana terhadap sitotoksik dua sel kanser payudara (MCF-7 dan MDA-MB-231) dan sel kanser usus besar (HT-29). Walaubagaimanapun, rauwolfina B (**123**) menunjukkan kesan yang tinggi terhadap sel kanser usus besar (HCT-116) dengan IC₅₀ 46.86, 39.93 and 33.38 μ M selepas rawatan selama 24, 48 dan 72 jam.

ACKNOWLEDGEMENTS

My first and sincere appreciation goes to my supervisors, Professor Dr. Hapipah Mohd Ali and Dr. Najihah Mohd Hashim for all I have learned from them and for their continuous help and support in all stages of this thesis. I would also like to thank them for being an open persons to ideas, and for encouraging and helping me to shape my interest and ideas.

I would like to express my deep gratitude and respect to my first supervisor, the late Professor Datuk Dr. A. Hamid A. Hadi whose advices and insight was invaluable to me. For all I learned from him. His in-depth knowledge and interest in research inspired me to start my PhD study. May his soul rest in peace.

I would like to thank Dr. Syam and Mr Hamed from Department of Pharmacy, University of Malaya, Professor Dr. Afidah, Dr. Vicky, Dr. Yalda Kia, Dr. Alireza Basiri, Dr. Bothi Raja from University Science Malaysia and Dr. Atty from Airlangga University, Indonesia for running the biological activities tests.

My deepest appreciation is also dedicated to Professor Dr. Iqbal Choudhary form HEJ Karachi, Pakistan, Professor Hiroshi Morita from Hoshi University, Japan, Professor Dr. Mawardi Rahmani from University Putra Malaysia, Professor Dr. Khalijah Awang from University of Malaya, Dr. Azlan Mohd Nafiah from UPSI and Dr. Nurdin Saidi from Syah University, Indonesia for lending their helps in this research.

I also wish to extend my thanks to the department of chemistry staffs; Ms. Norzalida, Mrs. Fiona, Mr. Fateh, Mr. Nordin Mr. Sew for recording the NMR and LC-MS spectra.

I wish to extend my thanks to my friends in the HIR laboratory; Mrs. Hairin Taha, Mrs. Hanita Omar, Ms Ainnul, Ms Azie, Ms Jad, and my dear friends; Aziemah, Dr. Yasodha from Malaysia, Mr. Arshia and Dr. Masoumeh from Iran, Mr. Ahmad Kaleem from Pakistan and Mr. Omer Hamdi from Sudan for their kind help, support and friendship.

Finally I would like to express my special appreciation to my family. My parents deserve special mention for their inspirable support and prayers. I am very thankful to my lovely sisters and brother for their encouragement.

CONTENTS

Content	Page
ABSTRACT	i
ABSTRAK	iv
ACKNOWLEDGEMENT	vii
CONTENTS	ix
LIST OF SCHEMES	xii
LIST OF FIGURES	xiv
LIST OF TABLES	xviii
ABBREVIATIONS	xxi
 CHAPTER 1: INTRODUCTION	 1
 CHAPTER 2: LITERATURE REVIEW	 3
2.1 Apocynaceae: Distribution and Classification	3
2.1.1 General Appearance and Morphology	4
2.1.2 Classification of Apocynaceae	5
2.1.2.1 Genus: <i>Ochrosia</i>	7
2.1.2.2 <i>Ochrosia oppositifolia</i>	7
2.1.2.3 Genus: <i>Rauvolfia</i>	11
2.1.2.4 <i>Rauvolfia reflexa</i>	11
2.1.3 Medicinal Value of Apocynaceae Family	14
2.2 Lauraceae: Distribution and Classification	14
2.2.1 General Appearance and Morphology	15
2.2.2 Classification of Lauraceae	16
2.2.2.1 Genus: <i>Actinodaphne</i>	18
2.2.2.2 <i>Actinodaphne machrophylla</i>	20
2.2.3 Medicinal Value of Lauracea Family	23
2.3 Alkaloids	24
2.3.1 True Alkaloid	24
2.3.2 Proto Alkaloid	24
2.3.3 Pseudo Alkaloid	25
2.4 Classification of Alkaloids	32
2.4.1 Indole Alkaloids	35
2.4.1.1 Biosynthesis of Indole Alkaloids	40
2.4.1.2 Pharmacological Activity of Indole Alkaloids	42
2.4.2 The β -Carboline Alkaloids	43
2.4.3 Isoquinoline Alkaloids	44
2.4.3.1 Simple Isoquinoline	47
2.4.3.2 Aporphines	49
2.4.3.3 Benzyloisoquinolines	50
2.4.3.4 Bisbenzyloisoquinolines (BBIQ)	52
2.4.3.5 Pharmacological Activity of Isoquinolines	53

CHAPTER 3: EXPERIMENTAL	55
3.1 General Methods	55
3.2 Reagents	56
3.3 Plants Material	57
3.4 Purification	57
3.4.1 Extraction of <i>Ochrosia oppositifolia</i> (Bark and Leaves)	57
3.4.2 Isolation and Purification of Alkaloids from <i>Ochrosia oppositifolia</i> (Bark)	58
3.4.3 Extraction of <i>Rauvolfia reflexa</i> (Bark)	59
3.4.4 Isolation and Purification of Alkaloids from <i>Rauvolfia reflexa</i> (Bark)	61
3.4.5 Extraction of <i>Rauvolfia reflexa</i> (Leaves)	63
3.4.6 Isolation and Purification of Constituents from <i>Rauvolfia reflexa</i> (Leaves)	64
3.4.7 Extraction of <i>Actinodaphne macrophylla</i> (Bark)	65
3.4.8 Isolation and Purification of Alkaloids from <i>Actinodaphne macrophylla</i> (Bark)	66
3.5 Physical and Spectral Data of Isolated Constituents	68
3.5.1 <i>Ochrosia oppositifolia</i> Alkaloids	68
3.5.2 <i>Rauvolfia reflexa</i> Constituents	69
3.5.3 <i>Actinodaphne macrophylla</i> Alkaloids	74
3.6 Antiplasmodial Test Against <i>Plasmodium Falciparum</i> Strains	77
3.6.1 Preparation of the Antiplasmodial Test	77
3.6.1.1 Parasite Strain	77
3.6.1.2 Malaria Culture Media	78
3.7 Cholinesterase Enzymes Inhibitory Assay	79
3.8 Cytotoxicity Assay	80
3.8.1 Cell Culture and MTT Assay	80
3.8.2 Annexin-V-FITC Assay	80
CHAPTER 4: RESULTS AND DISCUSSION	82
4.1 Isolation and Structural Elucidation of Compounds from the Bark of <i>Ochrosia oppositifolia</i>	84
4.1.1 Isoreserpiline (120)	84
4.1.2 Neisosposinine (121)	89
4.1.3 Reserpiline (122)	94
4.2 Isolation and Structural Elucidation of Compounds from <i>Rauvolfia reflexa</i>	99
4.2.1 Alkaloids from the Bark of <i>Rauvolfia reflexa</i>	100
4.2.1.1 Rauvolfine B (123)	100
4.2.1.2 Rauvolfine C (124)	106
4.2.1.3 Vinorine (125)	112
4.2.1.4 Rescinnamine (126)	117
4.2.1.5 Cantleyine (127)	122

4.2.1.6	Akuammilan-17-oic acid, 1,2- dihydro-3- hydroxyl-1-methyl-, methyl ester (128)	127
4.2.1.7	Undolifoline (129)	132
4.2.1.8	Macusine B (130)	137
4.2.1.9	Isoreserpiline (120)	142
4.2.1.10	Akuammilan-17-oic acid, 12- hydroxyl, methyl ester (131)	142
4.2.2	Compounds from the Leaves of <i>Rauvolfia reflexa</i>	147
4.2.2.1	17- Methoxycarbonyl- 14- heptadecaenyl- 4- hydroxyl-3- methoxy cinnamate (132)	147
4.2.2.2	3- Methyl- 10, 11- dimethoxyl-6- methoxy carbonyl- β - Carboline (133)	153
4.2.2.3	(E)- Methyl 3- (4- hydroxyl-3, 5- dimethoxyphenyl) acrylate (134)	158
4.2.2.4	1,2,3,4- Tetrahydro-1-1 oxo- β - Carboline (135)	163
4.2.2.5	3- Hydroxyl- β - Carboline (136)	167
4.2.2.6	(E)-3- (3,4,5- Trimethoxyphenyl) acrylic acid (137)	171
4.2.2.7	Benzenepropanoic acid, 3- methoxy (138)	175
4.3	Isolation and Structural Elucidation of Compounds from the Bark of <i>Actinodaphne macrophylla</i>	179
4.3.1	Cycleanine (139)	179
4.3.2	(-)- 10- Demethylxylopinine (140)	185
4.3.3	Reticuline (141)	190
4.3.4	(+)- Laurotetanine (142)	195
4.3.5	(+)- Bicuculine (143)	200
4.3.6	(-)- α - hydrastine (144)	205
4.3.7	(+)- Parfumine (145)	209
4.3.8	(+)- Anolobine (146)	214
4.4	Biological Activities	219
4.4.1	Introduction	219
4.4.2	Antiplasmodial Activity	219
4.4.3	Antialzheimer Activity	221
4.4.4	Anti Cancer Activity	223
4.4.4.1	Effects of Isolated Compounds on Cell Proliferation of Different Cell Lines	223
4.4.4.2	Quantification of Apoptosis Using Fluorescent Microscopy and AO/PI Double-Staining	224
		226
CHAPTER 5: CONCLUSION		
REFERENCES		229
APPENDICES		

LIST OF SCHEMES

	Description	Page
Scheme 2.1	Classification of Apocynaceae	6
Scheme 2.2	Condensation of Secologanin with Tryptamine	41
Scheme 2.3	Steps in the Biosynthesis of Indole Alkaloids	42
Scheme 2.4	Biosynthetic Origin of the Benzyltetrahydroisoquinoline	46
Scheme 2.5	Biogenetic Relationship of the Major Alkaloids Groups Derived from Tetrahydroisoquinoline Precursor	51
Scheme 3.1	Extraction of <i>Ochrosia oppositifolia</i> (Bark and Leaves)	58
Scheme 3.2	Isolation and Purification of Alkaloids from <i>Ochrosia oppositifolia</i> (Bark)	59
Scheme 3.3	Extraction of <i>Rauvolfia reflexa</i> (Bark)	60
Scheme 3.4	Isolation and Purification of Alkaloids from <i>Rauvolfia reflexa</i> (Bark)	62
Scheme 3.5	Extraction of <i>Rauvolfia reflexa</i> (Leaves)	63
Scheme 3.6	Isolation and Purification of Constituents from <i>Rauvolfia reflexa</i> (Leaves)	65
Scheme 3.7	Isolation and Purification of Alkaloids from <i>Actinodaphne machrophylla</i> (Bark)	67
Scheme 4.1	The HMBC Correlations of Isoreserpiline (120)	88
Scheme 4.2	The HMBC Correlations of Neisosposinine (121)	93
Scheme 4.3	The HMBC Correlations of Reserpiline (122)	98
Scheme 4.4	(—) COSY and (→) selected HMBC correlations of Rauvolfine B (123)	106
Scheme 4.5	The HMBC Correlations of Rauvolfine C (124)	111
Scheme 4.6	The HMBC Correlations of Vinorine (125)	116
Scheme 4.7	The HMBC Correlations of Rescinnamine (126)	122
Scheme 4.8	The HMBC Correlations of Cantleyine (127)	126
Scheme 4.9	The HMBC Correlations of Akuammilan (128)	131
Scheme 4.10	The HMBC Correlations of Undolifoline (129)	136
Scheme 4.11	The HMBC Correlations of Macusine B (130)	141
Scheme 4.12	The HMBC Correlations of Akuammilan (131)	146
Scheme 4.13	The HMBC Correlations of Cinnamate (132)	152
Scheme 4.14	The HMBC Correlations of β - carboline (133)	158

Scheme 4.15	The HMBC Correlations of Acrylate (134)	162
Scheme 4.16	The HMBC Correlations of β - carboline (135)	166
Scheme 4.17	The HMBC Correlations of β - carboline (136)	170
Scheme 4.18	The HMBC Correlations of Acrylic Acid (137)	174
Scheme 4.19	The HMBC Correlations of Benzenepropanoic acid (138)	178
Scheme 4.20	The HMBC Correlations of Cycleanine (139)	184
Scheme 4.21	The HMBC Correlations of (-) -10- demethylxylopinine (140)	189
Scheme 4.22	The HMBC Correlations of Reticuline (141)	194
Scheme 4.23	The HMBC Correlations of (+) - laurotetanine (142)	199
Scheme 4.24	The HMBC Correlations of Bicuculine (143)	204
Scheme 4.25	The HMBC Correlations of (+) - Parfumine (145)	213
Scheme 4.26	The HMBC Correlations of (+) - Anolobine (146)	218

LIST OF FIGURES

	Description	Page
Figure 2.1	Bark and Leaves of <i>Ochrosia oppositifolia</i>	10
Figure 2.2	Bark and Leaves of <i>Rauvolfia reflexa</i>	13
Figure 2.3	Bark and Leaves of <i>Actinodaphne machrophylla</i>	22
Figure 2.4	Example of Alkaloids Ring Skeletons	34
Figure 4.1	¹ H NMR Spectrum of Isoreserpiline (120)	87
Figure 4.2	¹³ C NMR Spectrum of Isoreserpiline (120)	87
Figure 4.3	LC-MS Spectrum of Isoreserpiline (120)	88
Figure 4.4	¹ H NMR Spectrum of Neisosposinine (121)	92
Figure 4.5	¹³ C NMR Spectrum of Neisosposinine (121)	92
Figure 4.6	LC-MS Spectrum of Neisosposinine (121)	93
Figure 4.7	¹ H NMR Spectrum of Reserpiline (122)	97
Figure 4.8	¹³ C NMR Spectrum of Reserpiline (122)	97
Figure 4.9	LC-MS Spectrum of Reserpiline (122)	98
Figure 4.10	¹ H NMR Spectrum of Rauvolfine B (123)	103
Figure 4.11	¹³ C NMR Spectrum of Rauvolfine B (123)	103
Figure 4.12	HSQC Spectrum of Rauvolfine B (123)	104
Figure 4.13	HMBC Spectrum of Rauvolfine B (123)	104
Figure 4.14	COSY Spectrum of Rauvolfine B (123)	105
Figure 4.15	LC-MS Spectrum of Rauvolfine B (123)	105
Figure 4.16	¹ H NMR Spectrum of Rauvolfine C (124)	109
Figure 4.17	¹³ C NMR Spectrum of Rauvolfine C (124)	109
Figure 4.18	HSQC Spectrum of Rauvolfine C (124)	110
Figure 4.19	HMBC Spectrum of Rauvolfine C (124)	110

Figure 4.20	LC-MS Spectrum of Rauvolfine C (124)	111
Figure 4.21	¹ H NMR Spectrum of Vinorine (125)	115
Figure 4.22	¹³ C NMR Spectrum of Vinorine (125)	115
Figure 4.23	LC-MS Spectrum of Vinorine (125)	116
Figure 4.24	¹ H NMR Spectrum of Rescinnamine (126)	120
Figure 4.25	¹³ C NMR Spectrum of Rescinnamine (126)	121
Figure 4.26	LC-MS Spectrum of Rescinnamine (126)	121
Figure 4.27	¹ H NMR Spectrum of Cantleyine (127)	125
Figure 4.28	¹³ C NMR Spectrum of Cantleyine (127)	125
Figure 4.29	LC-MS Spectrum of Cantleyine (127)	126
Figure 4.30	¹ H NMR Spectrum of Akuammilan (128)	130
Figure 4.31	¹³ C NMR Spectrum of Akuammilan (128)	130
Figure 4.32	LC-MS Spectrum of Akuammilan (128)	131
Figure 4.33	¹ H NMR Spectrum of Undolifoline (129)	135
Figure 4.34	¹³ C NMR Spectrum of Undolifoline (129)	135
Figure 4.35	LC-MS Spectrum of Undolifoline (129)	136
Figure 4.36	¹ H NMR Spectrum of Macusine B (130)	140
Figure 4.37	¹³ C NMR Spectrum of Macusine B (130)	140
Figure 4.38	LC-MS Spectrum of Macusine B (130)	141
Figure 4.39	¹ H NMR Spectrum of Akuammilan (131)	145
Figure 4.40	¹³ C NMR Spectrum of Akuammilan (131)	145
Figure 4.41	LC-MS Spectrum of Akuammilan (131)	146
Figure 4.42	¹ H NMR Spectrum of Cinnamate (132)	150
Figure 4.43	¹³ C NMR Spectrum of Cinnamate (132)	150
Figure 4.44	HSQC Spectrum of Cinnamate (132)	151

Figure 4.45	HMBC Spectrum of Cinnamate (132)	151
Figure 4.46	LC-MS Spectrum of Cinnamate (132)	152
Figure 4.47	¹ H NMR Spectrum of β- carboline (133)	155
Figure 4.48	¹³ C NMR Spectrum of β- carboline (133)	155
Figure 4.49	HSQC Spectrum of β- carboline (133)	156
Figure 4.50	HMBC Spectrum of β- carboline (133)	156
Figure 4.51	DEPT 135 Spectrum of β- carboline (133)	157
Figure 4.52	LC-MS Spectrum of β- carboline (133)	157
Figure 4.53	¹ H NMR Spectrum of Acrylate (134)	161
Figure 4.54	¹³ C NMR Spectrum of Acrylate (134)	161
Figure 4.55	LC-MS Spectrum of Acrylate (134)	162
Figure 4.56	¹ H NMR Spectrum of β- carboline (135)	165
Figure 4.57	¹³ C NMR Spectrum of β- carboline (135)	165
Figure 4.58	LC-MS Spectrum of β- carboline (135)	166
Figure 4.59	¹ H NMR Spectrum of β- carboline (136)	169
Figure 4.60	¹³ C NMR Spectrum of β- carboline (136)	169
Figure 4.61	LC-MS Spectrum of β- carboline (136)	170
Figure 4.62	¹ H NMR Spectrum of Acrylic Acid (137)	173
Figure 4.63	¹³ C NMR Spectrum of Acrylic Acid (137)	173
Figure 4.64	LC-MS Spectrum of Acrylic Acid (137)	174
Figure 4.65	¹ H NMR Spectrum of Benzenepropanoic Acid (138)	177
Figure 4.66	¹³ C NMR Spectrum of Benzenepropanoic Acid (138)	177
Figure 4.67	LC-MS Spectrum of Benzenepropanoic Acid (138)	178
Figure 4.68	¹ H NMR Spectrum of Cycleanine (139)	182
Figure 4.69	¹³ C NMR Spectrum of Cycleanine (139)	182

Figure 4.70	DEPT 135 Spectrum of Cycleanine (139)	183
Figure 4.71	LC-MS Spectrum of Cycleanine (139)	183
Figure 4.72	¹ H NMR Spectrum of (-)-10- Demethylxylopinine (140)	188
Figure 4.73	¹³ C NMR Spectrum of (-)-10- Demethylxylopinine (140)	188
Figure 4.74	LC-MS Spectrum of (-)-10- Demethylxylopinine (140)	189
Figure 4.75	¹ H NMR Spectrum of Reticuline (141)	193
Figure 4.76	¹³ C NMR Spectrum of Reticuline (141)	193
Figure 4.77	LC-MS Spectrum of Reticuline (141)	194
Figure 4.78	¹ H NMR Spectrum of (+) - laurotetanine (142)	198
Figure 4.79	¹³ C NMR Spectrum of (+) - laurotetanine (142)	198
Figure 4.80	LC-MS Spectrum of (+) - laurotetanine (142)	199
Figure 4.81	¹ H NMR Spectrum of Bicuculine (143)	203
Figure 4.82	¹³ C NMR Spectrum of Bicuculine (143)	203
Figure 4.83	LC-MS Spectrum of Bicuculine (143)	204
Figure 4.84	¹ H NMR Spectrum of (-) - α - Hydrastine (144)	208
Figure 4.85	¹³ C NMR Spectrum of (-) - α - Hydrastine (144)	208
Figure 4.86	LC-MS Spectrum of (-) - α - Hydrastine (144)	209
Figure 4.87	¹ H NMR Spectrum of (+) - Parfumine (145)	212
Figure 4.88	¹³ C NMR Spectrum of (+) - Parfumine (145)	212
Figure 4.89	LC-MS Spectrum of (+) - Parfumine (145)	213
Figure 4.90	¹ H NMR Spectrum of (+) - Anolobine (146)	217
Figure 4.91	¹³ C NMR Spectrum of (+) - Anolobine (146)	217
Figure 4.92	LC-MS Spectrum of (+) - Anolobine (146)	218
Figure 4.93	Fluorescent micrographs of AO/PI double stained HCT-116 cells	225

LIST OF TABLES

	Description	Page
Table 2.1	Classification of Lauraceae general	16
Table 2.2	Different species of the genus <i>Actinodaphne</i> and their distribution	19
Table 2.3	Different species of Lauraceae plant and its medicinal properties	23
Table 2.4	Physiological activities of some alkaloids	26
Table 2.5	Types of indole skeleton, classes and the examples	37
Table 2.6	Classification of isoquinolines base on skeletal of the structure	45
Table 3.1	Standard <i>Plasmodium falciparum</i> strains	78
Table 4.1	Compounds isolated from <i>Ochrosia oppositifolia</i> , <i>Rauvolfia reflexa</i> and <i>Actinodaphne macrophylla</i>	82
Table 4.2	¹ H NMR (400 MHz) and ¹³ C NMR (100 MHz) spectral data of isoreserpiline (120) in CDCl ₃ (δ in ppm, <i>J</i> in Hz)	86
Table 4.3	¹ H NMR (400 MHz) and ¹³ C NMR (100 MHz) spectral data of neisosposinine (121) in CDCl ₃ (δ in ppm, <i>J</i> in Hz)	91
Table 4.4	¹ H NMR (400 MHz) and ¹³ C NMR (100 MHz) spectral data of reserpiline (122) in CDCl ₃ (δ in ppm, <i>J</i> in Hz)	96
Table 4.5	¹ H NMR (400 MHz) and ¹³ C NMR (100 MHz) spectral data of rauwolfine B (123) in Acetone- <i>d</i> ₆ (δ in ppm, <i>J</i> in Hz)	102
Table 4.6	¹ H NMR (400 MHz) and ¹³ C NMR (100 MHz) spectral data of rauwolfine C (124) in CDCl ₃ (δ in ppm, <i>J</i> in Hz)	108
Table 4.7	¹ H NMR (400 MHz) and ¹³ C NMR (100 MHz) spectral data of vinorine (125) in acetone- <i>d</i> ₆ (δ in ppm, <i>J</i> in Hz)	114
Table 4.8	¹ H NMR (400 MHz) and ¹³ C NMR (100 MHz) spectral data of rescinnamine (126) in CDCl ₃ (δ in ppm, <i>J</i> in Hz), ^b signal overlapped by solvent peak	119
Table 4.9	¹ H NMR (400 MHz) and ¹³ C NMR (100 MHz) spectral data of cantleyine (127) in CDCl ₃ (δ in ppm, <i>J</i> in Hz)	124

Table 4.10	^1H NMR (400 MHz) and ^{13}C NMR (100 MHz) spectral data of akuammilan (128) in CDCl_3 (δ in ppm, J in Hz)	129
Table 4.11	^1H NMR (400 MHz) and ^{13}C NMR (100 MHz) spectral data of undolifoline (129) in CDCl_3 (δ in ppm, J in Hz)	134
Table 4.12	^1H NMR (400 MHz) and ^{13}C NMR (100 MHz) spectral data of macusine B (130) in MeOD (δ in ppm, J in Hz), ^b signal overlapped by solvent peak.	139
Table 4.13	^1H NMR (400 MHz) and ^{13}C NMR (100 MHz) spectral data of akuammilan (131) in CDCl_3 (δ in ppm, J in Hz)	144
Table 4.14	^1H NMR (400 MHz) and ^{13}C NMR (100 MHz) spectral data of cinnamate (132) in CDCl_3 (δ in ppm, J in Hz)	149
Table 4.15	^1H NMR (400 MHz) and ^{13}C NMR (100 MHz) spectral data of β - carboline (133) in CDCl_3 (δ in ppm, J in Hz)	154
Table 4.16	^1H NMR (400 MHz) and ^{13}C NMR (100 MHz) spectral data of acrylate (134) in CDCl_3 (δ in ppm, J in Hz)	160
Table 4.17	^1H NMR (400 MHz) and ^{13}C NMR (100 MHz) spectral data of β - carboline (135) in CDCl_3 (δ in ppm, J in Hz).	164
Table 4.18	^1H NMR (400 MHz) and ^{13}C NMR (100 MHz) spectral data of β - carboline (136) in CDCl_3 (δ in ppm, J in Hz).	168
Table 4.19	^1H NMR (400 MHz) and ^{13}C NMR (100 MHz) spectral data of acrylic acid (137) in CDCl_3 (δ in ppm, J in Hz).	172
Table 4.20	^1H NMR (400 MHz) and ^{13}C NMR (100 MHz) spectral data of benzenepropanoic acid (138) in CDCl_3 (δ in ppm, J in Hz).	176
Table 4.21	^1H NMR (400 MHz) and ^{13}C NMR (100 MHz) spectral data of cycleanine (139) in CDCl_3 (δ in ppm, J in Hz).	181
Table 4.22	^1H NMR (400 MHz) and ^{13}C NMR (100 MHz) spectral data of (-)-10- demethylxylopinine (140) in CDCl_3 (δ in ppm, J in Hz).	187
Table 4.23	^1H NMR (400 MHz) and ^{13}C NMR (100 MHz) spectral data of reticuline (141) in CDCl_3 (δ in ppm, J in Hz).	192
Table 4.24	^1H NMR (400 MHz) and ^{13}C NMR (100 MHz) spectral data of (+) - laurotetanine (142) in CDCl_3 (δ in ppm, J in Hz).	197
Table 4.25	^1H NMR (400 MHz) and ^{13}C NMR (100 MHz) spectral data of bicuculine (143) in CDCl_3 (δ in ppm, J in Hz).	202

Table 4.26	¹ H NMR (400 MHz) and ¹³ C NMR (100 MHz) spectral data of (-) - α- hydrastine (144) in CDCl ₃ (δ in ppm, <i>J</i> in Hz).	207
Table 4.27	¹ H NMR (400 MHz) and ¹³ C NMR (100 MHz) spectral data of (+) - parfumine (145) in CDCl ₃ (δ in ppm, <i>J</i> in Hz).	211
Table 4.28	¹ H NMR (400 MHz) and ¹³ C NMR (100 MHz) spectral data of (+) - anolobine (146) in CDCl ₃ (δ in ppm, <i>J</i> in Hz).	216
Table 4.29	Inhibition growth percentage of <i>Plasmodium falciparum</i> and probit analysis with SPSS 11.5 (crude extracts of <i>Ochrosia oppositifolia</i>)	220
Table 4.30	Inhibition growth percentage of <i>Plasmodium falciparum</i> and probit analysis with SPSS 11.5 (alkaloids of <i>Ochrosia oppositifolia</i>)	220
Table 4.31	Inhibition growth percentage of <i>Plasmodium falciparum</i> and probit analysis with SPSS 11.5 (alkaloids of <i>Actinodaphne macrophylla</i>)	221
Table 3.32	IC ₅₀ values of <i>Rauvolfia reflexa</i> extracts (leaves and bark) for inhibitory activities on Cholinesterase enzymes.	222
Table 4.33	IC ₅₀ values of <i>Rauvolfia reflexa</i> chemical constituents for inhibitory activities on Cholinesterase enzymes.	222
Table 4.34	IC ₅₀ values of the isolated compounds on eight different cell lines after 24 h treatment.	224

ABBREVIATION

α	Alpha
β	Beta
λ	Maximum wave length
δ	Chemical shift
μM	Micromolar
μl	Microlitre
$\mu\text{g/ml}$	Microgram per mililitre
mM	Milimolar
mg/ml	Milligram per mililitre
g	Gram
kg	Kilogram
U/ml	Unit per mililitre
ml	Mililitre
m	Meter
MHz	Mega Hertz
Hz	Hertz
UV	Ultraviolet
IR	Infrared
mM	Milimolar
ppm	Part per million
MeOH	Methanol
CHCl_3	Chloroform
CH_2Cl_2	Dichloromethane
OCH_2O	Methylenedioxy
CH_3	Methyl group
OCH_3	Methoxyl group
OH	Hydroxyl group
NH_3	Ammonia
pH	Potency of Hydrogen
HCl	Hydrogen Chloride

TLC	Thin layer chromatography
PTLC	Preparative thin layer chromatography
CC	Column chromatography
NMR	Nuclear Magnetic Resonance
FT-NMR	Fourier Transform Nuclear Magnetic Resonance
cm ⁻¹	Per centimeter
<i>J</i>	Coupling constant
<i>d</i>	Doublet
<i>s</i>	singlet
<i>dd</i>	Doublet of doublet
<i>t</i>	triplet
<i>m</i>	multiplet
BBIQ	Bisbenzylisoquinoline
1D-NMR	One Dimension Nuclear Magnetic Resonance
2D-NMR	Two Dimension Nuclear Magnetic Resonance
¹ H	Proton NMR
¹³ C	13-Carbon NMR
COSY	¹ H- ¹ H Correlation Spectroscopy
DEPT	Distortionless Enhancement by Polarization Transfer
HMQC	Heteronuclear Multiple Quantum Coherence
HMBC	Heteronuclear Multiple Bond Coherence
NOE	Nuclear Overhauser Enhancement
GC-MS	Gas Chromatography-Mass Spectroscopy
MS	Mass Spectroscopy
HREIMS	High Resolution Electron Impact Mass Spectroscopy
FAB	Fast Atomic Bombardment
ESI	Electrospray Ionization
m/z	Mass per charge
CDCl ₃	Deuterated chloroform
MeOD	Deuterated methanol
Acetone <i>d</i> ₆	Deuterated acetone
OD	Optical density

CHAPTER 1

INTRODUCTION

INTRODUCTION

Natural products have played an important role in drugs discovery. Natural products are those chemical compounds derived from living organisms such as plants, animals, insects, and the study of natural products is the investigation of their structures, formations, use, and purpose in the organism. Drug derived from natural products are usually secondary metabolites and derivatives. The natural products that were studied and used tend to be compounds that occurred in the largest amounts, mostly from plants, and were most easily isolated in pure, or sometimes not very pure, from the technique such as simple distillation, steam distillation or extraction with acid or base. We now employ different solvents, for example hexane and CO₂ nowadays are used to extract the non-polar constituents, methanol and ethanol to extract the polar constituents. Modern isolation techniques include all types of chromatography (HPLC, TLC, CC, GC), often guided by bioassays, to isolate the active compounds.

Two main approaches exist for the finding of new bioactive chemical entities from natural sources; both random collection and screening of material, or exploitation of ethnopharmacological knowledge in the selection. The former approach bases itself on the fact that only a very small part of glob's biodiversity has ever been tested for any biological activity, and on the other hand, particularly organisms living in a species-rich environment need to evolve defense and competition mechanisms to survive. Thus, collection of plant, animal and microbial samples from rich ecosystems may give rise to isolation of novel compounds with significant biological activities (Koehn, 2005).

Malaysia is known for its richness in plants that have been around for millions of years. Strategically located on the equator where there is an existence of hot and wet climate, thas the environment has a wide range of plants to form a majestic plant kingdom.

From ancient times, preparations of plants have been used as remedies against disease. Today, with the advent of modern technology scientists are able to identify the active principles of medicinal plants such as morphine in opium poppy which acts as a pain killer. By the end of nineteenth century organic chemists had begun the investigation on alkaloids and their usage in traditional or modern medicine (Grey, 2006). Therefore, studies on various compounds such as alkaloids have been carried out widely due to the demand of the pharmaceutical industries.

The richness of Malaysian flora provides opportunities for the discovery of many novel compounds. Therefore, we have embarked on a study of chemical constituents of *Ochrosia oppositifolia*, *Rauvolfia reflexa* (Apocynaceae) and *Actinodaphne macrophylla* (Lauraceae) and their anti plasmodial, anti- alzheimer and anti- cancer activities.

The objectives of this research are:

- i. To extract, isolate and purify the phytochemicals from the *Ochrosia oppositifolia*, *Rauvolfia reflexa* and *Actinodaphne macrophylla* using various chromatographic techniques.
- ii. To characterize and elucidate the chemical structures of the isolated compounds using various spectroscopic methods such as NMR, UV, IR and MS.
- iii. To evaluate the *in vitro* anti plasmodial, anti-alzheimer and anti-cancer activities of the crudes and the isolated compounds.

CHAPTER 2

LITRATURE REVIEW

2.1 Apocynaceae: Distribution and Classification

The Apocynaceae or dogbane family is a family of flowering plants, including trees, shrubs, herbs, or lianas. Many species are tall trees, found in the tropical rainforest, and most are from the tropic and subtropics, but some grow in tropical environments. There are also some perennial herbs from temperate zones. Many of these plants have milky sap; and some species are poisonous if ingested. Some genera of Apocynaceae, such as *Adenium*, *Alafia*, and *Nerium* have both clear and milky latex sap, and others, such as *Pachypodium*, *Vinca* and *Kopsia* possess clear sap (Whitmore , 1989).

The Apocynaceae family is one of the largest plant families; comprises of 400 genera and 1500 species. In Peninsular Malaysia, there are only 32 genera and 120 species. Apocynaceae is a large Family with about 1500 species found mainly in tropical regions. It includes many of the most well-known tropical ornamental plants (Oleander, Frangipani, Allamanda, and Mandevilla). Many are large trees with buttress roots found in rainforests some are smaller, evergreen or deciduous trees, shrubs or climbers from other warm areas of the world, and one or two are found in temperate regions (*Vinca*). The sap of most plants is milky latex, which is often of economic importance for medicinal use, or further production of natural rubber. This sap is often toxic.

Fruit type is highly diversified in the Apocynacea family, and it is diagnostic of many genera. Genera 1-produce 1, 2-celled berries from a flower; genus 5 produces 2, 1-celled berries from a flower; 6 and 7 produce mostly fleshy follicles containing deeply indented seeds with ruminant endosperm; 8 has follicles and winged seeds; 9 produces follicles and seeds with 2 comas; 10-12 have follicles with globose seeds; 13-18 have drupes mostly with fleshy mesocarp; 19 has samaroid fruit; 20 has spiny capsules with seeds winged all around; and 21-44 have free or fused follicles and

comose seeds. Double flowers are known only from cultivated forms of *Nerium oleander*, *Tabernaemontana divaricata*, and *Wrightia religiosa*. Plants of the Apocynaceae are often poisonous and rich in alkaloids or glycosides, especially in the seeds and latex. Some species are valuable sources of medicine, insecticides, fibers, and rubber (Bingtao & David, 1998).

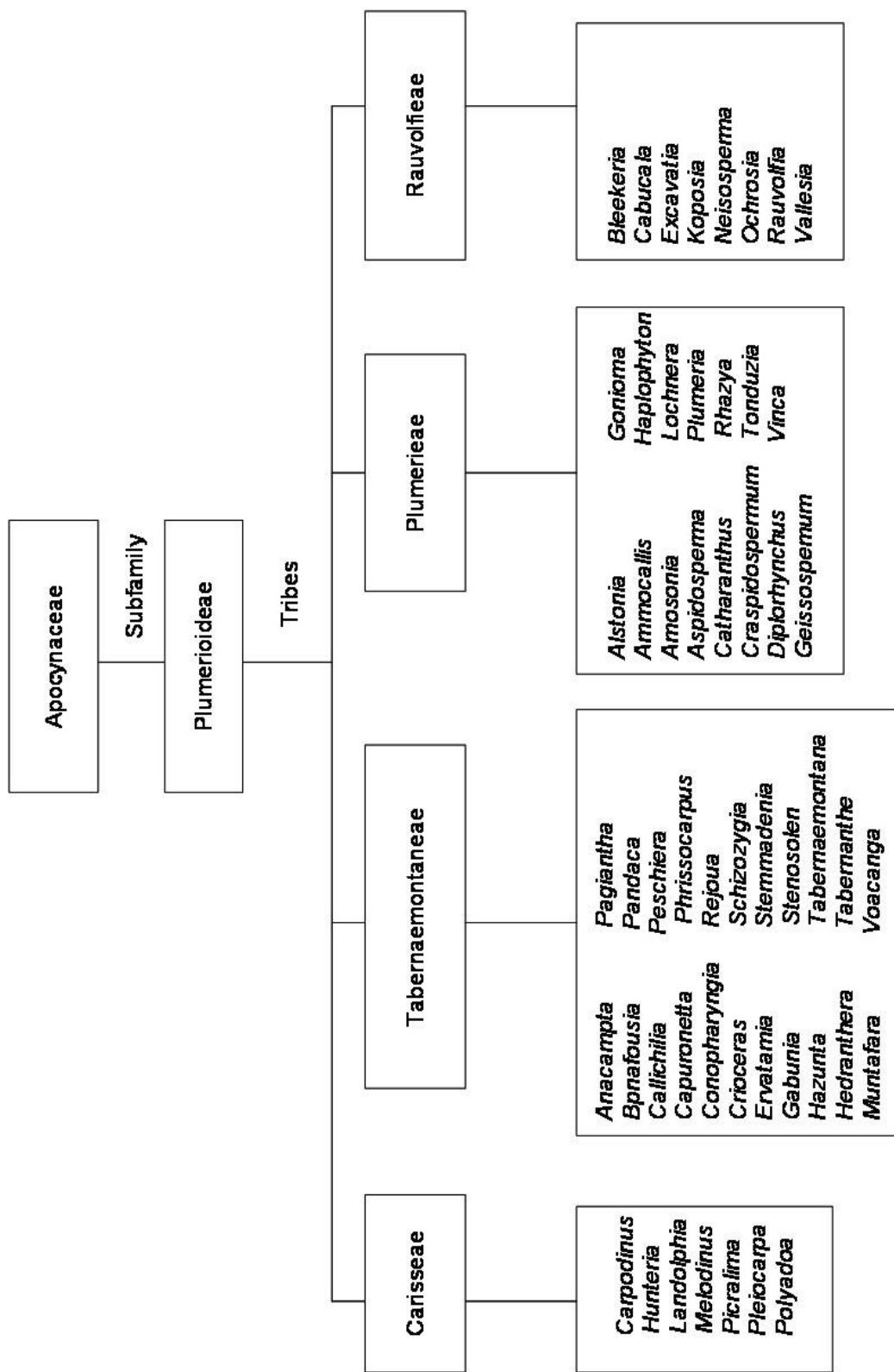
2.1.1 General Appearance and Morphology.

The leaves are simple, usually opposite and decussate, or whorled; stipules are usually absent. The flowers are bisexual and actinomorphic or sometimes weakly zygomorphic. The calyx and the corolla, both are usually 5-lobed however the calyx is synsepalous while corolla is sympetalous. The stamens are distinct, as many as corolla lobes and alternate with them, and adnate to the corolla tube (or erigynous zone). The anthers are introrse and commonly adherent to the surface of the stigma. The gynoecium consists of a single compound pistil of 2 carpels that may be distinct at the level of the superior or rarely partly inferior ovary but which are united by a single style. When distinct, each ovary typically has few to numerous ovules on marginal placentae; when connate, the placentation is axile or intruded parietal.

A nectary consisting of 5 glands or an annular ring is usually found at the base of the ovary. The fruit is commonly a follicle, capsule, or berry. The seeds usually are flat and winged or have tuft hairs at one end (Jia *et al.*, 1995).

2.1.2 Classification of Apocynaceae

Apocynaceae can be divided into Plumerioideae subfamily, which is further divided into a few tribes (Scheme 2.1). Each tribe comprises of several genera. The genus *Ochrosia* and *Rauvolfia* are classified as member of the tribe Rauvolfieae (Kisakurek *et al.*, 1983).



Scheme 2.1: Classification of Apocynaceae

2.1.2.1 Genus *Ochrosia*

Ochrosia is a genus of sea-shores, which was observed in Singapore a century ago. There are 32 *ochrosia* in Malaysia which mostly occurs in the Pangkor Island. The trees produce latex and the branches are stout. The leaves are arranged in whorls 3-5, and rarely opposite. The lateral veins are numerous; sub parallel, almost at a right angle to midvein. Calyx are deeply divided and usually without glands. The tree is in corolla salver form and the tube is slightly dilated above middle with lobes overlapping to right. The stamens are inserted in widening of corolla tube and the anthers are free from pistil head which is narrowly oblong, rounded at the base and disc absent. The ovaries are free or basally connate comprising of 2-6 ovules, biseriate on each side of a prominent placenta. The filaments are in filiform style and the pistil head is short. The drupes are smooth with thick and hard endocarp and the seeds are flat, not composed with no endosperm, and the cotyledons are large and flat (Hendrian, 2004)

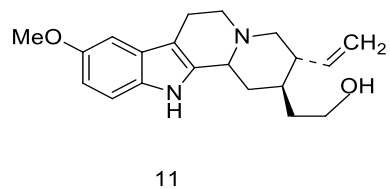
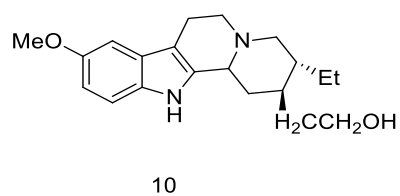
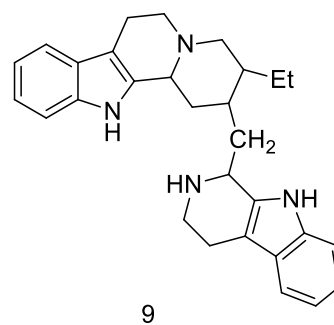
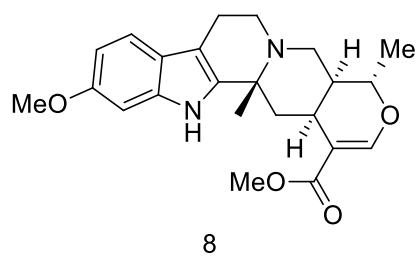
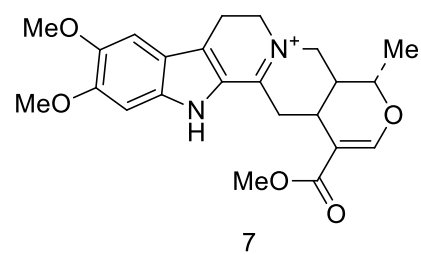
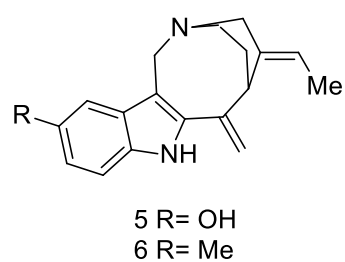
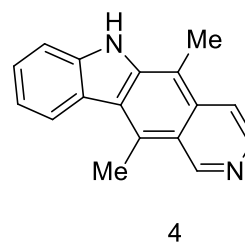
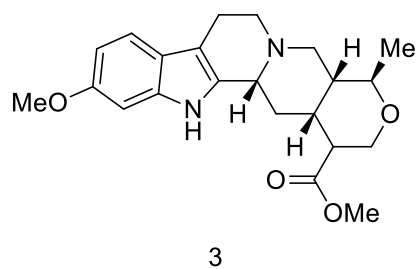
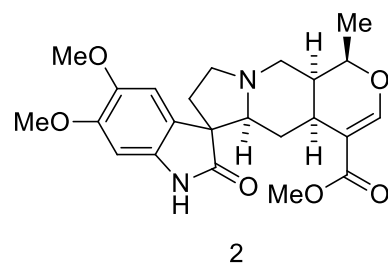
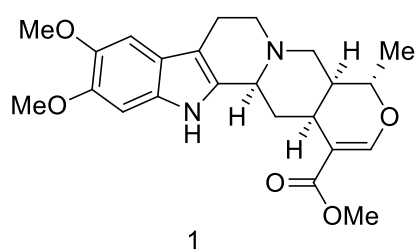
2.1.2.2 *Ochrosia oppositifolia*

Ochrosia oppositifolia is an evergreen tree that can vary greatly in size, growing to a maximum height of 15 m (50ft) or more. This species produces five-petalled white flowers with yellow centers. The flowers usually drop to the ground like confetti. The fallen flowers provide a clue to finding the tree. The fruit comes in pairs, is elliptical in shape, and is about 5-8 cm long and turns yellow when it is ripe. The seed is about 10-20 cm, apparently growing quite slowly.

Ochrosia oppositifolia occurs in Indonesia and along the southern coastal region of Sri Lanka. This plant is commonly called Muda Kaduru in Sri Lanka. The timber is moderately hard and even grained. Its roots are reputed to nullify the effect of eating

poisonous fish and crabs. It is also used as a bitter, stomachic and carminative. The seeds of *Ochrosia oppositifolia* are edible and also reputed in indigenous medicine (Peube & Koch, 1972).

Ochrosia oppositifolia, an alkaloid-rich plant belongs to Apocynaceae family. Plants of this genus are widely used in the traditional medicine. The alkaloids was first observed by J.Polsson. A literature search on the alkaloids of *Ochrosia oppositifolia* revealed the presence of isoreserpiline (**1**), neisosposinine (**2**), reserpine (**3**), 9-methoxyellipticine (**4**), hydroxyapparacine (**5**), 10-methoxyapparacine (**6**) ochroprosinine (**7**) isoreserpine (**8**), ochrolifuanine (**9**), 10- ethoxydihydrocorynantheol (**10**), 10- methoxycorynantheol (**11**). (Guanatilaka, 1998), (Liu Ching & Knochel, 2007) and (Fujii & Ohaba, 1998).





(a)



(b)

Figure 2.1: Bark (a) and Leaves (b) of *Ochrosia oppositifolia*

2.1.2.3 Genus: *Rauwolfia*

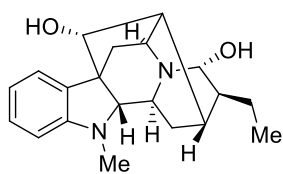
Rauwolfia (also spelled *Rauwolfia*) is a genus of evergreen and shrubs in the dogbane family, Apocynaceae. Approximately 85 species in the genus can mainly be found in tropical regions (Arvind *et al.*, 2011). The chemistry of the *Rauwolfia* species has been comprehensively investigated for the presence of alkaloids over a long period of time (Kato *et al.*, 2002).

Rauwolfia exists as shrubs or trees with whorled or opposite leaves. The flowers are in corymbose or umbellate cymes, axillary and pseudo- terminal. The lobes are broad, overlapped to left. The stamens are above middle of tube and the anthers are rounded at base. The disc cup is shaped or annular. The carpels are connate or free; style filiform; stigma calyptriform or peltate. Fruit of 2 drupes each with 1 pyrene. About 50 species were found, chiefly in American, and about 15 species were in Asia (Ridley, 1924).

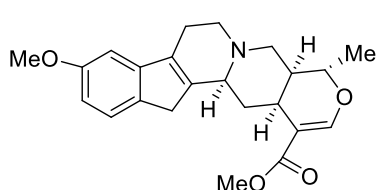
2.1.2.4 *Rauwolfia reflexa*

The tree are 40 to 50 feet and tall with thin and sub coriaceous leaves, whorled 3 to 4 or opposite, oblong to obovate- spatulate blunt or very shortly acuminate. The nerves are parallel, over 30 pairs; 6 to 8 inches long, 2 to 3 inches. wide. The flowers in compound umbels, 3 to 6 terminal on peduncles 3 inches long; umbels 2 inches long and 3 inches across on peduncles 25 inches long. The calyx-lobes are small and orbicular. The corolla campanulates 2 inches long, 1 inch wide, pubescent in mouth and white colour. The drupe are oblong- globose 6 to 7 inches long, Goping (Kunsler); Tambun (Burkill). (Ridley, 1924). *Rauwolfia reflexa*, commonly known as or Indian snakeroot or *Sarpagandha*, contains a number of bioactive chemicals including, isoreserpiline (**1**), ajmaline (**12**), aricine (**13**), corynanthine (**14**), deserpidine (**15**), rescinnamine (**16**), reserpine (**17**) and serpentinine (**18**) (Chatterjee *et al.*, 1956).

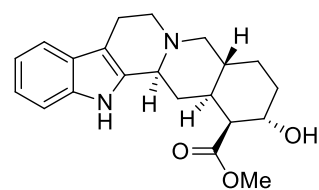
Reserpine is an alkaloid was first isolated from *Rauvolfia serpentina* and was widely used as an antihypertensive drug. It has psychological side effects and has been replaced as a first-line antihypertensive drug by other compounds that lack such adverse effects, however in some countries a combination drug that include reserpine are still available as a second-line antihypertensive drugs (Plummer *et al.*, 1954).



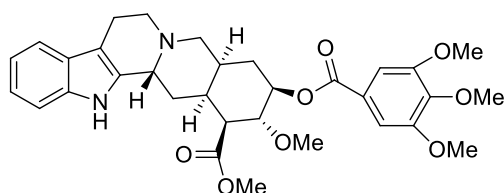
12



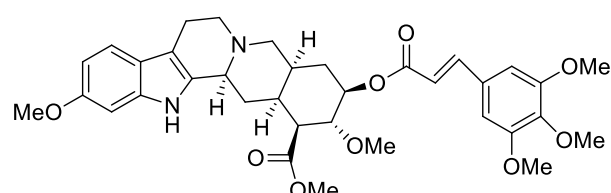
13



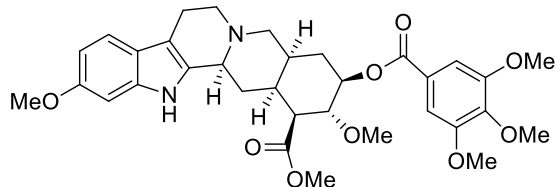
14



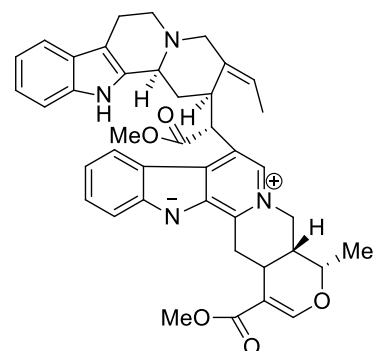
15



16



17



18



(a)



(b)

Figure 2.2: Bark (a) and Leaves (b) of *Rauvolfia reflexa*

2.1.3 Medicinal Value of Apocynaceae Family.

The alkaloids in the Apocynaceae are important in native medicine, such as bark of *Ochrosia oppositifolia* which had been used as a medicine to treat cancer in ancient Hawaii and China. *Rauvolfia* species have been used as antidote for poisons and to treat malaria (Mia *et al.*, 2009), while *Ochrosia* species widely used in combination chemotherapy regimens for treating leukemias and to treat malaria (Jordan & Scheuer, 1965). These plants are distributed mainly in the tropical and sub-tropical region.

2.2 Lauraceae: Distribution and Classification

In Malaysia, Lauraceae family is known as *medang* or *Tejur*. The Lauraceae or laurel family comprises a group of flowering plants included on the order laurales. The family contains about 62 genera and over 2000 species world-wide, mostly from warm or tropical regions, especially Southeast Asia and tropical America (Little *et al.*, 2009). The tree of Lauraceae are usually evergreen, shrubs and without buttresses.

Ecology of Lauraceae is dependent on type of the lands, whether lowlands or highlands. In the lowlands, Lauraceae are typically small trees except for a few species which may reach 30 m tall. In the highlands, Lauraceae like fagaceae, becoming more abundant reaches the top layer of the forest, which lies at 1200- 1600 m. Such Oak- laurel forest is a feature of the mountains of tropical Asia from Himalayas to New Guinea (Corner, 1988).

2.2.1 Lauraceae: General Appearance and Morphology

The bark is usually smooth, rarely fissured, scaly or dipple, often covered with large lenticels, grey- brown to reddish-brown. The inner bark is usually very thick, granular, mottled or laminated, often with strong aromatic smell, yellow, orange-brown, pinkish or reddish. Sapwood is pale yellow to pale brown with satiny lustre when freshly cut. Terminal bud naked or covered with bud scales which sometimes appear like small leaves.

The leaves of this family appear in a simple way. They are spiral, alternate, opposite, subopposite, or whorled (*Actinodaphne*), entire and leathery. The secondary veins pinnate have only one pair as in *Cinnamomum*. The colors of the new leaves is vary from nearly white to pink, purple or brown.

The flowers of Lauraceae usually are small, regular, greenish, white or yellow, fragrant or with rancid smell, bisexual or unisexual, perianth free or united with six tepals in two rows. The flowers are pollinated chiefly by flies and beetles which are attracted by the smell emitted from the flowers.

The fruit of this family are small to large (one seed berry), sometimes envelopes by the accrescent perianth tube or persiting and clasping the base of fruit. In some genera perianth lobes are dropping but the tube developing into a shallow or deep cup at base of fruit. The fruits stalk enlarging and becoming highly coloured in some species of *Dehaasia* and *Alseodaphne*. The seed of Lauraceae are without albumen, with thin testa. Cotyledons are large, flat, convex and pressed against each other.

Wood of Lauraceae is soft to moderately hard, light to moderately heavy to varying from 350-880 kg/m³ air dry. Grain straight or slightly interlocked, texture moderately

fine and even. Sapwood usually is a distinctly lighter shade than the heartwood. The heartwood is yellow-white (*Beilschmiedia*), yellow brown or red-brown in most species of *Cinnamomum*, *Cryptocarya*, and *Endiandra*, olive green in species of *Litsea*, *Actinodaphne*, *Alseodaphne*, *Notaphoebe*, *Phoebe*, and dark olive green-brown in *Dehaasia*.

The family of Lauraceae provided many useful economic products. Most of them are economically important species, other than sources of excellent wood, there are species as flavoring agents for example avocado (*Persea*) is one of important tropical fruit (Bost, 2009).

2.2.2 Classification of Lauraceae

Classification of Lauraceae can be illustrated in 60 genera, mainly in Southeast Asia and Latin America Table 2.1. (Little *et al.*, 2009).

Table 2.1: Classification of Lauraceae genera

1. <i>Actinodaphne</i>	31. <i>Lindera</i>
2. <i>Adenodaphne</i>	32. <i>litsea</i>
3. <i>Aiouea</i>	33. <i>Machilus</i>
4. <i>Alseodaphne</i>	34. <i>Mezilarus</i>
5. <i>Anaueria</i>	35. <i>Mochinnodaphne</i>
6. <i>Aniba</i>	36. <i>Mutisiopersea</i>
7. <i>Apollonias</i>	37. <i>Nectandra</i>
8. <i>Aspidostemon</i>	38. <i>Neocinnamomum</i>
9. <i>Beilschmiedia</i>	39. <i>Neolitsea</i>
10. <i>Brassiodendron</i>	40. <i>Nothaphoebe</i>

11. <i>Caryodaphnopsis</i>	41. <i>Ocotea</i>
12. <i>Cassytha</i>	42. <i>Paraia</i>
13. <i>Chlorocardium</i>	43. <i>Parasassafras</i>
14. <i>Cinadenia</i>	44. <i>Persea</i>
15. <i>Cinnamomum</i>	45. <i>Phoebe</i>
16. <i>Clinostemon</i>	46. <i>Phyllostemonodaphne</i>
17. <i>Cryptocarya</i>	47. <i>pleurothyrium</i>
18. <i>Dahlgrenodendrone</i>	48. <i>Potameia</i>
19. <i>Dehaasia</i>	49. <i>Potoxylon</i>
20. <i>Dicypellium</i>	50. <i>Povedadaphne</i>
21. <i>Dodecadenia</i>	51. <i>Ravensara</i>
22. <i>Endiandra</i>	52. <i>Rhodostemonodaphne</i>
23. <i>Endlicheria</i>	53. <i>Sassafras</i>
24. <i>Eusideroxylon</i>	54. <i>Sextonia</i>
25. <i>Gamanthera</i>	55. <i>Sinosassafras</i>
26. <i>Hexapora</i>	56. <i>Syndiclis</i>
27. <i>Hypodaphnis</i>	57. <i>Triadodaphne</i>
28. <i>Iteadaphne</i>	58. <i>Umbellularia</i>
29. <i>Kubitzkia</i>	59. <i>Urbanodendron</i>
30. <i>Laurus</i>	60. <i>Williamodendron</i>

2.2.2.1 Genus *Actinodaphne*.

Actinodaphne belongs to the family of Lauraceae, of the tribe *Cinnamomone*. This genus is readily distinguished from the foregoing by the arrangement of the flowers. From each other they differ fundamentally only in minute details of the stamens. However the arrangement of the leaves is a rather useful, if imperfect, guide to the Malayan species. The genus *Actinodaphne* has about 70 species, mainly in Asiatic mainland and malesia where 14 species were found in Malaysia (Table 2.2).

The plant of this genus is either shrub or small to medium sized trees. In *Actinodaphne* the leaves are arranged on whorls (except *A. Sphaerocarpa*); leaf bud enclosed by large bud scales which leaves circular markings on twigs. The flowers are dioecious; perianth villous outside, with six lobes. Flower- heads generally in small dense clusers in the leaf- axils, or on the twigs and branches behind the leaves. Inflorescences in shortened racemes appearing as pseudoumbels, surrounded by deciduous bracts. Each flower shortly stalked and grouped with two eight (or more) other flowers in a tiny stalked head surrounded (at least when young) with bracts a perianth.

The fruits are small or large, round or oblong berries. They appear orange, red or black when ripening. The fruits are seated on the small or swollen calayx- cup where the rim of cup generally entire, that is without sepals (Kochummen, 1972).

Table 2.2: Different species of the genus *Actinodaphne* and their distribution

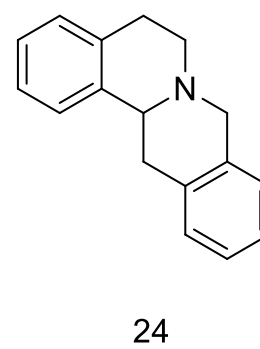
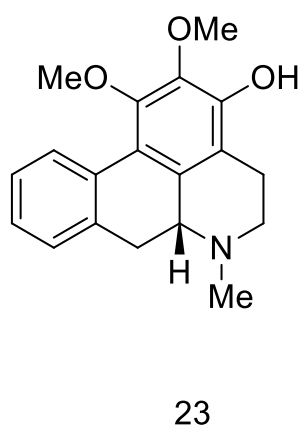
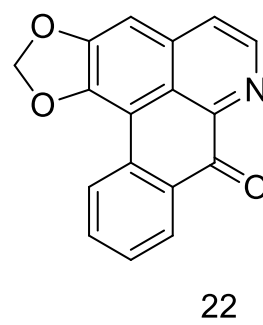
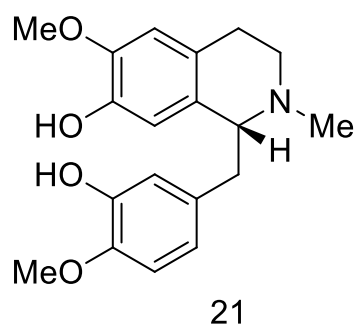
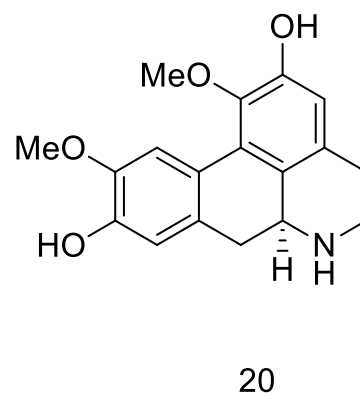
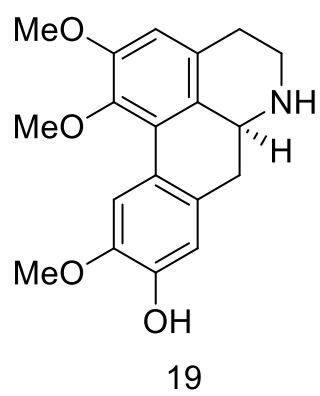
Species	Distribution
<i>A. Borneensis Meissn</i>	Lowland forest near swamps; Terengganu, Johor, Borneo
<i>A.concinna Ridl</i>	Mountain forest; Terengganu, Pahang, Selangor
<i>A.Cuspidata Gamp</i>	Ulu Bera, Perak
<i>A.fragilis Gamp</i>	Lowland; Perak
<i>A.glomerata (Bl.) Nees</i>	Lowland forest; Perak, Terengganu, Johor, Singapore, Borneo, Java, Sumatra
<i>A.johorensis Gamp</i>	Hill forest; Pahang & Johor
<i>A.macrophylla (Bl.) Nees</i>	Lowland to mountain forest; Kelantan, Pahang, Perak, Selangor, Melaka, Singapore
<i>A.malaccensis Hk.f</i>	Mountain forest; Melaka, Perak, Singapore
<i>A.montana Gamp</i>	Mountain forest between 900-1500 m. Rarely on low hills; Kedah, Perak, Kelantan
<i>A.obovata Bl.</i>	Mountain forest at Gunung Tahan, Pahang
<i>A.oleifolia Gamp</i>	Mountain forest; Perak, Pahang, Borneo
<i>A.pruinosa Nees</i>	Lowland and hill forest; Kedah, Penang, Perak, Singapore
<i>A.ridleyi Gamp</i>	Mountain forest between 600-900 m in Gunung Pulai, Johor, Borneo
<i>A.sesquipedalis Hook.f. & Th</i>	Widely distributed throughout peninsular Malaysia except Melaka and Johor from lowland to mountain forest up to 1200 m

2.2.2.2 *Actinodaphne macrophylla*

The leaves are hairy below and sometimes only petiole and midrib below hairy. The leaves undersurface appear woolly reddish brown and the apex usually blunt. Tertiary nerves prominently raised below. The buds are covered with large leaf-like scale leaves.

The trees are normally medium sized to 24 meters tall with 150 cm girth. The crowns are dense and domed. Bole with steep buttresses up to one meter high. The barks appear dull brown in color and smooth while the inner bark appear bright orange-brown and granular. Twigs are densely covered with long reddish brown hairs. Buds are covered with 2.5- 5 cm long scale leaves. The leaves are in whorls of 6-12; stalk 2.5-5 cm long with woolly hairy; blade thickly leathery. Flowers are in clusters on bare twigs between leaf whorls. Fruits are globose, rather flattened and seated on woody perianth. It appears yellow and then bright red when ripening. This species are found in the lowland to mountain forest; very common Fraser's Hill in Pahang or Kelantan, Perak, Selangor, Melaka and Johor (Kochummen, 1972).

A number of bioactive chemicals have been isolated from *Actinodaphne macrophylla* like; (+) laurotetanine (**19**), norboldine (**20**), reticuline (**21**), lirodenine (**22**), lirinine (**23**) and berbine (**24**). (Rashid, 2008).





(a)



(b)

Figure 2.3: Bark (a) and Leaves (b) of *Actinodaphne macrophylla*.

2.2.3 Medicinal Value of Lauraceae Family

The Lauraceae genus is important, both for its sheer number of species and for its therapeutic properties (Meissner & Friedrich, 1964). They are found in the tropical areas of American and Asia. The lists below (Table 2.3) show some examples of Lauraceae plant with its medicinal properties.

Table 2.3: Different species of Lauraceae plant and its medicinal properties

Species	Medicinal Used
<i>Actinodaphne sesquipedalis</i>	Used as anesthetic
<i>Actinodaphne moluccana</i> Blume	Used against boils
<i>Actinodaphne cupularis</i> (leaf)	Beverage tea, remedy for trauma and stomachache
<i>Actinodaphne lancifolia</i> (root)	Traditional Chinese medicine used for treatment of stomachache, arthritis, overexertion and edema
<i>Cinnamomum zeylanicum</i>	Warming stimulant, carminative, antispasmodic, antifungal, antiseptic
<i>Cinnamomum camphora</i>	Antiseptic, antispasmodic, analgesic
<i>Cassytha filiformis</i>	Useful medicinally for gonorrhea, kidney, ailments, as a diuretic
<i>Lindera benzoin</i>	Anthelmintic, antipyretic
<i>Lindera strychnifolia</i> (twigs)	Control pain, disperse cold and strengthen stomach
<i>Litsea cubeba</i> (fruits, roots, stems)	Disperse cold, control pain
<i>Laurus nobilis</i>	To treat upper digestive tract disorders and to ease arthritic aches and pains
<i>Sassafras albidum</i>	Anodyne, antiseptic, diuretic, stimulant

2.3 Alkaloids

The term alkaloids or alkali-like was first proposed by W. Meisner in 1819. Alkaloids are defined as nitrogen containing basic substances, having a complex structure, naturally origin and limited distribution on earth (Haslam, 1986). Alkaloids always contain nitrogen atom as a part of the heterocyclic system, and they usually possess some pharmacological activity. Particular alkaloid is usually restricted to certain genera and families of plant kingdom, rarely being present in large groups of plants. They are biosynthetically exist as salt and related to acid amino such as ornithine and lysine. Many of alkaloids are derived from plant sources. They are basic, contain one or more nitrogen atoms (usually in a heterocyclic ring) and usually have a marked physiological action on man or other animals (Trease & Evans, 1989) (Table 2.4).

Alkaloids can be categorized into three groups based on their biogenesis; true alkaloids, protoalkaloids and pseudoalkaloids.

2.3.1 True Alkaloid

The true alkaloids normally contain nitrogen in heterocyclic rings, they derived from amino acid. They normally occur in the plants in form of salt of an organic acid. Examples of this group are hygrine (**25**) and cryptostyline (**26**).

2.3.2 Proto Alkaloid

The protoalkaloids are relative simple amine in which the amino acid nitrogen is not in a heterocyclic ring. Like the true alkaloids, they are derived from amino acid and they are

basic. Some examples of this group are mescaline (27), ephedrine (28), *N,N*-dimethyltriethamine (29), serotonin (30) and cathinone (31).

2.3.3 Pseudo Alkaloid

The pseudoalkaloids are not derived from amino acid precursor and usually basic. They are nitrogen containing in the molecule but they have a carbon skeletons derived from terpenoids (mono-, sesqui-, di-, and triterpenoids), steroidal, hemiterpenoids and other acetate derivatives. Some examples of this group are actinidine (32), deoxynupharidine (33) and alchorneine (34).

Alkaloids represent a fascinating group of natural product for a number of reasons. Many reveal important biological and pharmacological activities and for several decades have been therapeutically applied in the treatments of various diseases. Some of the alkaloids with impressive activities which have prompted the development of broadly applied drugs on the pharmaceutical market, include the well-known cytotoxic bisindole alkaloids vincleucoblastine (35) and vinblastine (36) from *Catharanthus*, the diterpenoid alkaloid taxol from *Taxus*, the highly important analgesic morphine (37), spasmolytics tubocurarine (38) and papaverine (39), the vasodilating agents vincamine (40) and ajmalicine (41), emetine (42) with its emetic activity, and the antiarrhythmic alkaloids quinidine (43) and ajmaline (44) (Scholz & Winterfeldt, 2000).

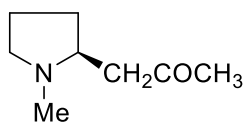
The diversity of alkaloid structures forced scientists to concentrate during recent decades on the elucidation of biosynthetic pathways at the enzymatic level. Now the first examples exist for the detection of series of enzymes catalyzing multistep biosynthetic sequences, e.g. in the field of isoquinoline alkaloids (Tanahashi & Zenk, 1985), indole bases (Victor &

Roberto, 2007) and pyrrolizadine alkaloids (Boeder, 1999). Successful study of the molecular genetics of alkaloid formation has been undertaken including the first example of heterologous expression of appropriate enzymes catalyzing alkaloid metabolism (Kutchan *et al.*, 1991), (Facchini, 2001).

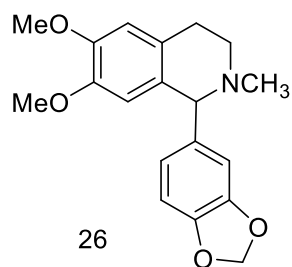
Table 2.4: Biological activities of some alkaloids

Alkaloids	Biological activities
Nicotine (54)	Toxic, stimulate respiratory processes, inhibition in all sympathetic and parasympathetic
Atropine (55)	Antagonism to muscarinic receptors (parasympathetic inhibition)
Cytochalasin D (56)	Cytotoxic and antitumor activity
Haplophyllidine (57)	Ataractic and sedative
Perforine (58)	Hypoglycemic activity
Bucharaine (59)	Suppress aggressive tendencies
Mescaline (60)	Inhibit the pressor effect epinephrine and produce hyperthermia and uterine contraction
Ephedrine (61)	Therapeutic agent
Gliotoxin (62)	Bacteriostatic agent
Papaverine (63)	Decrease the tonus of the smooth muscle
Laudanosine (64)	Reduce intraocular pressure
(+)-Cepharanthine (65)	Effective against human tuberculosis and leprosy
(-)-mecambrine (66)	
Thebaine (67)	Increases motility of isolated rat or rabbit duodenum
Heroine (68)	
Erysotrine (69)	Increased intestinal muscle tone in rabbit
Coccuvinine (70)	Exhibited significant cytotoxicity
Tylophorine (71)	Neuromuscular blocking agents
Canthin-6-one (72)	Antifungal and leishmanicidal activities
Tecomine (73)	Toxic to many bacteria and other unicellular organism

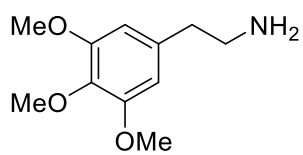
(Verporte, 1986), (Ajay, 2010)



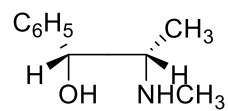
25



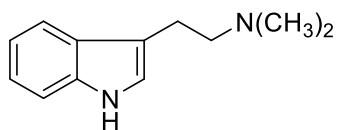
26



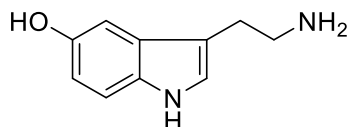
27



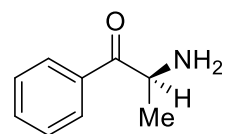
28



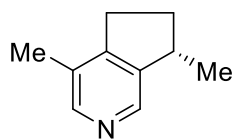
29



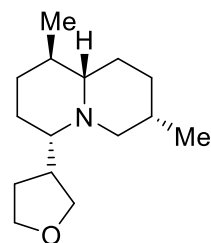
30



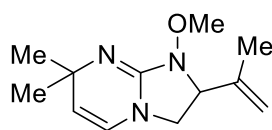
31



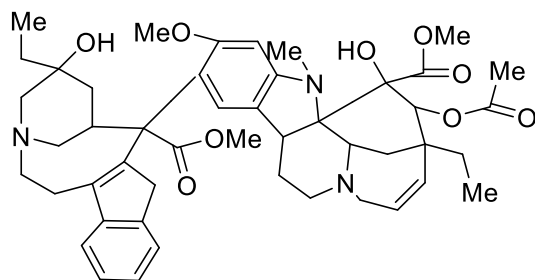
32



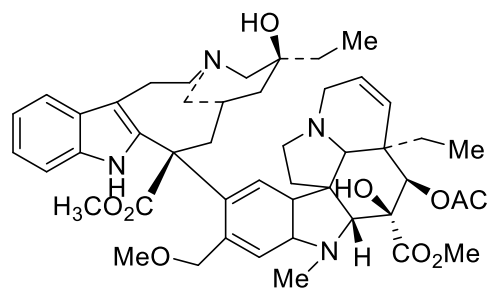
33



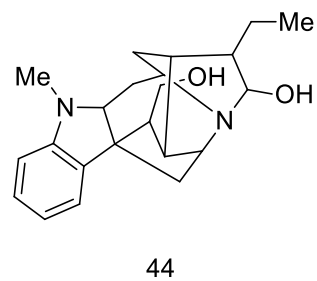
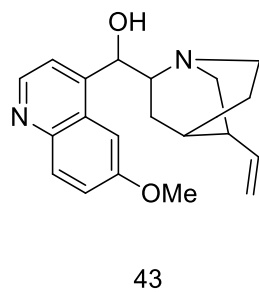
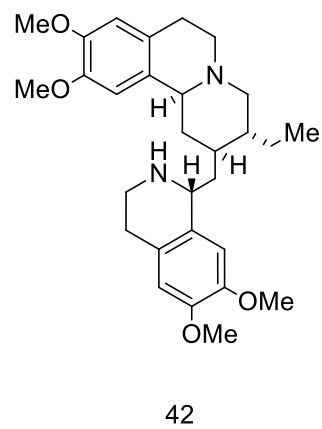
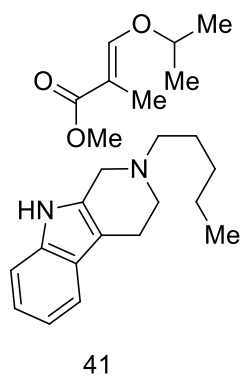
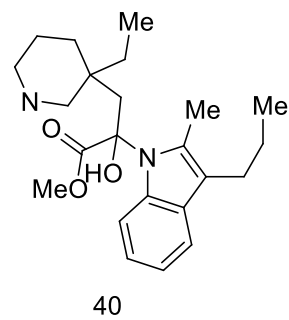
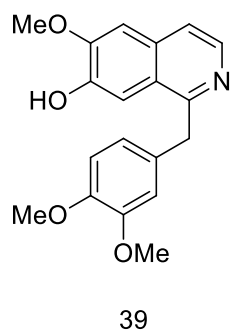
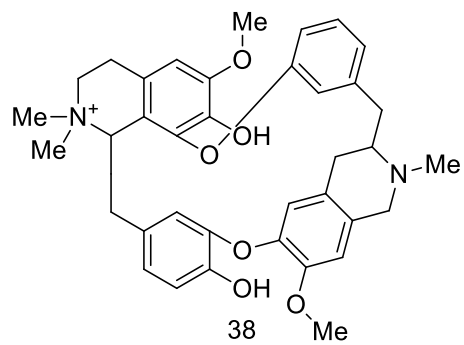
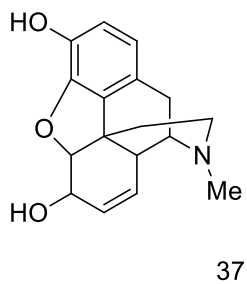
34



35



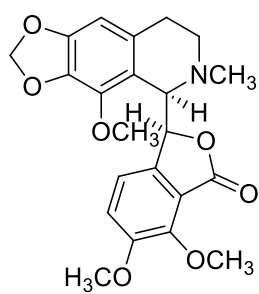
36



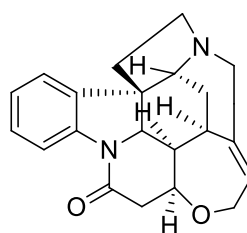
Usually alkaloids occur in a multicomponent mixture and separation of alkaloids from other groups of natural product is the first requirement for detailed qualitative, quantitative and structural analysis of a single alkaloid.

The first crude drug to be investigated chemically was opium from the dried latex of the poppy *Papaver somniferum*. In 1803, Derosne isolated a semipure alkaloid from opium and named it as narcotine (45). Further examination of opium by Serturner in 1805 had led to the isolation of morphine. In the years 1817-1820 in the laboratory of Pelletier and Caventou at the Faculty of Pharmacy in Paris, the researchers obtained many active alkaloids. Among the alkaloids obtained were strychnine (46), brucine (47), piperine (48), caffeine (49), quinine (50), cinchonine (51) and colchicine (52). They also obtained coniine (53) in 1826 (Phillipson, 2001).

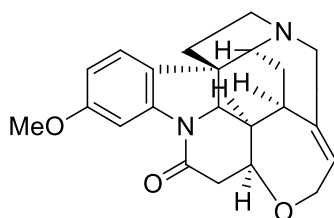
Certain plant families have a marked tendency to elaborate alkaloids and this is true for the monocotyledons such as Annonaceae, Apocynaceae, Fumariaceae, Lauraceae, Loganiaceae, Magnoliaceae, Menispermaceae, Papaveriaceae, Ranunculaceae, Rubiaceae, Rutaceae, and Solanaceae (Cordell *et al.*, 2001). Within these families, some genera produce alkaloids and others do not. The biological activity of the alkaloids, together with their impressive structural diversity, largely accounts for the enormous research effort that has been devoted to their characterization, pharmacologic evaluation and synthesis (Raven *et al.*, 2005).



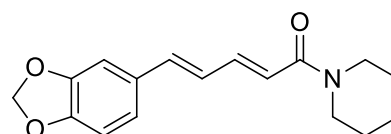
45



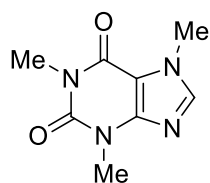
46



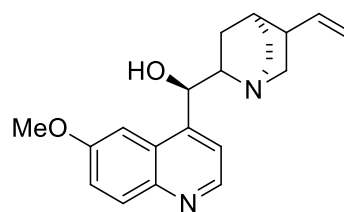
47



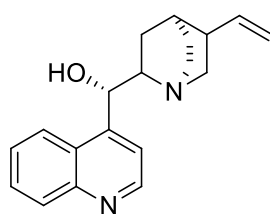
48



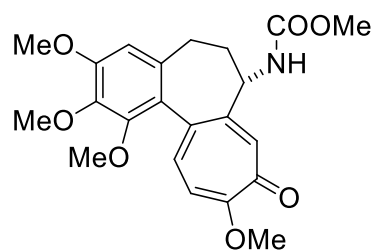
49



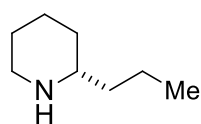
50



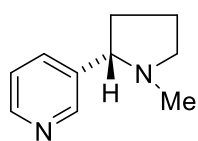
51



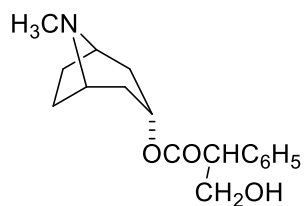
52



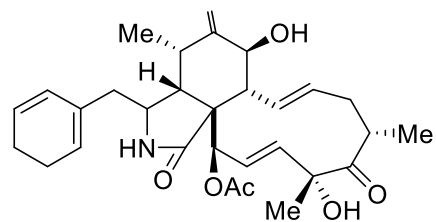
53



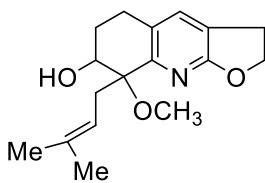
54



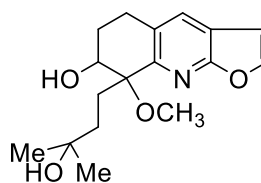
55



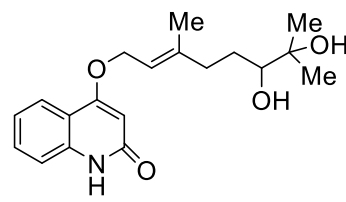
56



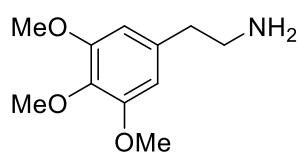
57



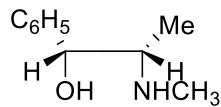
58



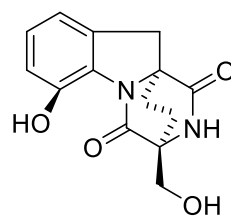
59



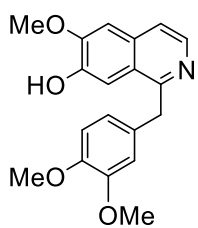
60



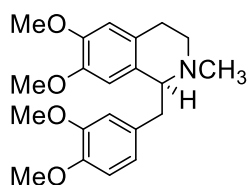
61



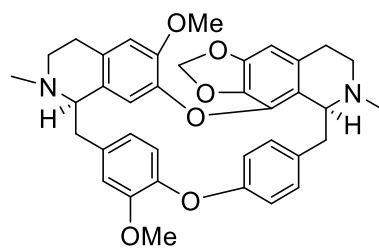
62



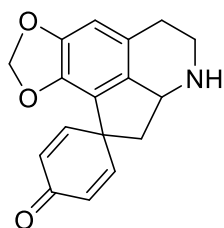
63



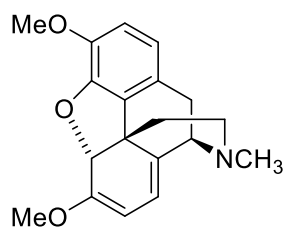
64



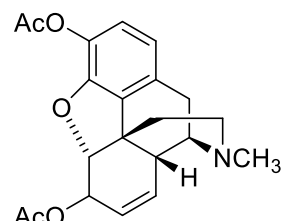
65



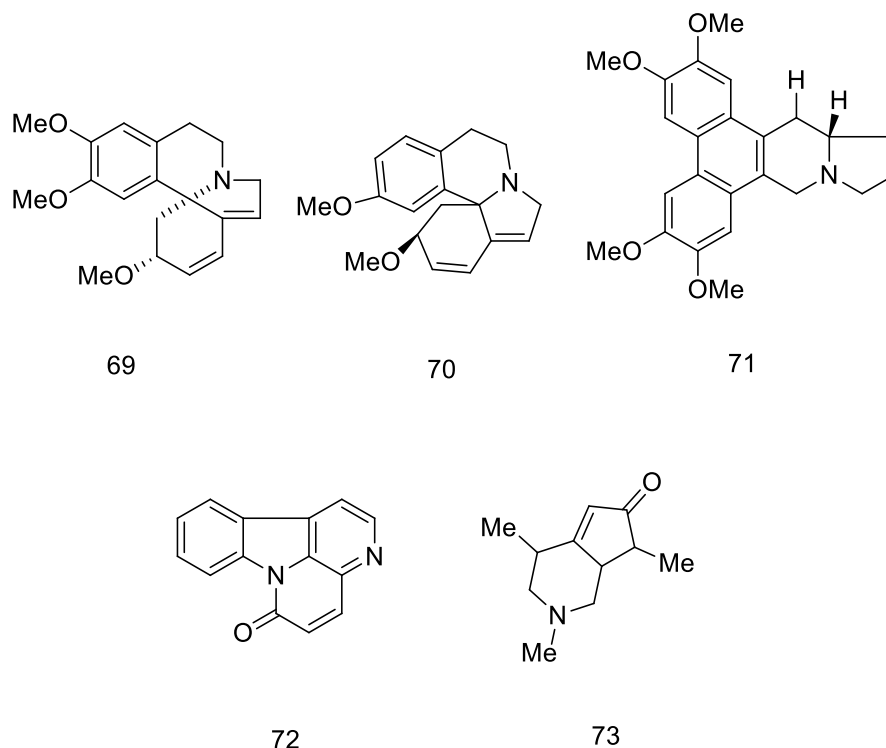
66



67



68



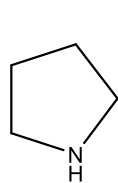
The role of alkaloids in plants are still unknown, however some have suggested that alkaloids are as the end product of metabolism or waste products, and they function as a protection against predator attack, storage reservoir of nitrogen for protein synthesis, plants stimulants or regulator in many activities, such as growth, metabolism and reproduction and a model for the chemical synthesis of analogue with excellent properties (Bruneton, 1995).

2.4 Classification of Alkaloids.

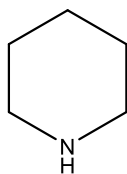
Alkaloids are usually classified according to their common structural motif, based on the metabolic pathway used to construct the molecule. When not much was known about the biosynthesis of alkaloids, they were grouped under the names of known compounds, even some non-nitrogenous ones, for example the phenanthrenes, since this moiety appeared in the finished product or by the plant or animals from which they were isolated. When more

is learned about a certain alkaloid, the grouping is changed to reflect the new knowledge, usually talking the name of a biologically-important amine that stands out in the synthesis process. Alkaloids may be classified by various methods which are based on the nature of the classification such as: biogenesis, structural relationship based on chromophore of fundamental skeleton, nitrogen atom and its immediate environment, botanical origin, spectroscopic criteria (Roberts, 1998).

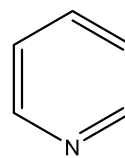
Several examples of common alkaloids ring skeleton are illustrated in Figure 2.4 (Bruneton, 1995).



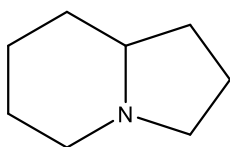
Pyrrolidine



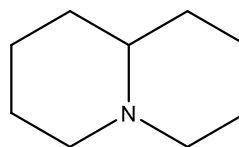
Piperidine



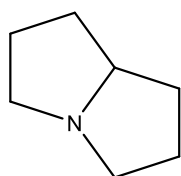
Pyridine



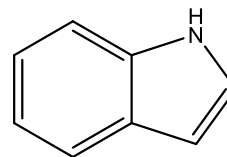
Indolizidine



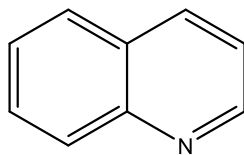
Quinolizidine



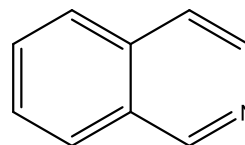
pyrrolizidine



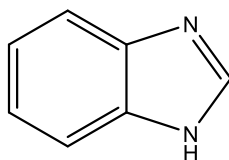
Indole



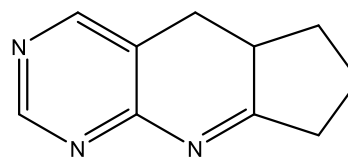
Quinoline



Isoquinoline



Purine



Quinazoline

Figure 2.4: Example of Alkaloids Ring Skeletons

2.4.1 Indole Alkaloids

Indole is an electron-rich aromatic compound and is widely distributed in natural product. In proteins it is an important constituent of essential amino acid tryptophan (**91**). It is known to form a hydrophobic environment in proteins and to be involved in enzymatic reactions, in addition to the redox activities and various weak interactions (de Souza *et al.*, 2010). It shows versatile metal binding abilities through the nitrogen and carbon atoms. They include the 'animal alkaloids'; adrenaline, noradrenaline, serotonin (5-hydroxytryptamine or 5-HT), the tranquillizing alkaloids of passion flower, the ophthalmic alkaloids related to physostigmine from the calabar bean, the uterine stimulants ergotamine and ergometrine from the fungus ergot of rye, and lysergic acid diethylamide (LSD). Also included are the alkaloids of the Indian snakeroot (*Rauwolfia serpentina*), including reserpine, having powerful hypotensive effects. In addition, there are some examples of central nervous stimulants: strychnine, johimbine and psilocybin. All these alkaloids have their effect on the neuromuscular system by interacting with adrenergic receptors. Finally, the infamous two antileukaemic medications vincristine and vinblastine isolated from the Madagascar periwinkle (*Catharanthus rosea*) (Gurib- Fakim, 2006).

Indole alkaloids exhibit numerous biological activities (anti-tumor, anti-microbial, anti-hypertensive and central nervous system stimulant. They can be found in plants of the Apocynaceae, Rubiaceae, and Loganiaceae families.

In Apocynacea the majority of indole alkaloids can be classified into nine main types according to the structural characteristics of their skeleton (Table 2.5) (Schutte, 1986).

Eight main types have been defined. There are vincosan, vallesiachotaman, corynanthean, strychnan, aspidospermatan (all belong to the class I skeleton with an intact secologanin), plumeran, eburnan (belong to the class II skeleton, rearranged secologanin) and ibogan (class III skeleton, rearranged monoterpene). The ninth type, tacaman (class III skeleton) has been added by Verpoorte and Beek, 1983 to account for the isolation of a few tacamines (Table 2.5) (Gower *et al.*, 1986).

Table 2.5: Types of indole skeleton, classes and the examples.

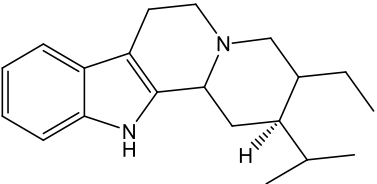
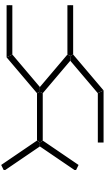
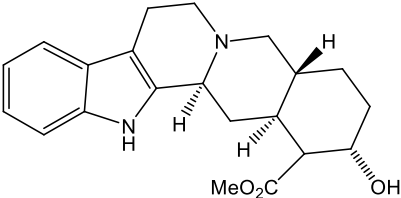
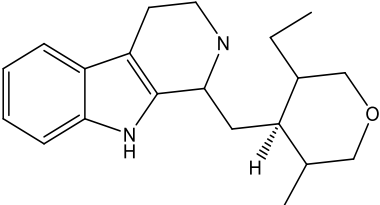
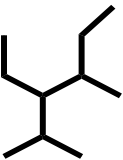
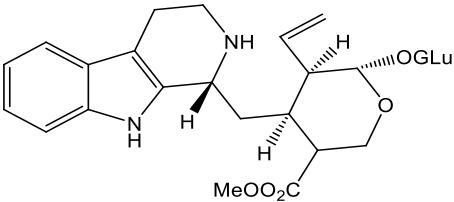
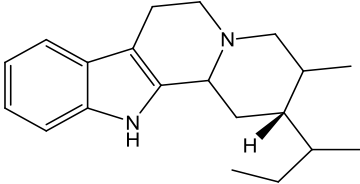
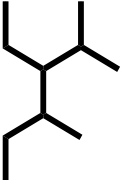
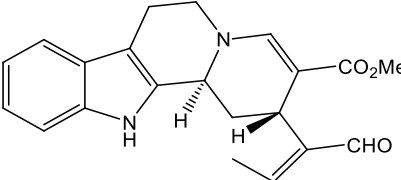
Type of indole alkaloid	Skeleton	Example
 <p>Corynanthean or C-type</p>	 <p>Class I</p>	 <p>corynanthine 74</p>
 <p>Vincosan or D-type</p>	 <p>Class I</p>	 <p>Vincoside 75</p>
 <p>Vallesiachtamon or V-type</p>	 <p>Class I</p>	 <p>vallesiachotamine 76</p>

Table 2.5: Types of indole skeleton, classes and the examples (continued)

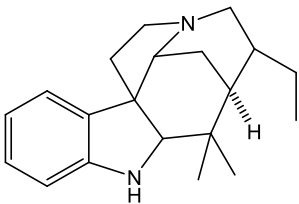
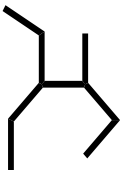
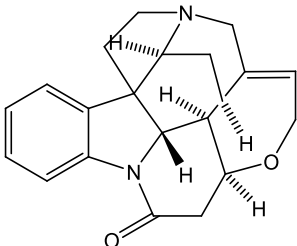
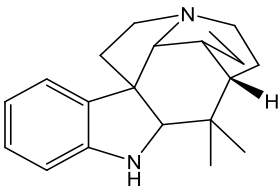
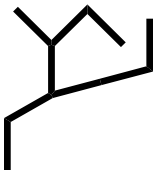
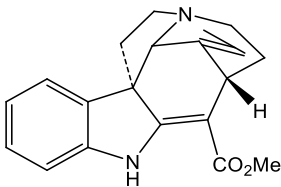
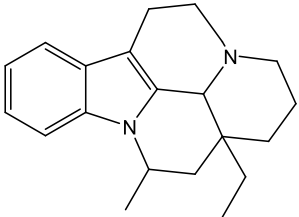
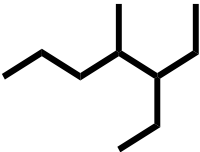
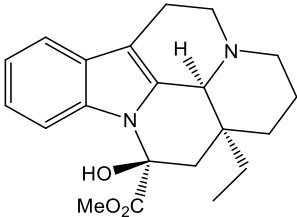
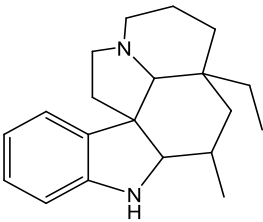

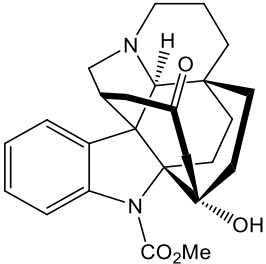
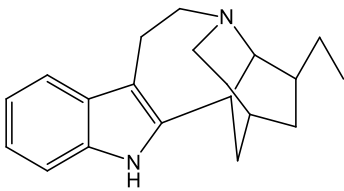

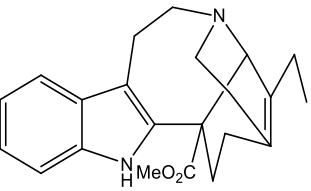
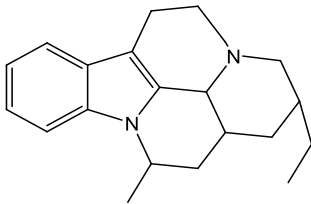
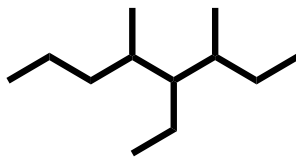
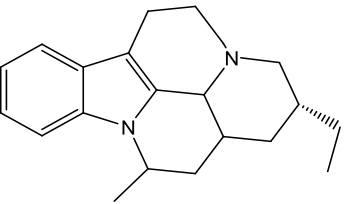
Type of indole alkaloid	Skeleton	Example
 <p>Strychnan or S-type</p>	 <p>Class I</p>	 <p>strychnine 46</p>
 <p>Aspidospermatan or A-type</p>	 <p>Class I</p>	 <p>condylocarpine 77</p>
 <p>Eburanan or E-type</p>	 <p>Class II</p>	 <p>vincamine 78</p>

Table 2.5: Types of indole skeleton, classes and the examples (continued)

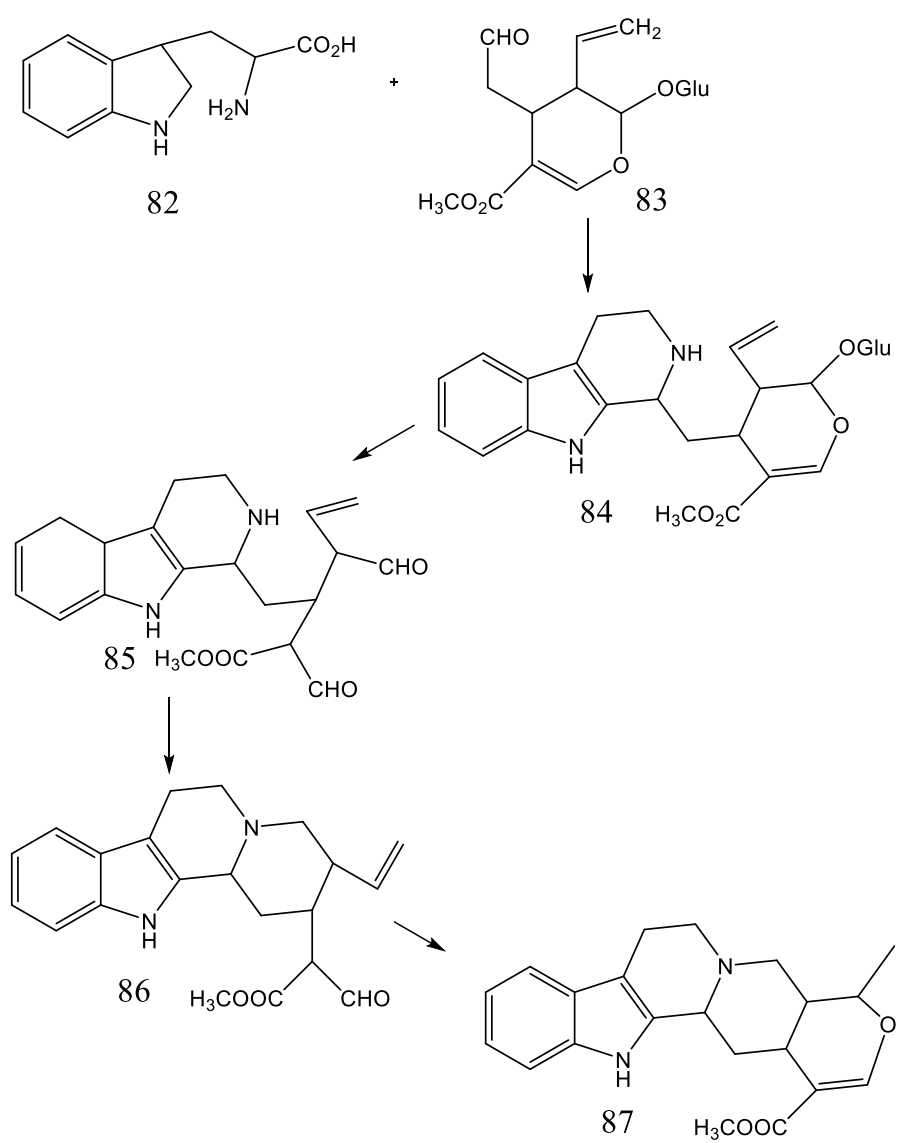
Type of indole alkaloid	Skeleton	Example
 <p>Plumeran or P-type</p>	 <p>Class II</p>	 <p>kopsine 79</p>
 <p>Ibogan or J-type</p>	 <p>Class III</p>	 <p>catharantine 80</p>
 <p>Tacaman type</p>	 <p>Class III</p>	 <p>tacamine 81</p>

2.4.1.1 Biosynthesis of Indole Alkaloids:

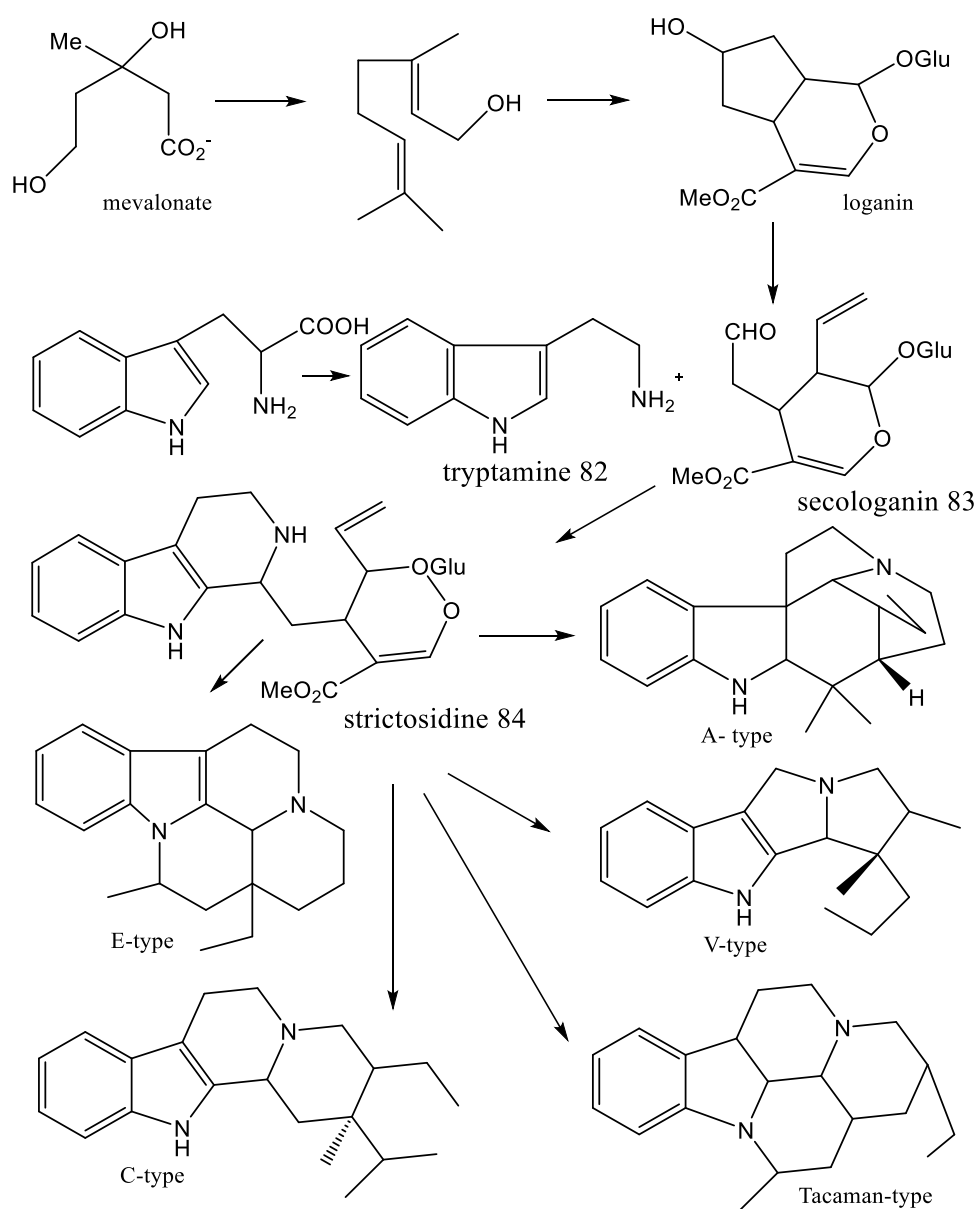
Biosynthesis refers to the manner in which organic substances are synthesized, altered or degraded by organism (plant or animal). The complexity of indole alkaloid structure are formally derived from a Mannich condensation of tryptamine (**82**) as the indole nucleus and a C9 or C10 monoterpene moiety, derived from secologanin (**83**). Secologanin is made up of two molecules of mevalonic acid (El-Sayed & Verpoorte, 2007).

Condensation of secologanin (**83**) with tryptamine (**82**) leads to strictosidine (**84**), a vincosan skeleton alkaloid. Hydrolysis of the sugar residue and the opening of the cyclic acetal function give the dialdehyde (**85**). Ring closure of (**85**) yields the tetracyclic system (**86**). Minor rearrangements generate ajmalicine (**87**), a corynanthian type of alkaloid (type C). These transformations are described in scheme 2.2.

Strictosidine (**84**) (Stockigt & Zenk, 1977) is also the precursor of many other type of indole alkaloids; (type A), (type C), (type V), (type E) and Tacaman type. (Scheme 2.3)



Scheme 2.2: Condensation of Secologanin (**83**) with Tryptamine (**82**)

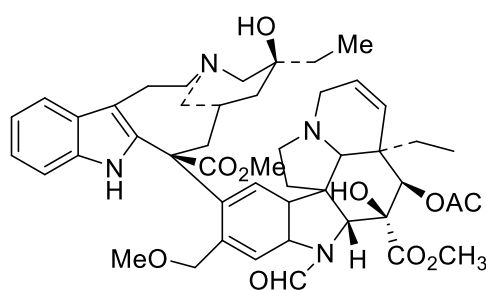


Scheme 2.3: Steps in the Biosynthesis of Indole Alkaloids

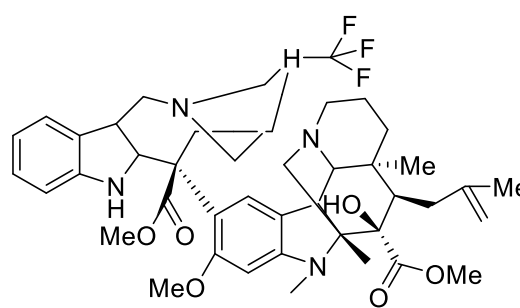
2.4.1.2 Pharmacological Activity of Indole Alkaloids

Before their recognition as useful therapeutic agents, alkaloids were renowned for their poisonous properties. Only a few of bioactive indole alkaloids were used today as therapeutic agents, in human for example vincristine (**88**) was used to treat acute leukemia

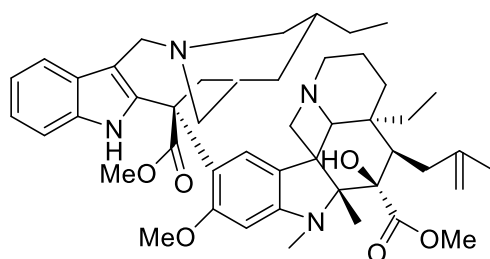
(Slater *et al.*, 1986). The dimeric alkaloids from *Catharanthus roseus* form an important class of antitumour agents, widely used in combination chemotherapy regimens for treating leukamias and many solid tumours. Vinflunine (**89**) which is a novel *vinca* alkaloid synthesized from vinorelbine (**90**) using superacidic chemistry and characterised by superior *in vivo* activity to vinorelbine in preclinical tumour models (Krunczynski & Jean, 1998), (Philipson & Zenk, 1980).



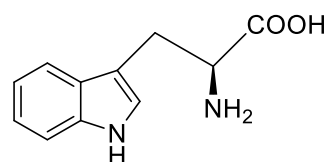
88



89



90



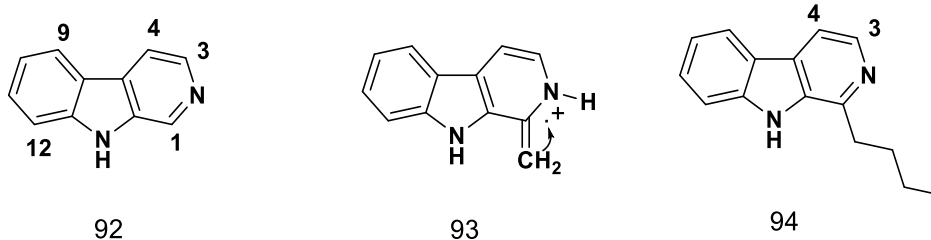
91

2.4.2 The β -Carboline Alkaloids

The β -Carboline Alkaloids are a large group of natural and synthetic indole alkaloids with different degrees of aromaticity. The Harmala alkaloids are derivatives of β -carboline (**92**), sometimes also known as norharman. The pyridine nitrogen atom is basic, while the indole nitrogen atom is virtually non-basic. β -carboline (**92**) and its homologues showed a

brilliant bluish- violet fluorescence in dilute solution (Swan, 1967) and a characteristic absorption in the ultraviolet due to its highly conjugated system.

The mass spectrum of β - carboline alkaloids always show a peak at m/z 182 typical (**93**) and in addition a peak at m/z 168 is also characteristic of β - carboline (**92**) structure (Biemann, 1962).



The NMR spectrum of 1- butyl- β - carboline (94) measured in $CDCl_3$ solution showed a broad one- proton peak at δ 7.58- 7.62 (indole NH), a four proton multiplet at δ 6.83- 7.58 assigned to the four aryl protons. A pair of AB doublets ($J= 5\text{Hz}$) appear at δ 8.30 and 7.75 due to the proton at position 3 and 4. The remainder of the spectrum showed an extended system of broad multiplets at δ 1.17- 2.17 may be assigned to three methylene groups (Morikawa *et al.*, 2004).

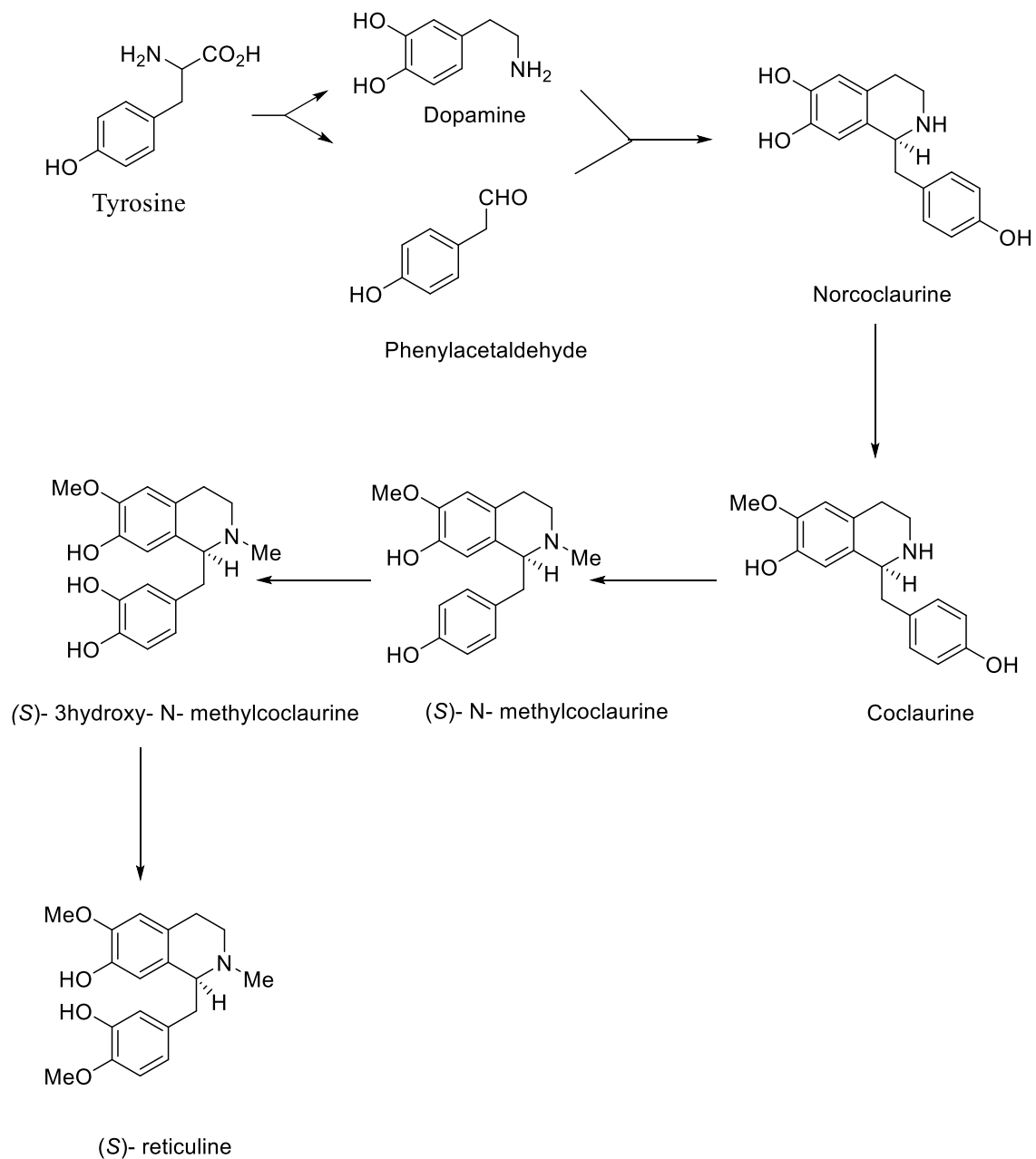
2.4.3 Isoquinoline Alkaloids

Isoquinolines are hetrocyclic aromatic compounds. Benzyltetrahydroisoquinolines are intermediate in the metabolism of isoquinoline alkaloids. They are formed by a Manich-type condensation between two metabolites of phenylalanine. The experiments with labeled precursors and cell culture showed that the true precursors are dopamine on one hand and 4- hydroxyphenylacetaldehyde on the other hand. The condensation of these two molecules

leads to (*S*) - 6- demethylcoclaurine, which is subsequently methylated (on the 6- position of the phenol and on the nitrogen atom) before being hydroxylated at C-12 and finally methylated to (*S*) – reticuline (Bruneton, 1995) (Scheme 2.4). Isoquinoline can be divided into several classes base on the skeletal of the structure. Shamma & Moniot, 1987 divided isoquinoline into 34 categories. (Table 2.6)

Table 2.6: Classification of isoquinolines base on skeletal of the structure

1. Simple isoquinolines	18. Dibenzazonines
2. Benzyloisoquinolines	19. Protoberberines and retroprotoberberines
3. Isoquinolones	20. Secoberberines
4. Pavines and isopavines	21. Benzophenantridhines
5. Bisbenzyloisoquinolines	22. Aryloisoquinolines
6. Baluchistanamines	23. Protopines
7. Cularines	24. Phthlideisoquinolines
8. Dibenzopyrrocolines	25. Spirobenzyloisoquinolines
9. Proaporphines	26. Rhoeadines
10. Aporphines	27. Emetine
11. Pakistanamine (proaporphine-benzyloisoquinoline dimmers)	28. Phenethylisoquinolines
12. Aporphine-benzyloisoquinoline dimmers	29. Homoaporphines and homoproaporphines
13. Aporphine- pavine dimmers	30. 1- Phenylisoquinolines
14. Oxoaporphines	31. <i>N</i> - benzyltetrahydroisoquinolines
15. Phenantrenes	32. Cheryllines (a 4-aryloisoquinolines)
16. 4,5- dioxoaporphines	33. Azafluoranthenes and tropoloisoquinolines
17. Aristolochic acid and aristolactams	34. Eupolauridine (a 1,6-diazafluoranthenes)

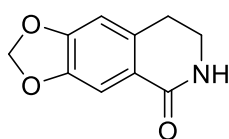


Scheme 2.4: Biosynthetic Origin of the Benzyltetrahydroisoquinoline

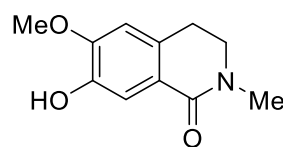
2.4.3.1 Simple Isoquinoline

The simple isoquinolines are the simplest of isoquinoline type and usually bicyclic. These alkaloids are divided from tetrahydroisoquinoline and they may be found in the fully aromatic form or in partially reduced form (Krane & Shamma, 1982). The nitrogen function in the ring B is often substituted with methyl or hydrogen. The carbon C-6 and C-7 usually have methoxyl or hydroxyl groups.

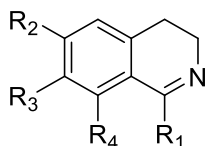
Simple isoquinoline alkaloids have been reported in *Cactaceae*, as well as the family of *Leguminosae* and *Papaveraceae* (Cordell, 1981). Aly *et al.*, 1989 isolated two isoquinolines, noroxyhydrastine (**95**) and thalifoline (**96**) from *Thalictrum minus*. *Beckbergia militaris*, contains a number of alkaloids, including fully aromatic oxygenated isoquinolines. Examples of the simple isoquinoline are dehydroheliamine (**97**), dehydrolemaireocereine (**98**), backerbergine (**99**), and isobackerbergine (**100**) (Ferrigni *et al.*, 1984).



95

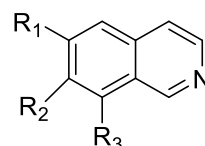


96



97 R₁, R₄ = H, R₂, R₃ = OMe

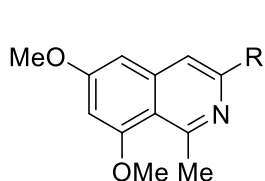
98 R₁, R₂ = H, R₃, R₄ = OMe



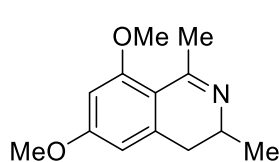
99 R₁, R₂ = OMe, R₃ = H

100 R₁ = H, R₂, R₃ = OMe

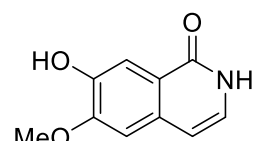
Montagnac *et al.*, 1995, reported a major simple isoquinoline alkaloids, namely 6,8-dimethoxy-3-hydroxymethyl-1-methylisoquinoline (**101**), 6,8-dimethoxy-1,3-methylisoquinoline (**102**) and 6,8-dimethoxy-1,3-dimethyl-3,4-dihydroisoquinoline (**103**) from the bark of *Ancistrocladus tectorius*. Three isoquinolines were isolated by Zhang *et al.*, 2004 from the roots of *Menispermum dauricum*, namely 7-hydroxy-6-methoxy-1-(2H)-isoquinoline, (**104**), 3,4-dioxo-6,7-dimethoxy-N-methyl-1-(2H)-isoquinoline (**105**) and 6-hydroxy-5-methoxy-N-methylphthalimide (**106**). Ten flavonols, one simple isoquinoline, 6,7-methylenedioxy-1-(2H)-isoquinoline (**107**), and one isoquinoline type were isolated from *Corydalis bungeana* (Xie *et al.*, 2004).



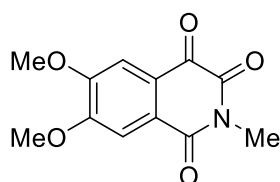
101 R = CH₂OH
102 R = Me



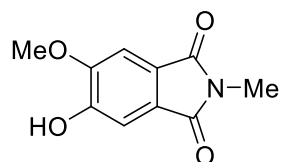
103



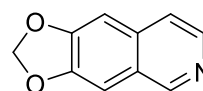
104



105



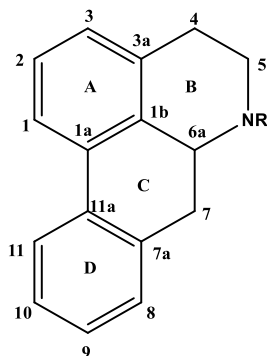
106



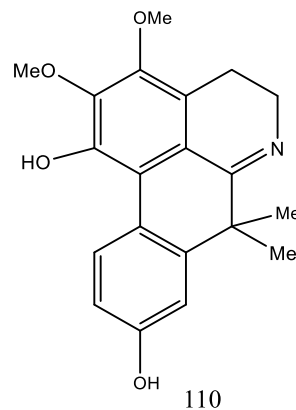
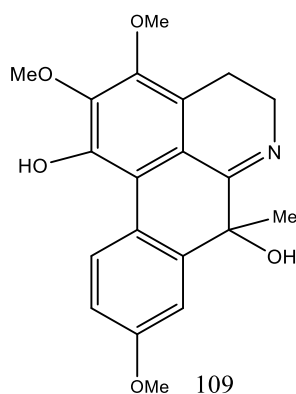
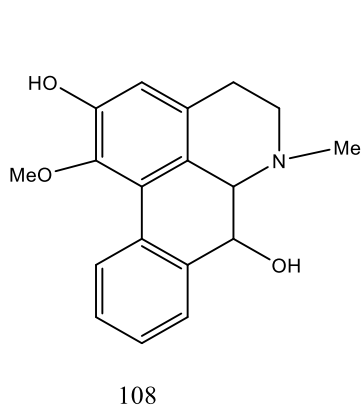
107

2.4.3.2 Aporphines

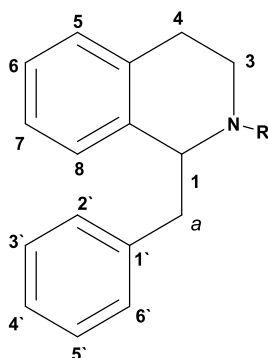
The aporphines alkaloids contain a twisted biphenyl system. Aporphine is the largest group of isoquinoline alkaloids and represented by the general structure below. The plants families that contain aporphine alkaloid type are Anonaceae, Lauraceae, Berberidaceae, Menispermaceae, Ranunculaceae, Monimiaceae, Pavaperaceae and Rhamnaceae (Guinaudeau *et al.*, 1979), (Guinaudeau *et al.*, 1983), (Guinaudeau *et al.*, 1988),



The most diverse structural feature of the aporphine was the oxygenation pattern. Position C-1 and C-2 were sometimes oxygenated, either by hydroxyl, methylenedioxy or methoxy groups. In few cases a hydroxyl or methyl function group is located at C-7. Some examples of compounds which have these special structures are pachyconfine (**108**) (Perez & Cassels, 2010), guattouregine (**109**) (Cave, 1989) and melosmine (**110**) (Zabel *et al.*, 1982).

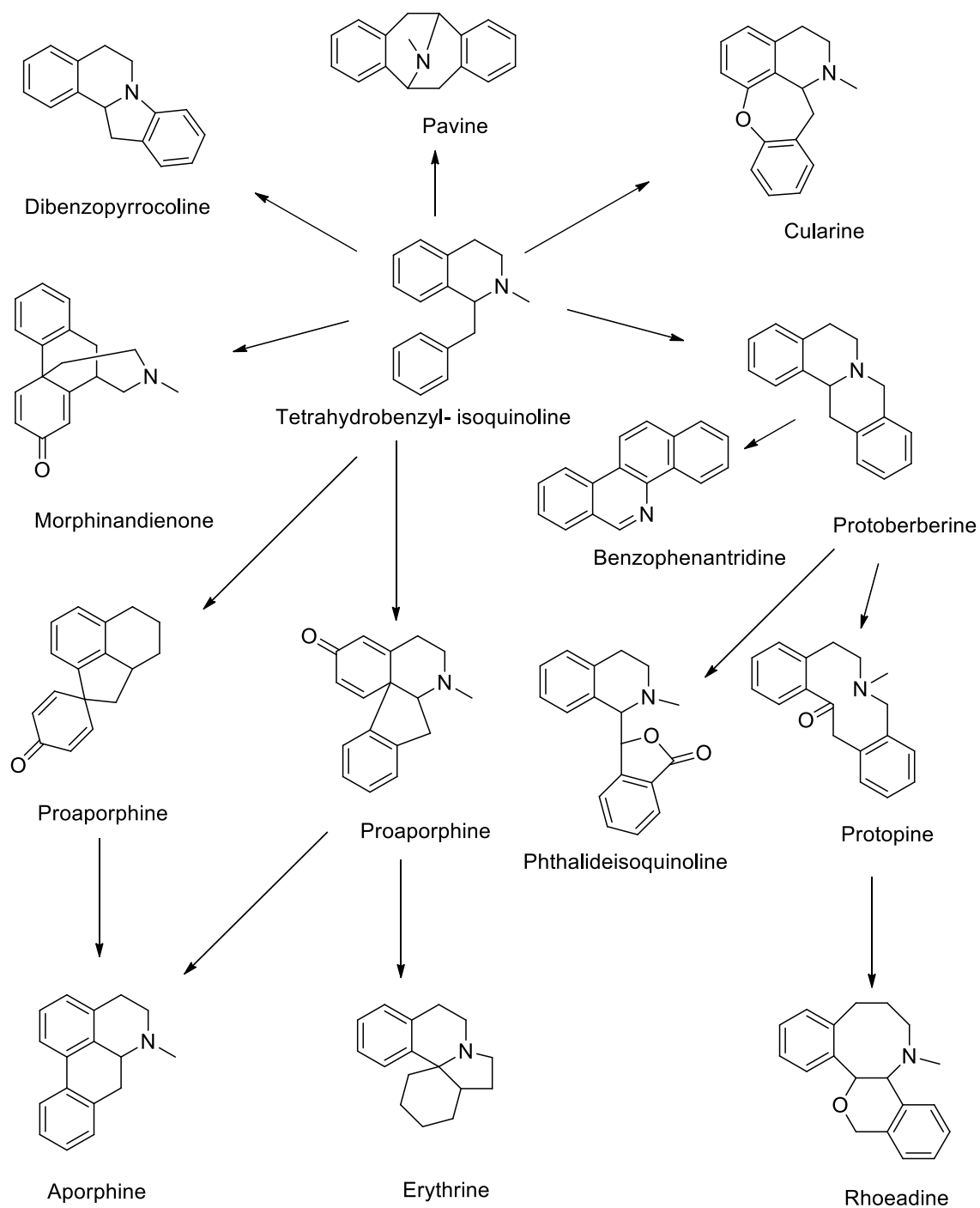


2.4.3.3 Benzyloisoquinolines



The benzyloisoquinoline type of alkaloid is derived from phenylalanine or tyrosine. There are two types of benzyloisoquinoline; 1,2,3,4- tetrahydro isoquinoline such as reticuline (**21**) and a fully aromatic type such as papaverine (**63**).

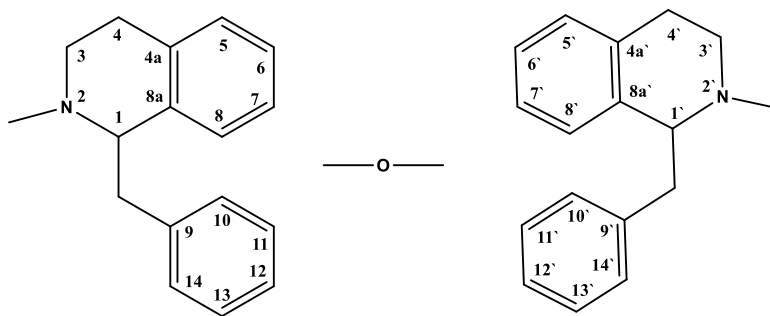
Benzyloisoquinoline alkaloids are widely distributed in the family Anonaceae (Chen *et al.*, 2001), (Zawawi *et al.*, 2012), Lauraceae (Lee *et al.*, 1993), (Lamberton & Vashist, 2011), Menispermaceae (de Lira *et al.*, 2002), (Rasoanaivo *et al.*, 1995), Papaveraceae (Lim, 2013), (Benn & Mitchell, 1972), Fumariaceae (Suau *et al.* 1994), (Hussain *et al.*, 1981), Ranunculaceae (Wu *et al.*, 1980), and Berberidaceae (Suau *et al.*, 1998), (Valencia *et al.*, 1984), some biogenetic relationship of these alkaloids is shown in Scheme 2.5.



Scheme 2.5: Biogenetic Relationship of the Major Alkaloids Groups Derived from Tetrahydroisoquinoline Precursor

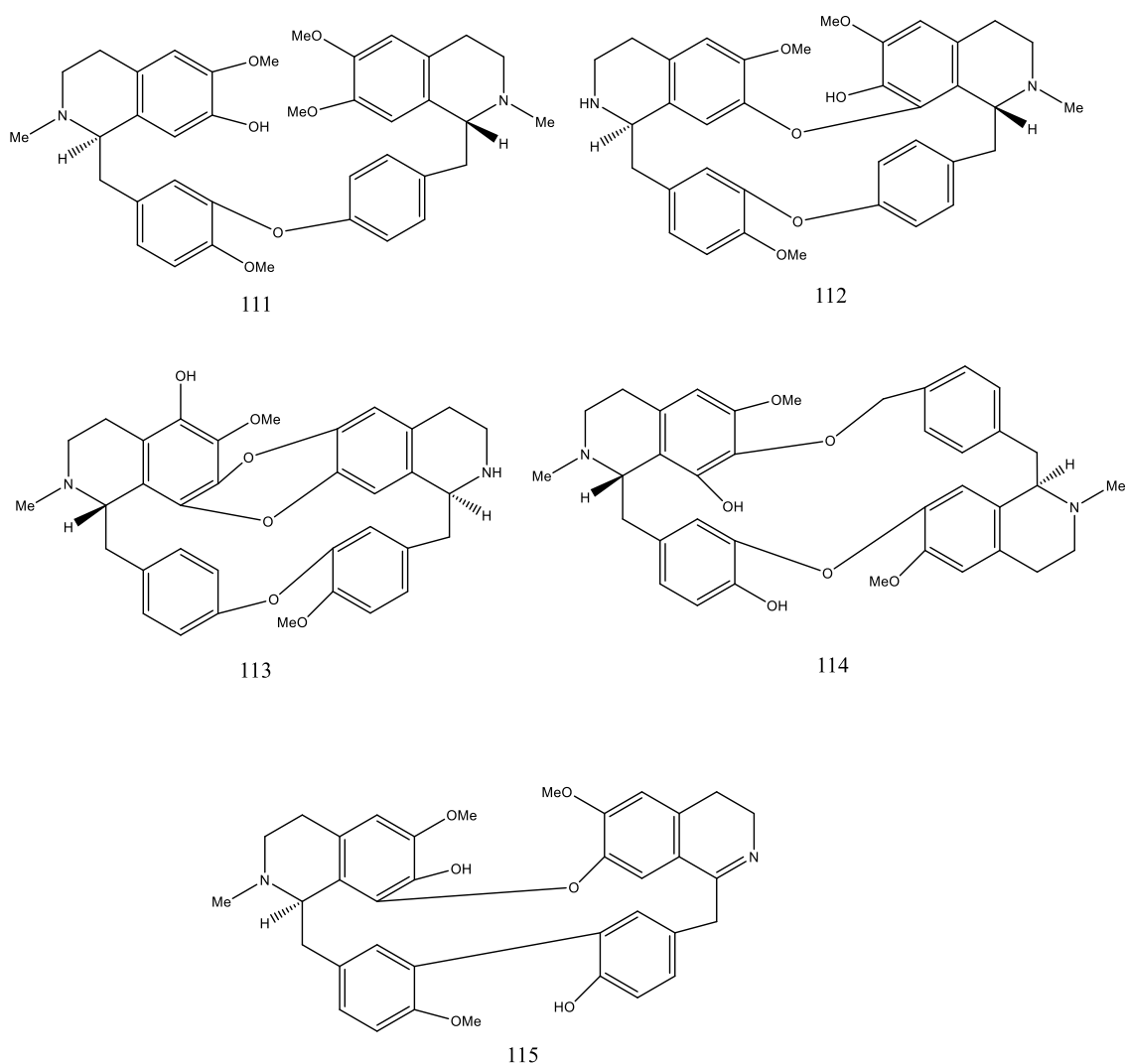
2.4.3.4 Bisbenzylisoquinolines

The BBIQ alkaloid consists of two benzylisoquinoline units attached to each other by one, two or three bonds. In the most structures, the units were joined via ether linkages.



Bisbenzylisoquinolines can be found primarily in Berberidaceae, Menispermaceae, Monimiaceae, Ranunculaceae and Lauraceae (Angerhofer *et al.*, 1999). These alkaloids were reported to have many pharmacological activities. Bisbenzylisoquinolines were classified into five major groups (Guha *et al.*, 1979);

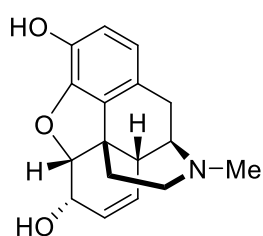
- One diphenyl ether linkage, for example 7-O-methylcuspidaline (**111**), (El-Sebakhy & Waterman, 1984), the ether linkage between C-11 and C-12`.
- Two diphenyl ether linkage, for example 2- norlimacusine (**112**), (Nafiah *et al.*, 2010), the ether linkage between the aromatic rings of tetrahydroisoquinoline component and the benzyl rings.
- Three diphenyl ether linkage, for example kohatamine (**113**), (Barbosa *et al.* 2000).
- One diphenyl ether and one benzyl phenyl ether, for example cissampentin (**114**) (Galiniš *et al.*, 1993).
- One or two diphenyl ether linkage and benzyl linkage, for example cordobimine (**115**), (Frappier *et al.*, 1996).



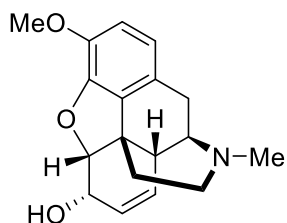
2.4.3.5 Pharmacological Activity of Isoquinoline Alkaloids.

The isoquinoline alkaloids are a large class of medicinally active alkaloids whose properties are variable. Their properties include being antispasmodic, antimicrobial, antitumour, antifungal, anti-inflammatory, cholagogue, hepatoprotective, antiviral, amoebicidal, and anti-oxidant and can act as enzyme inhibitors (Mukherjee *et al.*, 2007). This class notably includes, morphine (a narcotic pain reliever used to treat moderate to severe pain), (**116**), codeine (an opioid pain medicine used to treat mild to moderate pain), (**117**), thebaine (has no direct medical use, it serves as the raw material in industry for

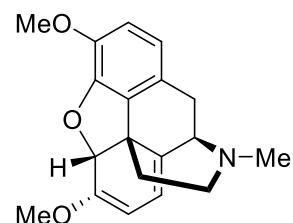
increasing the production of codeine) (**118**), and papaverine (used to increase blood flow throughout the body, including the heart and the brain) (**119**). They are typically found in the Papaveraceae, Berberidaceae and Ranunculaceae families. They are derived from the amino acids phenylalanine or tyrosine formed from a precursor of 3, 4- dihydroxytyramine (dopamine) linked to an aldehyde or ketone (Suau *et al.*, 1998).



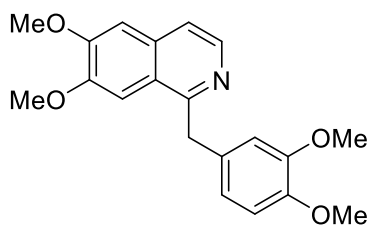
116



117



118



119

CHAPTER 3

METHODOLOGY

EXPERIMENTAL

3.1 General Experimental

Spectra were recorded on the following instruments as follows:

Ultra Violet Spectra (UV)

Ultra violet spectra were obtained in methanol on a Shimadzu UV-250 uv-visible spectrophotometer and the wavelength which the spectrum was recorded is 190-500nm.

Infrared Spectra (IR)

The infrared spectra were recorded on a Perkin Elmer FTIR (model 1600) spectrophotometer. Solvent used for dilution the sample is CHCl_3 .

Optical Rotation (OR)

The optical rotation was obtained on Jasco DIP-1000 Digital polarimeter with tungsten lamp at 25°C.

Mass Spectra (MS)

The mass spectra were measured on Absciex, triple tof 4600. The Automass Thermofinnigan was used for HR ESI^+ and ESI^- analysis.

NMR Spectra

NMR spectra were recorded in deuterated chloroform (CDCl_3), deuterated methanol (CD_3OH) and deuterated acetone ($\text{C}_3\text{D}_6\text{O}$) on a JEOL ECA 400MHz, Bruker 400 and 600MHz. Chemical shifts (δ) were expressed in ppm and the coupling constants are given in Hz.

Column Chromatography (CC), Thin Layer Chromatography (TLC) and High Performance Liquid Chromatography (HPLC)

Column chromatography was prepared by using Silica Gel 60F, 70-230 mesh ASTM (Merck 7734); Silica Gel 60F, 230-400 mesh ASTM (Merck 9385); Silica gel 40-63 μ m (Silicycle R12030B); Silica gel 60-200 μ m (Silicycle R10040B); Silica Gel 60GF₂₅₄, (Merck 1.07730.1000) and sephadex (LH-20). Analytical Thin Layer Chromatography (TLC) was performed on commercially aluminum supported silica gel 60F₂₅₄ TLC sheets (Merck 1.05554.0001); Glass supported silica gel 60F₂₅₄ TLC plates (Merck 1.05715.0001); Glass backed TLC Amino plates (Silicycle TLG-R52030B-203). Preparative HPLC was conducted using a Waters 2707 instrument with a PDA 2998 detector and a C-18 luna column (250 \times 21.2 mm, 5 μ m).

3.2 Reagents

Mayer's Reagent (Potassium mercuric iodide) was used for screening the alkaloid compounds. A positive result indicated when white precipitate was formed under acidic condition. The Mayer's Reagent was prepared as follows:

1.4 g mercuric iodide was dissolved in 60 ml distilled water were mixed with a solution of 5.0 g of potassium iodide in 10 ml of distilled water.

Dragendorff's Reagent (Potassium bismuth iodide) was also used to identify the presence of alkaloids spotting on TLC. A positive result is indicated by the formation of orange spots on the developed TLC. The Dragendorff's Reagent was made as follows:

Solution A: Bismuth (III) nitrate (1.7 g) was dissolved in a mixture of 20 ml glacial acetic acid and 80 ml of distilled water.

Solution B: Potassium iodide (16 g) was dissolved in 40 ml of distilled water.

Solution A and B were mixed together to give stock solution. Finally, the spray reagent was prepared by diluting stock solution (40 ml) with 40 ml glacial acetic acid in 120 ml distilled water.

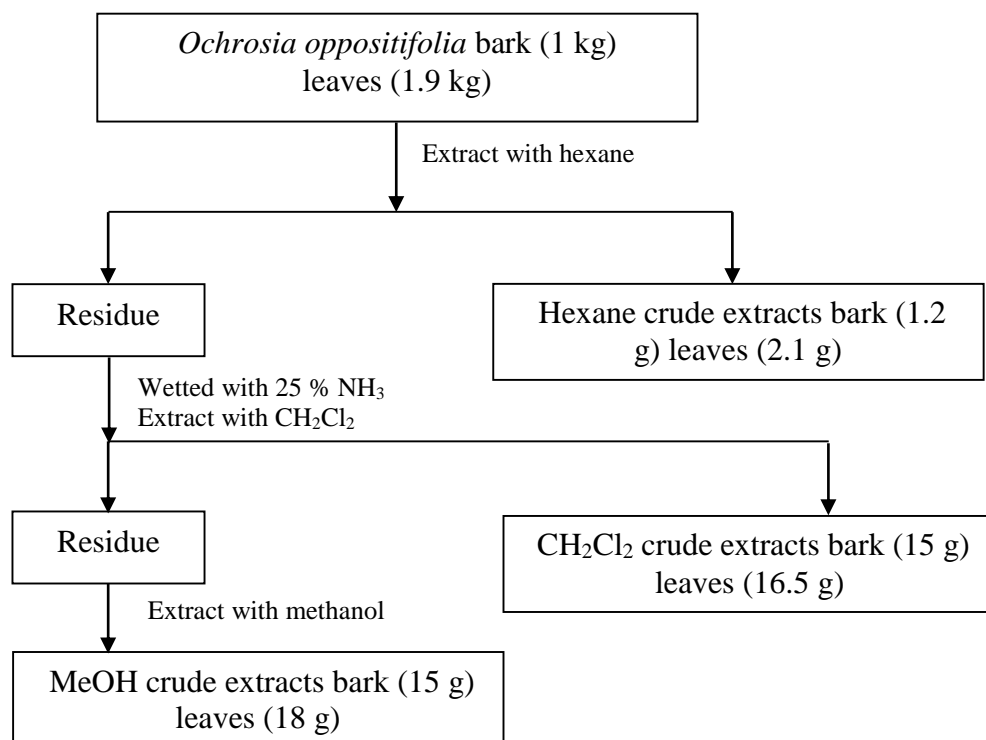
3.3 Plants Material

Ochrosia oppositifolia and *Rauvolfia reflexa* were collected from Pangkor island in 2007 and Kelantan in 2009 respectively. *Actinodaphne macrophylla* was collected from Johor in 2000. The samples were identified by Mr L.E.Teo , University of Malaya and deposited at the herbarium unit (specimen no; KL 5349, KL 4900, and KL 4940 respectively).

3.4 Purification

3.4.1 Extraction of *Ochrosia oppositifolia* (Bark and Leaves)

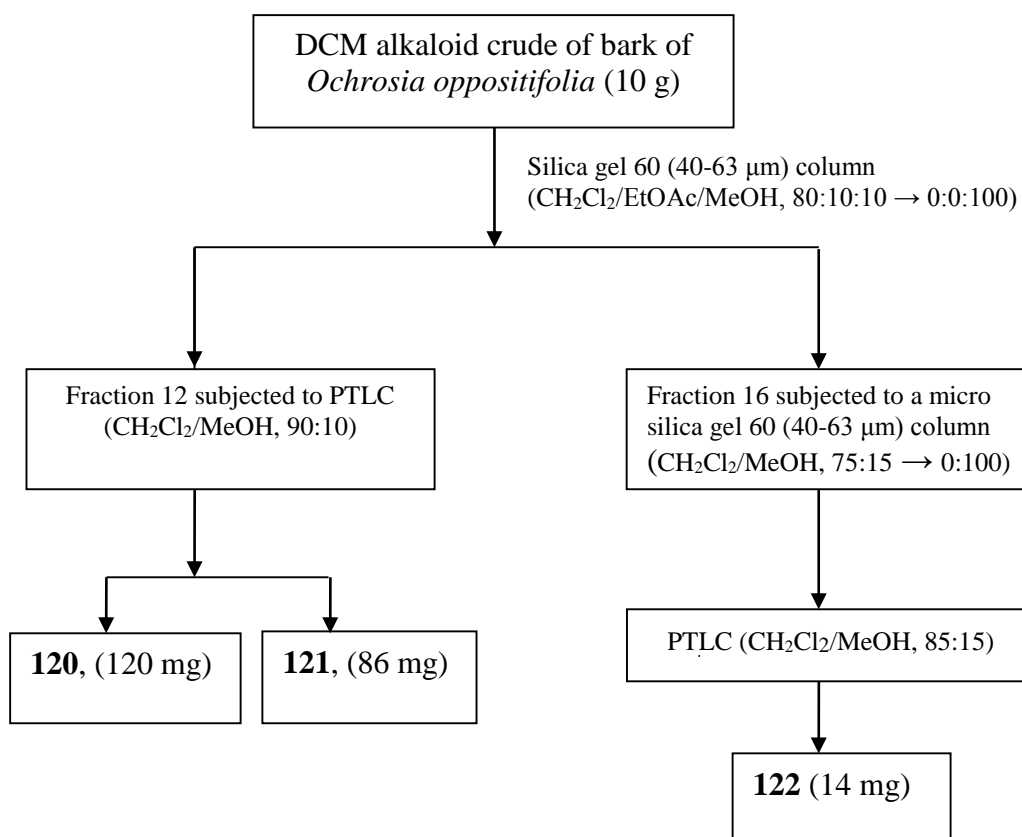
The dried bark (1kg) and leaves (1.9 kg) were extracted exhaustively with hexane for 48 hours to removed non-polar organic compound, waxes and fats. The plant materials were dried and wetted with 25 % ammonia solution and left for overnight. They were then re-extracted successively with dichloromethane and methanol. After removal of the solvents, the hexane crude extracts of bark (1.2 g), leaves (2.1 g), dichloromethane crude extracts of bark (15 g), leaves (16.5 g) and methanol crude extracts of bark (15 g) and leaves (18 g) were obtained. The extraction procedure was shown in Scheme 3.1.



Scheme 3.1: Extraction of *Ochrosia oppositifolia* (Bark and Leaves)

3.4.2 Isolation of Alkaloids from *Ochrosia oppositifolia* (Bark)

The dichloromethane crude extract (10 g) was subjected to a silica gel 60 (40-63 μm) column chromatography ($\text{CH}_2\text{Cl}_2/\text{EtOAc}/\text{MeOH}$, 80:10:10 \rightarrow 0:0:100), 24 fractions were collected. Fraction 12 was subjected to a preparative silica gel TLC ($\text{CH}_2\text{Cl}_2/\text{MeOH}$, 90:10) to give isoreserpiline (**120**) (120 mg, 0.012 %) and neisosposinine (**121**) (86 mg, 0.0086 %). Fraction 16 was subjected to a micro silica gel 60 (40-63 μm) column chromatography ($\text{CH}_2\text{Cl}_2/\text{MeOH}$, 75:15 \rightarrow 0:100) followed by a preparative silica gel TLC ($\text{CH}_2\text{Cl}_2/\text{MeOH}$, 85:15) to give reserpine (**122**), (14 mg, 0.0014 %). The isolation and purification procedure were summarized in the flow diagram shown in scheme 3.2.

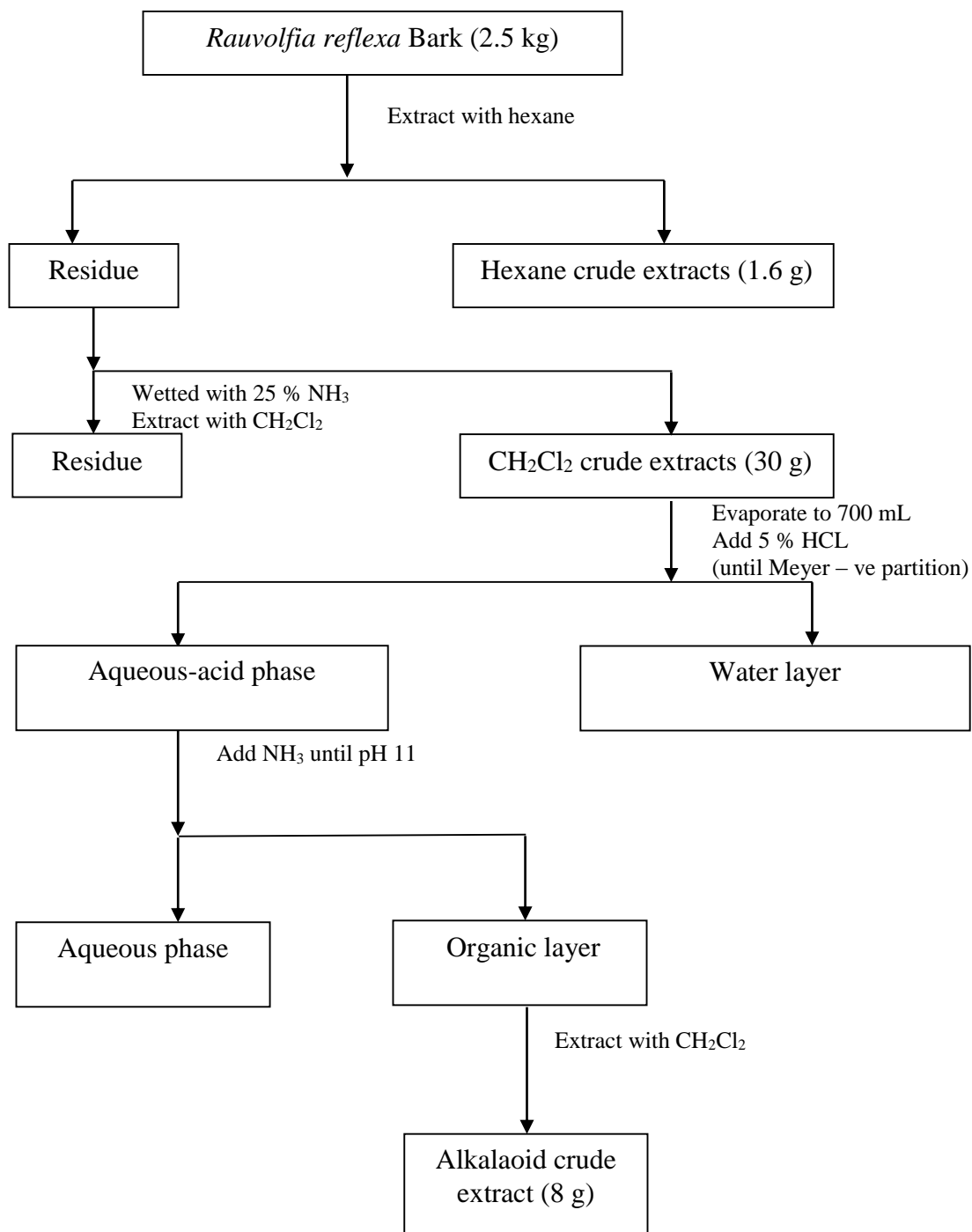


Scheme 3.2: Isolation and Purification of Alkaloids from *Ochrosia oppositifolia* (Bark)

3.4.3 Extraction of *Rauvolfia reflexa* (Bark)

The bark of *Rauvolfia reflexa* (2.5 kg) was first defatted in hexane for 48 hours. Then the extract was dried on the rotary evaporator. The plant material was dried and again wetted with 25 % ammonia solution and left for 2 hours. They were then re-extracted successively with dichloromethane (CH₂Cl₂). After removal of the solvents, the hexane crude extract (1.6 g) were collected. Dichloromethane crude extract was dissolved in CH₂Cl₂ and re-extracted with 5% hydrochloric acid (HCl) until a negative result was formed with Mayer's reagent. The combined extracts were then basified with 25% NH₃ solution (pH 11) and re-extracted with CH₂Cl₂ until a negative mayers test was obtained and later washed with distilled water and sodium chloride solution and dried with

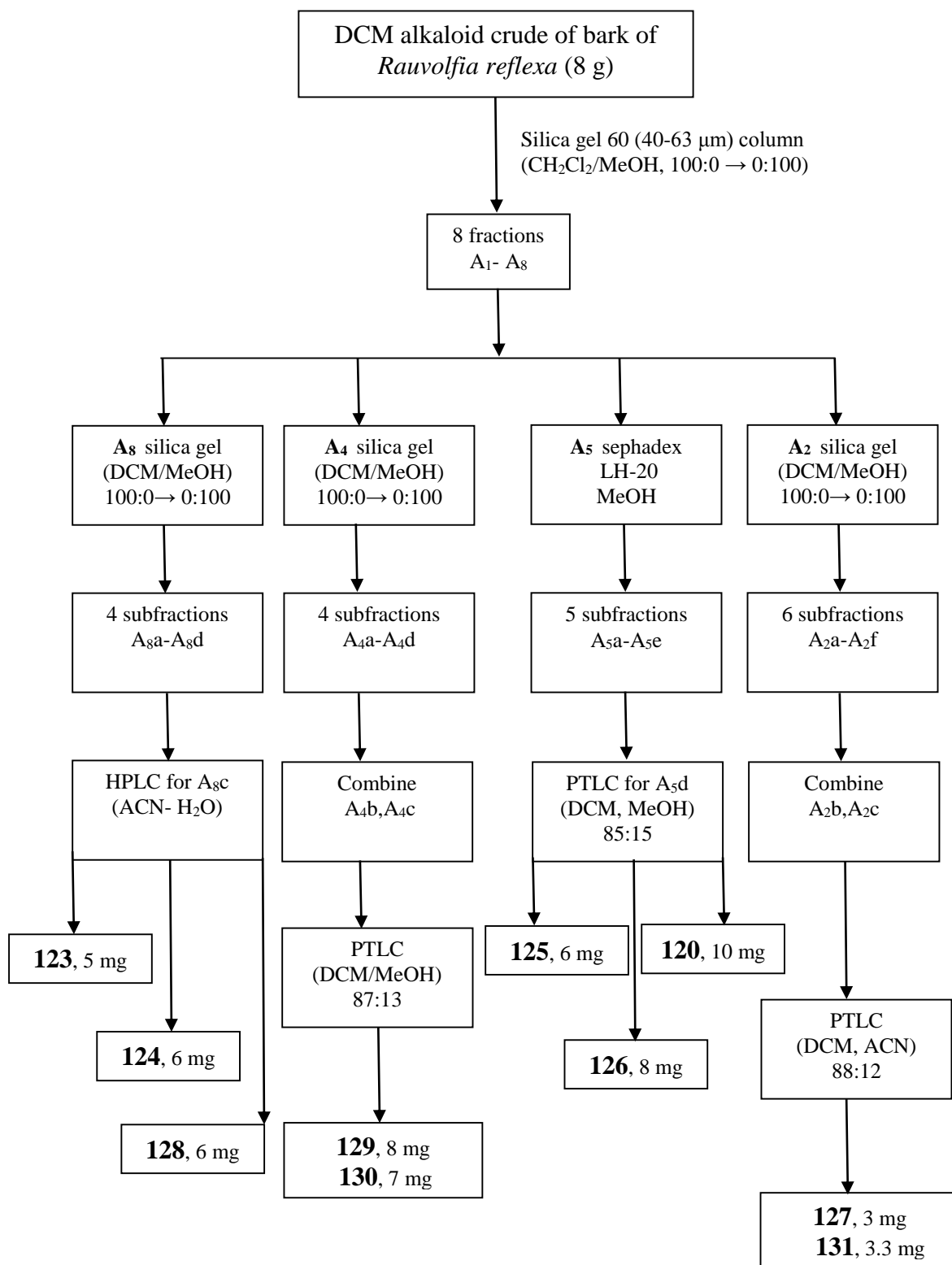
sodium sulfate anhydrous. Finally, the extract was evaporated to dryness to give an alkaloid crude extract (8 g). The extraction procedure is shown in scheme 3.3.



Scheme 3.3: Extraction of *Rauvolfia reflexa* (Bark)

3.4.4 Isolation of alkaloids from *Rauvolfia reflexa* (Bark)

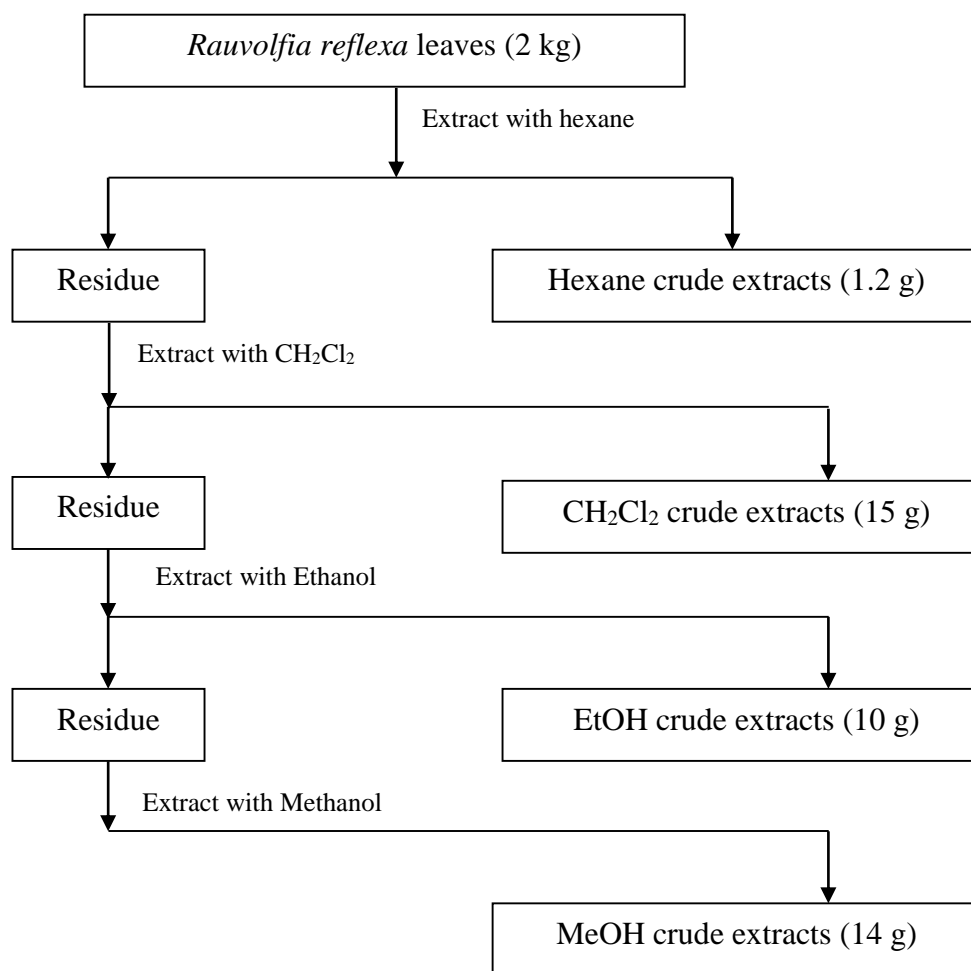
The dichloromethane alkaloid crude extract (8 g) was fractionated *via* silica gel CC eluting with dichloromethane- methanol ($\text{CH}_2\text{Cl}_2/\text{MeOH}$, 100:0 \rightarrow 0:100) to afford 8 fractions, A_1 - A_8 , on the basis of TLC analysis. Fraction A_8 (1.1 g) was chromatographed over silica gel 60 (40-63 μm) eluted with dichloromethane- methanol (100:0 \rightarrow 0:100) to give four subfractions, A_{8a} - A_{8d} . Separation of fraction A_{8c} (0.35 g) by preparative HPLC (50-100% $\text{ACN-H}_2\text{O}$, detection at 210 nm, 7 mL/min, C18 Column) successively, yielded rauvolfine B (**123**), (5 mg, 0.0002 %), rauvolfine C (**124**), (6 mg, 0.00024 %) and akuammilan-17-oic acid 1,2-dihydro-3-hydroxy-1-methyl- methyl ester (**128**), (6 mg, 0.00024 %). Fraction A_4 (1.2 g) was chromatographed over silica gel 60 (40-63 μm) eluted with dichloromethane- methanol (100:0 \rightarrow 0:100) to give five subfractions, A_{4a} - A_{4e} . Fraction A_{4b} and A_{4c} were combined (0.51 g) and purified by a PTLC ($\text{CH}_2\text{Cl}_2/\text{MeOH}$, 87:13) to yield macusine B (**130**), (8 mg, 0.00032 %) and undulifoline (**129**), (7 mg, 0.00028 %). Fraction A_5 (1.3 g) was chromatographed over a LH-20 sephadex by using methanol as mobile phase to give five subfractions, A_{5a} - A_{5e} . Fraction A_{5d} was subjected to a PTLC ($\text{CH}_2\text{Cl}_2/\text{MeOH}$, 85:15) to yield vinorine (**125**), (6 mg, 0.00024 %), isoreserpiline (**120**), (10 mg, 0.0004 %) and rescinnamine (**126**), (8 mg, 0.00032 %). Fraction A_2 (1.2 g) was applied on a silica gel 60 (40-63 μm) column with the mobile phase dichloromethane- methanol (100:0 \rightarrow 0:100) to give six subfractions, A_{2a} - A_{2c} . A_{2b} and A_{2c} were combined and purified by a PTLC ($\text{CH}_2\text{Cl}_2/\text{ACN}$, 88:12) to yield cantleyine (**127**), (3 mg, 0.00012 %) and akuammilan-17-oic acid 12-hydroxy- methyl ester (**131**), (3.3 mg, 0.000132 %). (Scheme 3.4).



Scheme 3.4: Isolation and Purification of Alkaloids from *Rauwolfia reflexa* (Bark)

3.4.5 Extraction of *Rauvolfia reflexa* (leaves)

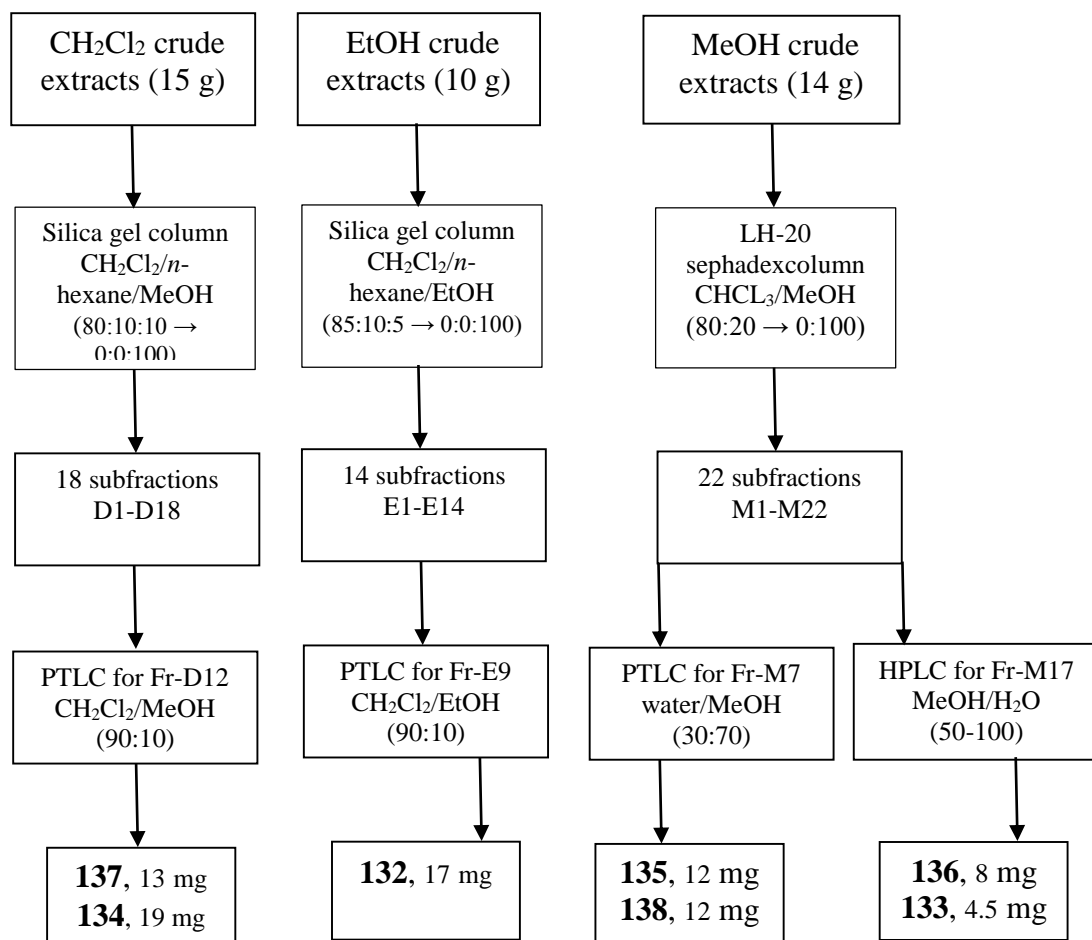
The dried leaves of *R. reflexa* (2 kg) were first defatted in *n*-hexane for 48 h. Then, the extract was filtered and dried on the rotary evaporator. The residue was sequentially re-extracted with dichloromethane CH_2Cl_2 , ethanol EtOH, and methanol MeOH and the resulting filtrates were dried under reduced pressure by a rotary evaporator at 40 °C to yield CH_2Cl_2 (15 g), EtOH (10 g) and MeOH (14 g) extracts, respectively. The extraction procedure is shown in scheme 3.5.



Scheme 3.5: Extraction of *Rauvolfia reflexa* (Leaves)

3.4.6 Isolation of Constituents from *Rauvolfia reflexa* (leaves)

Dichloromethane extract (12 g) was chromatographed on a silica gel 60 column (40–63 μm particle size) and eluted sequentially with $\text{CH}_2\text{Cl}_2/n\text{-hexane/MeOH}$ mixtures (80:10:10 \rightarrow 0:0:100). Eluates were collected and those displaying similar R_f values on TLC were pooled to yield 18 fractions. Fraction 12 was subjected to a preparative silica gel TLC with a solvent system of $\text{CH}_2\text{Cl}_2/\text{MeOH}$ (90:10) to yield (*E*)-3-(3,4,5-trimethoxyphenyl) acrylic acid (**137**), (13 mg, 0.00065%) and (*E*)-methyl 3-(4-hydroxy-3,5-dimethoxyphenyl) acrylate (**134**), (19 mg, 0.00095%). Ethanolic extract (10 g) was chromatographed on a silica gel 60 column (40–63 μm particle size) and was eluted sequentially with $\text{CH}_2\text{Cl}_2/n\text{-hexane/EtOH}$ mixtures (85:10:5 \rightarrow 0:0:100). Eluates were collected and those displaying similar R_f values on TLC were pooled to yield 14 fractions. Fraction 9 was subjected to a preparative silica gel TLC with a solvent system of $\text{CH}_2\text{Cl}_2/\text{EtOH}$ (90:10) to yield 17-Methoxycarbonyl-14-heptadecaenyl-4-hydroxy-3-methoxy cinnamate (**132**), (17 mg, 0.00085%). MeOH (14 g) extract was chromatographed on a LH-20 Sephadex column and was eluted sequentially with $\text{CHCl}_3/\text{MeOH}$ mixtures (80:20 \rightarrow 0:100). Eluates were collected and those displaying similar R_f values on TLC were pooled to yield 22 fractions. Fraction 7 was further subjected to a preparative TLC on a reversed-phase silica gel with a solvent system of water/MeOH (30:70) to yield 1,2,3,4- tetrahydro -1- oxo- β - carboline (**135**), (12 mg, 0.0006 %) and benzenepropanoic acid, 3- methoxy (**138**), (12 mg, 0.0006 %). Fraction 17 was further purified by a preparative HPLC (50-100% MeOH- H_2O , detection at 248 and 283 nm, 7 mL/min, C18 Column) successively, yielded 3- hydroxy- β - carboline (**136**), (8 mg, 0.0004 %) and 3- methyl-10,11-dimethoxyl-6- methoxycarbonyl- β - carboline (**133**), (4.5 mg, 0.00022 %). (Scheme 3.6).



Scheme 3.6: Isolation and Purification of Constituents from *Rauvolfia reflexa* (Leaves)

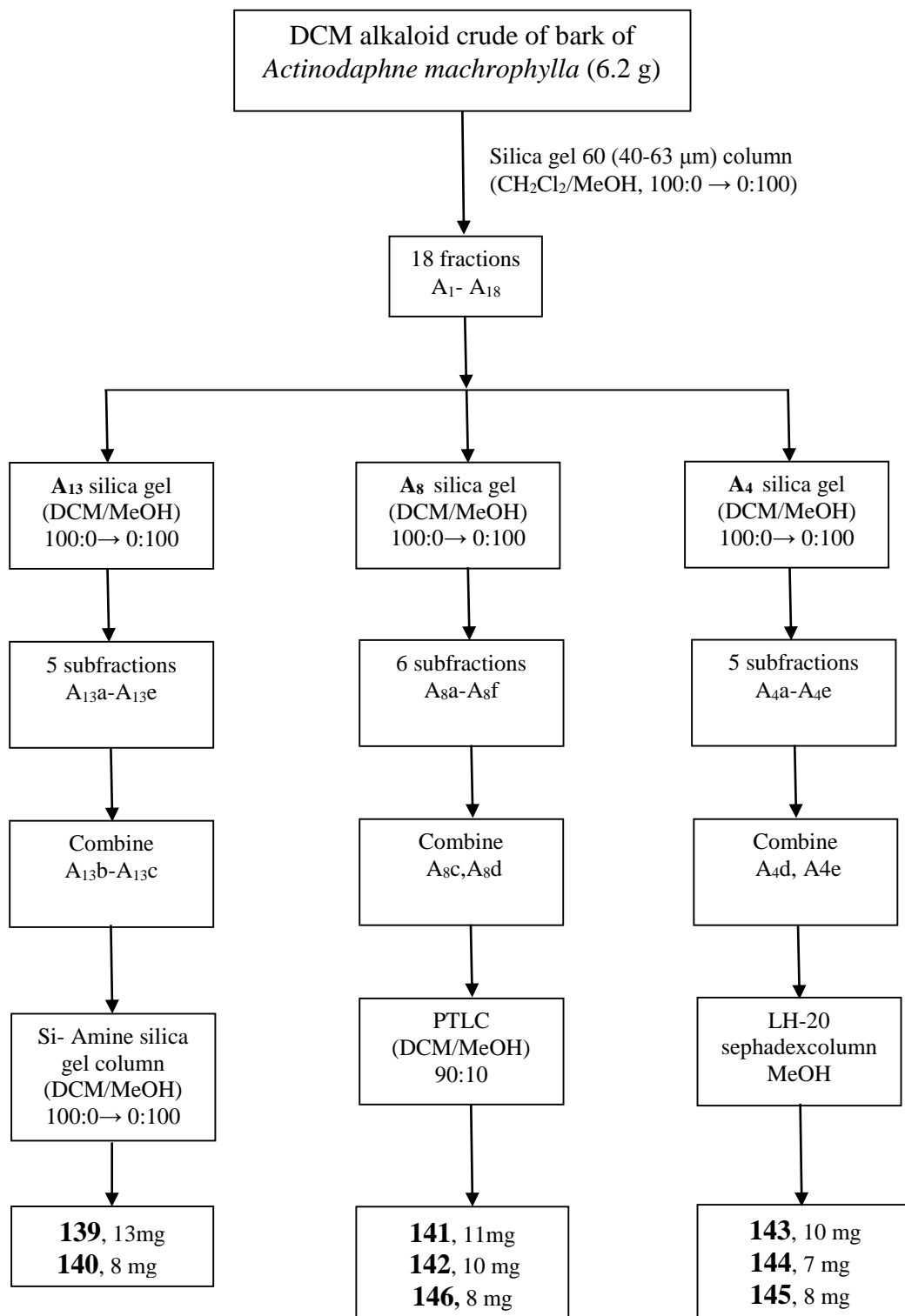
3.4.7 Extraction of *Actinodaphne macrophylla* (Bark)

The bark of *Actinodaphne macrophylla* (2.7 kg) was first defatted in hexane for 48 hours. Then the extract was dried on the rotary evaporator to give hexane crude extract (1.7 g). The plant material was dried and wetted with 25 % ammonia solution and left for 2 hours. They were then re-extracted successively with dichloromethane (CH_2Cl_2). The concentrated dichloromethane crude extract was dissolved in CH_2Cl_2 and re-extracted with 5% hydrochloric acid (HCl) until a negative result was formed with Mayer's reagent. The combined extracts were then basified with 25% NH_3 solution (pH 11) and re-extracted with CH_2Cl_2 until a negative Mayer's test was obtained and later

washed with distilled water and sodium chloride solution and dried with sodium sulfate anhydrous. Finally, the extract was evaporated to dryness to give an alkaloid crude extract (6.2 g). The extraction procedure was similar to *Rauvolfia reflexa* (bark) shown in Scheme 3.3.

3.4.8 Isolation of Alkaloids from *Actinodaphne macrophylla* (Bark).

The dichloromethane alkaloid crude extract of the bark (6.2 g) was fractionated by a silica gel 60 column (40–63 μm particle size). The mobile phase was ($\text{CH}_2\text{Cl}_2/\text{MeOH}$, 100:0 \rightarrow 0:100). Eighteen fractions were collected and have been used for further purification base on their alkaloids percentage on the aluminum TLC. Fraction A_{13} was subjected to a silica gel column (DCM/MeOH) 100:0 \rightarrow 0:100), from the five sub fractions (A_{13a} - A_{13e}) fractions A_{13b} and A_{13c} were combined and chromatographed on a Si- Amine silica gel column (DCM/MeOH , 100:0 \rightarrow 0:100) to give cycleanine (**139**), (13 mg, 0.00048 %) and 10- demethylxylopinine (**140**), (8 mg, 0.00029 %). Fraction A_8 was further purified by a silica gel column ($\text{CH}_2\text{Cl}_2/\text{MeOH}$, 100:0 \rightarrow 0:100), six sub fractions were collected (A_{8a} - A_{8f}). fractions A_{8c} and A_{8d} were combined and applied on a preparative TLC ($\text{CH}_2\text{Cl}_2/\text{MeOH}$, 90:10) to give reticuline (**141**), (11 mg, 0.0004 %) and laurotetanine (**142**), (10 mg, 0.000037 %) and anolobine (**146**), (8 mg, 0.00029 %). Fraction A_4 was chromatographed via silica gel column eluting with dichloromethane- methanol ($\text{CH}_2\text{Cl}_2/\text{MeOH}$, 100:0 \rightarrow 0:100). Among the five (A_{4a} - A_{4e}) two fractions were combined (A_{4d} and A_{4e}) and subjected to a LH-20 sephadex column by using MeOH as mobile phase to give bicuculine (**143**), (10 mg, 0.000037 %), α - hydrastine (**144**), (7 mg, 0.00025 %) and parafumine (**145**), (8 mg, 0.00029 %). (Scheme 3.7).



Scheme 3.7: Isolation and Purification of Alkaloids from *Actinodaphne macrophylla* (Bark).

3.5 Physical and Spectral Data of Isolated Constituents

3.5.1 *Ochrosia oppositifolia* Alkaloids:

Isoreserpiline (120) : pale brownish amorphous solid

Molecular formula : C₂₃H₂₈N₂O₅

UV λ_{max} (MeOH), nm : 226, 299

IR ν_{max} (CHCl₃), cm⁻¹ : 3370, 2928, 1692, 665

Mass spectrum, m/z : 413 (100)

¹H NMR (CDCl₃), ppm : See figure 4.1

¹³C NMR (CDCl₃), ppm : See figure 4.2

Neisosposinine (121) : pale brownish amorphous solid

Molecular formula : C₂₃H₂₈N₂O₆

UV λ_{max} (MeOH), nm : 246, 302

IR ν_{max} (CHCl₃), cm⁻¹ : 3583, 2359, 1704, 665

Mass spectrum, m/z : 429 (100)

¹H NMR (CDCl₃), ppm : See figure 4.4

¹³C NMR (CDCl₃), ppm : See figure 4.5

Reserpiline (122) : pale brownish amorphous solid

Molecular formula : C₂₂H₂₆N₂O₄

UV λ_{max} (MeOH), nm : 225, 300

IR ν_{max} (CHCl₃), cm⁻¹ : 3402, 2926, 1706, 665

Mass spectrum, m/z : 383 (100)

¹H NMR (CDCl₃), ppm : See figure 4.7

¹³C NMR (CDCl₃), ppm : See figure 4.8

3.5.2 *Rauvolfia reflexa* Compounds:

Rauvolfine B (123) : pale brownish amorphous solid

Molecular formula : C₂₃H₂₈N₂O₅

UV λ_{max} (MeOH), nm : 226,299

IR ν_{max} (CHCl₃), cm⁻¹ : 3435, 2928, 1730, 665

Mass spectrum, m/z : 413 (100)

¹H NMR (CDCl₃), ppm : See figure 4.10

¹³C NMR (CDCl₃), ppm : See figure 4.11

Rauvolfine C (124) : pale brownish amorphous solid

Molecular formula : C₂₁H₂₈N₂O

UV λ_{max} (MeOH), nm : 250,285

IR ν_{max} (CHCl₃), cm⁻¹ : 3378, 2944, 665

Mass spectrum, m/z : 325 (100)

¹H NMR (CDCl₃), ppm : See figure 4.16

¹³C NMR (CDCl₃), ppm : See figure 4.17

Vinorine (125) : pale brownish amorphous solid

Molecular formula : C₂₁H₂₂N₂O₂

UV λ_{max} (MeOH), nm : 226, 299

IR ν_{max} (CHCl₃), cm⁻¹ : 2926, 1742, 665

Mass spectrum, m/z : 335 (100)

¹H NMR (CDCl₃), ppm : See figure 4.21

¹³C NMR (CDCl₃), ppm : See figure 4.22

Rescinnamine (126) : pale brownish amorphous solid

Molecular formula : C₃₅H₄₂N₂O₆

UV λ_{max} (MeOH), nm : 215, 246, 302

IR ν_{max} (CHCl₃), cm⁻¹ : 3368, 2921, 1711, 665

Mass spectrum, m/z : 635 (100)

¹H NMR (CDCl₃), ppm : See figure 4.24

¹³C NMR (CDCl₃), ppm : See figure 4.25

Cantleyine (127) : pale brownish amorphous solid

Molecular formula : C₁₁H₁₃NO₃

UV λ_{max} (MeOH), nm : 222, 283

IR ν_{max} (CHCl₃), cm⁻¹ : 3402, 2976, 1706, 665

Mass spectrum, m/z : 208 (100)

¹H NMR (CDCl₃), ppm : See figure 4.27

¹³C NMR (CDCl₃), ppm : See figure 4.28

**Akuammilan-17-oic-acid
1,2- dihydro-3-hydroxy-1-
methyl ester (128)** : pale brownish amorphous solid

Molecular formula : C₂₁H₂₆N₂O₃

UV λ_{max} (MeOH), nm : 250, 285

IR ν_{max} (CHCl₃), cm⁻¹ : 1706, 3378

Mass spectrum, m/z : 355 (100)

¹H NMR (CDCl₃), ppm : See figure 4.30

¹³C NMR (CDCl₃), ppm : See figure 4.31

Undulifoline (129) : pale brownish amorphous solid

Molecular formula : C₂₀H₂₄N₂O₃

UV λ_{max} (MeOH), nm : 196, 273, 328

IR ν_{max} (CHCl₃), cm⁻¹ : 1704, 3401

Mass spectrum, m/z : 341 (100)

¹H NMR (CDCl₃), ppm : See figure 4.33

¹³C NMR (CDCl₃), ppm : See figure 4.34

Macusine B (130) : pale brownish amorphous solid

Molecular formula : C₂₀H₂₅N₂O

UV λ_{max} (MeOH), nm : 196, 273, 328

IR ν_{max} (CHCl₃), cm⁻¹ : 3431

Mass spectrum, m/z : 309 (100)

¹H NMR (CDCl₃), ppm : See figure 4.36

¹³C NMR (CDCl₃), ppm : See figure 4.37

**Akuammilan-17-oic,acid
12- hydroxyl, methyl
ester (131)** : pale brownish amorphous solid

Molecular formula : C₂₀H₂₂N₂O₃

UV λ_{max} (MeOH), nm : 250,285

IR ν_{max} (CHCl₃), cm⁻¹ : 3378, 2944, 1703, 665

Mass spectrum, m/z : 340 (100)

¹H NMR (CDCl₃), ppm : See figure 4.39

¹³C NMR (CDCl₃), ppm : See figure 4.40

17-Methoxy-carbonyl-14-heptadecaenyl-4-hydroxy-3-methoxy cinnamate (132) : white amorphous solid

Molecular formula : C₁₂H₁₄O₅
UV λ_{\max} (MeOH), nm : 196, 273, 328
IR ν_{\max} (CHCl₃), cm⁻¹ : 3401, 1704
Mass spectrum, m/z : 239 (100)
¹H NMR (CDCl₃), ppm : See figure 4.42
¹³C NMR (CDCl₃), ppm : See figure 4.43

3-Methyl-10,11-dimethoxyl-6-methoxycarbonyl- β -carboline (133) : brownish amorphous solid

Molecular formula : C₁₁H₁₀N₂O
UV λ_{\max} (MeOH), nm : 245, 285, 336
IR ν_{\max} (CHCl₃), cm⁻¹ : 3411, 1665
Mass spectrum, m/z : 187 (100)
¹H NMR (CDCl₃), ppm : See figure 4.47
¹³C NMR (CDCl₃), ppm : See figure 4.48

(E)-Methyl,3-(4-hydroxy-3,5-dimethoxyphenyl)acrylate (134) : brownish amorphous solid

Molecular formula : C₁₁H₈N₂O
UV λ_{\max} (MeOH), nm : 248, 283, 335
IR ν_{\max} (CHCl₃), cm⁻¹ : 3389
Mass spectrum, m/z : 185 (100)
¹H NMR (CDCl₃), ppm : See figure 4.53
¹³C NMR (CDCl₃), ppm : See figure 4.54

1,2,3,4-Tetrahydro-1-oxo- β -carboline (135) : white amorphous solid

Molecular formula : C₁₂H₁₄O₅

UV λ_{max} (MeOH), nm : 225, 307

IR ν_{max} (CHCl₃), cm⁻¹ : 3401, 1704

Mass spectrum, m/z : 239 (100)

¹H NMR (CDCl₃), ppm : See figure 4.56

¹³C NMR (CDCl₃), ppm : See figure 4.57

3-Hydroxy- β -carboline (136): white amorphous solid

Molecular formula : C₂₉H₄₄O₆

UV λ_{max} (MeOH), nm : 196, 273, 328

IR ν_{max} (CHCl₃), cm⁻¹ : 3431, 1711, 1738

Mass spectrum, m/z : 489 (100)

¹H NMR (CDCl₃), ppm : See figure 4.59

¹³C NMR (CDCl₃), ppm : See figure 4.60

(*E*)-3-(3,4,5-Trimethoxyphenyl)acrylic acid (137) : brownish amorphous solid

Molecular formula : C₁₆H₁₆ N₂O₄

UV λ_{max} (MeOH), nm : 245, 285, 336

IR ν_{max} (CHCl₃), cm⁻¹ : 1725, 3369

Mass spectrum, m/z : 301 (100)

¹H NMR (CDCl₃), ppm : See figure 4.62

¹³C NMR (CDCl₃), ppm : See figure 4.63

Benzenepropanoic acid, 3- methoxy (138) : white amorphous solid

Molecular formula : C₁₀H₁₂O₃

UV λ_{\max} (MeOH), nm : 225, 302

IR ν_{\max} (CHCl₃), cm⁻¹ : 3400, 1704

Mass spectrum, m/z : 181 (100)

¹H NMR (CDCl₃), ppm : See figure 4.65

¹³C NMR (CDCl₃), ppm : See figure 4.66

3.5.3 *Actinodaphne macrophylla* Alkaloids:

Cycleanine(139) : brownish amorphous solid

Molecular formula : C₃₈H₄₂N₂O₆

UV λ_{\max} (MeOH), nm : 238

IR ν_{\max} (CHCl₃), cm⁻¹ : 1500, 1220

Mass spectrum, m/z : 623 (100)

¹H NMR (CDCl₃), ppm : See figure 4.68

¹³C NMR (CDCl₃), ppm : See figure 4.69

10- Demethylxylopinine (140) : brownish amorphous solid

Molecular formula : C₂₀H₂₃NO₄

UV λ_{\max} (MeOH), nm : 301

IR ν_{\max} (CHCl₃), cm⁻¹ : 3382

Mass spectrum, m/z : 342 (100)

¹H NMR (CDCl₃), ppm : See figure 4.72

¹³C NMR (CDCl₃), ppm : See figure 4.73

Reteculine (141) : brownish amorphous solid

Molecular formula : C₁₉H₂₃NO₄

UV λ_{max} (MeOH), nm : 235, 283

IR ν_{max} (CHCl₃), cm⁻¹ : 3447

Mass spectrum, m/z : 330 (100)

¹H NMR (CDCl₃), ppm : See figure 4.75

¹³C NMR (CDCl₃), ppm : See figure 4.76

Laurotetanine (142) : brownish amorphous solid

Molecular formula : C₁₉H₂₁NO₄

UV λ_{max} (MeOH), nm : 217, 242

IR ν_{max} (CHCl₃), cm⁻¹ : 3385

Mass spectrum, m/z : 328 (100)

¹H NMR (CDCl₃), ppm : See figure 4.78

¹³C NMR (CDCl₃), ppm : See figure 4.79

Bicuculine (143) : brownish amorphous solid

Molecular formula : C₂₀H₁₇NO₆

UV λ_{max} (MeOH), nm : 217, 288

IR ν_{max} (CHCl₃), cm⁻¹ : 1692

Mass spectrum, m/z : 368 (100)

¹H NMR (CDCl₃), ppm : See figure 4.81

¹³C NMR (CDCl₃), ppm : See figure 4.82

α - Hydrastine (144) : brownish amorphous solid

Molecular formula : C₂₁H₂₁NO₆

UV λ_{max} (MeOH), nm : 217, 288

IR ν_{max} (CHCl₃), cm⁻¹ : 1692

Mass spectrum, m/z : 384 (100)

¹H NMR (CDCl₃), ppm : See figure 4.84

¹³C NMR (CDCl₃), ppm : See figure 4.85

Parafumine (145) : brownish amorphous solid

Molecular formula : C₂₀H₁₉NO₅

UV λ_{max} (MeOH), nm : 218, 288

IR ν_{max} (CHCl₃), cm⁻¹ : 3431, 1692

Mass spectrum, m/z : 354 (100)

¹H NMR (CDCl₃), ppm : See figure 4.87

¹³C NMR (CDCl₃), ppm : See figure 4.88

(+) – Anolobine (146) : brownish amorphous solid

Molecular formula : C₁₇H₁₅NO₃

UV λ_{max} (MeOH), nm : 218, 238

IR ν_{max} (CHCl₃), cm⁻¹ : 3385

Mass spectrum, m/z : 281 (100)

¹H NMR (CDCl₃), ppm : See figure 4.90

¹³C NMR (CDCl₃), ppm : See figure 4.91

3.6 Antiplasmodial Test Against *Plasmodium falciparum* Strains

Malaria is a disease caused by a parasite, transmitted by the bite of infected mosquitoes. Malaria produces recurrent attacks of chills and fever. Malaria kills an estimated 1 million people each year worldwide (Desjardins, *et al.*, 1979).

This protocol for assessing compound efficacy against *Plasmodium falciparum in vitro* uses as a marker for inhibition of parasite growth (Fidock *et al.*, 1998). Many alternative protocols exist, including ones based on microscopic detection of Giemsa-stained, assays based on production of parasite lactate dehydrogenase, and the use of flow cytometry (Noedl *et al.*, 2003).

3.6.1 Preparation of the Antiplasmodial Test

3.6.1.1 Parasite Strain

Several well- characterized strains (Table 3.1) are available, either from academic laboratories or from www.malaria.mr4.org (reagents available to registered users) (Wellems & Tinsley, 1990). One recommendation would be to test activity against a drug-sensitive line such as 3D7 (West Africa), D6 (Sierra Leone) or D10 (Papua New Guinea), (Oduola *et al.*, 1988), (Walliker, 1987), as well as a drug-resistant line such as W2 or Dd2 (both from Indochina), (Jacqueline & Culvenor, 2000), (Schmidt, *et al.*, 1977), FCB (SE Asia), (Joy, 2003), (Clemens & Richard, 1995), 7G8 (Brazil), (Jonathan *et al.*, 1992) or K1 (Thailand), (Essam *et al.*, 2009).

Table 3.1: Standard *Plasmodium falciparum* strains

Name	Clone	Origin	Resistant to	Multiplication
Dd2	yes (from WR82)	Indochina	CQ,QN,PYR,SDX	5-6
W2	yes (from Indochina-3)	Indochina	CQ,QN,PYR,SDX	5-6
HB3	yes	Honduras	PYR	4
3D7	yes (from NF54)	West Africa	-	4
D6	yes (from Sierra Leon-1)	Sierra Leone	-	4
D10	yes	Papua New Guinea		4
CAMP	no	Malaysia	PYR	4-5
FCB	no	SE Asia	CQ,QN,CYC	7-9
7G8	yes	Brazil	CQ,PYR,CYC	4-5
K1	no	Thailand	CQ,PYR	4-5

Note: CQ, chloroquine; QN, quinine; PYR, pyrimethamine; SDX, sulfadoxine; CYC, cycloguanil. Multiplication rate refers to increase in total numbers of viable parasites per 48-hr generation. These rates and the drug phenotypes refer to data from the Fidock Laboratory (Albert Einstein College of Medicine, NY) and may not be the same elsewhere.

3.6.1.2 Malaria Culture Media

RPMI 1640 medium containing L-glutamine (Catalog number 31800, Invitrogen), 50 mg/liter hypoxanthine, 25 mM Hepes, 10 µg/ ml gentamicine, 0.225% NaHCO₃ and either 10% human serum or 0.5% Albumax I or II (purified lipid-rich bovine serum albumin, Invitrogen). Medium is typically adjusted to a pH of 7.3 to 7.4.

3.7 Cholinesterase Enzymes Inhibitory Assay

Cholinesterase enzymes inhibitory potential of test samples was evaluated using Ellman's microplate assay following the method described by Ahmed & Gilani, 2009. Physostigmine was used as a positive control. Test samples and physostigmine were prepared in dimethyl sulfoxide (DMSO). The concentration of DMSO in final reaction mixture was 1%. At this concentration, DMSO has no inhibitory effect on both acetylcholinesterase and butyrylcholinesterase enzymes (Obregon *et al.*, 2005). For acetylcholinesterase (AChE) inhibitory assay, 140 μ L of 0.1 M sodium phosphate buffer (pH 8) was first added to a 96-wells microplate followed by 20 μ L of test samples and 20 μ L of 0.09 units/mL acetylcholinesterase enzyme. After 15 min of pre-incubation at 25 °C, 10 μ L of 10 mM 5, 5'-dithiobis (2-nitrobenzoic acid) was added into each well, followed by 10 μ L of 14 mM acetylthiocholine iodide. After the initiation of enzymatic reaction, absorbance of the coloured end- product was measured for 15 min using Tecan Infinite 200 Pro Microplate Spectrophotometer (Männedorf, Switzerland) at 417 nm. For butyrylcholinesterase (BChE) inhibitory assay, the same procedures as described above were followed except for the use of enzyme and substrate, which were BChE from equine serum and *S*-butyrylthiocholine chloride, respectively. Each test was conducted in triplicate. Absorbencies of the test samples were corrected by subtracting the absorbance of their respective blank. A set of five concentrations was used to estimate the 50% inhibitory concentration (IC_{50}).

3.8 Cytotoxicity Assay

3.8.1 Cell Culture and MTT Assay

All cell lines used in this study were obtained from American Type Cell Collection (ATCC, Manassas, VA, USA). Cells were cultured in DMEM medium (Sigma, St. Louis, MO, USA) supplemented with 10% FBS (PAA, Pasching, Austria) at 37 °C with 5% CO₂.

The cytotoxicity of the three isolated indole alkaloids against different cell lines was measured using the MTT assay as originally described by Mosmann, 1983 in brief, cells were treated with different concentrations of the indole alkaloids in 96-well plates and incubated for 24 h. After the incubation time, MTT dye (20 µL, 5 mg/mL, Sigma) was added to the cells for 3 h followed by incubation with DMSO for 10 min. The colorimetric assay was measured at the absorbance of 570 nm using a microplate reader (Hidex, Turku, Finland). Antiproliferative potential of the compounds was expressed as IC₅₀ value. As rauvolfine B (123) showed the lowest IC₅₀ value against colon cancer HCT-116 cells, we used rauvolfine B (123) to continue this study against HCT-116 cells.

3.8.2 Annexin-V-FITC Assay

Induction of the early and late apoptosis by rauvolfine B was further studied via Annexin V/PI staining assay. Briefly, HCT-116 cells (1×10^6) were plated in 60 mm² culture dish and treated with vehicle DMSO and rauvolfine B at IC₅₀ concentrations for 24, 48 and 72 h. After harvest of adherent and suspension cells and washing them twice with PBS, they were re-suspended in annexin V binding buffer (BD Biosciences, San Jose, CA, USA) and stained with annexin V-FITC (BD) and PI (Sigma) according to

the manufacturer's instructions. The fluorescence intensity of HCT-116 cells were then analyzed by flow cytometry (BD FACSCanto™ II) through quadrant statistics for necrotic and apoptotic cell populations. PI was used for detection of the late apoptosis and necrosis while Annexin V was consumed for the detection of the early and late apoptosis.

CHAPTER 4

RESULTS AND DISCUSSION

RESULTS AND DISCUSSION

Two Malaysian species from the family of Apocynaceae, *Ochrosia oppositifolia* and *Rauvolfia reflexa* and one species from the Lauraceae family, *Actinodaphne macrophylla* have been studied for their bioactive components content. The isolation process was carried out using the conventional methods and the structural elucidation was carried out using spectroscopic techniques, notably NMR, IR, MS and UV and also by comparison with the literature values.

Table 4.1: Compounds isolated from *Ochrosia oppositifolia*, *Rauvolfia reflexa* and *Actinodaphne macrophylla*

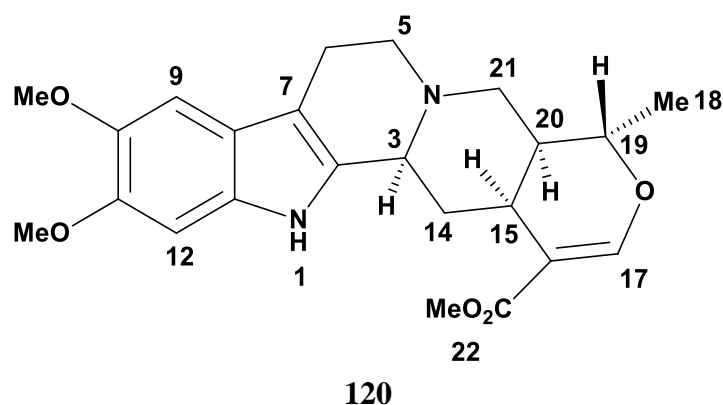
Number	Name of Compound	Plant's Name
1	isoreserpiline (120)	<i>Ochrosia Oppositifolia</i> (bark)
2	neisosposinine (121)	<i>Ochrosia Oppositifolia</i> (bark)
3	reserpine (122)	<i>Ochrosia Oppositifolia</i> (bark)
4	rauvolfine B (123)	<i>Rauvolfia reflexa</i> (bark)
5	rauvolfine C (124)	<i>Rauvolfia reflexa</i> (bark)
6	vinorine (125)	<i>Rauvolfia reflexa</i> (bark)
7	rescinamine (126)	<i>Rauvolfia reflexa</i> (bark)
8	cantleyine (127)	<i>Rauvolfia reflexa</i> (bark)
9	akuammilan-17-oic-acid, 1,2- dihydro-3-hydroxy-1-methyl ester (128)	<i>Rauvolfia reflexa</i> (bark)
10	undulifoline (129)	<i>Rauvolfia reflexa</i> (bark)
11	macusine B (130)	<i>Rauvolfia reflexa</i> (bark)
12	isoreserpiline (120)	<i>Rauvolfia reflexa</i> (bark)

Number	Name of Compound	Plant's Name
13	akuammilan-17-oic,acid,12- hydroxyl, methyl ester (131)	<i>Rauvolfia reflexa</i> (bark)
14	17-methoxy-carbonyl-14-heptadecaenyl-4-hydroxy-3-methoxy cinnamate (132)	<i>Rauvolfia reflexa</i> (leaves)
15	3-methyl-10,11-dimethoxyl-6-methoxycarbonyl- β - carboline (133)	<i>Rauvolfia reflexa</i> (leaves)
16	(<i>E</i>)-methyl,3-(4-hydroxy-3,5-dimethoxyphenyl)acrylate (134)	<i>Rauvolfia reflexa</i> (leaves)
17	1,2,3,4-tetrahydro-1-oxo- β -carboline (135)	<i>Rauvolfia reflexa</i> (leaves)
18	3-hydroxy- β -carboline (136)	<i>Rauvolfia reflexa</i> (leaves)
19	(<i>E</i>)-3-(3,4,5-trimethoxyphenyl)acrylic acid (137)	<i>Rauvolfia reflexa</i> (leaves)
20	benzenepropanoic acid, 3- methoxy (138)	<i>Rauvolfia reflexa</i> (leaves)
21	cycleanine (139)	<i>Actinodaphne macrophylla</i> (bark)
22	(-) - 10-demethylxylopinine (140)	<i>Actinodaphne macrophylla</i> (bark)
23	reticuline (141)	<i>Actinodaphne macrophylla</i> (bark)
24	(+) - laurotetanine (142)	<i>Actinodaphne macrophylla</i> (bark)
25	(+) - bicuculine (143)	<i>Actinodaphne macrophylla</i> (bark)
26	(-) α - hydrastine (144)	<i>Actinodaphne macrophylla</i> (bark)
27	(+) - parafumine (145)	<i>Actinodaphne macrophylla</i> (bark)
28	(+) - anolobine (146)	<i>Actinodaphne macrophylla</i> (bark)

4.1 Structural Elucidation of Alkaloids from the Bark of *Ochrosia oppositifolia*

The investigation on the crude extract from the bark of *Ochrosia oppositifolia* have resulted in the isolation of three known compounds namely, isoreserpiline (**120**), neisosposinine (**121**) and reserpiline (**122**).

4.1.1 Isoreserpiline (**120**)



Isoreserpiline (**120**) was isolated as a brownish amorphous solid, $[\alpha]_D^{24} -36$ (c 0.05, CHCl_3).

The mass spectrum showed pseudo-molecular ion peak at m/z 413.2662, $[\text{M}+\text{H}]^+$, which was consistent with the molecular formula of $\text{C}_{23}\text{H}_{28}\text{N}_2\text{O}_5$.

The UV spectrum revealed maxima at 226, 299 nm which were attributed typical of an indole system (Verporte, 1986). In addition, the IR spectrum showed a peak at 1692 cm^{-1} which indicate the presence of the carbonyl group, and a band at 3370 cm^{-1} presence of the NH group.

The ^1H NMR spectrum (Figure 4.1) indicated the presence of two aromatic protons at δ 6.88 and 6.79 attached to C-9 and C-12 respectively, and a deshielded singlet at δ 7.54 which belongs to H-17, indicative of a corynanthean skeleton (Waterman, 1998). Another

three singlets appeared at δ 3.90, 3.87 and 3.46 can be attributed to the protons of three methoxys attached to C-10, C-11 and C-22 respectively. The presence of the N-H protons was confirmed by the existence of a broad downfield signal at δ 7.73 in the ^1H NMR spectrum. There were a total of twelve aliphatic proton signals observed in the ^1H NMR spectrum. Eight methylene proton signals appeared between δ 1.47- 3.05 which belong to the protons attached to C-5, C-6, C-14 and C-21. The signal for another four aliphatic protons δ 3.30, 2.8, 4.4 and 1.5 were assigned to H-3, H-15, H-19 and H-20 respectively. Finally a doublet in the high field region at δ 1.40 (*d*, *J*= 6.8 Hz) may be attributed to the methyl group attached to C-19.

The ^{13}C data (Figure 4.2), (Table 4.2) indicated the presence of 23 carbons; eight quaternary carbons; δ 168.2 (C-22), 146.5 (C-11), 144.9 (C-10), 133.3 (C-2), 130.2 (C-13), 120.0 (C-8), 109.6 (C-16) and 107.9 (C-7), seven methines; δ 155.8 (C-17), 100.4 (C-9), 94.9 (C-12), 72.6 (C-19), 60.0 (C-3), 38.5 (C-20) and 31.4 (C-15), four methylenes; δ 56.5 (C-21), 53.7 (C-5), 34.4 (C-14) and 21.9 (C-6), 1 methyl; δ 18.6 (C-18), and three methoxys at δ 56.4 (C₁₀-OMe), 56.5 (C₁₁-OMe) and 50.8 (C₂₂-OMe) respectively.

The carbonyl (C-22) appeared at δ 168.1. Two aromatic methine signals were observed at 100.4 and 94.9 could be assigned to C-9 and C-12 respectively. C-17 appeared at δ 155.8 and the carbonyl is proven by the correlation between carbonyl and H-17 in HMBC (Scheme 4.1). The HMBC spectrum also showed correlation between C-20 and the methyl protons of C-18, while H-14 (δ 1.5) revealed correlation with C-3. The complete assignments of carbons and protons were confirmed with DEPT, HSQC and HMBC spectra. Analysis of all spectral data obtained and comparison with literature confirmed the

isolation of isoreserpiline (**120**) which was previously isolated from *Rauvolfia grandiflora* Mart (Cancelieri *et al.*, 2002).

Table 4. 2: ^1H NMR (400 MHz) and ^{13}C NMR (100) spectral data of isoreserpiline (**120**) in CDCl_3 (δ in ppm, J in Hz)

Position	^1H -NMR (δ ppm)	^{13}C -NMR (δ ppm)	^{13}C -NMR (δ ppm) (Cancelieri et al, 2002)
2	-	133.3	133.6
3	3.30 (1H, <i>d</i> , $J= 11.4$)	60.0	59.8
5	2.90 (2H, <i>m</i>)	53.7	52.9
6	2.74 (2H, <i>m</i>)	21.9	22.1
7	-	107.9	108.1
8	-	120.0	120.0
9	6.88 (1H, <i>s</i>)	100.3	101.0
10	-	144.9	145.2
11	-	146.5	146.6
12	6.79 (1H, <i>s</i>)	94.8	95.1
13	-	130.2	130.2
14	1.53 (2H, <i>q</i> , $J= 9.7$)	34.3	34.4
15	2.82 (1H, <i>m</i>)	31.4	31.4
16	-	109.6	110.3
17	7.54 (1H, <i>s</i>)	155.8	156.8
18	1.40 (3H, <i>d</i> , $J= 6.8$)	18.6	18.8
19	4.41 (1H, <i>m</i>)	72.5	72.8
20	1.52 (1H, <i>m</i>)	38.5	38.6
21	3.05 (2H, <i>dd</i> , $J= 1.6, 12.2$)	56.5	56.6
22	-	168.2	168.2
NH	7.73 (1H, <i>s</i>)	-	-
OMe -10	3.90 (3H, <i>s</i>)	56.4	56.4
OMe -11	3.87 (3H, <i>s</i>)	56.5	56.6
OMe -22	3.46 (3H, <i>s</i>)	50.8	51.2

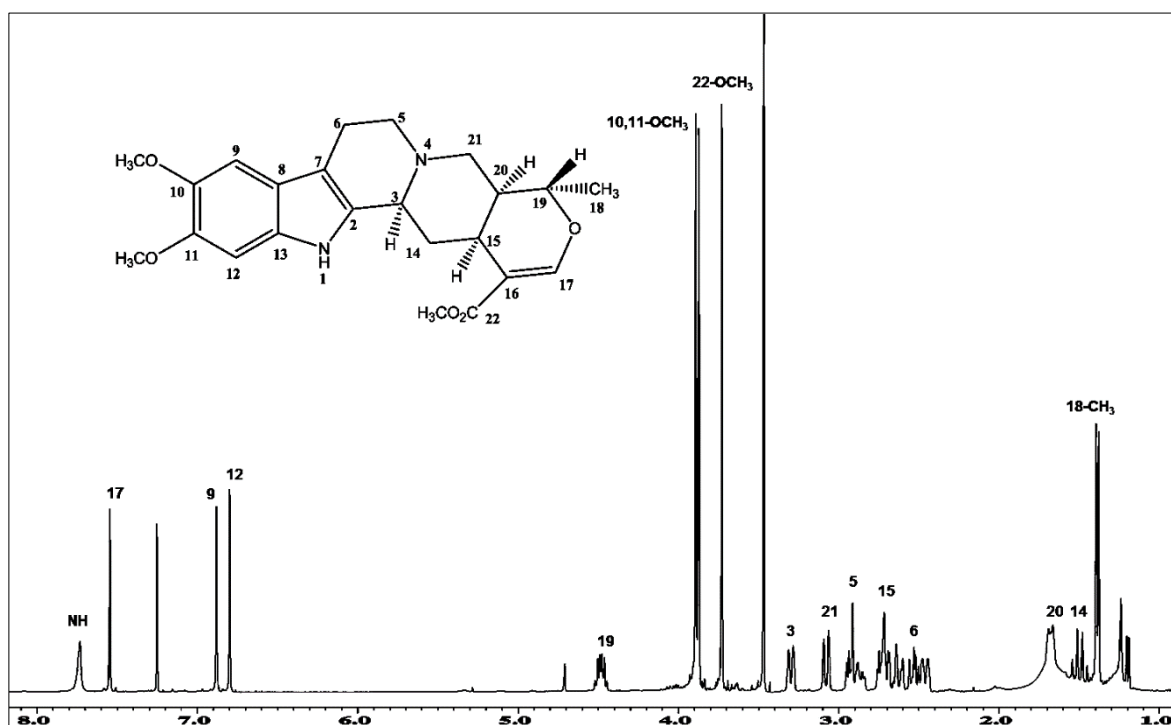


Fig. 4.1: ¹H NMR Spectrum of Isoreserpiline (120)

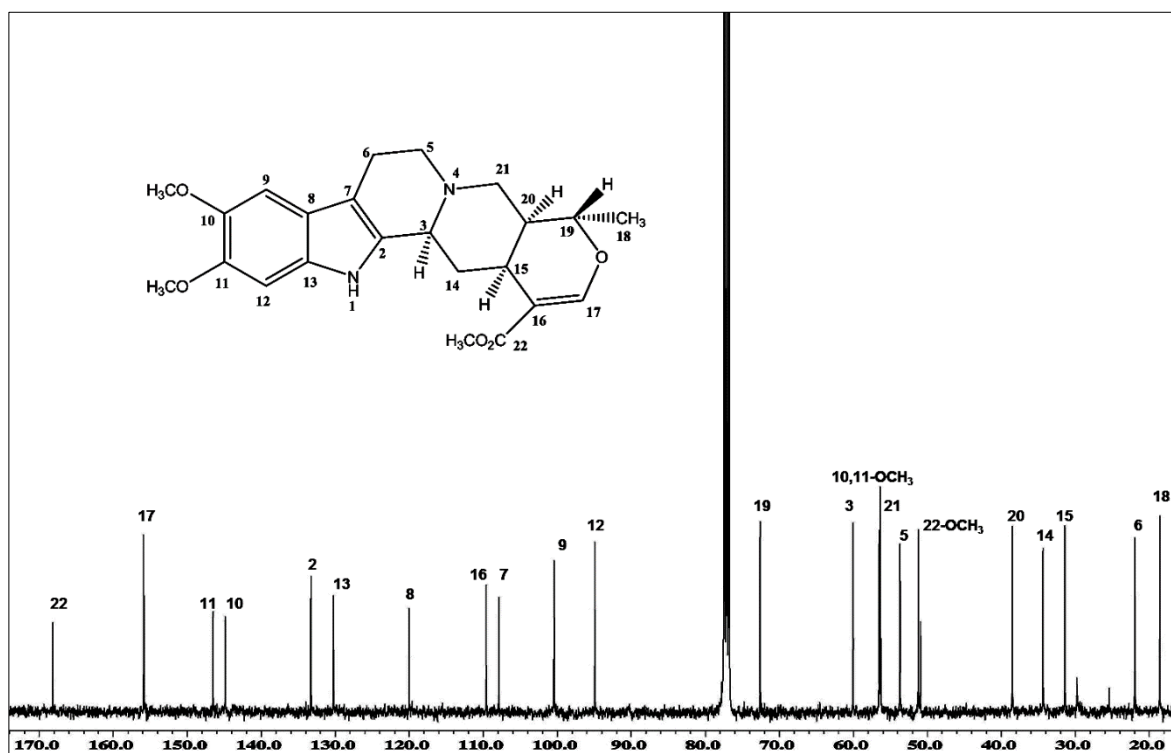


Fig. 4.2: ¹³C NMR Spectrum of Isoreserpiline (120)

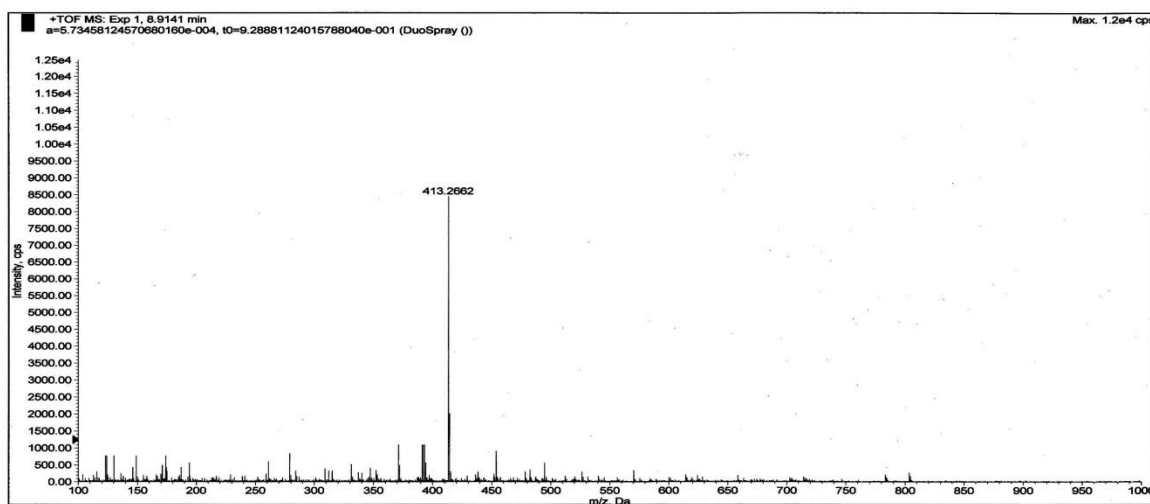
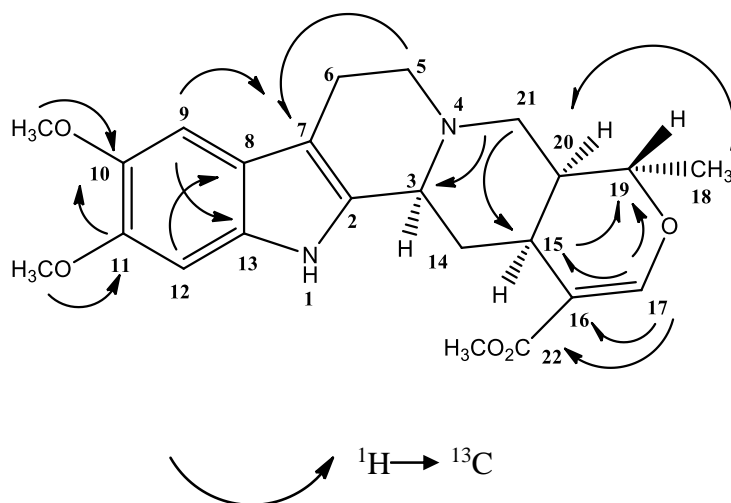
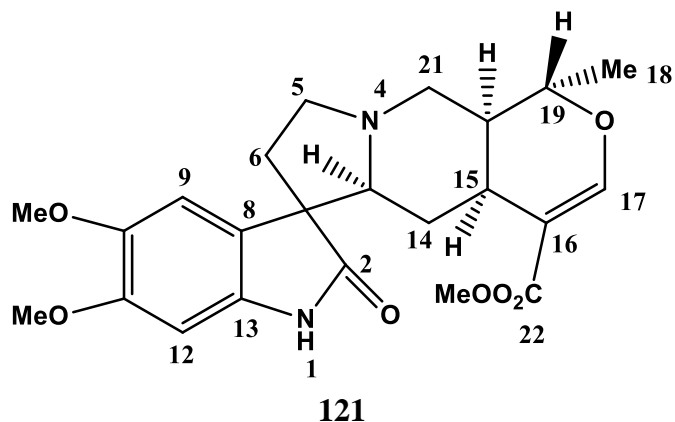


Fig. 4.3: LC-MS Spectrum of Isoreserpiline (**120**)



Scheme 4.1: The HMBC Correlations of Isoreserpiline (**120**)

4.1.2 Neisosposinine (121)



Neisosposinine (**121**) was isolated as a brownish amorphous solid, $[\alpha]_D^{24} -16$ (c 0.05, CHCl_3). The mass spectrum revealed a pseudo-molecular ion peak at m/z 429.1406 $[\text{M}+\text{H}]^+$ corresponding to the molecular formula of $\text{C}_{23}\text{H}_{28}\text{N}_2\text{O}_6$. The IR spectrum displayed a band at 3583 cm^{-1} presence of the NH group. In addition, a peak was observed at 1704 cm^{-1} (C=O) and 1190 cm^{-1} (C-O band).

The ^1H NMR spectrum (Figure 4.4) showed three singlets at δ 7.40, 6.81 and 6.49 which were assigned to the isolated an olefinic proton H-17 and two aromatic protons H-9 and H-12 respectively. The spectrum also showed a broad singlet in down-field region at δ 7.79 due to the presence of NH suggested the possibility of an oxindole skeleton (Matsuo *et al.*, 2011). This was further confirmed by the existence of a carbon signal at δ 181.20 (C=O). In up field region, three singlet signals were appeared at δ 3.87, 3.85 and 3.60 attributed to three methoxyl groups attached to C-10, C-11 and C- 22 respectively. The typical signal at δ 1.25 confirmed the existence of one methyl group C-18 attached to C-19. This signal appeared as a doublet with J value 5.96 Hz. The hypothesis was also supported further by the ^1H - ^1H COSY experiment that showed the following fragments; H-3-H-14, H-5-H-6 and

H-18-H-19. The ^{13}C NMR (Figure 4.5), DEPT and HSQC showed the presence of 23 carbon atoms; eight quaternary carbons, seven methines, four methylene, one methyl, and three methoxyls. The HMBC spectrum showed long range C-H cross peak correlations such as, H-5 C-7, H-17 C-22, H-18 C-20, H-5 C-7, H-9 C-11, H-12 C-8 (Scheme 4.2).

Detailed analysis of the spectral data and also data comparison with the literature value (Table 4.3) confirmed the isolation of neisosposinine (**121**) which was isolated previously from *Neisosperma oppositifolia* (Leslie *et al.*, 1989).

Table 4.3: ^1H NMR (400 MHz) and ^{13}C NMR (100 MHz) spectral data of neisosposinine (**121**) in CDCl_3 (δ in ppm, J in Hz)

Position	^1H -NMR (δ ppm)	^{13}C -NMR (δ ppm)	^{13}C -NMR (δ ppm) (Leslie et al, 1989)
2	-	181.2	180.0
3	2.48 (1H, <i>m</i>)	71.3	69.3
5	3.20 (2H, <i>m</i>)	54.0	55.2
6	1.59 (2H, <i>m</i>)	30.1	29.8
7	-	56.3	56.3
8	-	124.2	124.2
9	6.81 (1H, <i>s</i>)	109.3	110.2
10	-	144.9	145.0
11	-	146.5	147.2
12	6.49 (1H, <i>s</i>)	95.8	96.8
13		133.2	134.2
14	1.96 (2H, <i>m</i>)	34.3	34.6
15	2.40 (1H, <i>m</i>)	30.4	30.4
16	-	109.9	110.1
17	7.40 (1H, <i>s</i>)	155.1	155.1
18	1.25 (3H, <i>d</i> , $J=5.9$)	18.5	18.5
19	4.32 (1H, <i>m</i>)	72.0	72.0
20	1.48 (1H, <i>m</i>)	37.8	37.9
21	2.38 (2H, <i>m</i>)	54.0	54.1
22	-	168.2	168.4
NH	7.79 (1H, <i>s</i>)	-	-
OMe -10	3.87 (3H, <i>s</i>)	56.7	57.2
OMe -11	3.85 (3H, <i>s</i>)	56.6	56.6
OMe -22	3.60 (3H, <i>s</i>)	51.4	51.4

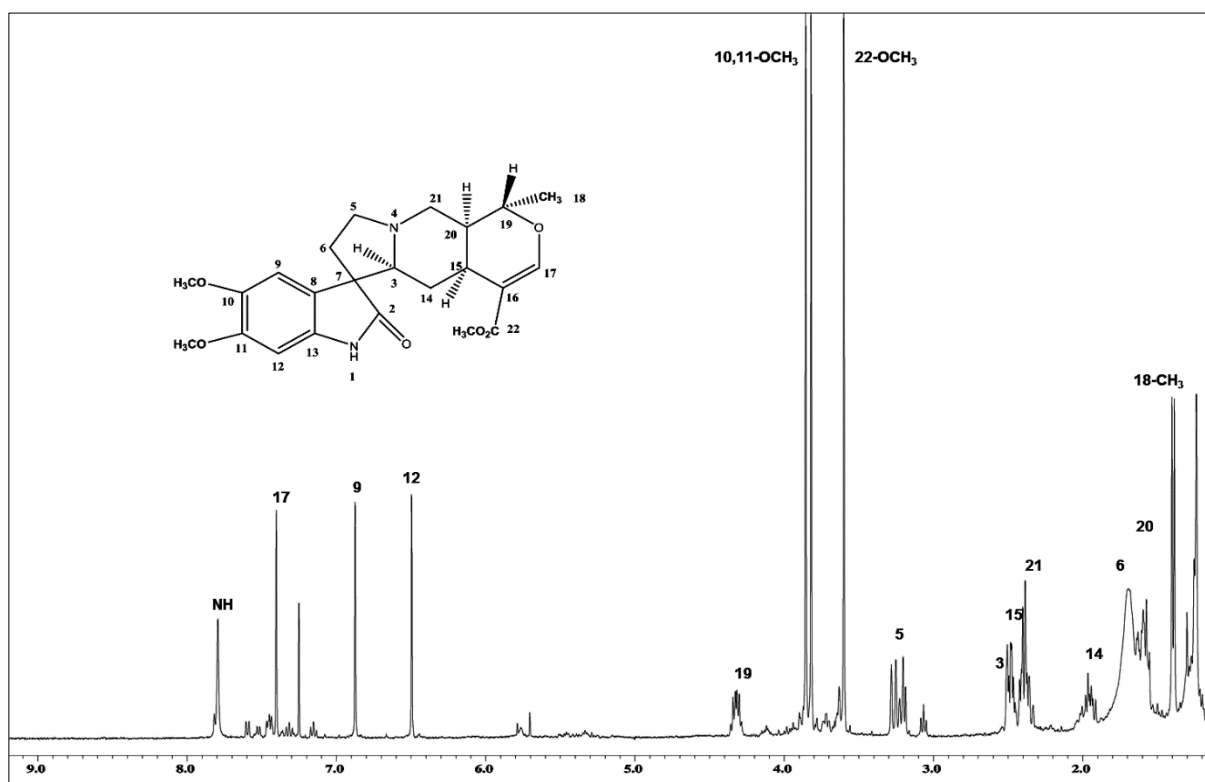


Fig. 4.4: ^1H NMR Spectrum of Neisosposinine (121)

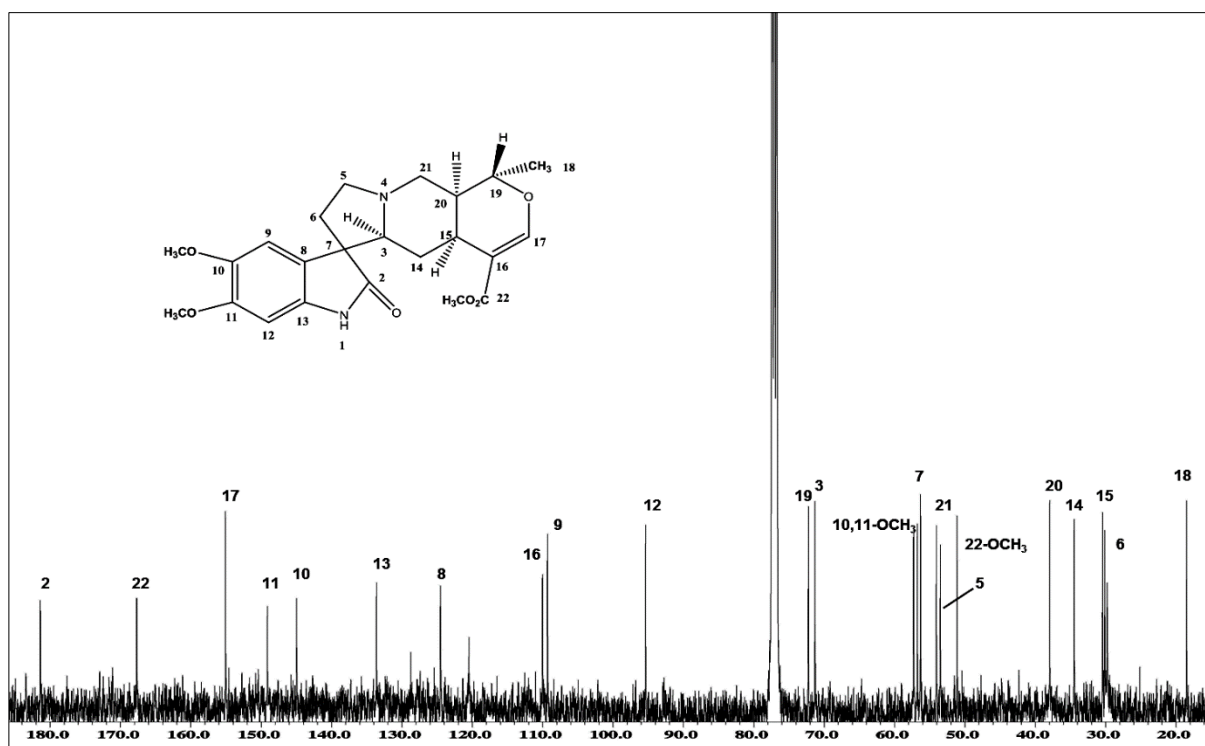


Fig. 4.5: ^{13}C NMR Spectrum of Neisosposinine (121)

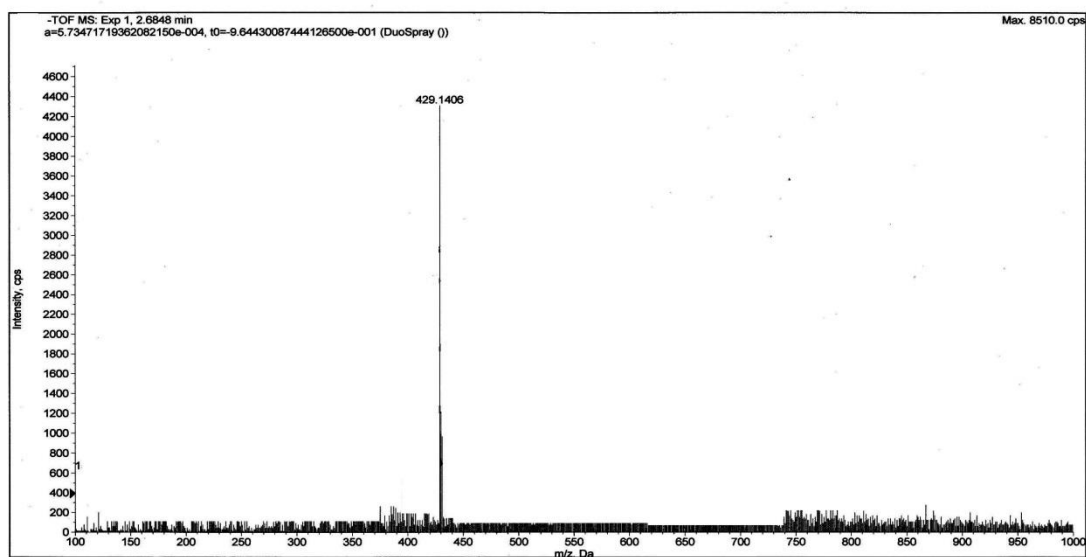
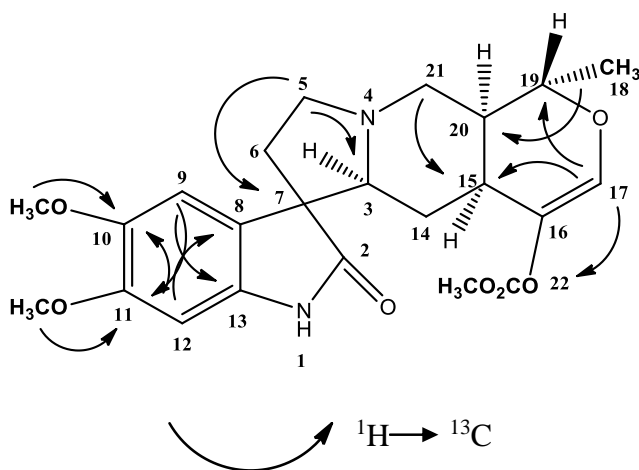
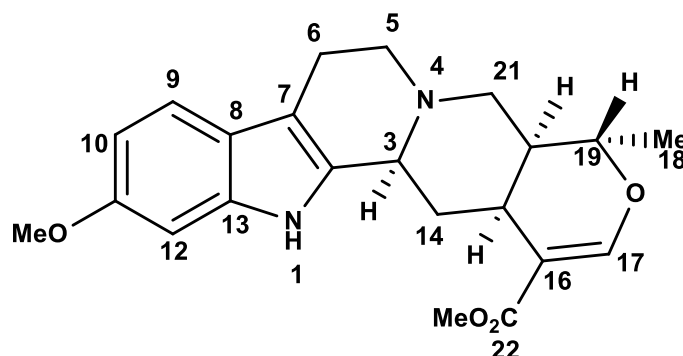


Fig. 4.6: LC-MS Spectrum of Neisosposinine (**121**)



Scheme 4.2: The HMBC Correlations of Neisosposinine (**121**)

4.1.3 Reserpinine (122)



122

Reserpinine (**122**) was isolated as a brownish amorphous solid, $[\alpha]_D^{24} -13.5$ (c 0.05, CHCl_3).

The mass spectrum showed a $[\text{M}+\text{H}]^+$ ion at m/z 383.1196 corresponding to the molecular formula of $\text{C}_{22}\text{H}_{26}\text{N}_2\text{O}_4$. The UV spectrum revealed maxima at 225 and 300 nm. The IR spectrum displayed a stretching of NH at 3402 cm^{-1} . In addition, a peak was observed at 1706 cm^{-1} which indicated the presence of the carbonyl group.

The ^1H NMR spectrum (Figure 4.7) of reserpinine (**122**) is reminiscent of isoreserpiline (**120**). The difference between isoreserpiline (**120**) and reserpinine (**122**) is the existence of one methoxyl group which is attached to the C-10 in the isoreserpiline. The spectrum indicated the presence of three aromatic protons at δ 7.28; 6.76 and 6.71 attached to C-9, C-12 and C-10 respectively. The deshielded signal of H-17 appeared at δ 7.53 for confirming the corynanthean skeleton type of reserpinine (**122**). In the aliphatic region, two singlets observed at δ 3.80 and 3.70 may be attributed to two methoxyl groups attached to C-11 and C-22 respectively. The signals for another four aliphatic protons

δ 3.27, 2.8, 4.6 and 1.7 were assigned to H-3, H-15, H-19 and H-20 respectively. Finally a doublet in the high field region at 1.4 (*d*, 6.8 Hz) attributed to the methyl group attached to C-19.

The ^{13}C NMR (Figure 4.8) and DEPT showed the presence of 22 carbon atoms; seven quaternary carbons; δ 168.2 (C-22), 156.5 (C-11), 136.8 (C-2), 133.4 (C-13), 121.7 (C-8), 109.6 (C-16) and 107.8 (C-7), eight methines; δ 155.8 (C-17), 118.6 (C-9), 109.5 (C-10), 95.0 (C-12), 72.3 (C-19), 59.9 (C-3), 38.4 (C-20) and 31.4 (C-15), four methylenes; δ 56.2 (C-21), 53.0 (C-5), 34.2 (C-14) and 21.8 (C-6), one methyl; δ 18.6 (C-18), and two methoxy groups at δ 55.8 (C₁₁-OMe) and 51.2 (C₂₂-OMe) respectively.

Detailed Analysis of the spectral data obtained and assessment with literature value confirmed that alkaloid (**122**) is reserpine (**122**) which was previously isolated from *Rauvolfia bahiensis* (Lucilia & Raquel, 2002). Complete assignments of reserpine (**122**) were listed in table 4.4.

Table 4.4: ^1H NMR (400 MHz) and ^{13}C NMR (100 MHz) spectral data of reserpinine (**122**) in CDCl_3 (δ in ppm, J in Hz)

Position	^1H -NMR (δ ppm)	^{13}C -NMR (δ ppm)	^{13}C -NMR (δ ppm) (Lucilia et al, 2002)
2	-	136.8	136.8
3	3.27 (1H, <i>d</i> , $J= 11.2$)	59.9	60.0
5	2.91 (1H, <i>m</i>)	53.0	53.0
6	2.56 (1H, <i>m</i>)	21.8	21.8
7	-	107.8	107.8
8	-	121.7	121.7
9	7.28 (1H, <i>d</i> , $J= 8.5$)	118.6	118.3
10	6.71 (1H, <i>dd</i> , $J= 2.4, 8.7$)	109.5	110.0
11	-	156.5	156.5
12	6.76 (1H, <i>d</i> , $J= 2.2$)	95.0	95.0
13	-	133.4	133.4
14	1.51 (2H, <i>m</i>)	34.2	34.2
15	2.82 (1H, <i>m</i>)	31.4	31.4
16	-	109.6	110.0
17	7.53 (1H, <i>s</i>)	155.8	155.6
18	1.41 (1H, <i>d</i> , $J= 6.8$)	18.6	18.5
19	4.63 (1H, <i>m</i>)	72.3	72.4
20	1.70 (1H, <i>m</i>)	38.4	38.6
21	2.72 (2H, <i>dd</i> , $J= 1.6, 12.2$)	56.2	56.4
22	-	168.2	168.0
NH	7.79 (1H, <i>s</i>)		
OMe -11	3.83 (3H, <i>s</i>)	55.8	55.6
OMe -22	3.71 (3H, <i>s</i>)	51.2	51.5

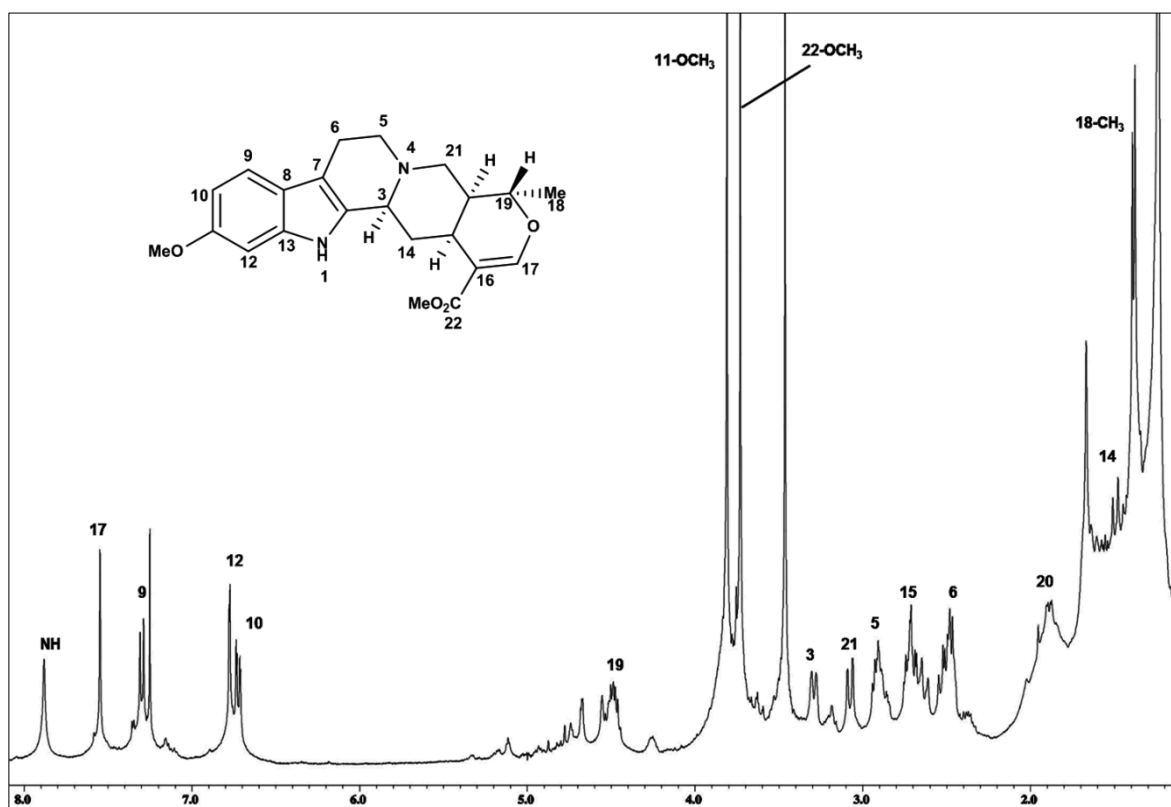


Fig. 4.7: ¹H NMR Spectrum of Reserpine (122)

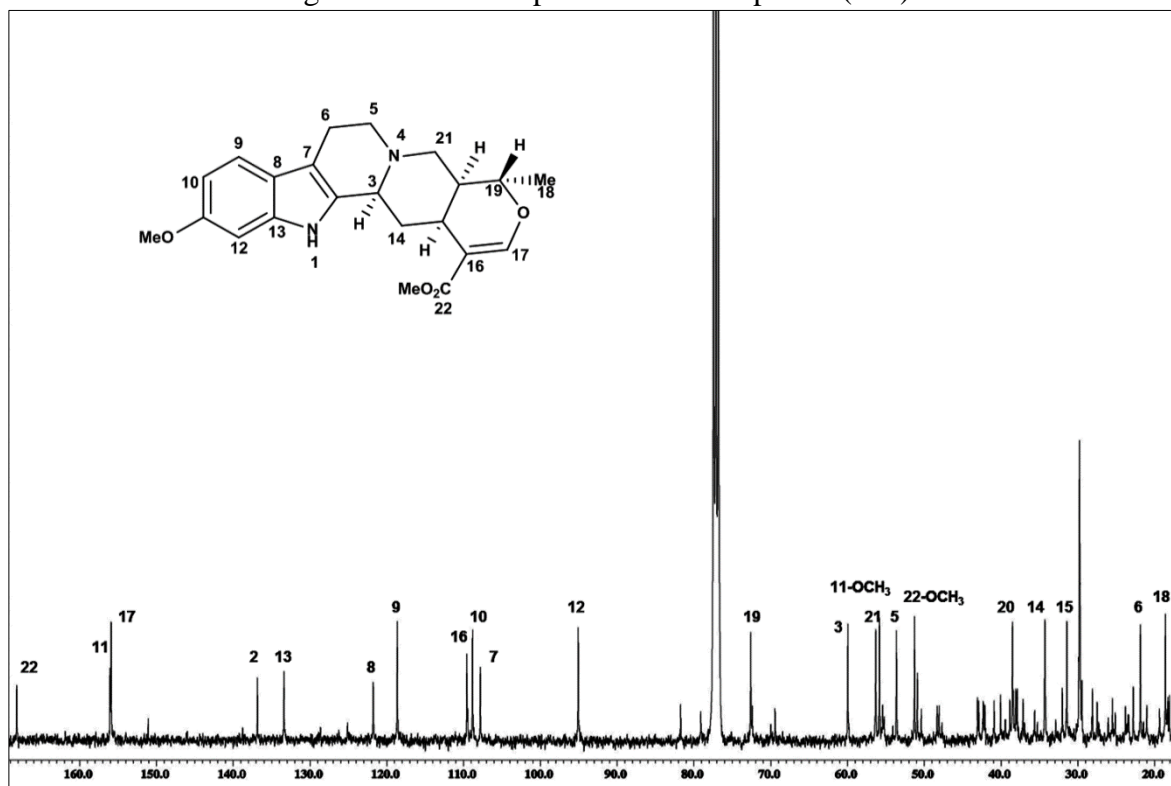


Fig. 4.8: ¹³C NMR Spectrum of Reserpine (122)

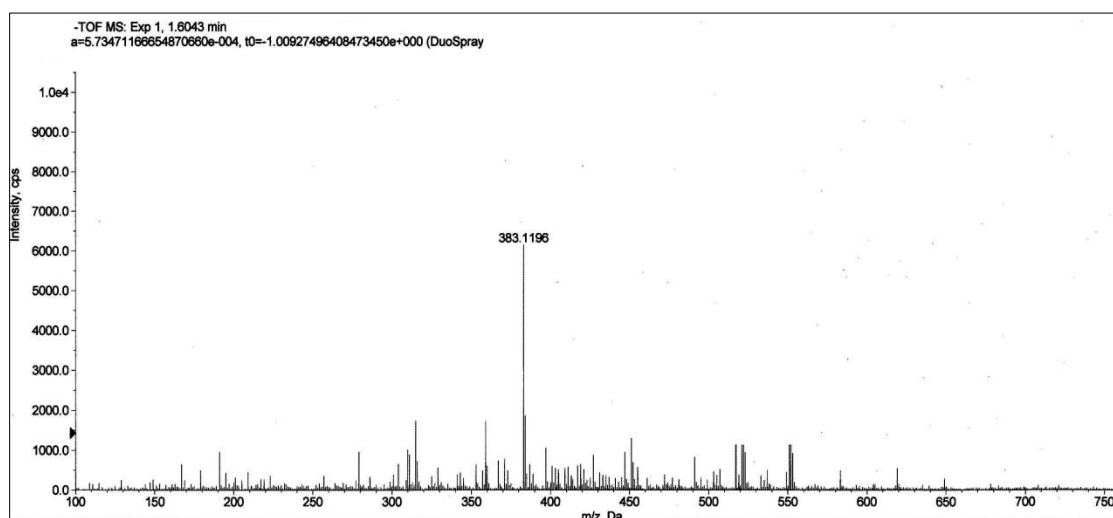
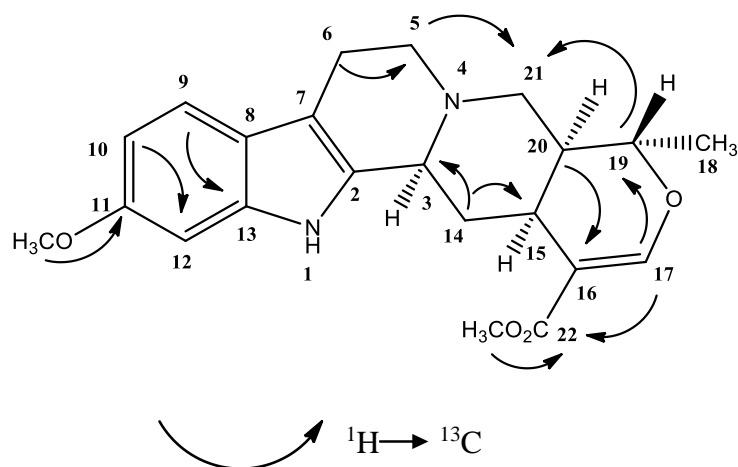


Fig. 4.9: LC-MS Spectrum of Reserpine (**122**)



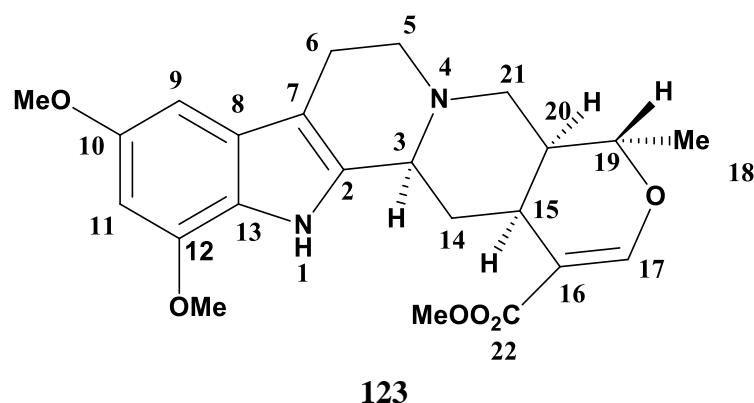
Scheme 4.3: The HMBC Correlations of Reserpine (**122**)

4.2 Structural Elucidation of Constituents from *Rauvolfia reflexa*

Seventeen compounds were isolated. The investigation on the crude alkaloids from the bark of *Rauvolfia reflexa* have resulted in the isolation of ten alkaloids which two of them are new, rauvolfine B (**123**) and rauvolfine C (**124**). Vinorine (**125**), rescinnamine (**126**), cantleyine (**127**), akuammilan-17-oic acid, 1,2-dihydro-3-hydroxy-1-methyl-, methyl ester (**128**), undulifoline (**129**), macusine B (**130**), isoreserpiline (**120**), akuammilan-17-oic acid, 12-hydroxy-, methyl ester (**131**) are the known alkaloids isolated from the bark of *Rauvolfia reflexa*. Two new compounds, 17-methoxy-carbonyl-14- heptadecaenyl- 4-hydroxy-3-methoxy cinnamate (**132**) and 3-methyl-10,11-dimethoxyl-6-methoxycarbonyl- β - carboline (**133**) were isolated from the leaves of *Rauvolfia reflexa* along with five known compounds which are, (*E*)-methyl 3-(4-hydroxy-3,5-dimethoxyphenyl) acrylate (**134**), 1,2,3,4- tetrahydro -1- oxo- β - carboline (**135**), 3-hydroxy- β -carboline (**136**), (*E*)-3-(3,4,5-trimethoxyphenyl) acrylic acid (**137**) and benzenepropanoic acid, 3- methoxy (**138**).

4.2.1 Alkaloids from the Bark of *Rauvolfia reflexa*

4.2.1.1 Ruavolfine B (123)



Ruavolfine B (**123**) was identified as Oxayohimban-16-carboxylic acid, 16,17 –didehydro-10,12 –dimethoxy- 19-methyl-, methyl ester, named as ruavolfine B; $[\alpha]_D^{24} -31$ (c 0.05, CHCl_3), was isolated as a brownish amorphous solid. The HRESIMS at m/z 413.2106 ($\text{M}+\text{H}^+$) (calcd for $\text{C}_{23}\text{H}_{28}\text{N}_2\text{O}_5$, 413.2101). The UV spectrum revealed maxima at 226, 299 nm which were characteristic for a substituted indole chromophore (Verporte, 1986). In addition, the IR (CHCl_3) spectrum showed a peak at 1730 cm^{-1} which indicate the presence of the carbonyl group, and a band at 3435 cm^{-1} presence of the NH group.

The ^1H NMR spectrum (Figure 4.10) indicated the presence of two overlapping aromatic protons at δ 6.93 (2H, d , $J = 1.8\text{ Hz}$) attached to C-9 and C-11 respectively, and a deshielded singlet at δ 7.51 which belongs to H-17. Another three singlets appeared at δ 3.79 (3H, s), 3.77 (3H, s) and 3.69 (3H, s) attributed to the protons of three methoxy groups attached to C-10, C-12 and C- 22 respectively.

The ^{13}C NMR and HSQC spectrum (Figure 4.11 and 4.12) indicated the presence of 23 carbons; eight quaternary carbons, seven methines, four methylenes, one methyl and three

methoxy groups. The carbonyl group (C=O 22) was proven by the correlation between carbonyl and H-17 in HMBC (Figure 4.13). The HMBC spectrum also showed a correlation between C-20 and the methyl protons of C-18, while H-14 revealed a correlation with C-3. The cross peak of COSY (Figure 4.14) showed series of correlations such as H-5/ H-6, H-19/ H-18, H-20 and H-3/ H-14. Ruavolfine B (**123**) is reminiscent of isoreserpiline (**120**). The relative configurations of C-3, C-15, C-19 and C-20 of ruavolfine B **123** were similar to isoreserpiline (**120**) (Cancelieri et al, 2002) configurations which were (3*R*, 15*R*, 19*S*, 20*R*). Hence, ruavolfine B (**123**) was characterized which has never been isolated before. Complete assignments of ruavolfine B (**123**) were listed in Table 4.5.

Table 4.5: ^1H NMR (400 MHz) and ^{13}C NMR (100 MHz) spectral data of rauvolfine B (**123**) in Acetone- d_6 (δ in ppm, J in Hz), ^bsignal overlapped by solvent peak.

Position	^1H -NMR	^{13}C -NMR	HMBC	COSY
2	-	133.8	-	-
3	3.20 (1H, <i>dd</i> , J = 10.3, 12.3)	60.4	-	14
5	2.90 ^b	53.5	-	6
6	2.51 (2H, <i>m</i>)	21.9	-	5
7	-	107.0	-	-
8	-	120.3	-	-
9	6.93 (<i>d</i> , J = 1.8)	101.3	11,13	-
10	-	146.9	-	-
11	6.93 (<i>d</i> , J = 1.8)	95.9	8,10	-
12	-	145.1	-	-
13	-	131.0	-	-
14	2.30 (2H, <i>m</i>)	34.2	15	3
15	2.71 (1H, <i>m</i>)	31.4	19	14
16	-	110.0	-	-
17	7.51 (1H, <i>s</i>)	154.9	19,16	-
18	1.38 (3H, <i>d</i> , J = 6.8)	17.8	20,19	19
19	4.49 (1H, <i>m</i>)	72.4	-	18,20
20	1.70 (1H, <i>m</i>)	38.5	-	21,15,19
21	2.90 ^b	53.5	15,20	20
22	-	168.7	-	-
NH	9.80 (1H, <i>s</i>)	-	-	-
OMe -10	3.79 (3H, <i>s</i>)	56.1	10	-
OMe -12	3.77 (3H, <i>s</i>)	56.0	12	-
OMe -22	3.69 (3H, <i>s</i>)	50.3	22	-

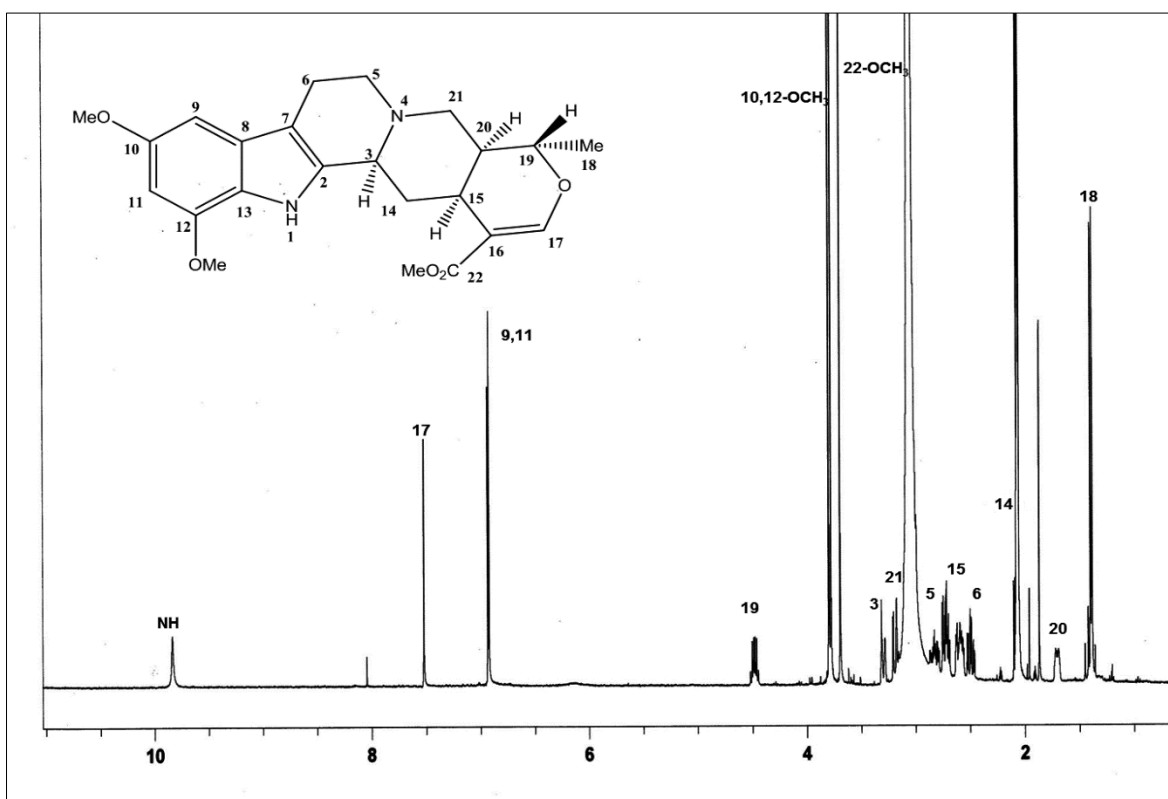


Fig. 4.10: ^1H NMR Spectrum of Rauvolfine B (123)

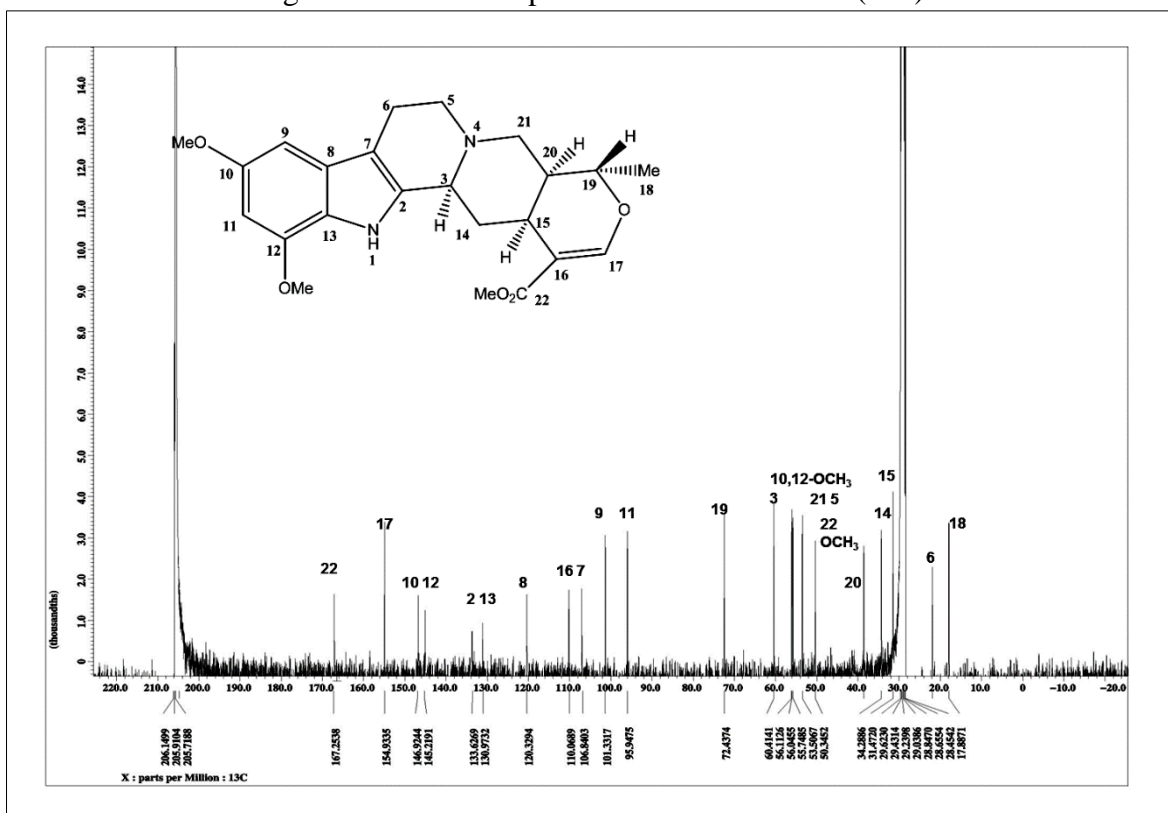


Fig. 4.11: ^{13}C NMR Spectrum of Rauvolfine B (123)

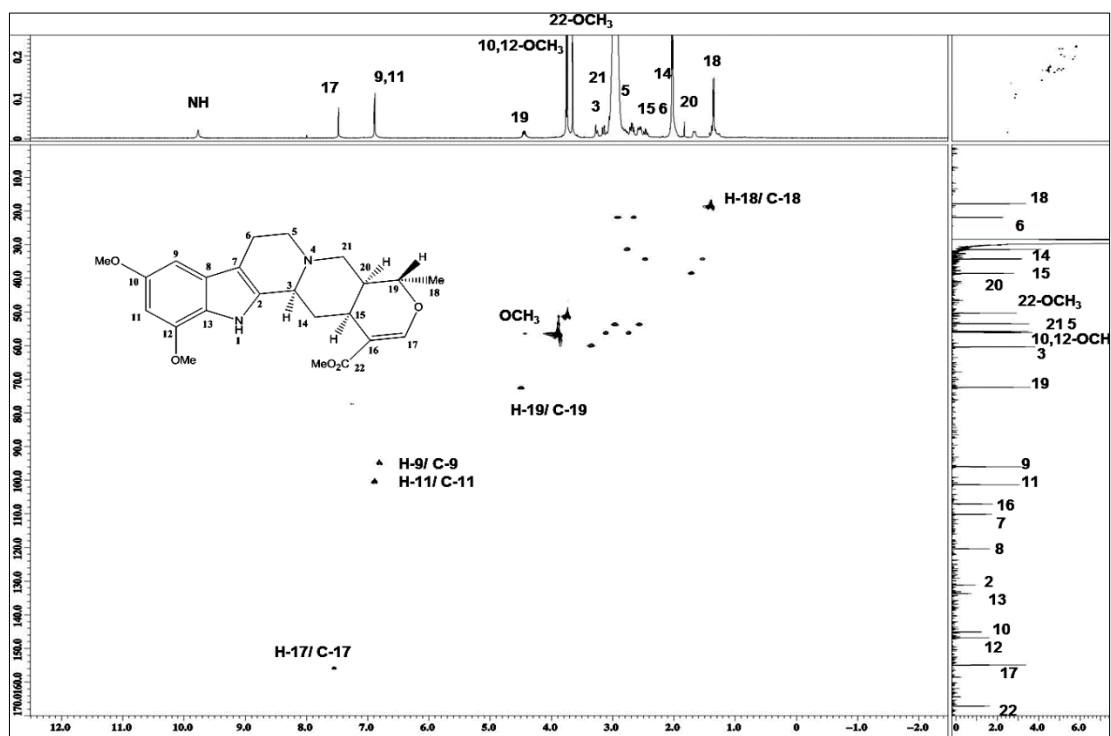


Fig. 4.12: HSQC Spectrum of Rauvolfine B (123)

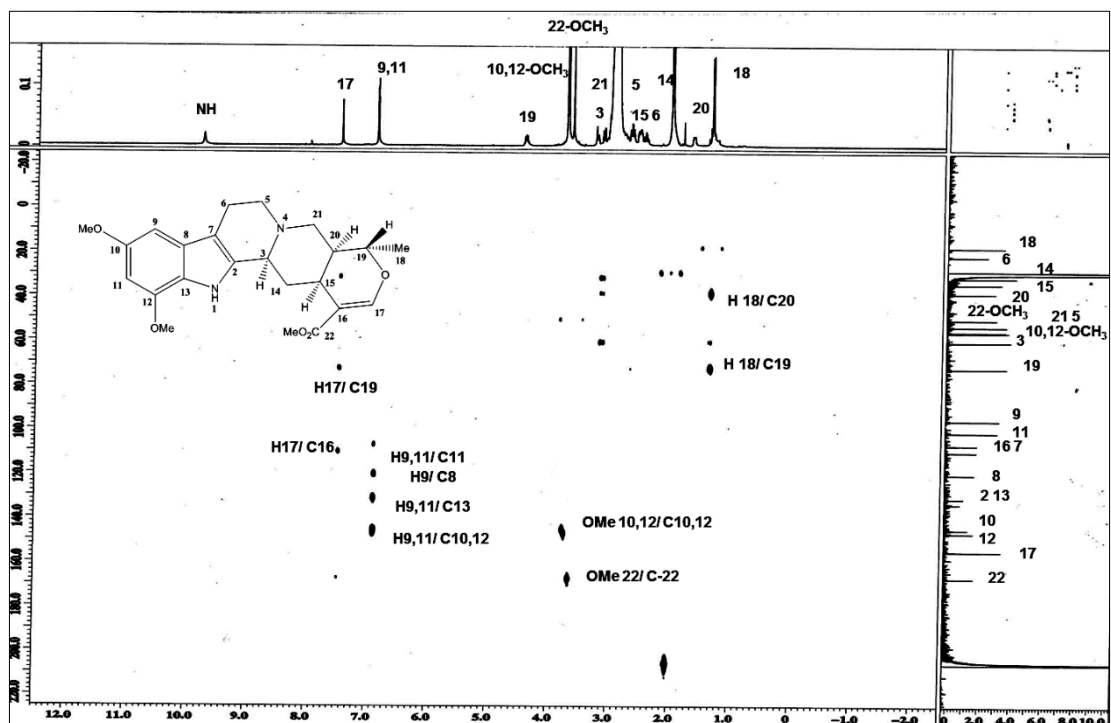


Fig. 4.13: HMBC Spectrum of Rauvolfine B (123)

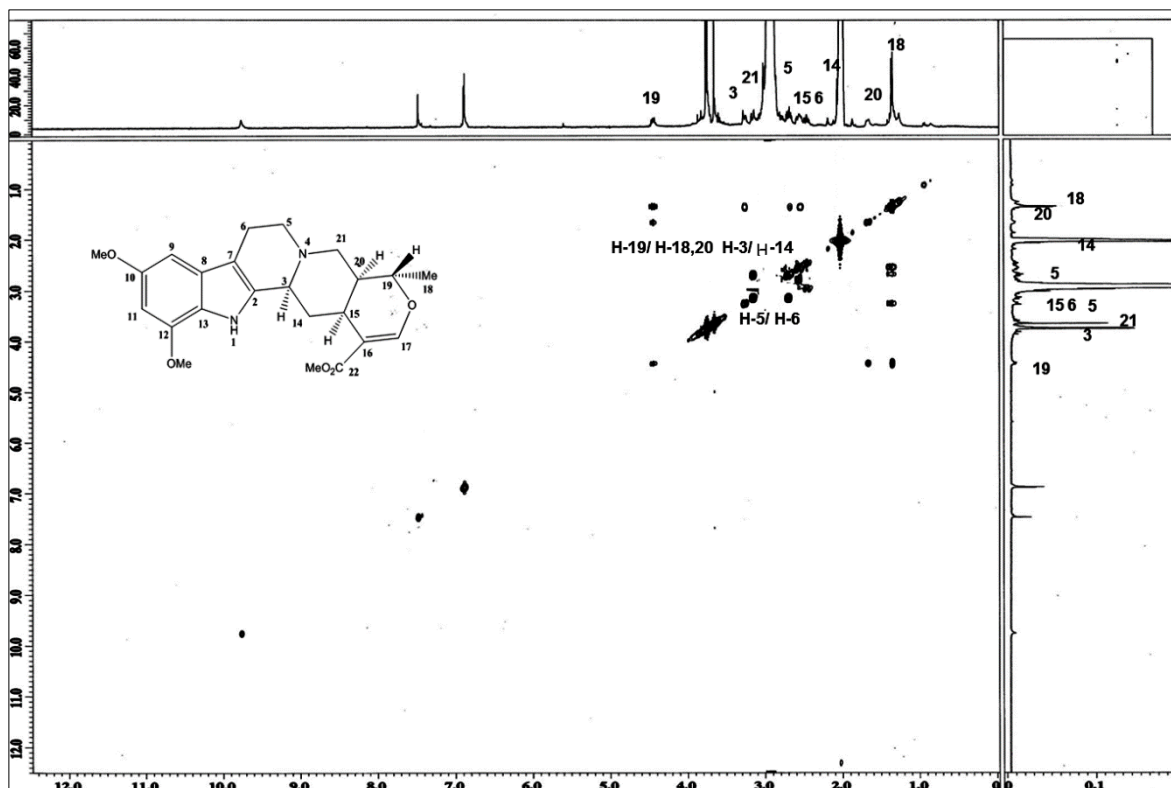


Fig. 4.14: COSY Spectrum of Rauvolfine B (123)

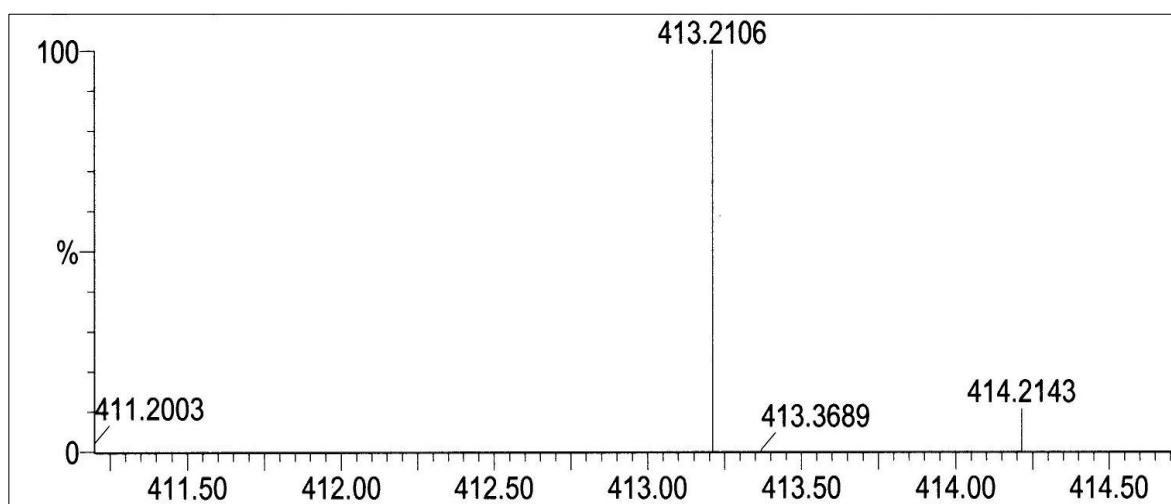
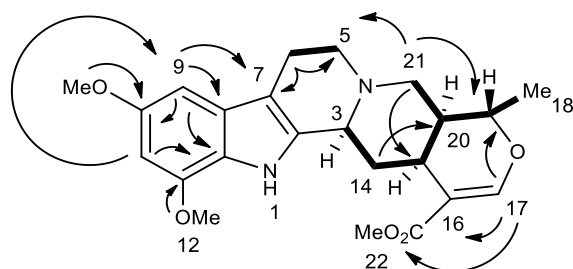
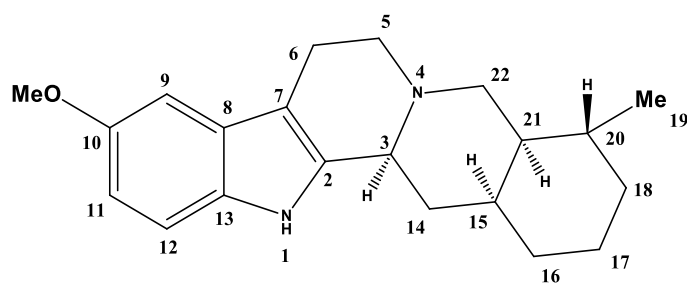


Fig. 4.15: LC-MS Spectrum of Rauvolfine B (123)



Scheme 4.4: (—) COSY and (→) Selected HMBC Correlations of Rauvolfine B (**123**)

4.2.1.2 Rauvolfine C (**124**)



124

Alkaloid (**124**) was identified as Yohimban, 10-methoxy-19-methyl and named as rauvolfine C, $[\alpha]_D^{24} -16$ (*c* 0.05, CHCl_3). Rauvolfine C (**124**) was isolated as a brownish amorphous solid. The HRESIMS at m/z 325.1924 ($\text{M}+\text{H}^+$) (calcd for $\text{C}_{21}\text{H}_{28}\text{N}_2\text{O}$, 325.1918). The UV spectrum revealed maximum at 250, 285 nm were characteristic for a substituted indole chromophore (Verporte, 1986). The IR spectrum showed a band of NH at 3378 cm^{-1} .

The ^1H NMR spectrum (Figure 4.16) indicated the presence of three aromatic protons at δ 7.12, 6.83 and 6.73 attached to C-12, C-9 and C-11, respectively. In up field region, one singlet peak was appeared at δ 3.79 attributed to one methoxy group. There were a total of

twelve aliphatic proton signals observed in the ^1H NMR spectrum. Fourteen methylene proton signals appeared between δ 1.2- 3.3 which attributed to the protons attached to C-5, C-6, C-14, C-16, C-17, C-18 and C-22. The signal for another four aliphatic protons δ 3.2, 1.5, 1.3 and 3.6 were assigned to H-3, H-15, H-20 and H-21 respectively. Finally a doublet in the high field region at δ 0.96 attributed to the methyl group attached to C-20.

The ^{13}C NMR (Figure 4.17) and HSQC (Figure 4.18) showed the presence of 21 carbon atoms; five quaternary carbons; δ 154.2 (C-10), 135.8 (C-2), 131.2 (C-13), 127.0 (C-8) and 107.9 (C-7), seven methines; δ 111.5 (C-12), 111.0 (C-11), 100.4 (C-9), 60.0 (C-3), 41.4 (C-21), 41.4 (C-15) and 37.1 (C-20), seven methylenes; δ 60.0 (C-22), 53.3 (C-5), 35.2 (C-14), 35.3 (C-18), 30.0 (C-16), 23.5 (C-17) and 21.7 (C-6), one methyl; δ 11.1 (C-19) and one methoxy; δ 55.9 (OMe-10). The HMBC spectrum (Figure 4.19 and Scheme 4.5) showed a correlation between C-10 and the 10-OMe which proved the place of methoxy group. The series of HMBC correlations are; H-19/ C-15, C-17, H-17/ C-15, H-14/ C-3, and the correlations between aromatic protons and their neighboring carbons in J_2 and J_3 . The relative configurations of C-3, C-15, C-20 and C-21 of rauwolfine C 124 were confirmed by comparing with the isoreserpiline (**120**) configurations (3*R*, 15*R*, 20*S*, 21*R*) (Cancelieri et al, 2002). Thus the structure of rauwolfine C (124) was determined which was isolated for the first time.

The assignments of the position of each carbon were established with DEPT, HSQC and HMBC spectra. Complete assignments of rauwolfine C (**124**) were listed in table 4.6.

Table 4.6: ^1H NMR (400 MHz) and ^{13}C NMR (100 MHz) spectral data of raувolfine C (**124**) in CDCl_3 (δ in ppm, J in Hz)

Position	^1H -NMR	^{13}C -NMR	HMBC
2	-	135.8	-
3	3.20 (1H, <i>dd</i> , $J=10.3, 12.3$)	60.0	-
5	3.13 (2H, <i>m</i>)	53.3	-
6	2.53 (2H, <i>m</i>)	21.7	-
7	-	107.9	-
8	-	127.0	-
9	6.83 (1H, <i>d</i> , $J= 2.3$)	100.4	13
10	-	154.2	-
11	6.73 (1H, <i>dd</i> , $J= 8.7, 2.3$)	111.0	9, 13
12	7.12 (1H, <i>d</i> , $J= 8.7$)	111.5	8, 10
13	-	131.2	-
14	2.23 (2H, <i>m</i>)	35.2	3
15	1.74 (1H, <i>m</i>)	41.4	-
16	1.33 (1H, <i>m</i>)	30.0	-
17	1.01 (2H, <i>m</i>)	23.5	15
18	1.44 (2H, <i>m</i>)	35.3	-
19	0.96 (3H, <i>d</i> , $J= 6.8$)	11.1	17, 15
20	1.30 (1H, <i>m</i>)	37.1	-
21	1.63 (1H, <i>m</i>)	41.4	-
22	2.23 (2H, <i>m</i>)	60.0	-
NH	8.10 (1H, <i>s</i>)	-	-
OMe	3.79 (3H, <i>s</i>)	55.9	10

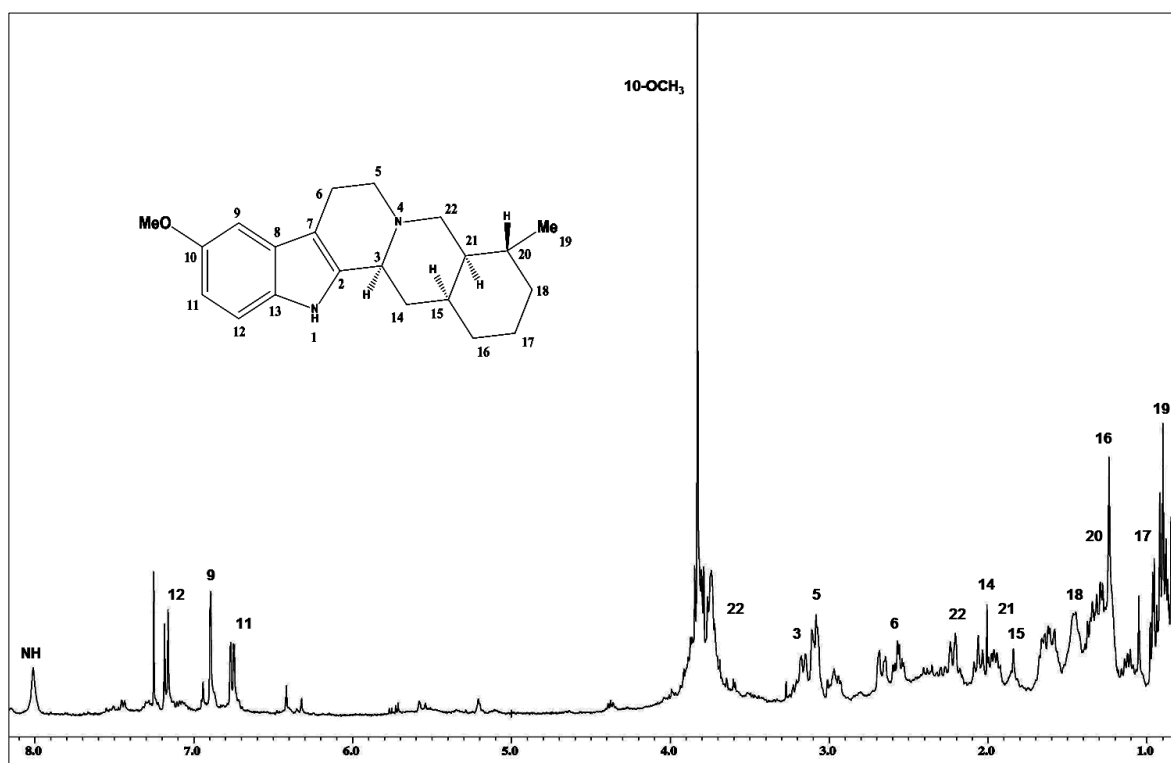


Fig. 4.16: ¹H NMR Spectrum of Rauvolfine C (124)

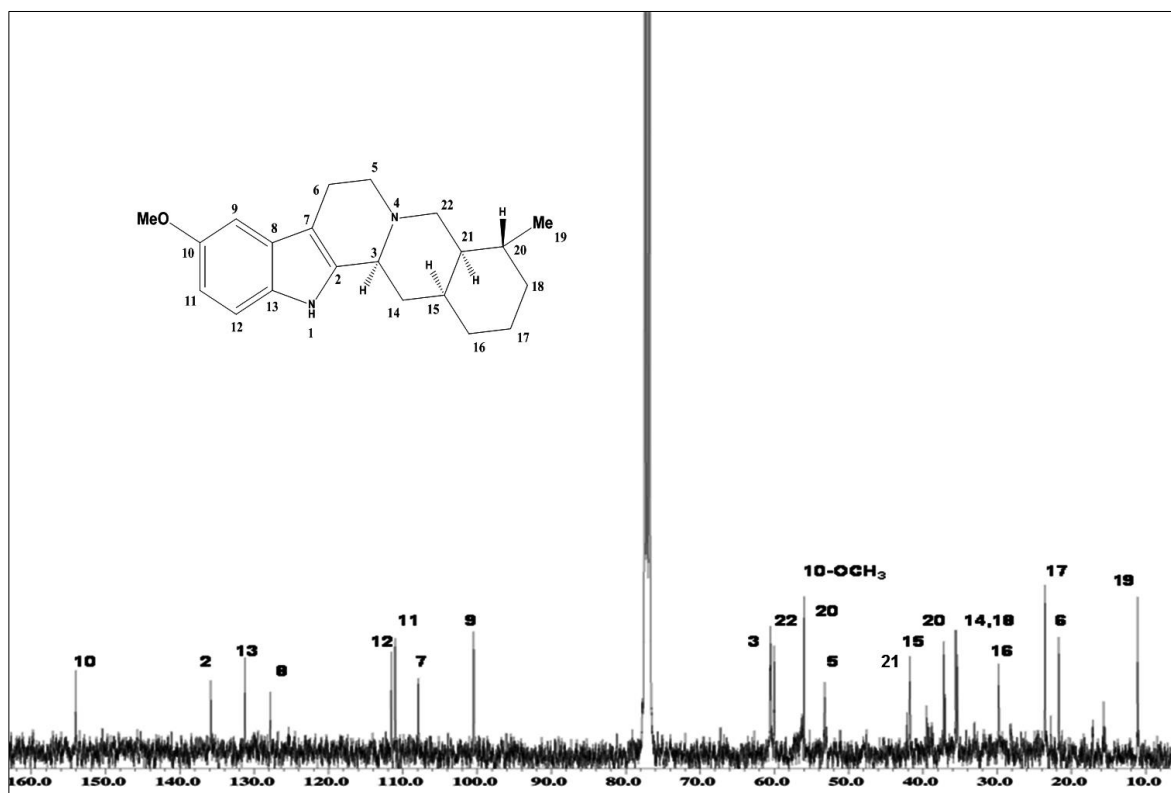


Fig. 4.17: ¹³C NMR Spectrum of Rauvolfine C (124)

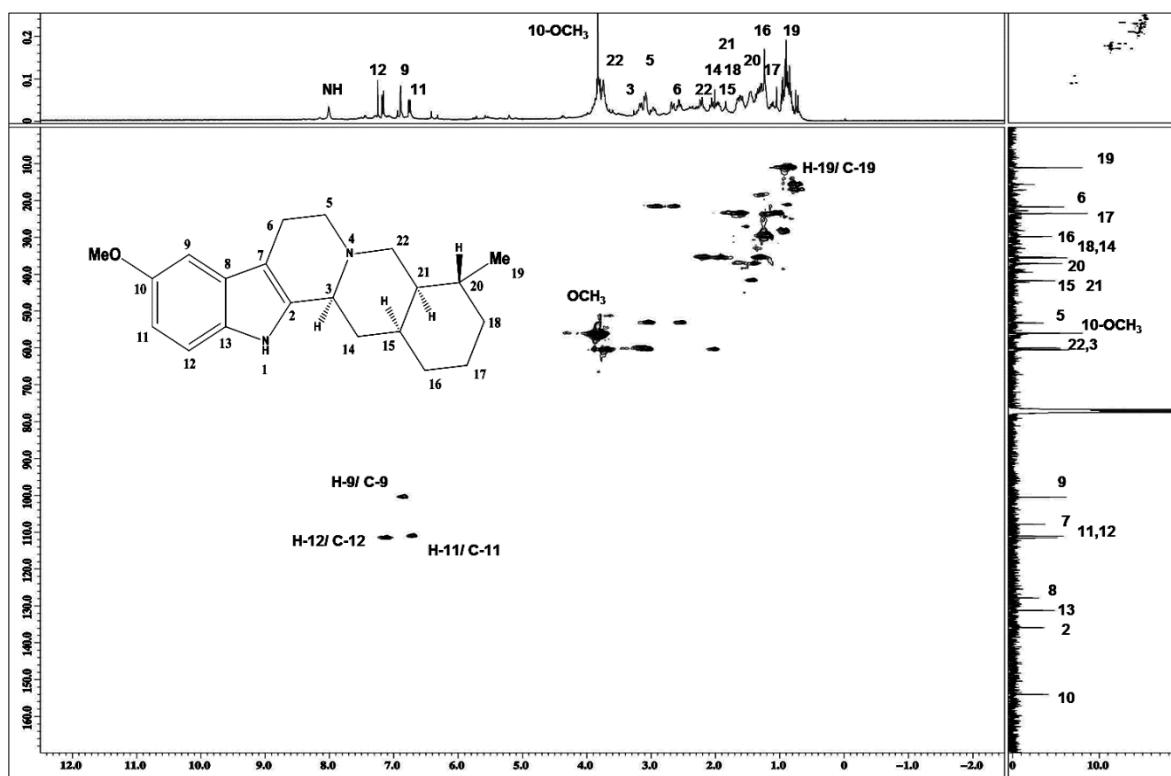


Fig. 4.18: HSQC Spectrum of Rauvolfine C (124)

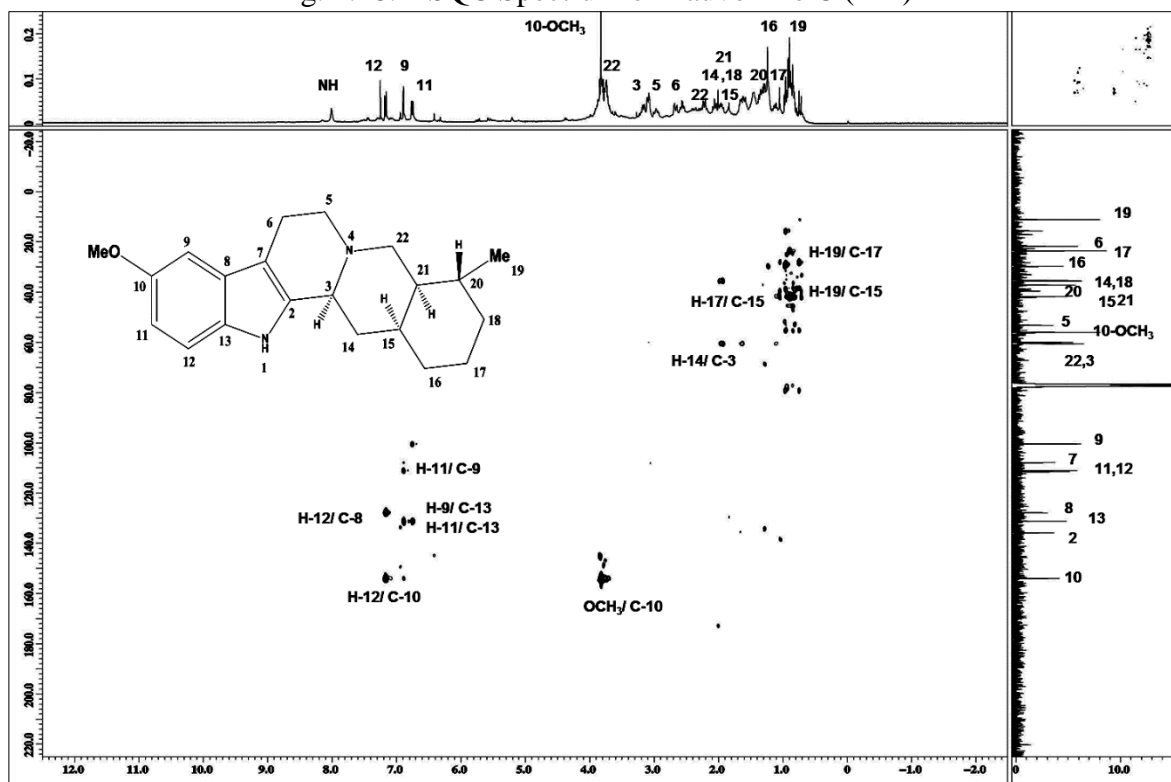


Fig. 4.19: HMBC Spectrum of Rauvolfine C (124)

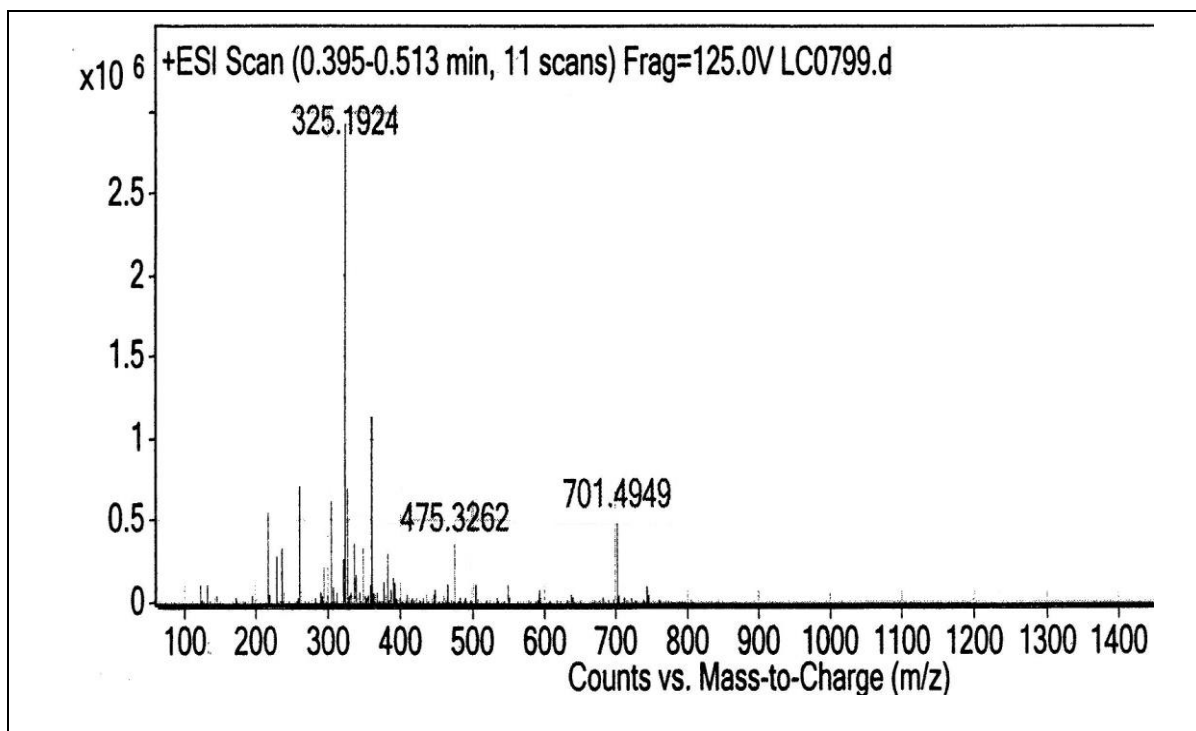
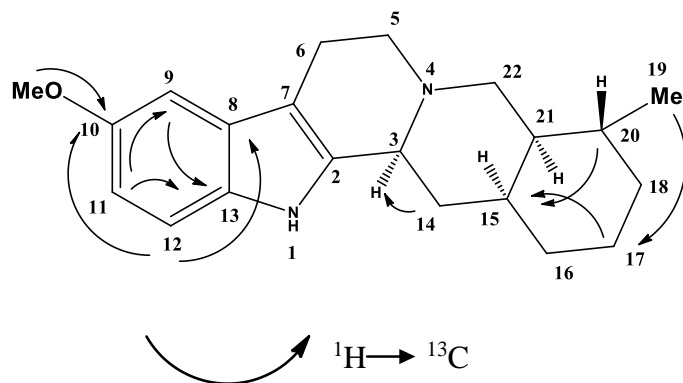
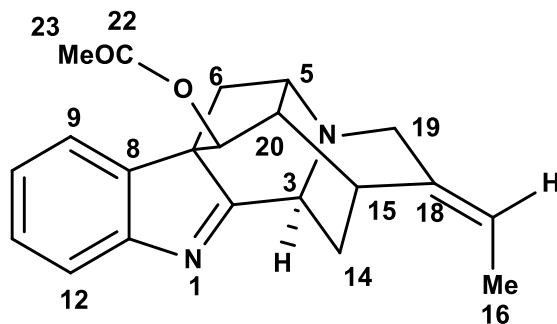


Fig. 4.20: LC-MS Spectrum of Rauvolfine C (**124**)



Scheme 4.5: The HMBC Correlations of Rauvolfine C (**124**)

4.2.1.3 Vinorine (125)



125

Vinorine (**125**) was isolated as a brownish amorphous solid. $[\alpha]_D^{24} -66$ (c 0.05, CHCl_3). The mass spectrum showed pseudo-molecular ion peak at m/z 335.1956, $[\text{M}+\text{H}]^+$, which was consistent with the molecular formula of $\text{C}_{21}\text{H}_{22}\text{N}_2\text{O}_2$.

The UV spectrum revealed maxima at 226, 299 nm which were characteristic of an unsubstituted indole chromophore (Kato et al, 2002). In addition, the IR spectrum showed a peak at 1742 cm^{-1} which indicate the presence of the carbonyl group.

The ^1H NMR spectrum (Figure 4.21) showed the presence of signals for four aromatic protons at δ 7.40 (d , $J= 8.5$ Hz, H-9), δ 7.07 (dt , $J= 1.2, 6.4$ Hz, H-10), δ 7.24 (dt , $J=1.2, 6.4$ Hz, H-11) and δ 7.40 (d , $J= 8.5$ Hz, H-12). The ^1H NMR also showed the existence of ethylidene group (δ 1.53, d , $J= 6.7$ Hz, H-16; δ 5.17, q , $J= 6.8$ Hz, H-17), one methyl signal at δ 2.02 (s) corresponding to OCOMe , three methylene signals appeared at δ 2.60 (d , $J= 4.6$ Hz, and δ 1.36 d , $J= 11.5$ Hz, H-6), δ 1.79 m , H-14 and δ 3.10 m , H-19. There are five aliphatic proton signals were observed at δ 3.12 (t , $J=5.8$ Hz, H-3), δ 2.31 (t , $J= 6.6$ Hz, H-5), δ 3.10 (m , H-15), δ 3.12 (t , $J=5.8$ Hz, H-20) and δ 3.98 (d , $J= 8.2$ Hz, H-21).

The ^{13}C NMR spectrum (Figure 4.22) showed 21 signals corresponding to five sp^2 methines, five sp^2 quaternary carbons, three sp^3 methylenes, five sp^3 methines, one sp^3 quaternary carbon and two methyl groups. Application of ^1H - ^1H COSY and C-H correlations from HSQC and HMBC (Scheme 4.6) allowed the complete assignment of all signals (Table 4.7). In conclusion, data comparison with the literature confirmed the isolation of vinorine (**125**) which previously isolated from *Rauvolfia bahiensis* (Lucilia & Raquel, 2002).

Table 4.7: ^1H NMR (400 MHz) and ^{13}C NMR (100 MHz) spectral data of vinorine (**125**) in acetone- d_6 (δ in ppm, J in Hz)

Position	^1H -NMR (δ ppm)	^{13}C -NMR (δ ppm)	^{13}C -NMR (δ ppm) (Lucilia et al, 2002)
2	-	184.7	185.0
3	3.12 (1H, <i>t</i> , J = 5.8)	58.6	58.8
5	2.31(1H, <i>t</i> , J = 6.6)	49.7	50.1
6	2.60 (1H, <i>d</i> , J = 4.6)	38.2	39.4
	1.36 (1H, <i>d</i> , J = 11.5)	-	-
7	-	65.3	65.4
8	-	140.2	141.0
9	7.40 (1H, <i>d</i> , J = 8.5)	124.8	124.8
10	7.07 (1H, <i>dt</i> , J = 1.2, 6.4)	126.1	125.8
11	7.24 (1H, <i>dt</i> , J = 1.2, 6.4)	129.1	130.1
12	7.40 (1H, <i>d</i> , J = 8.5)	121.3	122.2
13	-	158.0	158.4
14	1.79 (2H, <i>m</i>)	26.7	26.7
15	3.10 (1H, <i>m</i>)	28.4	29.4
16	1.53 (3H, <i>d</i> , J = 6.7)	13.0	12.9
17	5.17 (1H, <i>q</i> , J = 6.8)	115.2	115.2
18	-	137.8	137.8
19	3.39 (2H, <i>m</i>)	54.6	54.6
20	3.12 (1H, <i>t</i> , J = 5.8)	58.6	58.7
21	3.98 (1H, <i>d</i> , J = 8.2)	53.5	53.6
22	-	170.3	170.4
23	2.02 (3H, <i>s</i>)	21.0	21.1

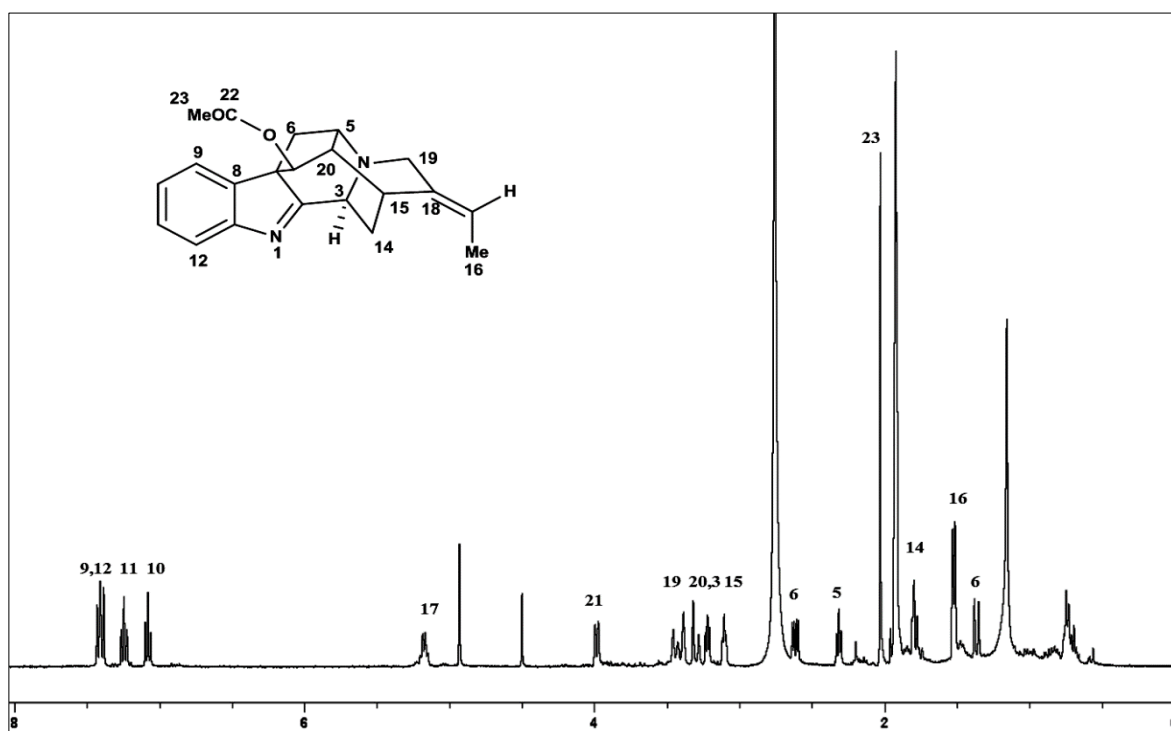


Fig. 4.21: ^1H NMR Spectrum of Vinorine (125)

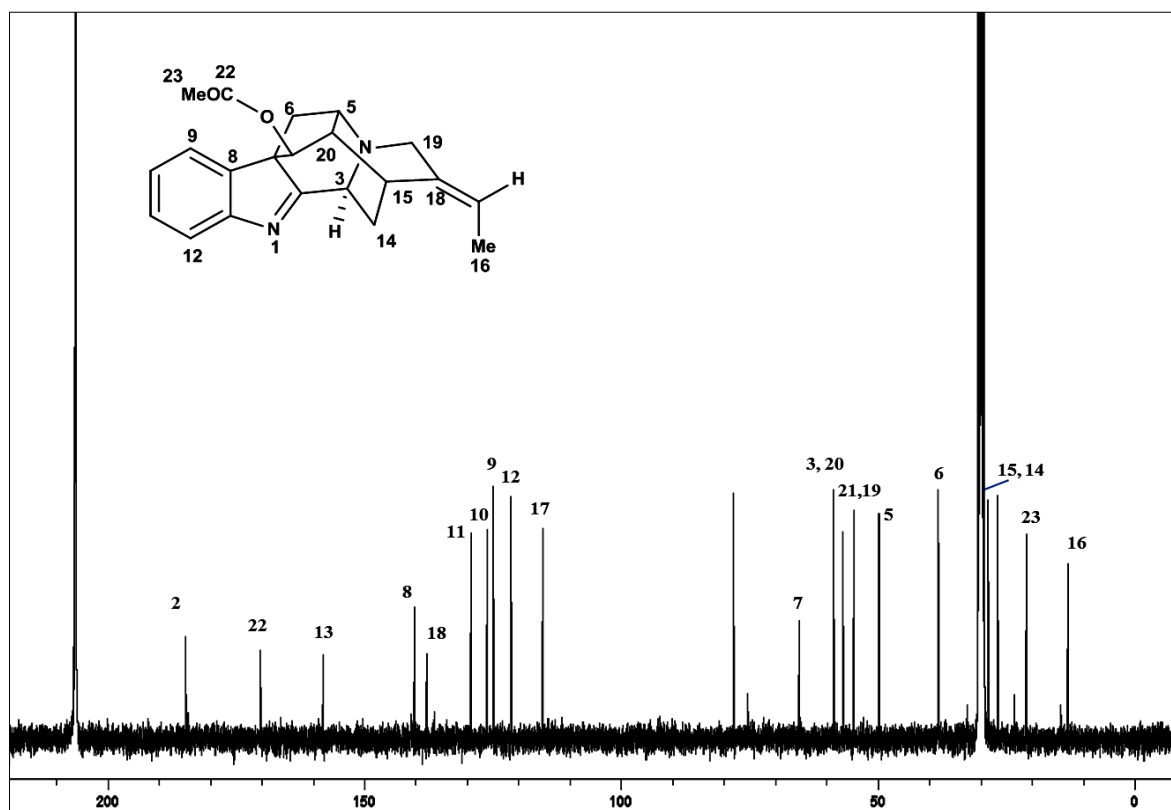


Fig. 4.22: ^{13}C NMR Spectrum of Vinorine (125)

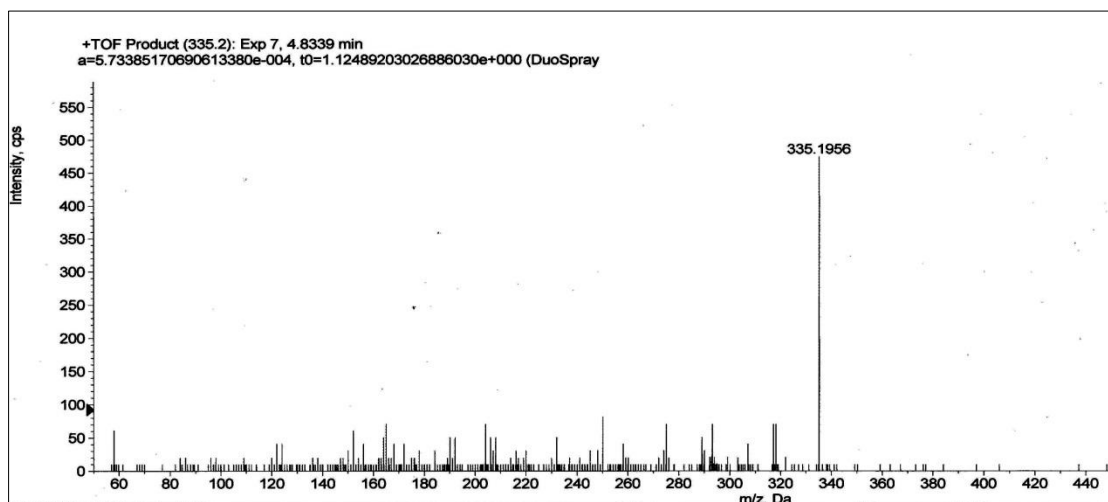
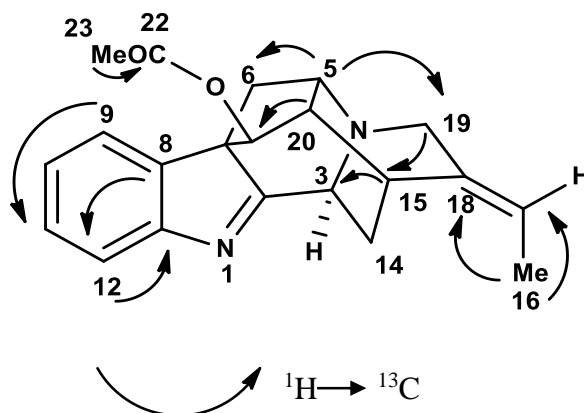
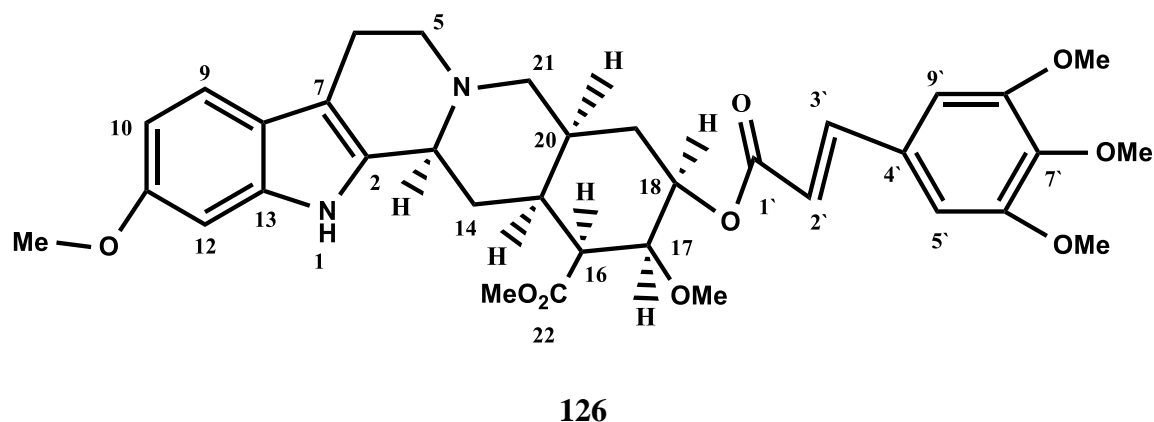


Fig. 4.23: LC-MS Spectrum of Vinorine (**125**)



Scheme 4.6: The HMBC Correlations of Vinorine (**125**)

4.2.1.4 Rescinnamine (126)



Rescinnamine (**126**) was isolated as a brownish amorphous solid. $[\alpha]_D^{24} -12$ (c 0.05, CHCl_3).

The mass spectrum revealed a pseudo-molecular ion peak at m/z 635.3518 $[\text{M}+\text{H}]^+$ corresponding to the molecular formula of $\text{C}_{35}\text{H}_{42}\text{N}_2\text{O}_9$. The UV spectrum revealed maxima at 215, 246 and 302 nm which were characteristic for an indole chromophore (Jia *et al.*, 1995). The IR spectrum displayed a band at 3368 cm^{-1} presence of the NH group. In addition, a peak was observed at 1711 cm^{-1} indicated a carbonyl group.

^1H NMR spectrum (Figure 4.24) exhibited two signals at δ 3.49 and 3.89 due to the presence of six overlapped methoxyl groups. The former was assigned to the methoxyl at C-6', C-7', C-8', C-11, C-17 and C-22. Moreover, signals at aromatic region indicated the presence of five protons attached to C-9 (δ 6.76, d , 8.0 Hz), C-10 (δ 6.76, d , 8.0 Hz), C-12 (δ 6.83, d , 1.8 Hz), C-5' (δ 7.32, d , 7.7 Hz) and C-9' (δ 7.32, d , 7.7 Hz), respectively. This was also confirmed by the aromatic carbon resonance in the HMBC spectrum (Scheme 4.7). The DEPT 135 and ^{13}C spectrum (Figure 4.25) (Table 4.8) indicated the presence of thirty five carbons, which consist of seven sp^2 methines, eleven sp^2 quaternary carbons, five sp^3 methylenes, six sp^3 methines and six methoxy groups. On the basis of the spectral data,

rescinnamine (**126**) was identified which previously isolated from *Rauvolfia serpentina* (Klohs *et al*, 1954).

Table 4.8: ^1H NMR (400 MHz) and ^{13}C NMR (100 MHz) spectral data of rescinnamine (**126**) in CDCl_3 (δ in ppm, J in Hz), ^bsignal overlapped by solvent peak.

Position	^1H -NMR (δ ppm)	^{13}C -NMR (δ ppm)	^{13}C -NMR (δ ppm) (Klohs et al, 1954)
2	-	136.3	135.0
3	3.15 (1H, <i>m</i>)	51.9	52.1
5	2.94 (2H, <i>m</i>)	53.7	52.8
6	3.03 (2H, <i>m</i>)	16.8	16.9
7	-	108.2	108.2
8	-	122.2	122.2
9	6.76 (1H, <i>d</i> , $J= 8.0$)	109.1	109.1
10	6.76 (1H, <i>d</i> , $J= 8.0$)	105.3	105.3
11	-	156.3	156.3
12	6.83 (1H, <i>d</i> , $J= 1.8$)	95.2	95.2
13		140.8	140.8
14	2.17 (2H, <i>m</i>)	29.7	29.8
15	2.16 (1H, <i>m</i>)	32.3	32.3
16	3.15 (1H, <i>m</i>)	51.2	51.3
17	4.44 (1H, <i>m</i>)	53.7	53.9
18	4.92 (1H, <i>m</i>)	77.9 ^b	76.2
19	1.81(2H, <i>m</i>)	24.3	24.2
20	1.95 (1H, <i>m</i>)	34.1	34.2
21	3.03 (2H, <i>m</i>)	49.1	50.2
22	-	172.9	168.7
1`	-	166.3	167.3
2`	6.33 (1H, <i>d</i> , $J= 16.0$)	117.4	117.3
3`	7.60 (1H, <i>d</i> , $J= 16.0$)	145.1	145.2
4`	-	130.5	130.5
5`	7.32 (1H, <i>d</i> , $J= 7.7$)	106.8	107.1
6`	-	153.0	153.2
7`	-	140.2	140.2

Position	^1H -NMR (δ ppm)	^{13}C -NMR (δ ppm)	^{13}C -NMR (δ ppm) (Klohs et al, 1954)
8`	-	153.5	153.2
9`	7.32 (1H, <i>d</i> , <i>J</i> = 7.7)	118.6	118.2
NH	7.56 (1H, <i>s</i>)	-	
OMe 6`,7`,8`,11	3.89 (12 H, <i>s</i>)	56.2	56.3
OMe 17,22	3.49 (6H, <i>s</i>)	61.0	61.2

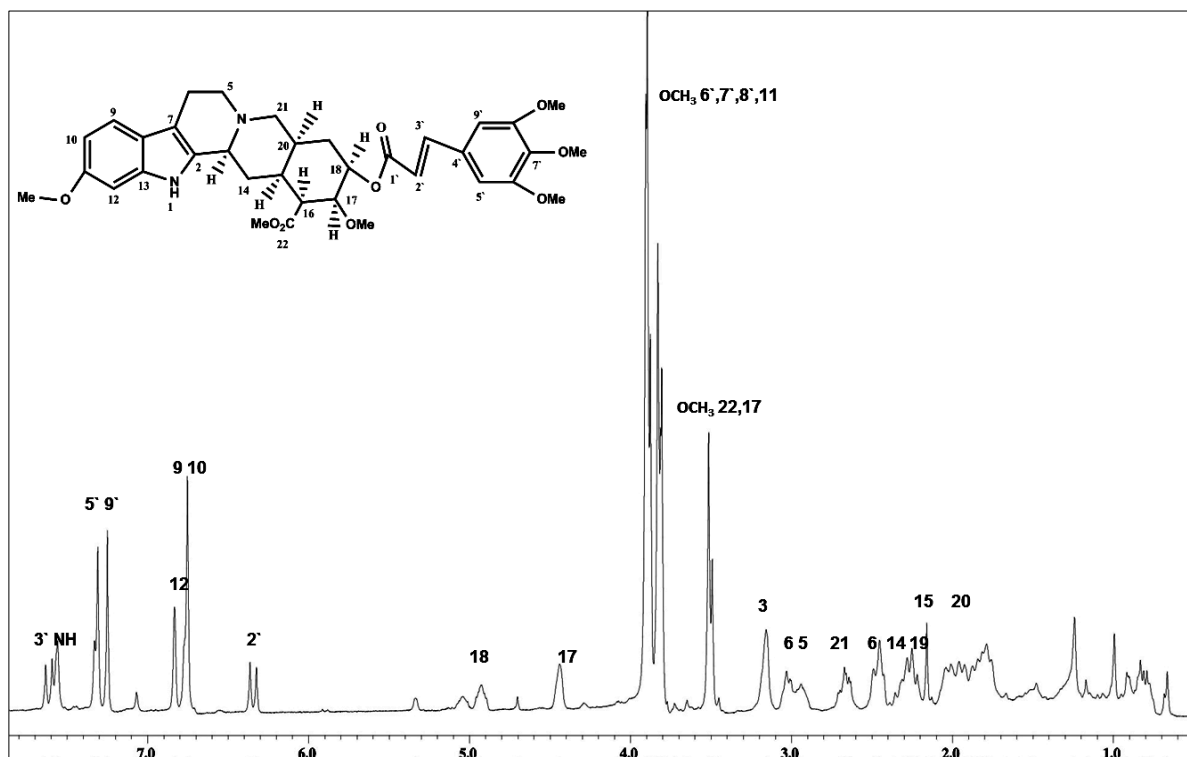


Fig. 4.24: ^1H NMR Spectrum of Rescinnamine (126)

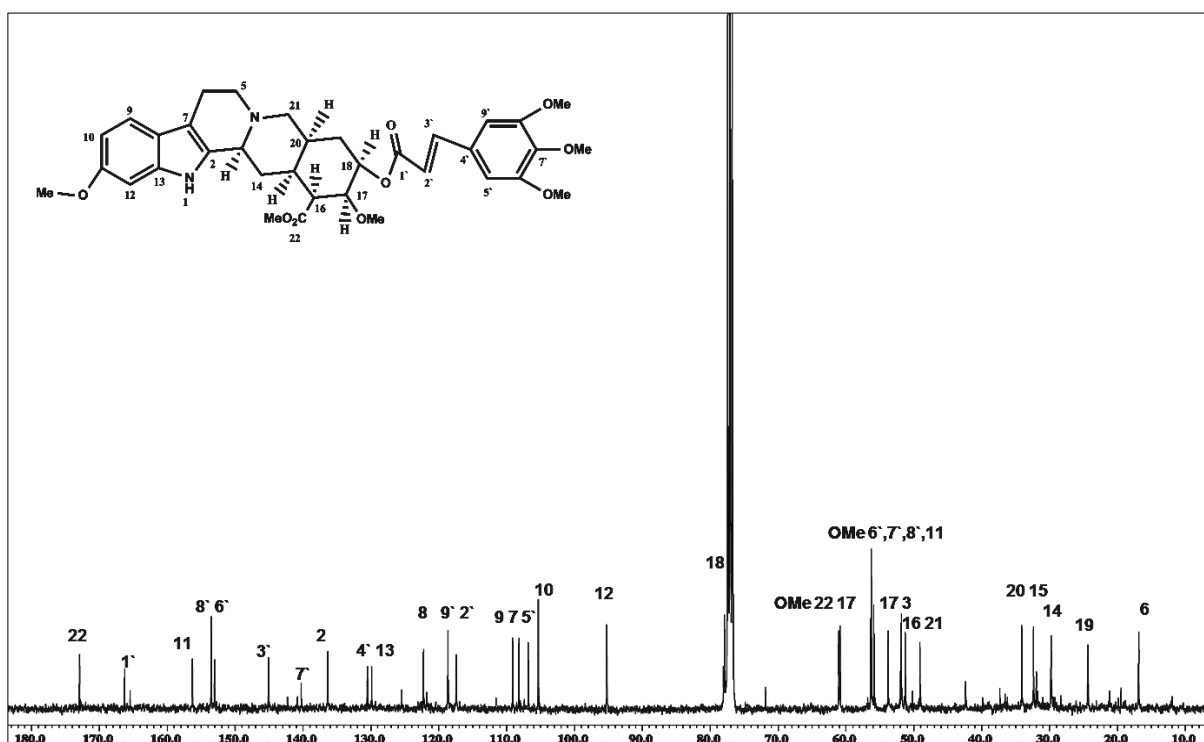


Fig. 4.25: ^{13}C NMR Spectrum of Rescinnamine (126)

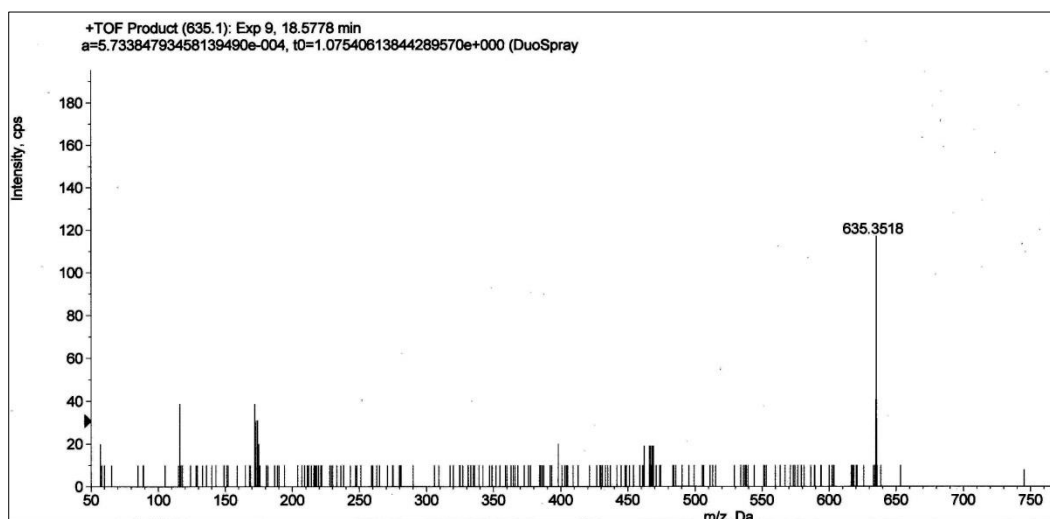
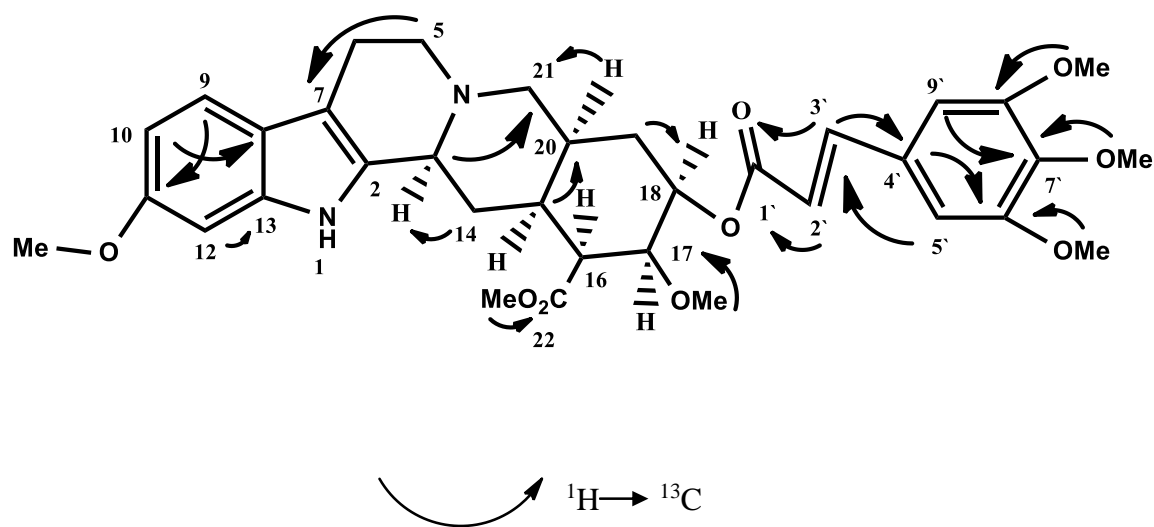
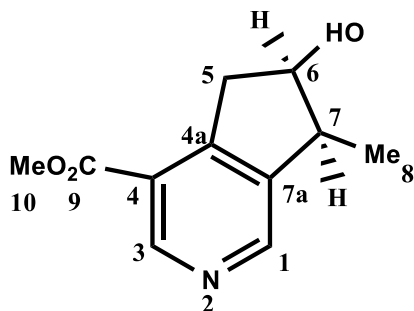


Fig. 4.26: LC-MS Spectrum of Rescinnamine (126)



Scheme 4.7: The HMBC Correlations of Rescinnamine (**126**)

4.2.1.5 Cantleyine (**127**)



127

Cantleyine (**127**) was isolated as a brownish amorphous solid. $[\alpha]_{\text{D}}^{24} -40$ (c 0.05, CHCl_3). The LC- Ms spectrum showed a $[\text{M}+\text{H}]^+$ ion peak at m/z 208.10 matched with the molecular formula of $\text{C}_{11}\text{H}_{13}\text{NO}_3$. The IR spectrum displayed a stretching of OH at 3402 cm^{-1} . In addition, a peak was observed at 1706 cm^{-1} which indicated the presence of the carbonyl group. The UV spectrum revealed maxima at 222 and 283 nm

The ^1H NMR spectrum (Figure 4.27) revealed a number of important features, including the presence of two aromatic protons at δ (8.51, *s*, H-1) and δ (9.00, *s*, H-3), one methoxy group at δ (3.88, *s*, OMe-10), two methines at δ (4.61, *m*, H-6) and (3.25, *m*, H-7), one methylene at δ (3.41, *d*, $J=1.8$ Hz), δ (3.37, *d*, $J= 5.0$ Hz, H-5) and one methyl group δ (1.41, *d*, $J= 7.3$ Hz).

The ^{13}C NMR spectrum (Figure 4.28) of cantleyine (**127**) showed eleven carbon signals corresponding to the eleven carbon atoms, whereas the DEPT 135 experiment displayed the presence of one methylene, two aromatic carbons, two aliphatic carbons and one methoxy group. The quaternary carbonyl carbon appeared at δ 166.2 and the remaining three quaternary carbon signals were observed at δ 123.1, 153.0 and 142.4. The complete assignment of ^1H and ^{13}C were aided by the HSQC, COSY and HMBC (Scheme 4.8) experiments and were listed in Table 4.9.

The analysis of the accumulated data and comparison with literature values confirms the isolation of cantleyine (**127**) which previously isolated from *Strychnos trinervis* (da Silva *et al.*, 1999).

Table 4.9: ^1H NMR (400 MHz) and ^{13}C NMR (100 MHz) spectral data of cantleyine (**127**) in CDCl_3 (δ in ppm, J in Hz).

Position	^1H -NMR (δ ppm)	^{13}C -NMR (δ ppm)	^{13}C -NMR (δ ppm)
			(da silva et al, 1999)
1	8.51(1H, <i>s</i>)	149.5	150.0
3	9.00 (1H, <i>s</i>)	148.3	148.3
4	-	123.1	123.3
4a	-	153.0	153.0
5	3.41 (2H, <i>d</i> , $J= 1.8$)	42.2	42.3
6	4.61 (1H, <i>m</i>)	76.7	76.8
7	3.25 (1H, <i>m</i>)	42.5	42.3
7a	-	142.4	142.5
8	1.41 (3H, <i>d</i> , $J= 7.3$)	11.9	11.9
9	-	166.2	166.2
OMe-10	3.88 (3H, <i>s</i>)	52.2	52.2

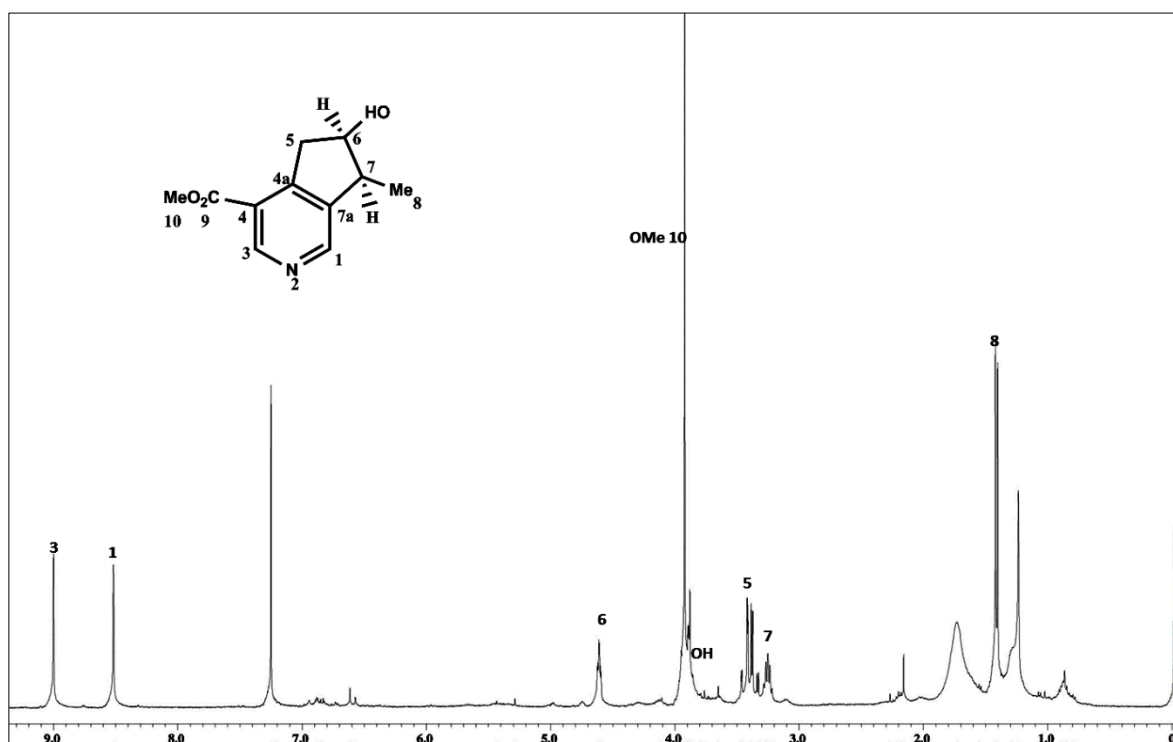


Fig. 4.27: ^1H NMR Spectrum of Cantleyine (127)

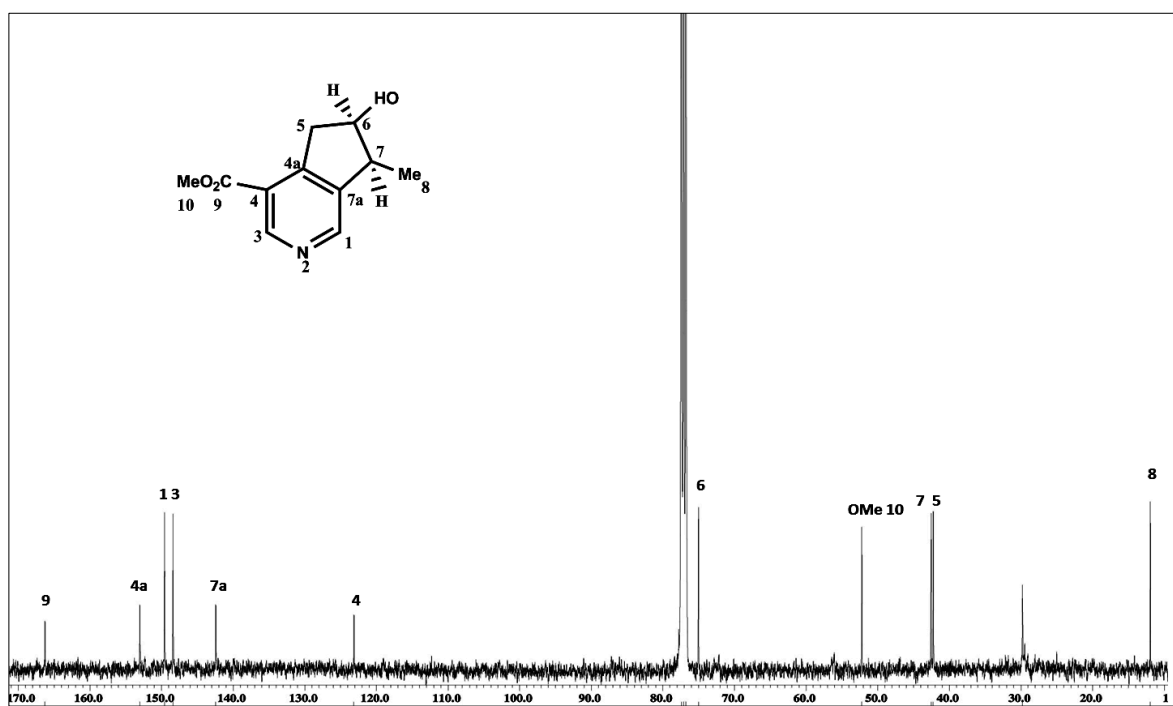


Fig. 4.28: ^{13}C NMR Spectrum of Cantleyine (127)

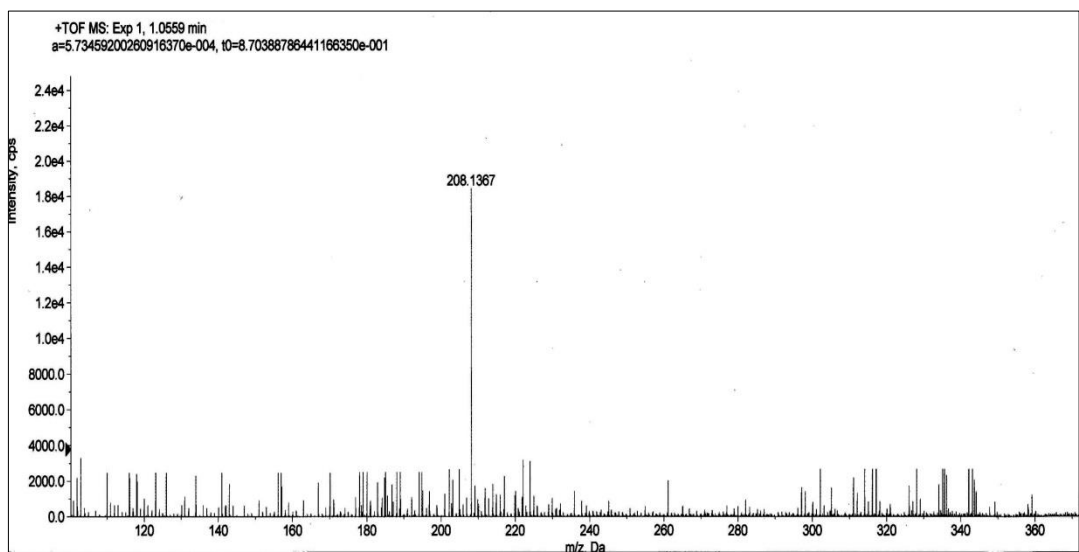
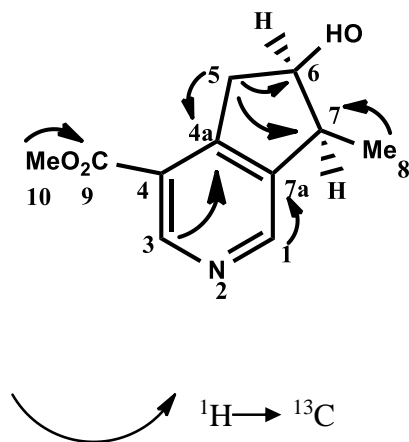
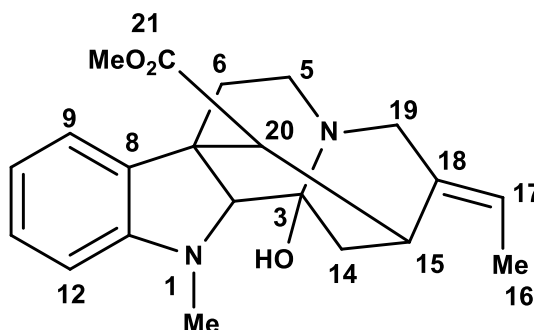


Fig. 4.29: LC-MS Spectrum of Cantleyine (**127**)



Scheme 4.8: The HMBC Correlations of Cantleyine (**127**)

4.2.1.6 Akuammilan-17-oic acid, 1,2-dihydro-3-hydroxy-1-methyl-, methyl ester (128)



128

Akuammilan (**128**) was isolated as a brownish amorphous solid. $[\alpha]_D^{24} -63$ (*c* 0.05, CHCl₃).

The mass spectrum revealed a pseudo-molecular ion peak at *m/z* 355.1409 [M+H]⁺ corresponding to the molecular formula of C₂₁H₂₆N₂O₃. The UV spectrum revealed maximum at 250, 285 nm. The IR spectrum showed a peak at 1706 cm⁻¹ which indicated the presence of the carbonyl group and the band of OH at 3378 cm⁻¹.

The ¹H NMR spectrum (Figure 4.30) showed the presence of signals for four aromatic protons at δ 7.51 (*dd*, *J*= 7.6, 2.1 Hz, H-9), δ 6.67 (*t*, *J*= 7.7, 2.1 Hz, H-10), δ 7.03 (*t*, *J*=7.7, 2.1 Hz, H-11) and δ 6.51(*dd*, *J*= 7.6, 2.1 Hz, H-12). The ¹H NMR also showed the existence of an ethylidene group (δ 1.73, *d*, *J*= 6.0 Hz, H-16; δ 5.50, *q*, *J*= 6.3 Hz, H-17), one *N*-methyl signal at δ 2.00 (*s*) and one methoxy group at δ 3.83 (*s*) corresponding to OCOMe, four methylene signals appeared at (δ 4.37, *m*, and 3.14, *m*, H-5), (δ 2.43, *m*, and 2.22, *m*, H-6), (δ 1.63, *m*, and 2.65, *m*, H-14) and (δ 3.97, *d*, *J*=14.6 Hz and 3.38, *d*, *J*= 12.3 Hz, H-19). There are three aliphatic proton signals were observed at δ 4.35 (*s*, H-2), δ 2.87 (*m*, H-15), and δ 3.13 (*d*, *J*=16.4 Hz, H-20).

The ^{13}C NMR spectrum (Figure 4.31) showed 21 signals corresponding to five sp^2 methines, four sp^2 quaternary carbons, four sp^3 methylenes, three sp^3 methines, two sp^3 quaternary carbon, one methyl, one methoxy and one *N*-Me group. Application of ^1H - ^1H COSY and C-H correlations from HSQC and HMBC (Scheme 4.10) allowed the complete assignment of all signals (Table 4.9). In conclusion, data comparison with the literature confirmed the isolation of Akuammilan-17-oic acid, 1, 2-dihydro-3-hydroxy-1-methyl-, methyl ester (**128**). (Massiot *et al.*, 1983).

Table 4.10: ^1H NMR (400 MHz) and ^{13}C NMR (100 MHz) spectral data of akuammilan (**128**) in CDCl_3 (δ in ppm, J in Hz).

Position	^1H -NMR (δ ppm)	^{13}C -NMR (δ ppm)	^{13}C -NMR (δ ppm) (Massiot et al, 1983)
2	4.35 (1H, <i>s</i>)	69.1	70.1
3	-	96.2	96.2
5	4.37 (1H, <i>m</i>)	53.3	53.2
	3.14 (1H, <i>m</i>)	-	-
6	2.43 (1H, <i>m</i>)	31.7	31.8
	2.22 (1H, <i>m</i>)	-	-
7	-	60.6	59.7
8	-	130.8	130.8
9	7.51 (1H, <i>dd</i> , $J=7.6, 2.1$)	126.4	126.4
10	6.67 (1H, <i>t</i> , $J=7.7, 2.1$)	118.7	118.8
11	7.03 (1H, <i>t</i> , $J=7.7, 2.1$)	128.7	128.7
12	6.51 (1H, <i>dd</i> , $J=7.6, 2.1$)	109.8	109.8
13	-	148.4	148.2
14	1.63 (1H, <i>m</i>)	29.8	29.6
	2.65 (1H, <i>m</i>)	-	-
15	2.87 (1H, <i>m</i>)	55.8	55.9
16	1.73 (3H, <i>d</i> , $J=6.0$)	14.4	14.6
17	5.50 (1H, <i>q</i> , $J=6.3$)	118.7	118.8
18	-	136.6	136.6
19	3.97 (1H, <i>d</i> , $J=14.6$)	66.9	67.2
	3.38 (1H, <i>d</i> , $J=12.3$)	-	-
20	3.13 (1H, <i>d</i> , $J=16.4$)	45.7	45.7
21	-	174.5	174.2
OH	6.15 (1H, <i>br s</i>)	-	-
N- Me	2.00 (3H, <i>s</i>)	36.3	36.3
OMe	3.83 (3H, <i>s</i>)	52.0	52.1

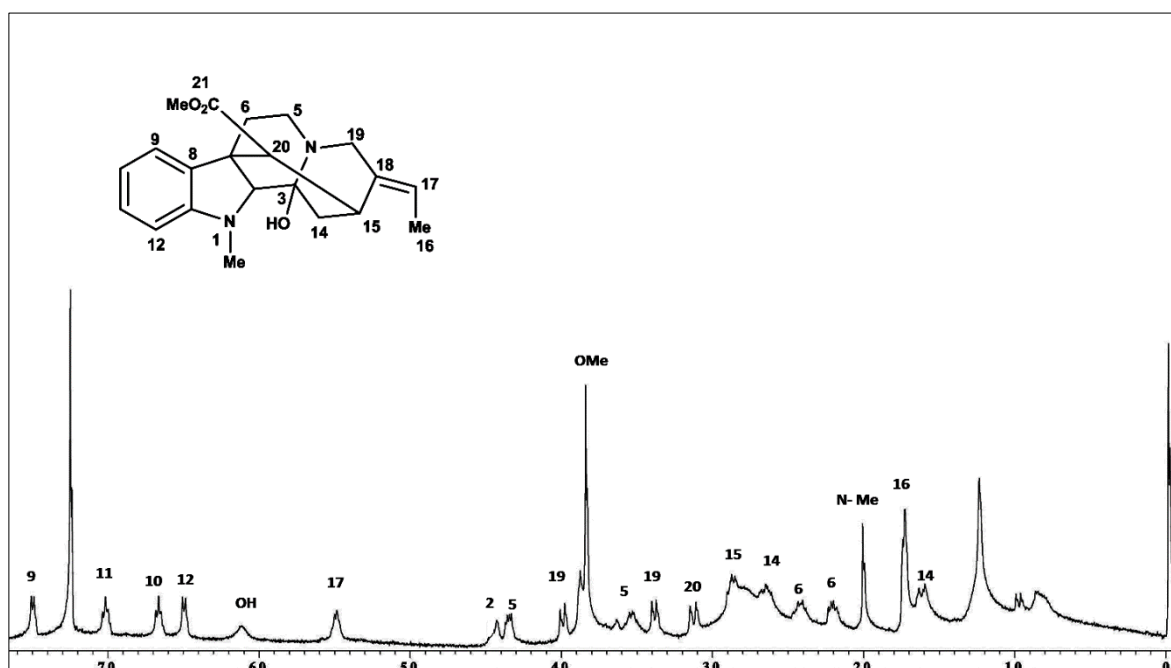


Fig. 4.30: ^1H NMR Spectrum of Akuammilan (128)

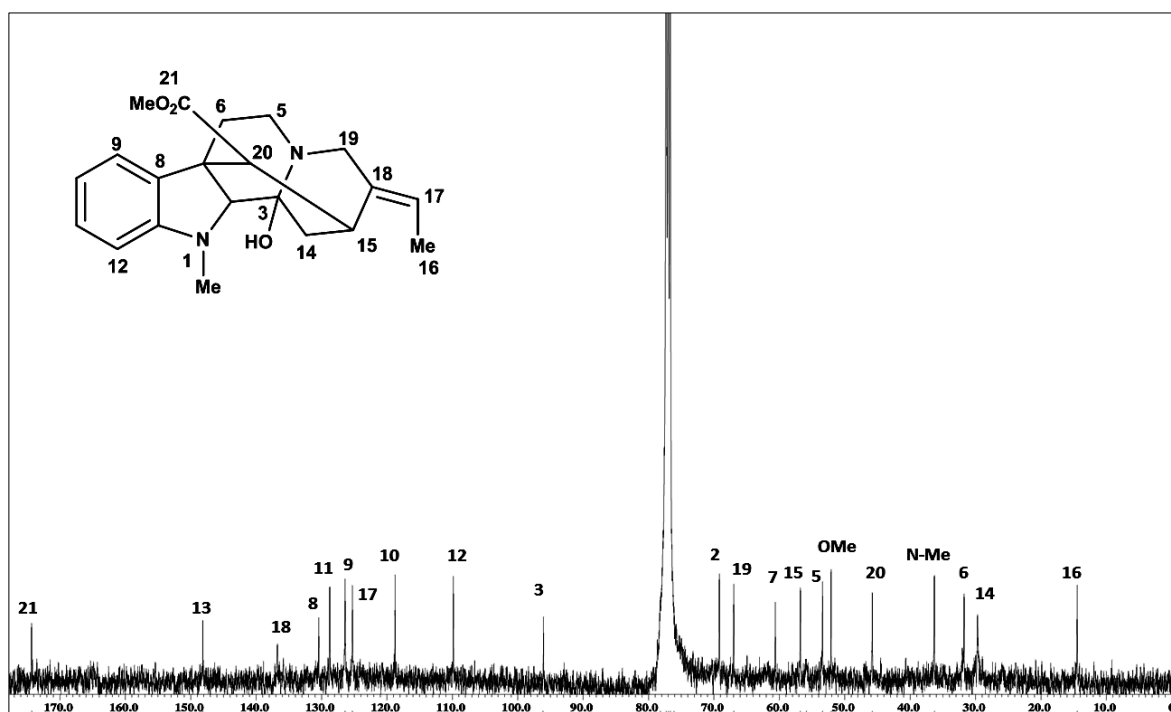


Fig. 4.31: ^{13}C NMR Spectrum of Akuammilan (128)

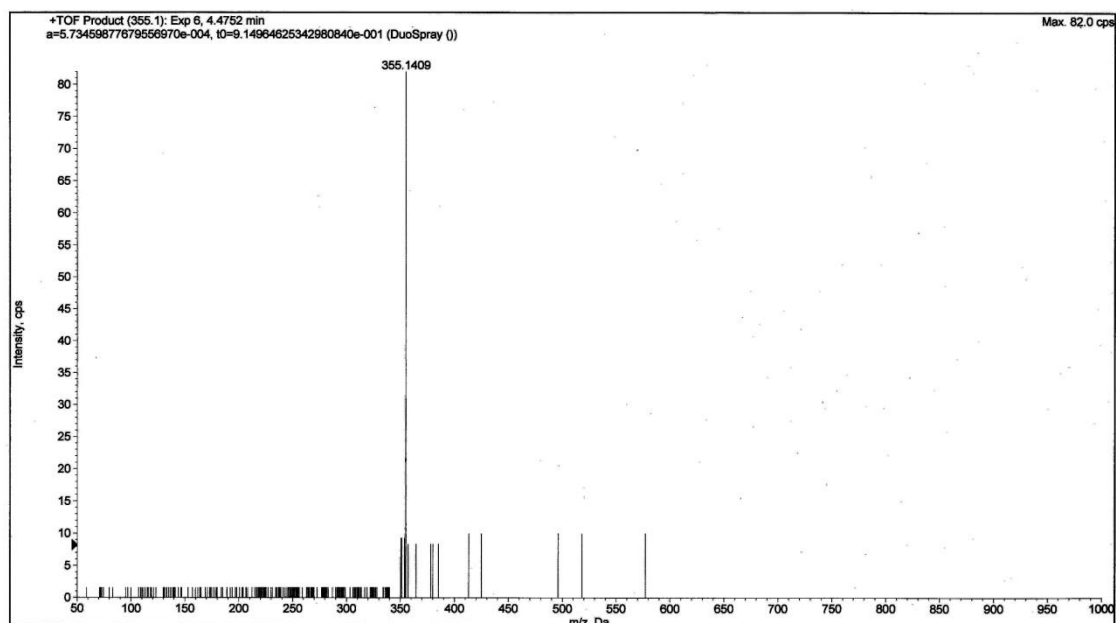
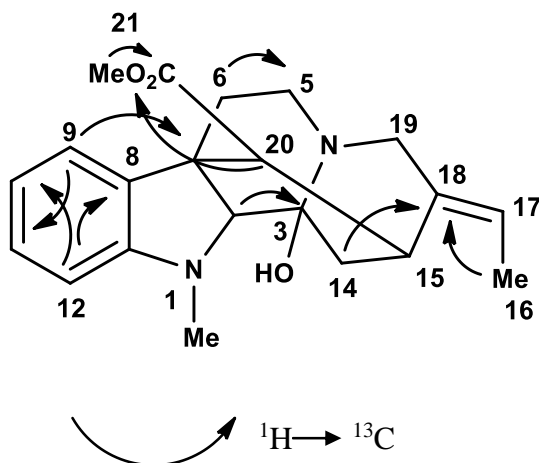
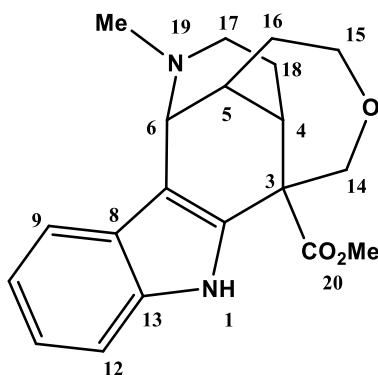


Fig. 4.32: LC-MS Spectrum of Akuammilan (**128**)



Scheme 4.9: The HMBC Correlations of Akuammilan (**128**)

4.2.1.7 Undulifoline (129)



129

Undulifoline (**129**) was isolated as a whitish amorphous solid. $[\alpha]_D^{24} -33$ (*c* 0.05, CHCl_3).

The mass spectrum revealed a pseudo-molecular ion peak at m/z 341.18 $[\text{M}+\text{H}]^+$ corresponding to the molecular formula of $\text{C}_{20}\text{H}_{24}\text{N}_2\text{O}_3$. The UV spectrum revealed maximum at 196, 273 and 328 nm which were characteristic of an indole system (Kam & Choo, 2004). The IR spectrum showed a broad band of NH at 3401 cm^{-1} . In addition, a peak was observed at 1704 cm^{-1} which indicated the presence of a carbonyl of an ester.

The ^1H NMR spectrum (Figure 4.33) showed four aromatic protons located at ring A. In aliphatic region, four signals at δ 4.13, 3.84, 3.47 and 3.71 were observed for two methylene attached to oxygen, H-14 and H-15 respectively. Two singlet signals were appeared at δ 2.33 and 3.77 attributed to one *N*-Me and a methoxyl group respectively.

The ^{13}C NMR spectrum (Figure 4.34) showed the presence of twenty carbon atoms; five quaternary carbons δ (136.9, 135.1, 128.7, 106.3 and 55.5), four methane aromatic carbons δ (122.1, 119.9, 118.8 and 111.4), three methane aliphatic carbons δ (58.9, 39.9 and 37.7),

five methylene carbons δ (69.6, 46.0, 33.0, 31.4 and 29.7), one methoxyl carbon δ (52.5) attached to the carbonyl carbon, consistent with the structure proposed.

The complete assignments of all carbons and protons (Table 4.11) were confirmed with DEPT, HSQC and HMBC spectra (Scheme 4.10). Analysis of all spectral data obtained and comparison with literature led to the conclusion that this alkaloid is undulifoline (**129**) which previously isolated from *Alstonia angustiloba* (Ku *et al.*, 2011).

Table 4.11: ^1H NMR (400 MHz) and ^{13}C NMR (100 MHz) spectral data of undulifoline (**129**) in CDCl_3 (δ in ppm, J in Hz).

Position	^1H -NMR (δ ppm)	^{13}C -NMR (δ ppm)	^{13}C -NMR (δ ppm) (Ku et al, 2011)
2	-	135.1	136.0
3	-	55.5	55.6
4	2.46 (1H, <i>m</i>)	39.9	39.8
5	2.01 (1H, <i>m</i>)	37.7	37.8
6	4.03 (1H, <i>d</i> , $J=1.4$)	58.6	58.7
7	-	106.3	106.3
8	-	128.7	128.2
9	7.47 (1H, <i>dd</i> , $J=7.8, 2.0$)	118.8	118.9
10	7.10 (1H, <i>t</i> , $J=7.0, 2.1$)	119.9	120.0
11	7.04 (1H, <i>t</i> , $J=7.3, 2.0$)	122.1	122.2
12	7.31 (1H, <i>dd</i> , $J=7.7, 2.0$)	111.4	112.5
13	-	136.9	136.9
14	4.13 (1H, <i>d</i> , $J=11.2$)	31.4	31.4
	3.84 (1H, <i>d</i> , $J=11.2$)	-	-
15	3.47 (1H, <i>m</i>)	69.6	70.2
	3.71 (1H, <i>m</i>)	-	-
16	0.92 (2H, <i>m</i>)	33.0	33.1
17	2.78 (2H, <i>m</i>)	46.0	46.1
18	1.62 (2H, <i>m</i>)	29.7	29.6
N-Me	2.33 (3H, <i>s</i>)	43.6	43.7
20	-	172.6	172.6
OMe	3.77 (3H, <i>s</i>)	52.5	52.5
NH	8.54 (1H, <i>s</i>)	-	-

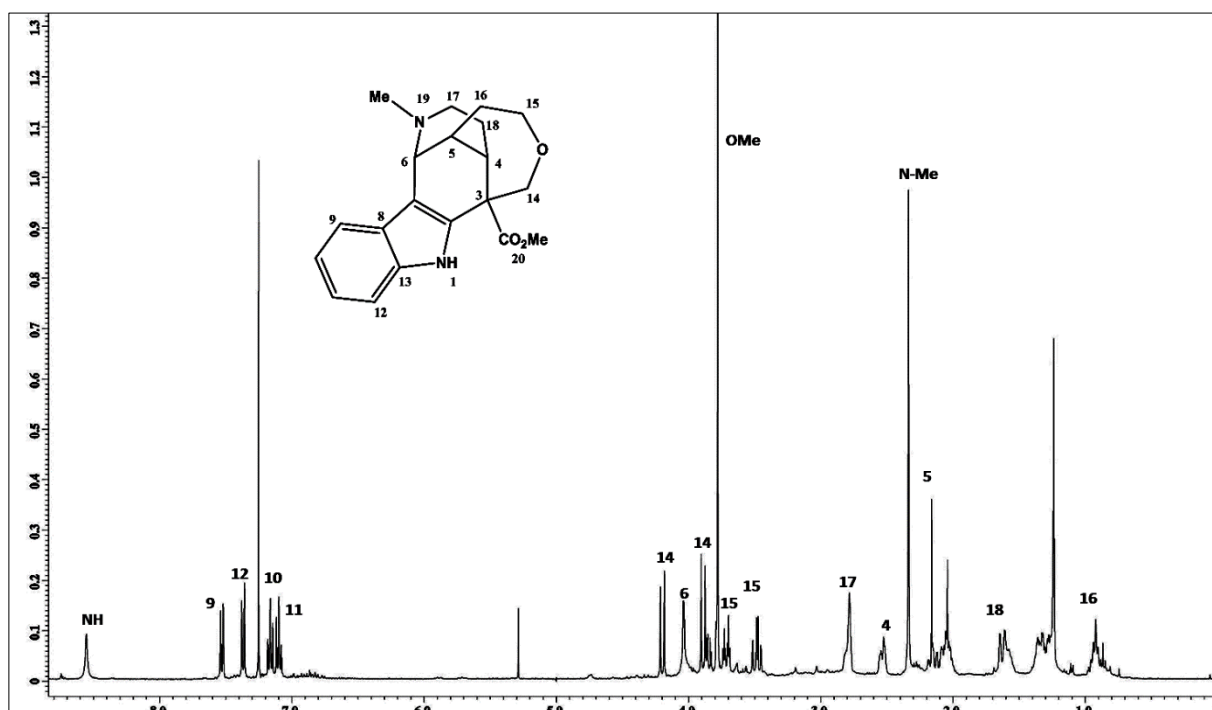


Fig. 4.33: ^1H NMR Spectrum of Undulifoline (129)

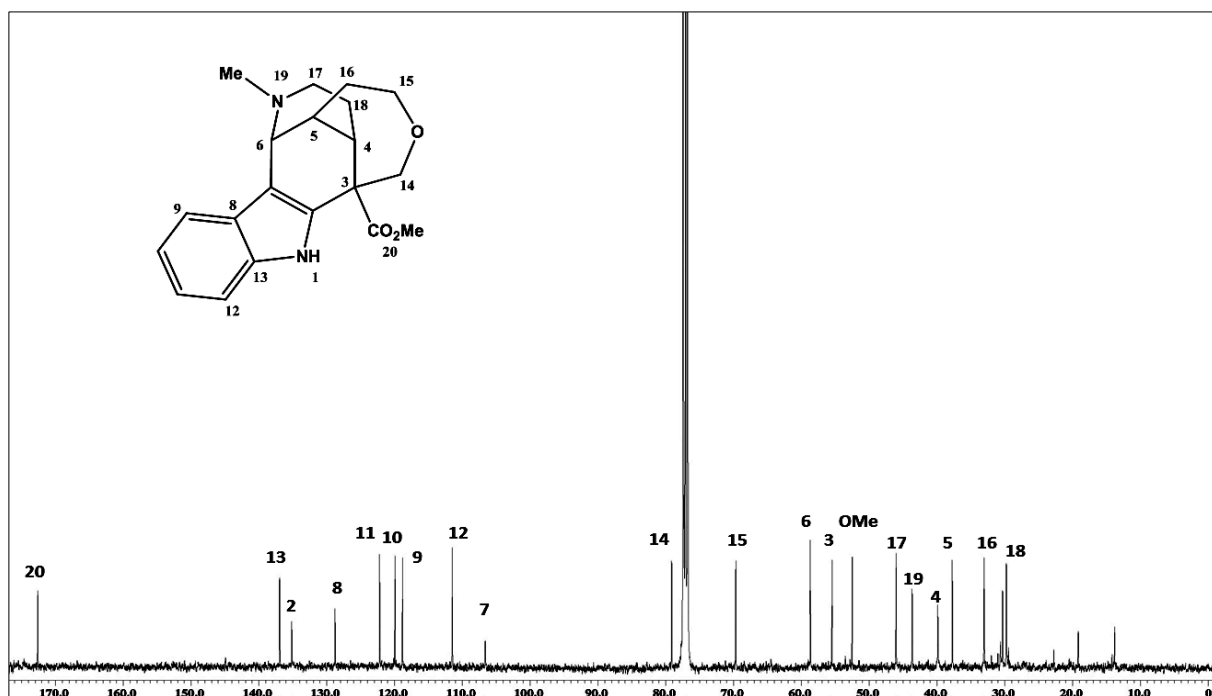


Fig. 4.34: ^{13}C NMR Spectrum of Undulifoline (129)

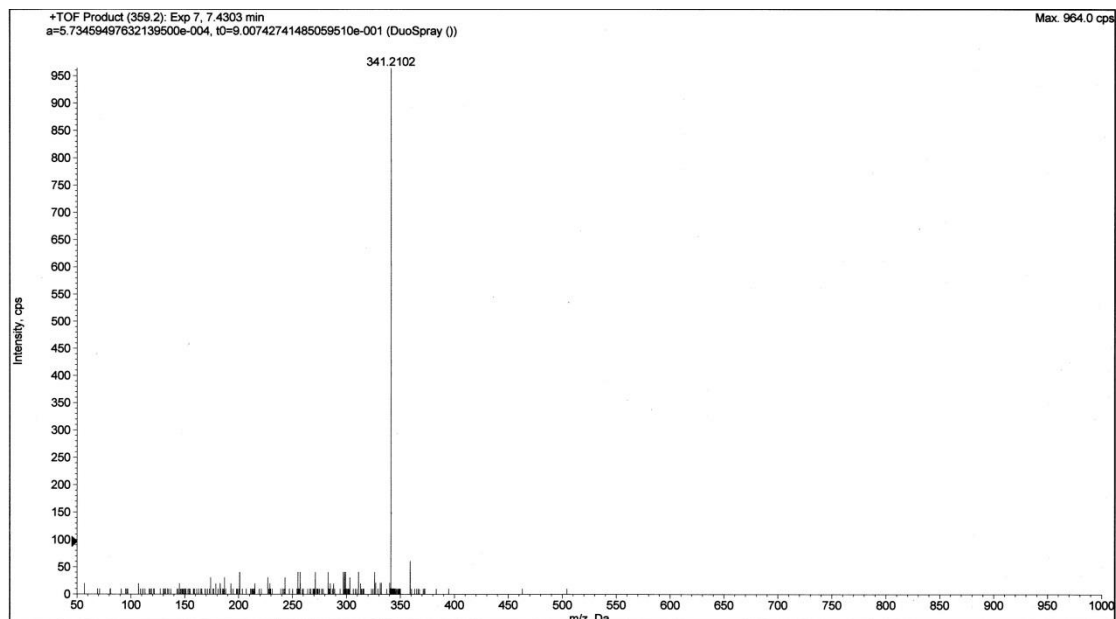
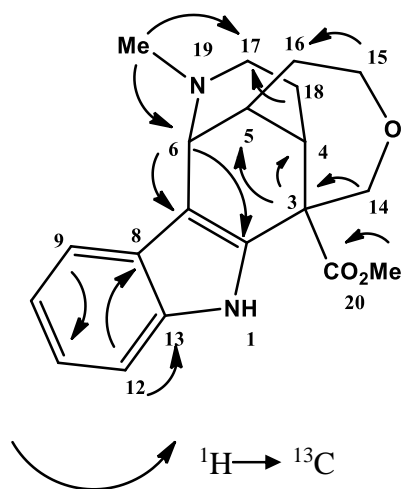
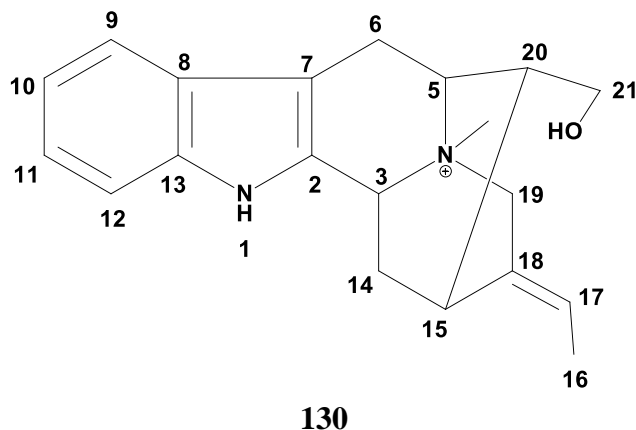


Fig. 4.35: LC-MS Spectrum of Undulifoline (**129**)



Scheme 4.10: The HMBC Correlations of Undulifoline (**129**)

4.2.1.8 Macusine B (130)



Macusine B (**130**) was isolated as a whitish amorphous solid. $[\alpha]_D^{24} +12$ (c 0.05, CHCl_3).

The mass spectrum revealed a pseudo-molecular ion peak at m/z 309.2270 $[\text{M}+\text{H}]^+$ corresponding to the molecular formula of $\text{C}_{20}\text{H}_{25}\text{N}_2\text{O}$. The UV spectrum revealed maximum at 196, 273 and 328 nm. The IR spectrum showed a band of OH at 3431 cm^{-1} .

The ^1H MNR spectrum (Figure 4.36) showed an unsubstituted aromatic ring at the range of δ 7.00 till 7.40 ppm, a broad peak at δ 8.52 indicated of a NH group and a ethylidene group (δ 1.71, d , $J= 6.8\text{ Hz}$, H-16; δ 5.63, m , H-17). A $\text{N}^+\text{-Me}$ group at δ 3.08 (s) which is a strong electron withdrawing group let the H-3, H-5 and H- 19 appear at δ 4.87, m ; 3.52, m and δ 4.42 d (16.0 Hz), 4.20 d (16.0 Hz) respectively and another signal that was shifted downfield at δ 3.52 corresponding for two protons at C-21. This condition may be due to the presence of a hydroxyl group attached to C-21.

The ^{13}C NMR (Figure 4.37) and DEPT 135 indicated the presence of five sp^2 methines, five sp^2 quaternary carbons, four sp^3 methylenes, four sp^3 methines, one methyl and one N -methyl group. In addition, the HMBC spectrum revealed correlations of H-15 to C-3, H-14 to C-2, H17 to C-15 and C-19, H-20 to C-6 and the correlations between aromatic protons

and carbons in J_2 and J_3 (Scheme 4.11). Through examination of ^1H , ^{13}C , (Table 4.12), DEPT, COSY, HSQC and HMBC spectra has made possible the complete assignments. In conclusion, data comparison with the literature confirmed the isolation of macusine B (**130**) previously isolated from the roots of *Rauvolfia serpentina* (Sheludko *et al.*, 2002).

Table 4.12: ^1H NMR (400 MHz) and ^{13}C NMR (100 MHz) spectral data of macusine B (**130**) in MeOD (δ in ppm, J in Hz), ^bsignal overlapped by solvent peak

Position	^1H -NMR (δ ppm)	^{13}C -NMR (δ ppm)	^{13}C -NMR (δ ppm) (Scheludku et al, 2002)
2	-	132.5	133.2
3	4.87 ^b	62.4	62.5
5	3.52 (1H, <i>m</i>)	71.7	71.7
6	3.11 (1H, <i>m</i>)	25.2	25.2
	3.29 (1H, <i>m</i>)	-	-
7	-	101.9	102.0
8	-	127.4	127.5
9	7.50 (1H, <i>dd</i> , $J=7.8, 2.2$)	119.3	119.3
10	7.08 (1H, <i>t</i> , $J=7.5, 2.0$)	120.9	120.9
11	7.18 (1H, <i>t</i> , $J=7.0, 2.0$)	123.8	123.3
12	7.38 (1H, <i>dd</i> , $J=8.0, 2.2$)	112.6	112.7
13	-	138.8	138.9
14	2.52 (2H, <i>m</i>)	33.3	33.3
15	3.11 (1H, <i>m</i>)	27.4	27.5
16	1.71 (3H, <i>d</i> , $J=6.8$)	12.9	13.1
17	5.63 (1H, <i>m</i>)	122.1	122.1
18	-	129.0	129.1
19	4.42 (1H, <i>d</i> , $J=16.0$)	66.8	66.9
	4.20 (1H, <i>d</i> , $J=15.8$)	-	-
20	2.16 (1H, <i>m</i>)	45.0	45.1
21	3.52 (2H, <i>m</i>)	63.8	63.1
N-Me	3.08 (3H, <i>s</i>)	49.0 ^b	49.2
NH	8.52 (1H, <i>s</i>)	-	-

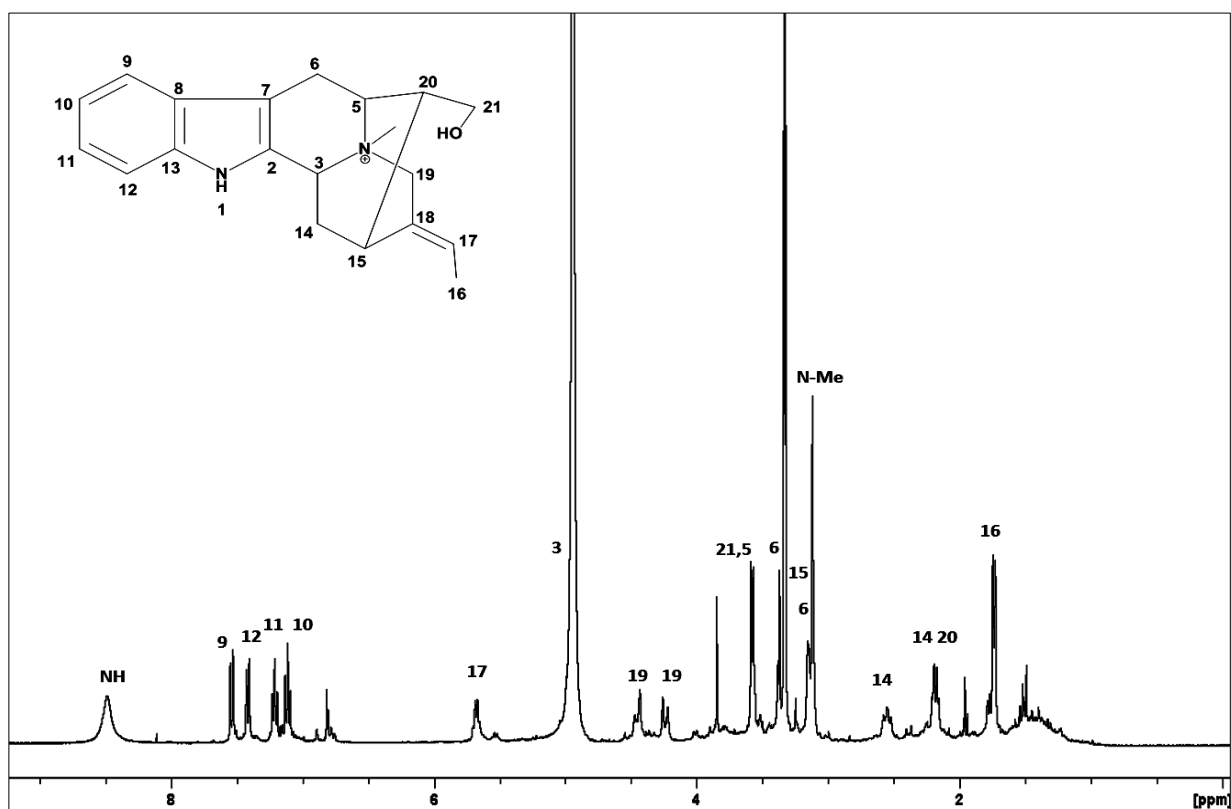


Fig. 4.36: ^1H NMR Spectrum of Macusine B (130)

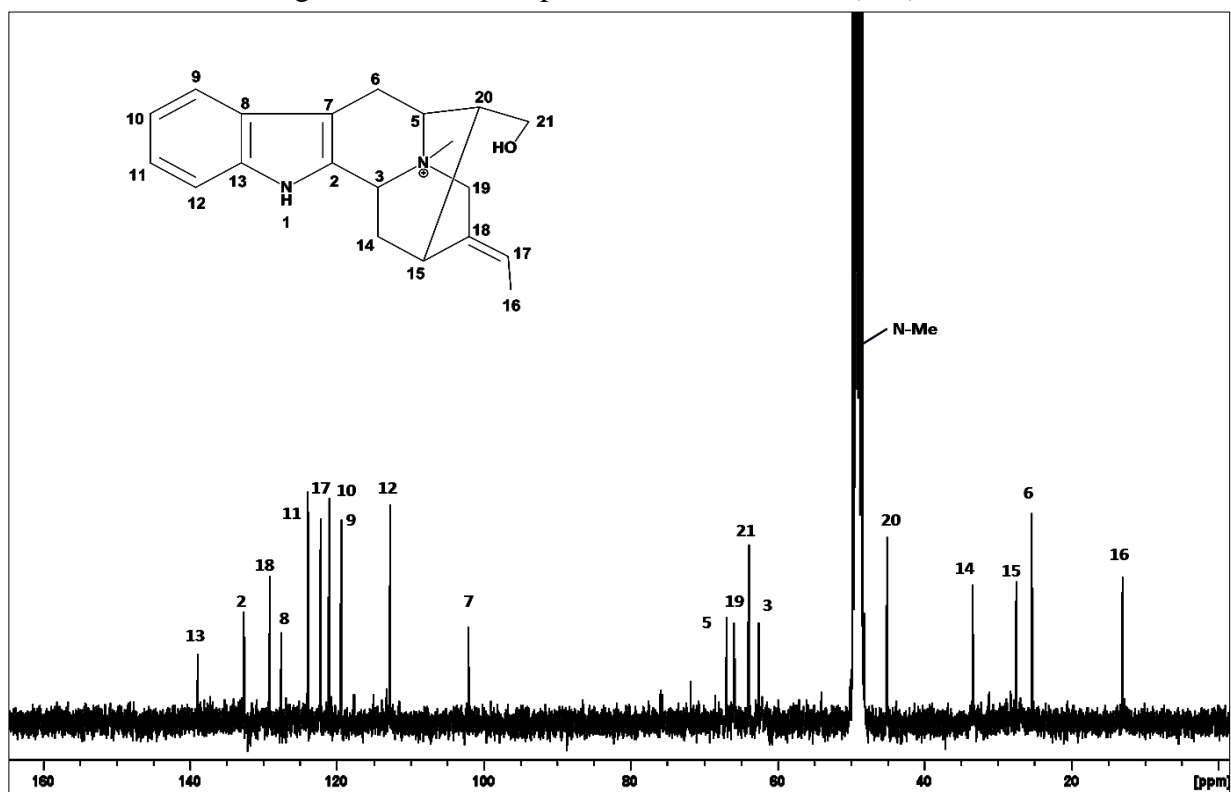


Fig. 4.37: ^{13}C NMR Spectrum of Macusine B (130)

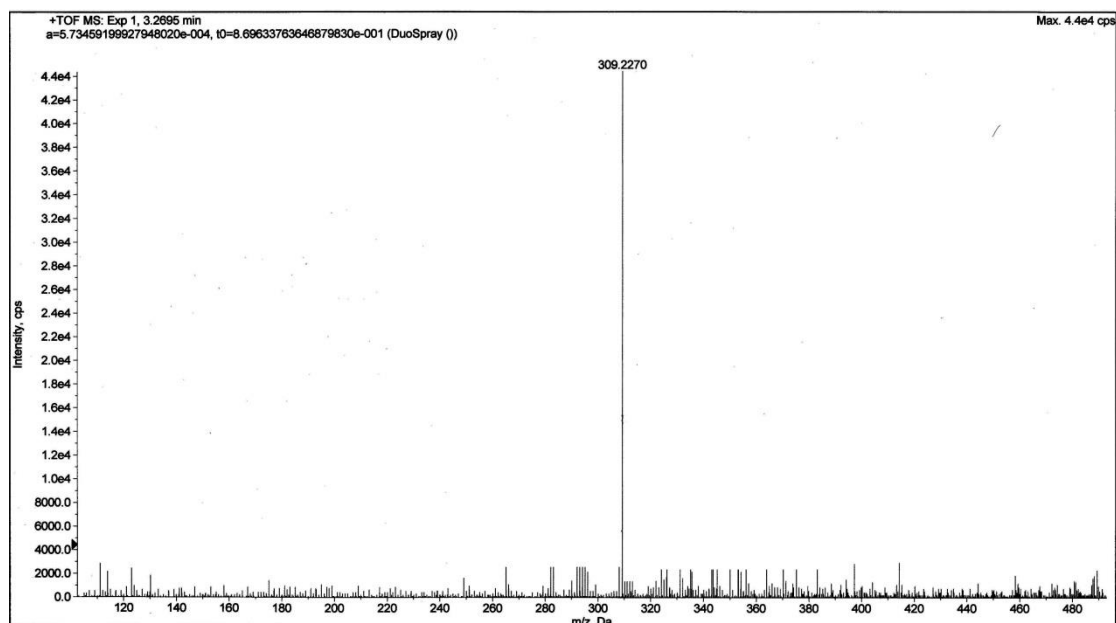
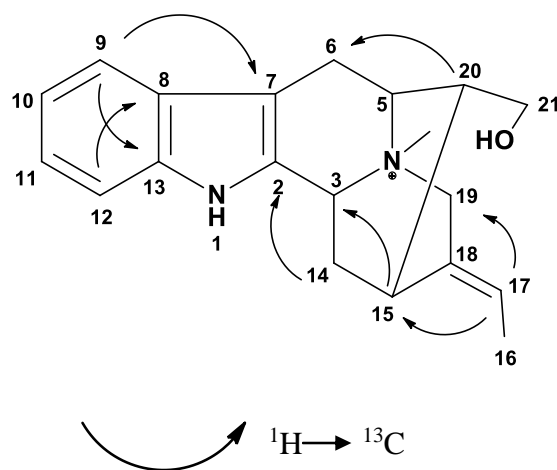
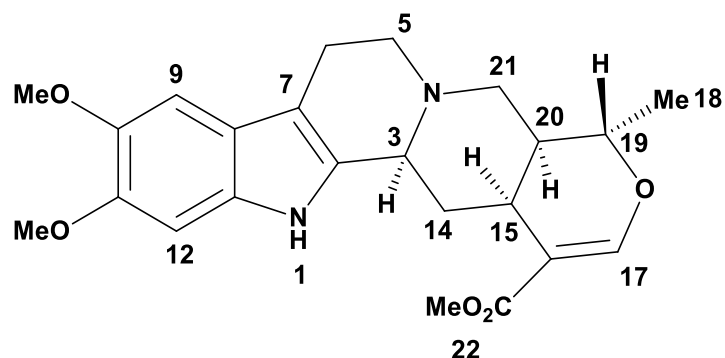


Fig. 4.38: LC-MS Spectrum of Macusine B (**130**)



Scheme 4.11: The HMBC Correlations of Macusine B (**130**)

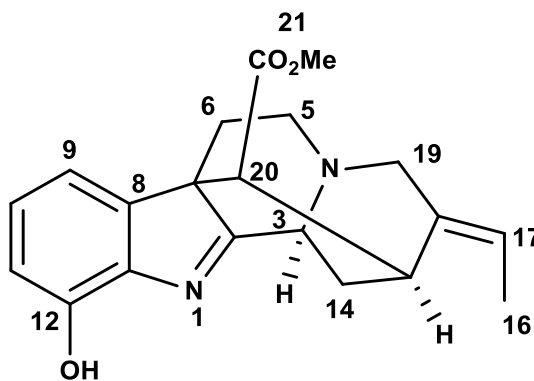
4.2.1.9 Isoreserpiline (120)



120

Isoreserpiline (**120**) was isolated as a brownish amorphous solid, $[\alpha]_D^{24} -32$ (c 0.05, CHCl_3). The UV spectrum revealed maxima at 225, 302 nm. In addition, the IR spectrum showed a peak at 1702 cm^{-1} which indicate the presence of the carbonyl group, and a band at 3374 cm^{-1} presence of a NH group. The LC-MS, ^1H NMR, ^{13}C NMR and 2D NMR data were resembled to isoreserpiline (**120**) which was isolated from the bark of *Ochroosia oppositifolia* and has been discussed in Section 4.1.1.

4.2.1.10 Akuammilan-17-oic acid, 12-hydroxy-, methyl ester (131)



131

Akuammilan (**131**) was isolated as a brownish amorphous solid. $[\alpha]_D^{24} -48$ (*c* 0.05, CHCl₃). The mass spectrum revealed a pseudo-molecular ion peak at *m/z* 339.1951 [M+H]⁺ corresponding to the molecular formula of C₂₀H₂₂N₂O₃. The UV spectrum revealed maximum at 250, 285 nm. The IR spectrum showed band of OH at 3378 and the carbonyl at 1703 cm⁻¹.

The ¹H NMR spectrum (Figure 4.39) showed the presence of signals for three aromatic protons at δ 6.86 (*dd*, *J*= 8.0, 2.0 Hz, H-9), δ 7.02 (*d*, *J*= 8.0 Hz, H-10), and δ 6.80 (*dd*, *J*=8.0, 2.0 Hz, H-11). The ¹H NMR also showed the existence of ethylidene group (δ 1.60, *d*, *J*= 6.0 Hz, H-16; δ 5.77, *m*, H-17), one methoxy group at δ 3.71 (*s*) corresponding to OCOMe, four methylene signals appeared at (δ 3.06, *m*, and 2.01, *m*, H-5), (δ 1.97, *m*, and 1.28, *m*, H-6), (δ 0.88, *m*, and 1.25, *m*, H-14) and (δ 4.06, *d*, *J*=15.6 Hz and 4.55, *d*, *J*= 15.4 Hz, H-19). There are three aliphatic proton signals were observed at δ 3.65 (*m*, H-3), δ 3.54 (*m*, H-15) and δ 3.50 (*d*, *J*=15.8 Hz, H-20).

The ¹³C NMR spectrum (Figure 4.40) showed 20 signals corresponding to four sp² methines, six sp² quaternary carbons, four sp³ methylenes, three sp³ methines, one sp³ quaternary carbon, one methyl and one methoxyl group. Application of ¹H-¹H COSY and C-H correlations from HSQC and HMBC (Scheme 4.12) allowed the complete assignment of all signals (Table 4.13). In conclusion, data comparison with the literature confirmed the isolation of Akuammilan-17- oic acid, 12- hydroxy-, methyl ester (**131**) which previously isolated from *Rauwolfia sumatrana* (Arbain *et al.*, 1991).

Table 4.13: ^1H NMR (400 MHz) and ^{13}C NMR (100 MHz) spectral data of akuammilan (**131**) in CDCl_3 (δ in ppm, J in Hz)

Position	^1H -NMR (δ ppm)	^{13}C -NMR (δ ppm)	^{13}C -NMR (δ ppm) (Arbain et al, 1991)
2	-	176.9	176.9
3	3.65 (1H, <i>m</i>)	68.4	68.4
5	3.06 (1H, <i>m</i>)	51.9	51.8
	2.01 (1H, <i>m</i>)	-	-
6	1.97 (1H, <i>m</i>)	30.4	30.5
	1.28 (1H, <i>m</i>)	-	-
7	-	71.6	71.7
8	-	145.9	145.7
9	6.86 (1H, <i>d</i> , $J= 8.0$)	119.3	119.4
10	7.02 (1H, <i>t</i> , $J= 7.5$)	128.3	128.4
11	6.80 (1H, <i>d</i> , $J= 7.0$)	113.8	113.8
12	-	151.4	151.2
13	-	145.9	145.9
14	0.88 (1H, <i>m</i>)	33.6	33.7
	1.25 (1H, <i>m</i>)	-	-
15	3.54 (1H, <i>m</i>)	29.3	29.4
16	1.60 (3H, <i>d</i> , $J= 6.0$)	13.4	13.4
17	5.77 (1H, <i>m</i>)	125.1	125.1
18	-	145.9	145.9
19	4.06 (1H, <i>d</i> , $J= 14.6$)	74.7	74.7
	4.55 (1H, <i>d</i> , $J= 16.2$)	-	-
20	3.50 (1H, <i>d</i> , $J= 15.8$)	45.0	45.1
21	-	170.7	170.8
OH	5.76 (1H, br <i>s</i>)	-	-
OMe	3.71 (3H, <i>s</i>)	53.7	53.7

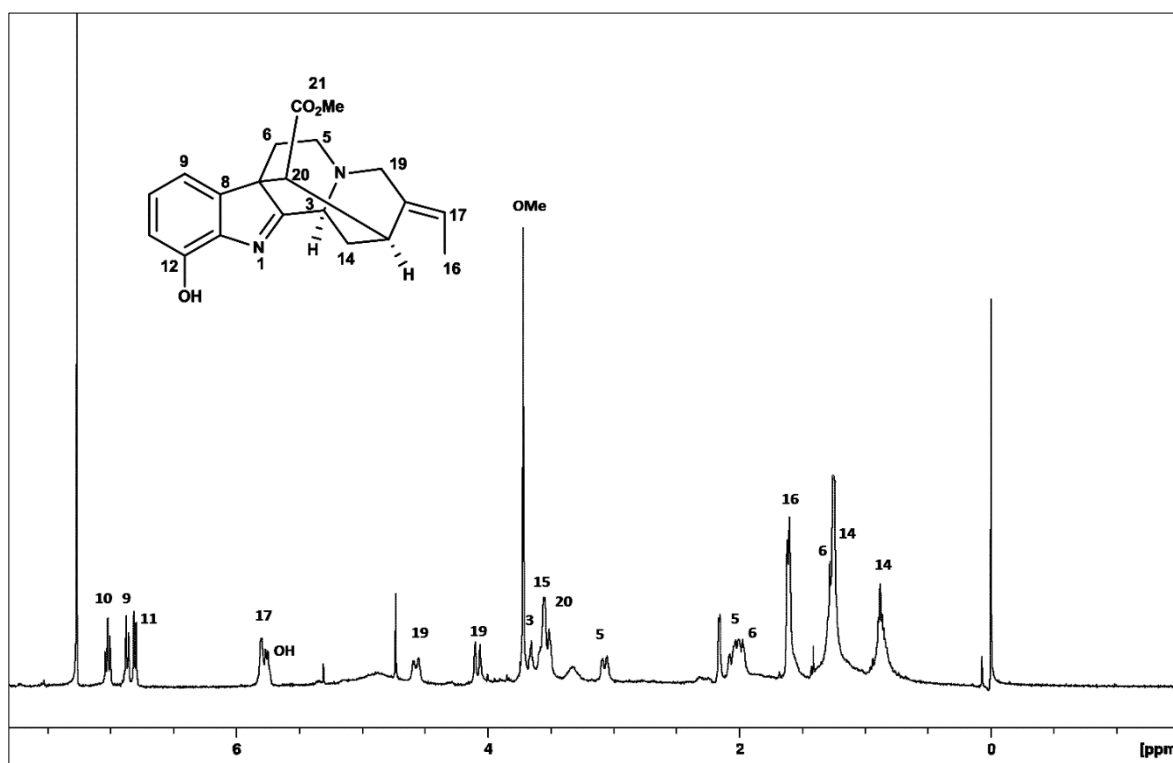


Fig. 4.39: ¹H NMR Spectrum of Akuammilan (**131**)

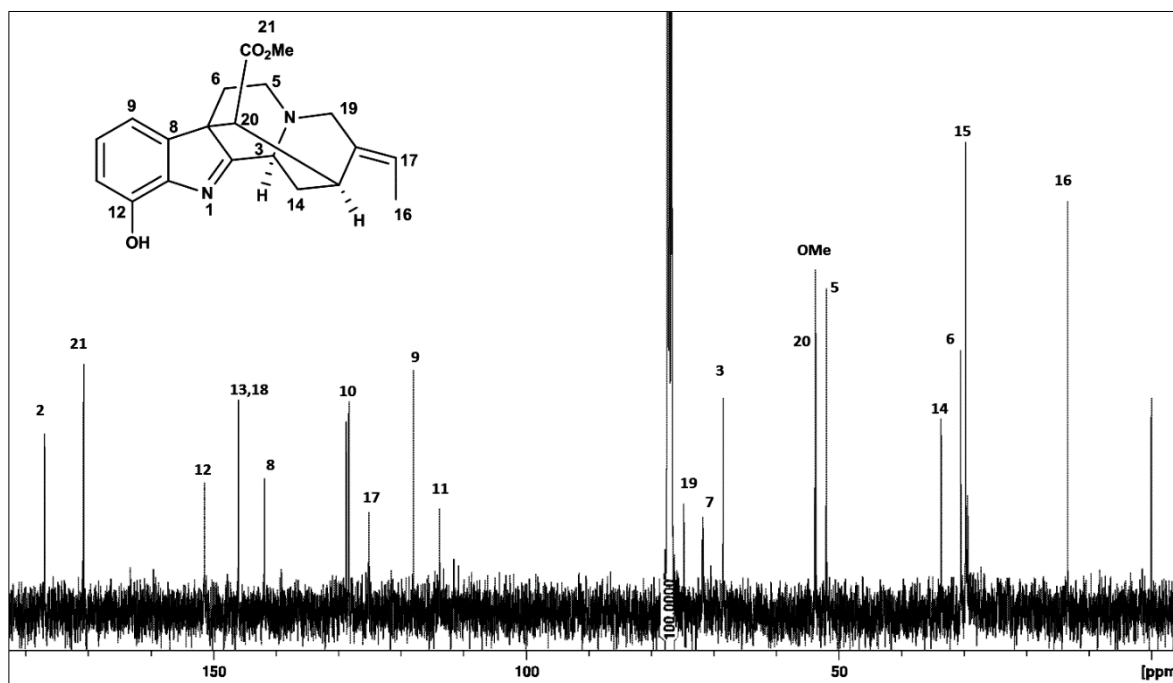


Fig. 4.40: ¹³C NMR Spectrum of Akuammilan (**131**)

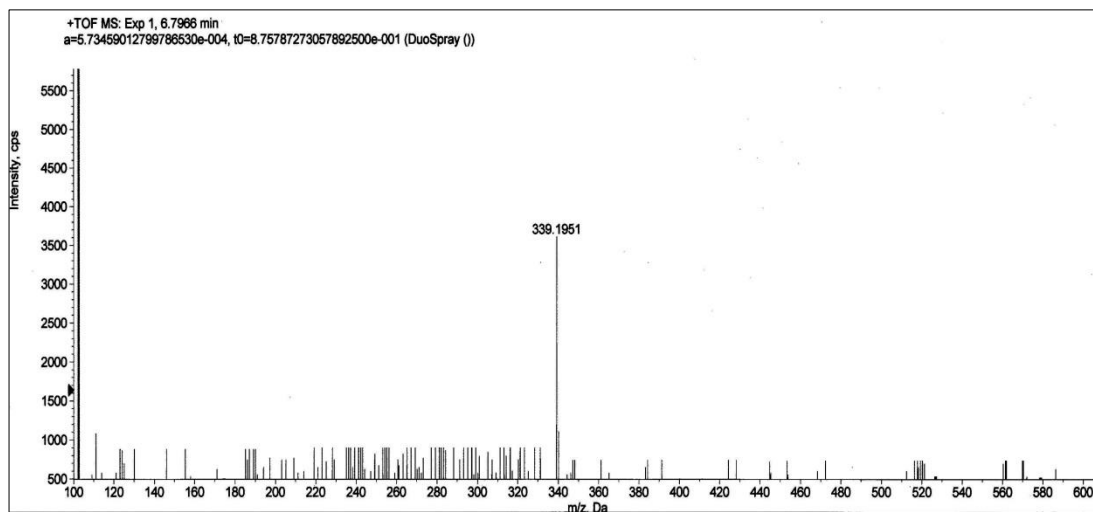
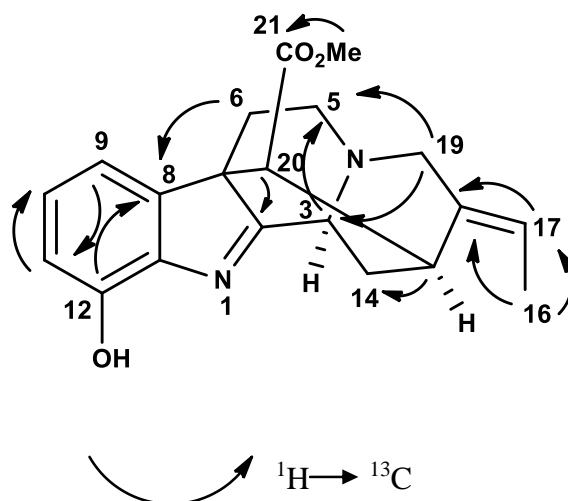


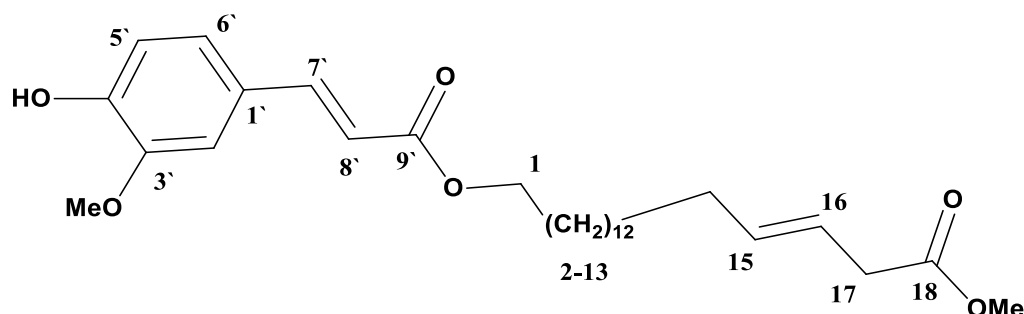
Fig. 4.41: LC-MS Spectrum of Akuammilan (**131**)



Scheme 4.12: The HMBC Correlations of Akuammilan (**131**)

4.2.2 Compounds from the Leaves of *Rauvolfia reflexa*

4.2.2.1 17-Methoxycarbonyl-14-heptadecaenyl-4-hydroxy-3-methoxy cinnamate (132)



132

17-Methoxycarbonyl-14-heptadecaenyl-4-hydroxy-3-methoxy

cinnamate (**132**) was isolated as a whitish amorphous solid. The mass spectrum revealed a pseudo-molecular ion peak at m/z 489.3332 $[M+H]^+$ (calcd for $C_{29}H_{44}O_6$, 489.3328). The UV spectrum revealed maximum at 196, 273 and 328 nm. The IR spectrum showed a band of OH at 3431 cm^{-1} . In addition, two peaks were observed at 1711 and 1738 cm^{-1} which implied the presence of two carbonyl group.

The ^1H NMR spectrum (Figure 4.42) indicated the presence of three aromatic protons at δ 7.10, 7.01 and 6.89 attached to C-6', C-2' and C-5', respectively. In up field region, two singlets appeared at δ 3.91 and 3.64 attributed to two methoxyl groups attached to C-3' and C-18 respectively. The cross peak of COSY showed one coupling set (H-7' - H-8'). This was confirmed by the existence of two sets of doublet ($J = 16.0\text{ Hz}$) in the ^1H NMR at δ 7.50 and 6.27 which corresponded to the resonances of H-7' and H-8', respectively. The correlation between H-14 and C-15, 16 in the HMBC established the position of double

bond in the long chain and also correlation between H-1 and C=O 9` supported the chain connections. (Figure 4.45).

The ^{13}C NMR (Figure 4.43) and HSQC (Figure 4.44) showed the presence of 29 carbon atoms; three quaternary carbons; δ 147.9 (C-4`), 146.8 (C-3`), and 127.1 (C-1`), seven methines; δ 144.7 (C-7`), 129.9 (C-15,16), 123.1 (C-6`), 115.7 (C-8`), 114.7 (C-5`) and 109.3 (C-2`), fifteen methylenes; δ 64.6 (C-1), 34.0 (C-17) and the rest thirteen methylenes overlapped in the region between δ 29.2 until 29.8. Two methoxys; δ 56.0 (C₃-OMe) and 51.5 (C₁₈-OMe). There are two carbonyls which appeared at δ 174.4 (C=O 18) and 167.4 (C=O 9`).

The assignments of the position of each carbon were confirmed with DEPT, COSY and HMBC spectra. Thus the structure was determined as 17-Methoxycarbonyl-14-heptadecaenyl-4-hydroxy-3-methoxy cinnamate (**132**) which was isolated for the first time from *Rauvolfia* species (Garcia *et al.*, 1997), (Fadaeinasab *et al.*, 2013). Complete assignments were listed in table 4.14.

Table 4.14: ^1H NMR (400 MHz) and ^{13}C NMR (100 MHz) spectral data of cinnamate (**132**) in CDCl_3 (δ in ppm, J in Hz).

Position	^1H -NMR	^{13}C -NMR	HMBC
1	4.16 (2H, <i>t</i> , $J= 6.8$)	64.6	2, 9 '
2-13	1.28- 1.58	29.2- 29.7	
14	2.14 (2H, <i>d</i> , $J= 5.4$)	29.8	15, 16
15	5.30 (1H, <i>m</i>)	129.9	-
16	5.30 (1H, <i>m</i>)	129.9	-
17	2.34 (2H, <i>t</i> , $J= 7.7$)	34.0	18
18	-	174.4	-
1 '	-	127.1	-
2 '	7.01 (1H, <i>d</i> , $J= 2.2$)	109.3	7 '
3 '	-	146.8	-
4 '	-	147.9	-
5 '	6.90 (1H, <i>d</i> , $J= 8.2$)	114.7	3 '
6 '	7.10 (1H, <i>dd</i> , $J= 8.2, 2.2$)	123.1	-
7 '	7.50 (1H, <i>d</i> , $J= 16.0$)	144.7	2 ' , 6 ' , 9 '
8 '	6.27 (1H, <i>d</i> , $J= 16.0$)	115.7	1 '
9 '	-	167.4	-
OMe-18	3.64 (3H, <i>s</i>)	51.5	18
OMe-3 '	3.91 (3H, <i>s</i>)	56.0	3 '
OH	5.90 (1H, <i>br s</i>)	-	-

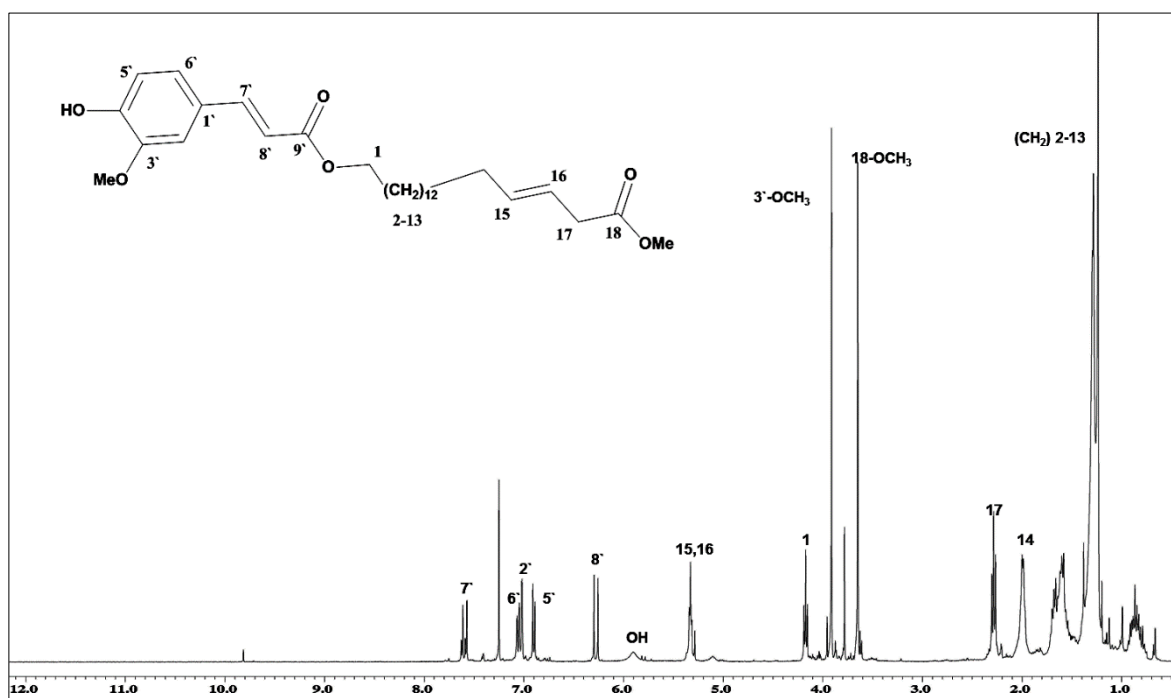


Fig. 4.42: ^1H NMR Spectrum of Cinnamate (**132**)

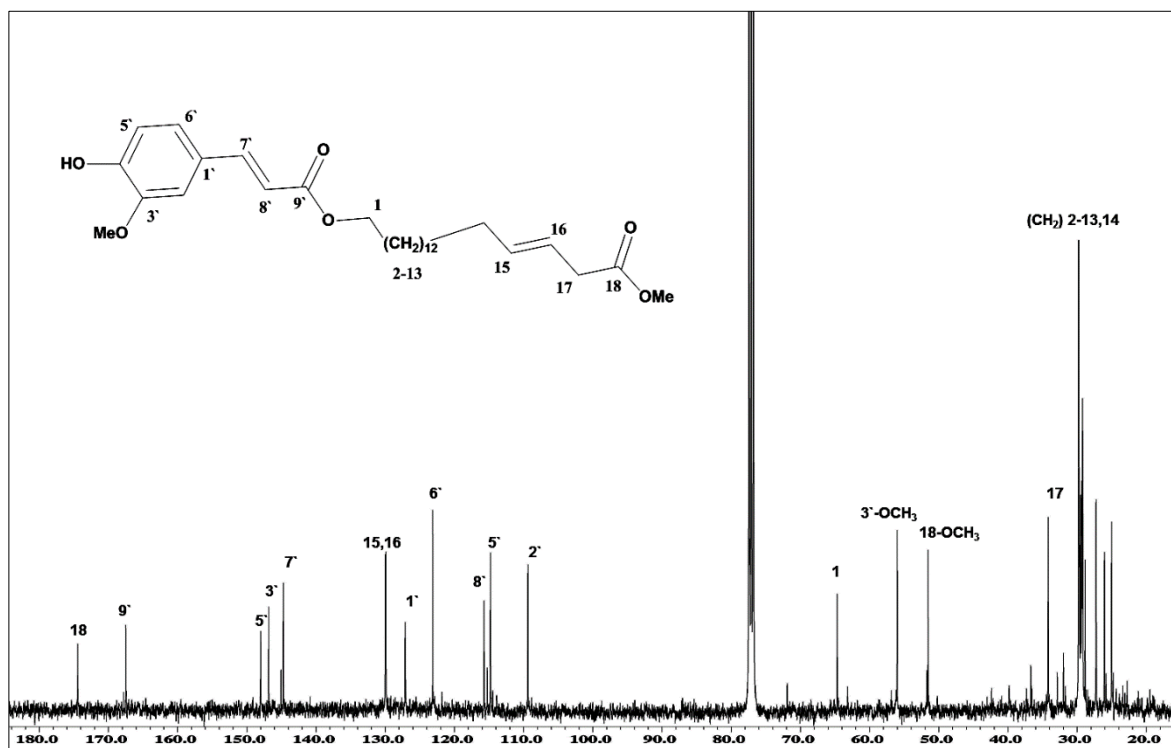


Fig. 4.43: ^{13}C NMR Spectrum of Cinnamate (**132**)

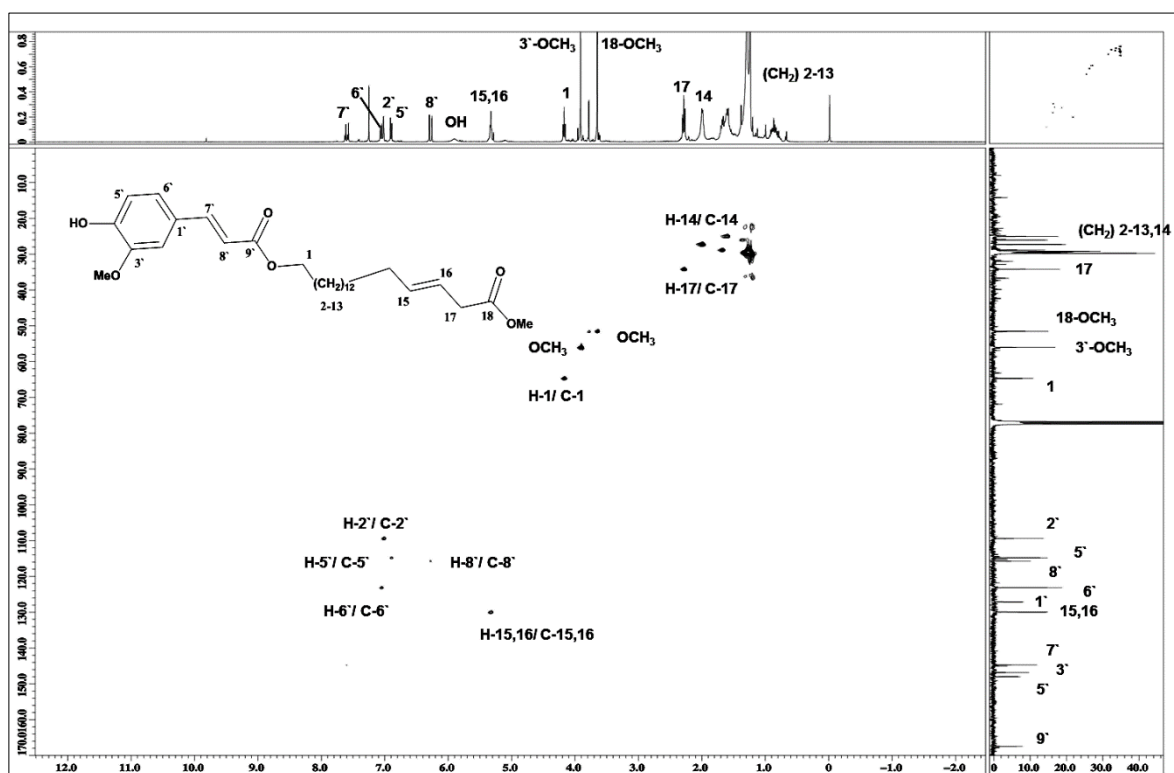


Fig. 4.44: HSQC Spectrum of Cinnamate (**132**)

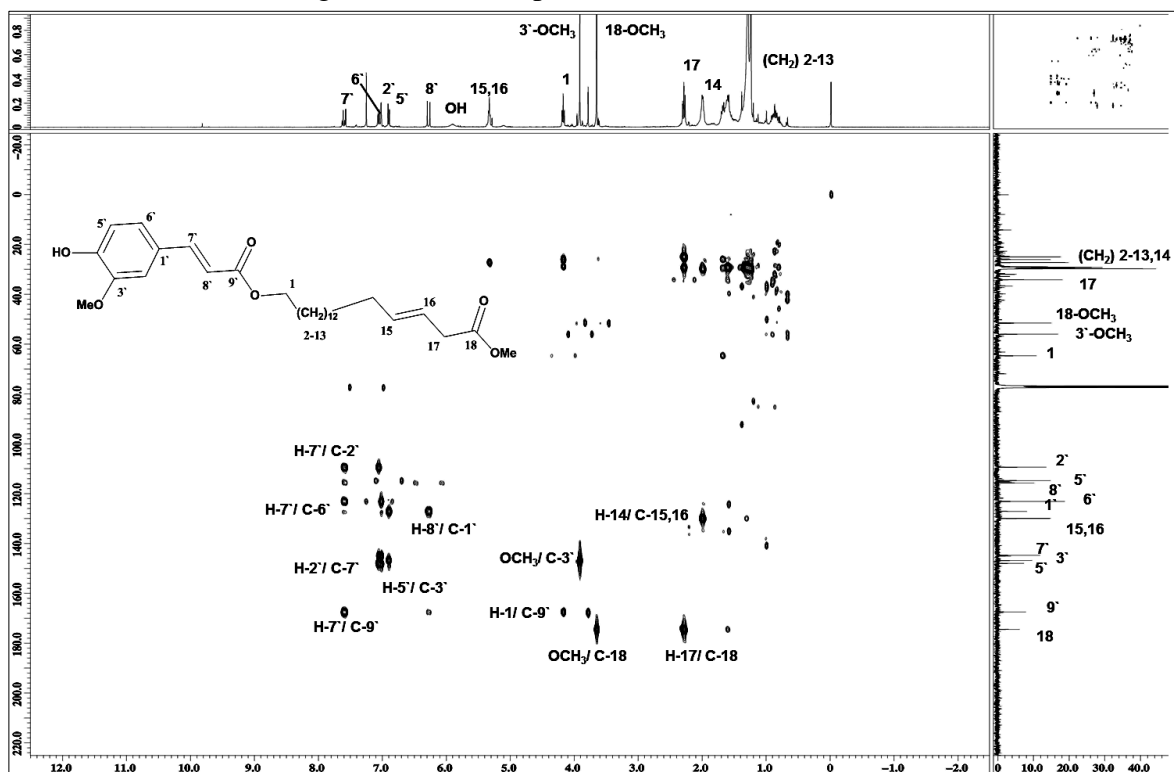


Fig. 4.45: HMBC Spectrum of Cinnamate (**132**)

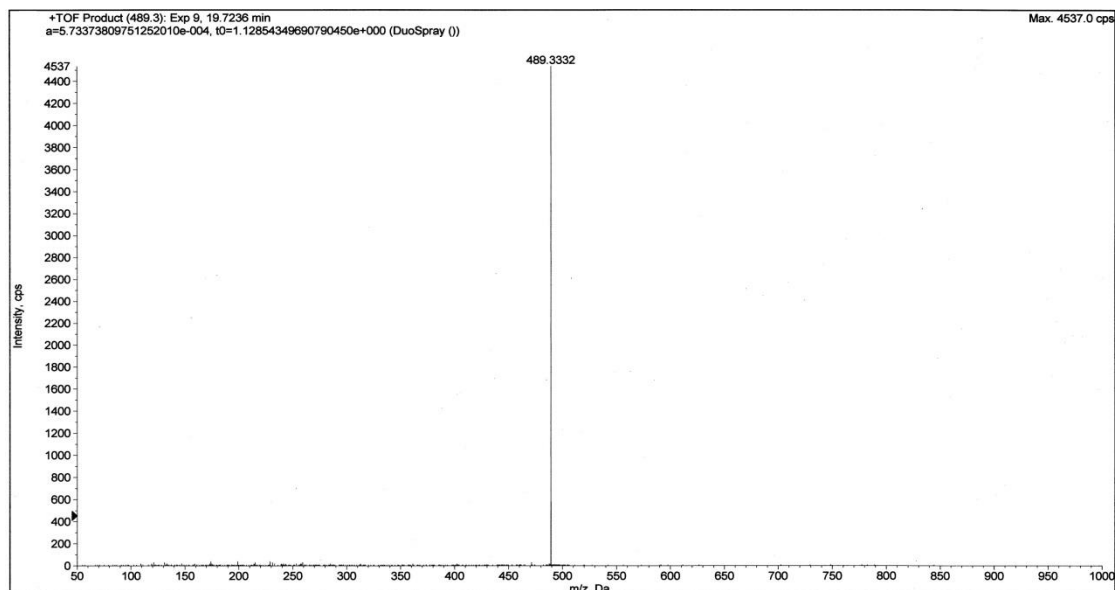
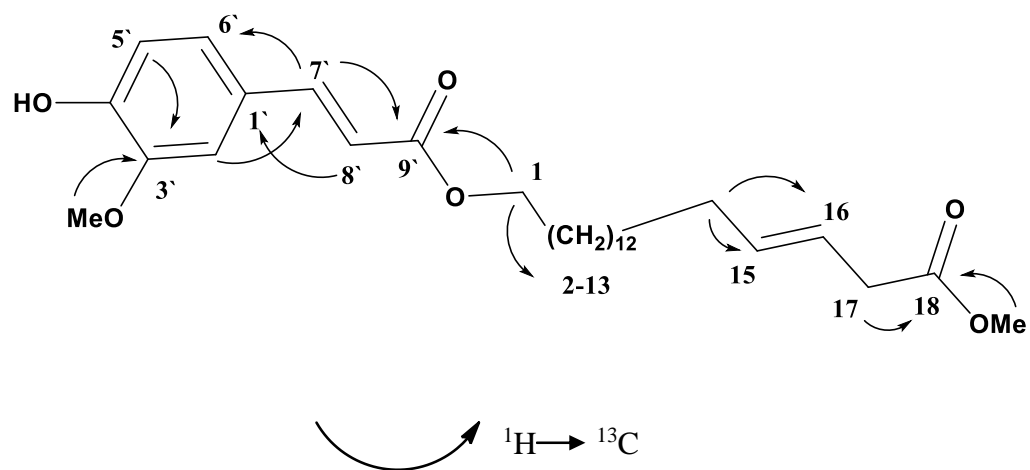
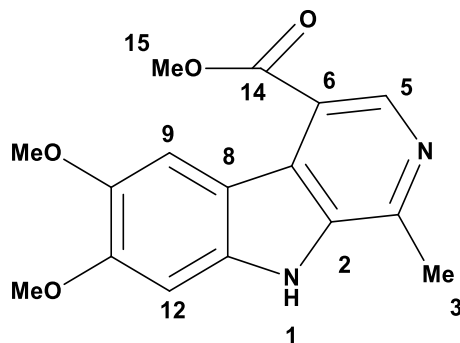


Fig. 4.46: LC-MS Spectrum of Cinnamate (**132**)



Scheme 4.13: The HMBC Correlations of Cinnamate (**132**)

4.2.2.2 3- Methyl-10,11-dimethoxyl-6- methoxycarbonyl- β - carboline (133)



133

3-Methyl-10,11-dimethoxyl-6-methoxycarbonyl- β - carboline (**133**) obtained as a yellowish amorphous solid. On the basis of its HRESIMS (m/z 301.1909, $[M+H]^+$) (calcd for $C_{16}H_{16}N_2O_4$, 301.1903) along with the 1H and ^{13}C NMR data, the molecular formula was established. The IR spectrum showed a peak at 1725 cm^{-1} which indicate the presence of the carbonyl group, and a band at 3369 cm^{-1} presence of the NH group. In the UV spectrum, the absorption bands at 245, 285 and 336 nm implied the presence of a β -carboline chromophore (Koike *et al.*, 1990). The 1H NMR spectrum (Figure 4.47) showed resonances attributable to a two isolated aromatic protons (2H, δ 6.86, s, H-9 and H-12), one methyl group (3H, δ 1.29, s), two methoxyl groups (3H, δ 3.88, s, 10-OMe, 3H, δ 3.84, s, 11-OMe), one methoxycarbonyl (3H, 3.69, s, 15-OMe). In addition, a broad singlet NH proton signal (1H, δ 8.51, br. s, H-1) and a singlet aromatic proton signal (1H, δ 7.52, s, H-5) were also displayed. The ^{13}C NMR (Figure 4.48) and DEPT 135 NMR spectra (Figure 4.51) for β - carboline (**133**) indicated the presence of 16 carbon signals, including three aromatic methines, eight aromatic quaternary carbon signals, three methoxyl groups and one carbonyl group. The above spectroscopic data suggested that (**133**) is a β - carboline

alkaloid bearing two methoxy groups, one methoxycarbonyl group and one methyl group. Furthermore, the HMBC correlations (Figure 4.50) between 10- OMe and C-10 (δ 144.75), 11- OMe and C-11 (δ 144.75), 15- OMe and C=O 14 (δ 168.10) determined the three methoxy groups were placed at C-10, C-11 and C=O 14, respectively. And the correlation of H-5 and C=O, 14 determined the carbonyl group was located at position 14. Thus the structure of (**133**) was determined as 3- methyl-10,11-dimethoxyl-6- methoxycarbonyl- β - carboline (**133**), Which has never been isolated before. Complete assignments were listed in table 4.15.

Table 4.15: ^1H NMR (400 MHz) and ^{13}C NMR (100 MHz) spectral data of β - carboline (**133**) in CDCl_3 (δ in ppm, J in Hz).

Position	^1H -NMR	^{13}C -NMR	HMBC
2	-	130.2	-
3	1.29 (3H, <i>s</i>)	18.5	-
4	-	146.4	-
5	7.52 (1H, <i>s</i>)	155.5	14
6	-	120.1	-
7	-	107.2	-
8	-	120.1	-
9	6.86 (1H, <i>s</i>)	100.2	8,10,11
10	-	144.7	-
11	-	144.7	-
12	6.86 (1H, <i>s</i>)	95.2	10,11
13	-	130.2	-
14	-	168.1	-
OMe-15	3.69 (3H, <i>s</i>)	51.2	14
OMe-10	3.88 (3H, <i>s</i>)	56.4	10
OMe-11	3.84 (3H, <i>s</i>)	56.3	11
NH	8.51 (1H, <i>br s</i>)	-	-

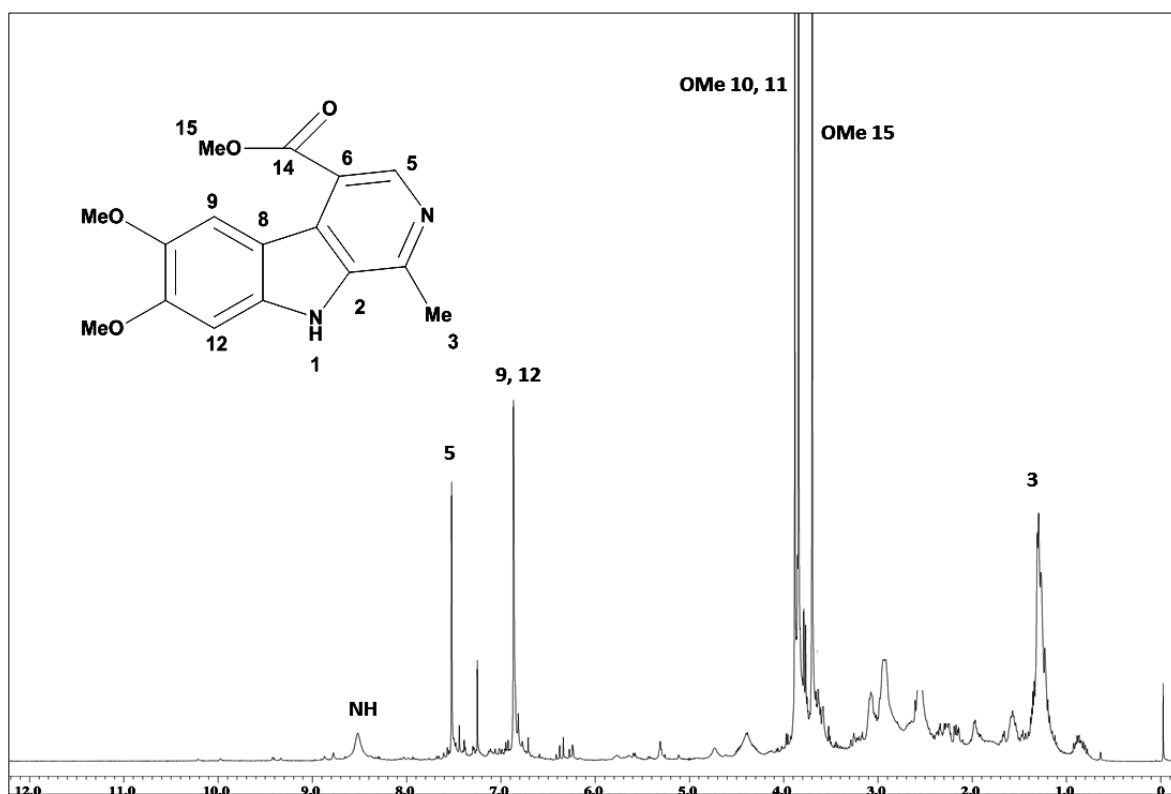


Fig. 4.47: ¹H NMR Spectrum of β- carboline (133)

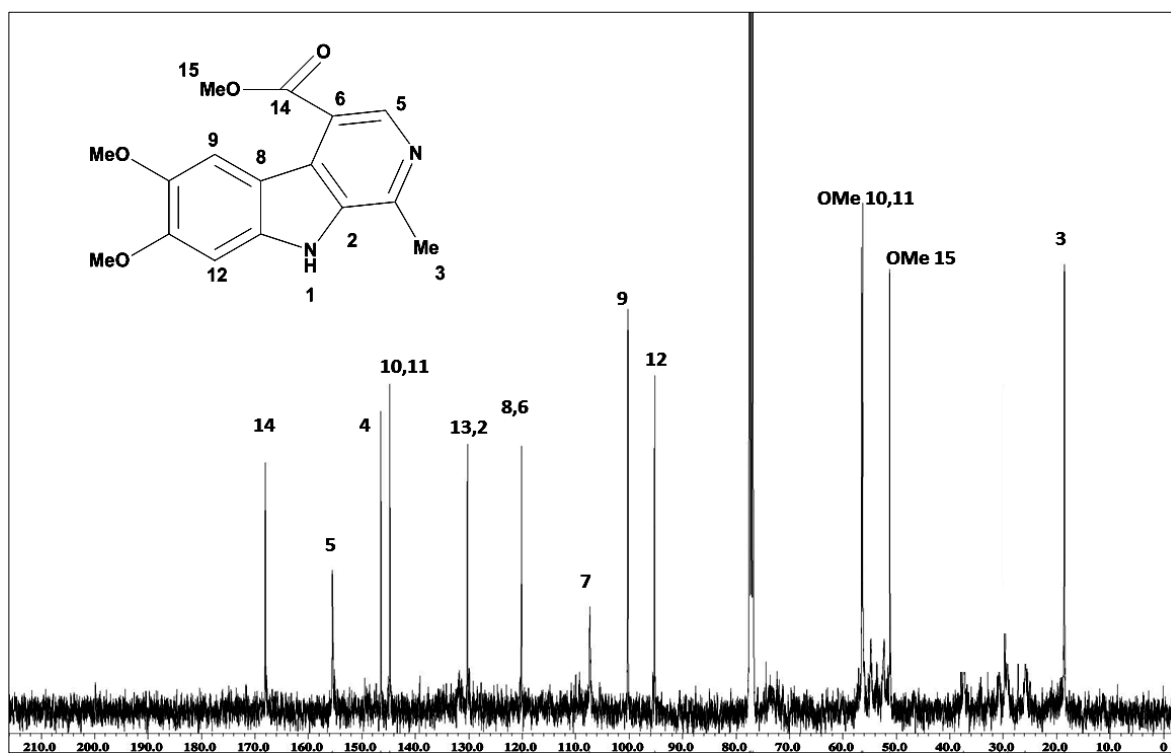


Fig. 4.48: ¹³C NMR Spectrum of β- carboline (133)

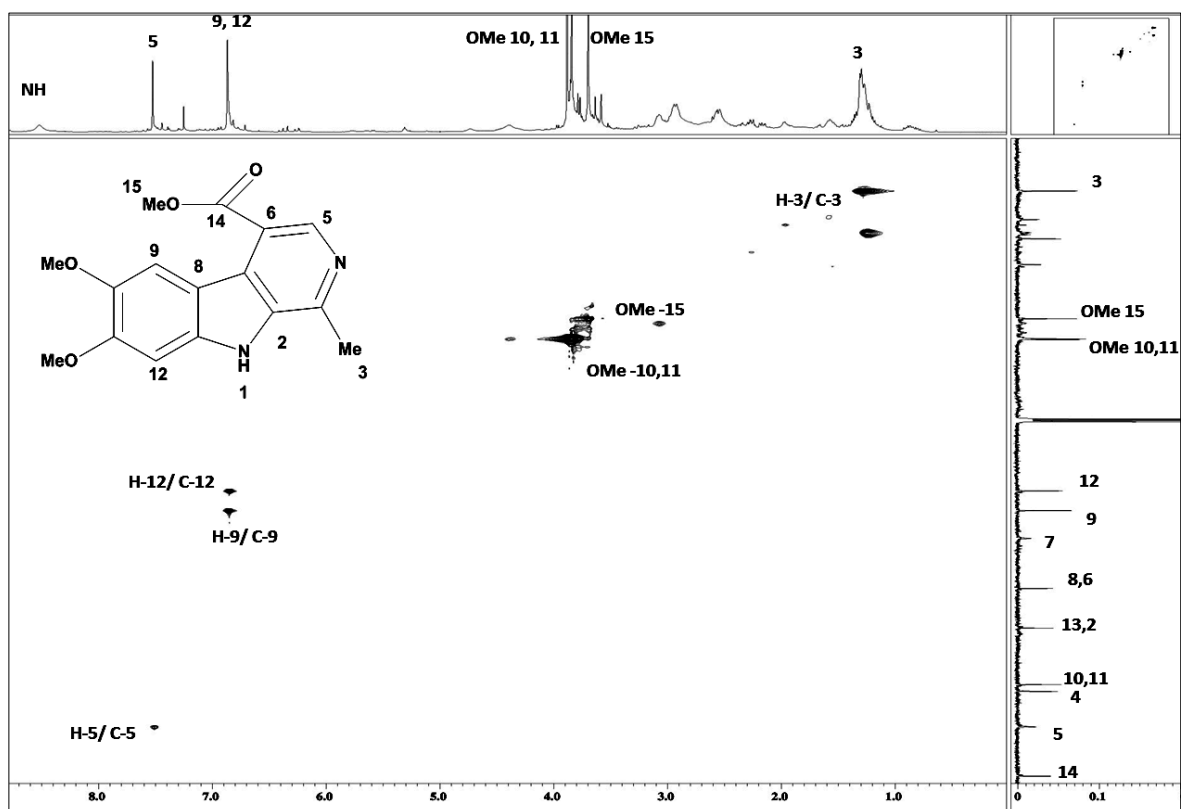


Fig. 4.49: HSQC Spectrum of β - carboline (133)

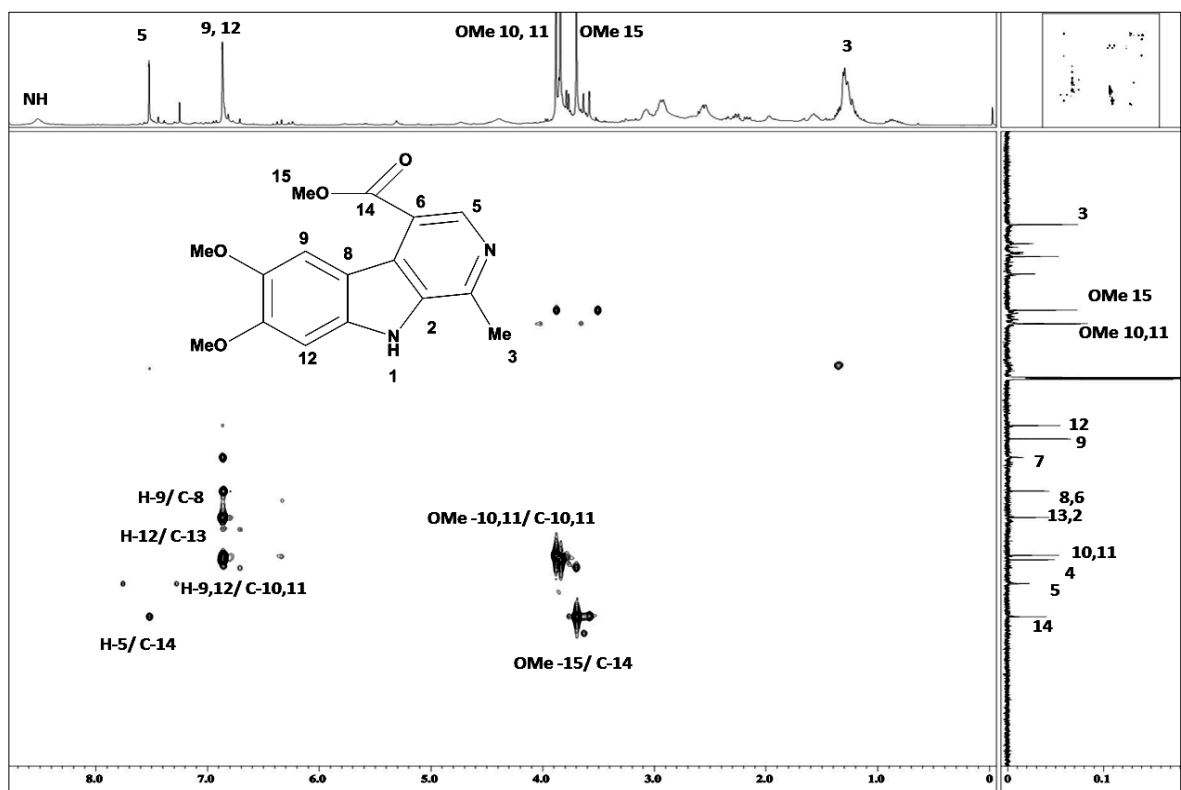


Fig. 4.50: HMBC Spectrum of β - carboline (133)

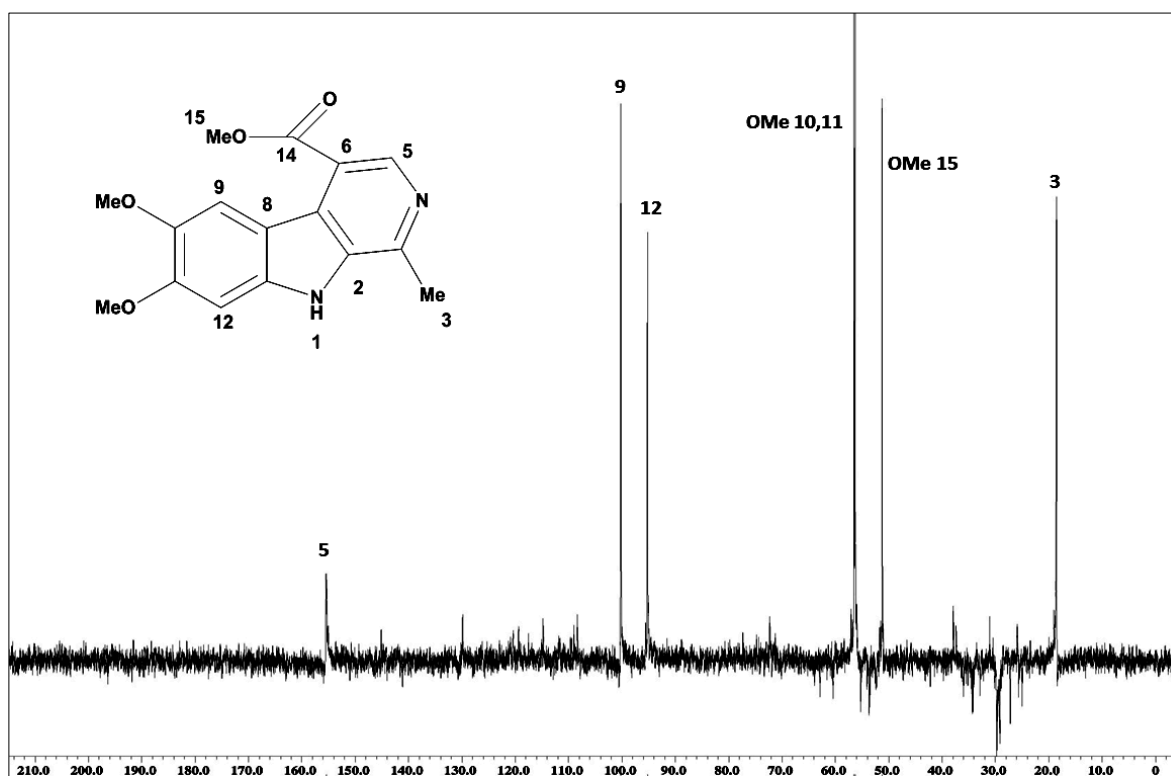


Fig. 4.51: DEPT 135 Spectrum of β - carboline (133)

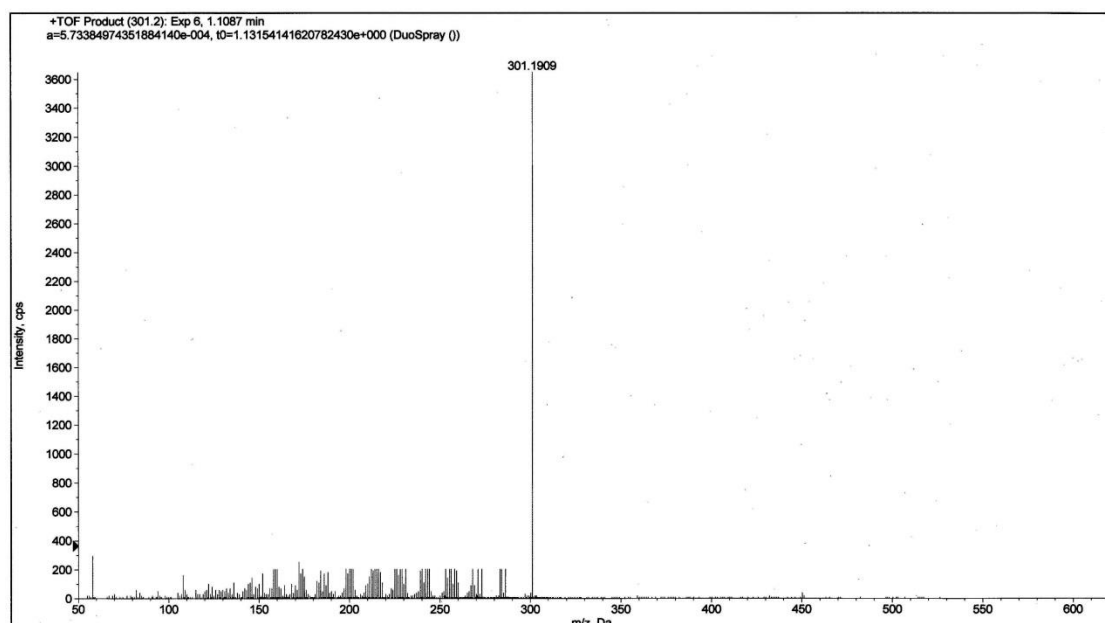
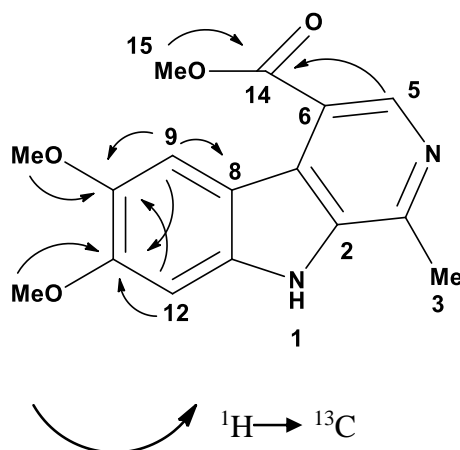
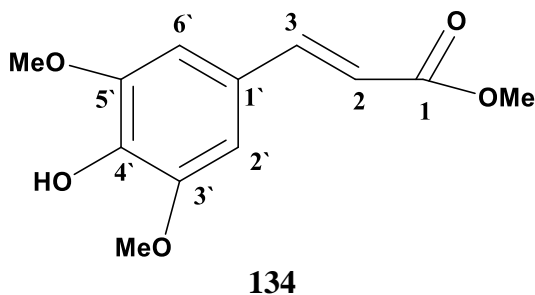


Fig. 4.52: LC-MS Spectrum of β - carboline (133)



Scheme 4.14: The HMBC Correlations of β - carboline (**133**)

4.2.2.3 (*E*)-Methyl 3-(4-hydroxy-3,5-dimethoxyphenyl) acrylate (**134**)



(*E*)-Methyl 3-(4-hydroxy-3,5-dimethoxyphenyl) acrylate (**134**) was isolated as a whitish amorphous solid. The mass spectrum revealed a pseudo-molecular ion peak at m/z 239.1071 $[M+H]^+$ corresponding to the molecular formula of $C_{12}H_{14}O_5$. The UV spectrum revealed maximum at 196, 273 and 328 nm. The IR spectrum showed a band of OH at 3401 cm^{-1} . In addition, a peak was observed at 1704 cm^{-1} which indicated the presence of the conjugated carbonyl of an ester.

The ^1H NMR spectrum (Figure 4.53) showed two overlapping aromatic protons at δ 6.77 attributed to H-6' and H-2' respectively. In the up field region, three singlets appeared at δ 3.92 and 3.91 and 3.79 attributed to three methoxys attached to C- 3', C- 5' and C- 1 respectively.

The hypothesis was also supported further by the cross peaks of COSY experiment that showed existence of two sets of doublet ($J = 16$ Hz) in the ^1H NMR at δ 6.29 and 7.59 which corresponded to the resonances of H-2 and H-3.

The ^{13}C NMR (Figure 4.54) and DEPT 135 showed the presence of 12 carbon atoms; four quaternary δ 147.2 (C-3'), 147.2 (C-5'), 137.3 (C-4'), and 125.9 (C-1'); four methines δ 145.5 (C-3), 115.6 (C-2), 105.1 (C-2'), and 105.1 (C-6'); three methoxyl δ 56.4 (OMe 3' and OMe 5') and 51.7 (OMe 1). One peak appeared in δ 167.6 which is carbonyl of (C-1). The cross peak between H-3 and C-1 as observed from the HMBC spectrum indicated that C-1 is vicinal to the olefinic carbon, C-3.

The comprising of data; DEPT, HSQC and HMBC (Scheme 4.15), established the isolation of (*E*)-methyl 3-(4-hydroxy-3, 5-dimethoxyphenyl) acrylate (**134**) which was previously isolated from the leaves of *Palicourea coriacea* (da Silva *et al.*, 2008). Complete assignments of (**134**) were listed in table 4.16.

Table 4.16: ^1H NMR (400 MHz) and ^{13}C NMR (100 MHz) spectral data of acrylate (**134**) in CDCl_3 (δ in ppm, J in Hz)

Position	^1H -NMR (δ ppm)	^{13}C -NMR (δ ppm)	^{13}C -NMR (δ ppm) (da Silva et al, 2008)
1	-	167.6	168.0
2	6.29 (1H, <i>d</i> , $J= 16.0$)	115.6	115.5
3	7.59 (1H, <i>d</i> , $J= 16.0$)	145.5	145.4
1'	-	125.9	125.3
2'	6.77 (1H, <i>s</i>)	105.1	105.1
3'	-	147.2	147.2
4'	-	147.3	147.3
5'	-	147.2	147.1
6'	6.77 (1H, <i>s</i>)	105.1	105.1
OMe 3'	3.92 (3H, <i>s</i>)	56.4	56.4
OMe 5'	3.92 (3H, <i>s</i>)	56.4	56.2
OMe 1	3.79 (3H, <i>s</i>)	51.7	51.7
OH	5.80 (1H, <i>s</i>)	-	-

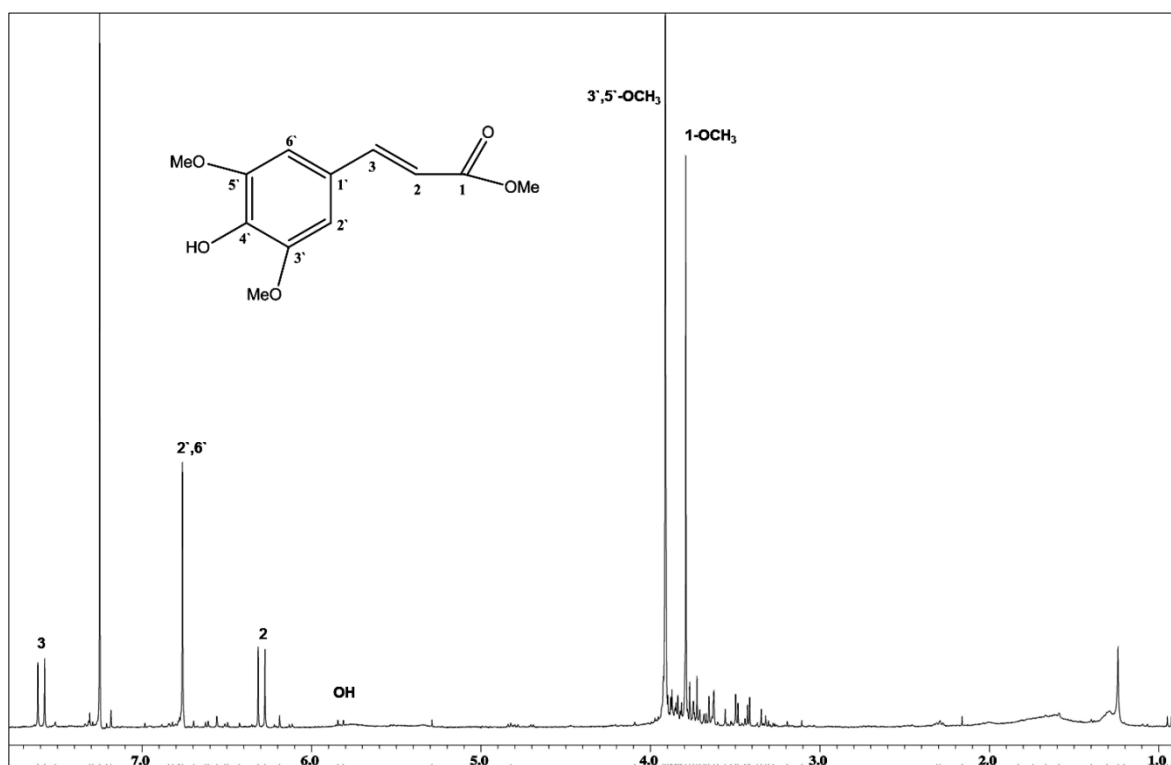


Fig. 4.53: ^1H NMR Spectrum of Acrylate (134)

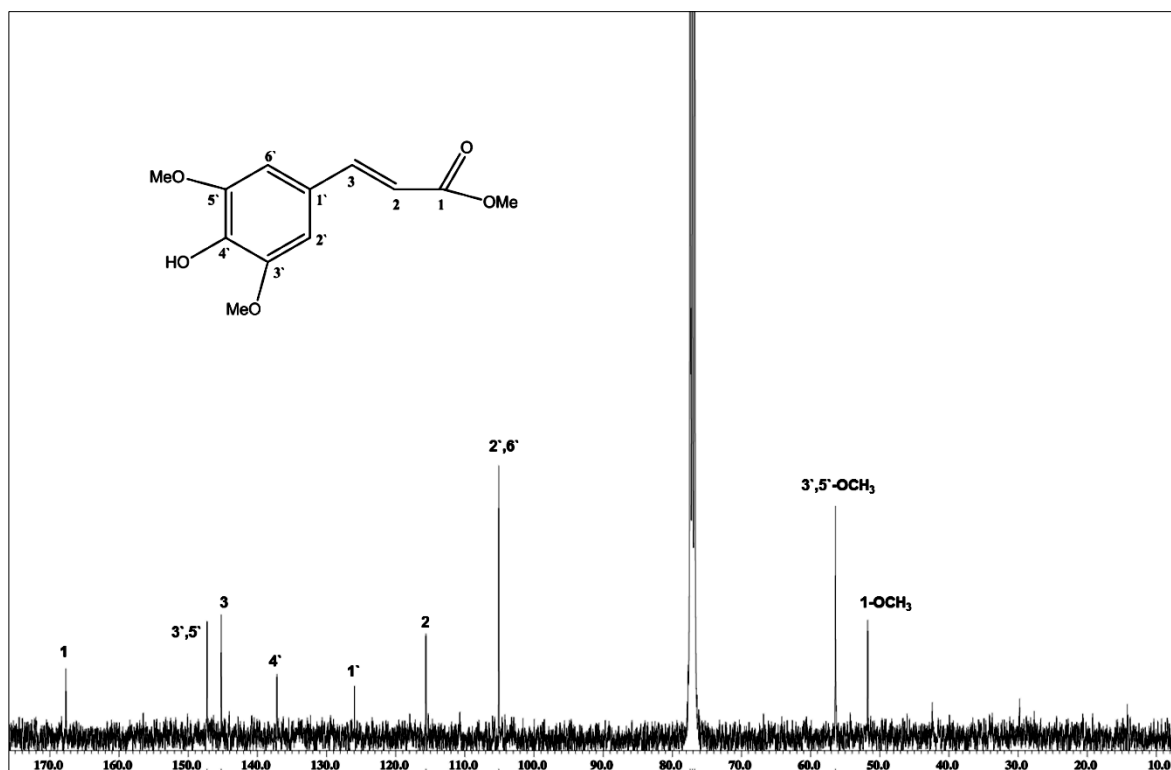


Fig. 4.54: ^{13}C NMR Spectrum of Acrylate (134)

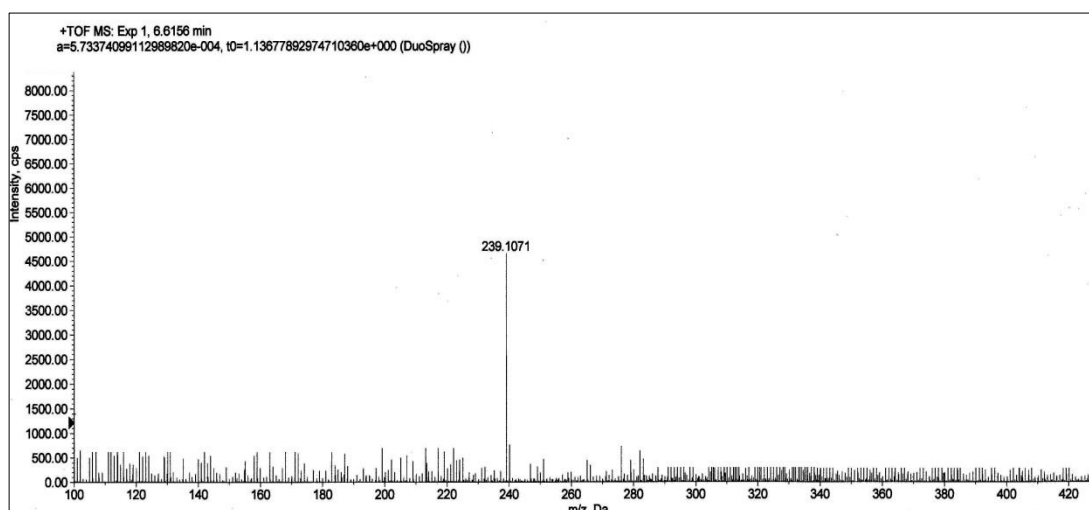
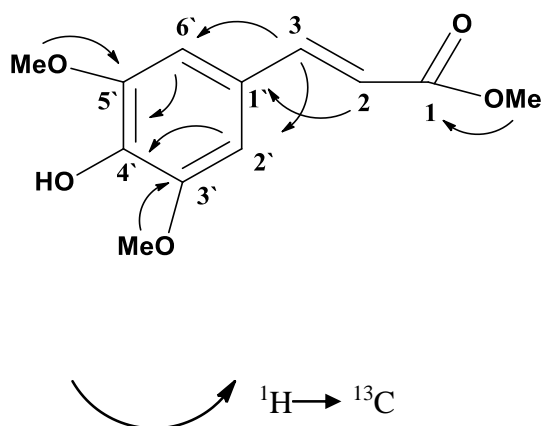
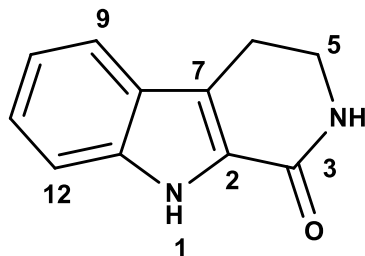


Fig. 4.55: LC-MS Spectrum of Acrylate (**134**)



Scheme 4.15: The HMBC Correlations of Acrylate (**134**)

4.2.2.4 1,2,3,4- Tetrahydro -1- oxo- β - carboline (135)



135

1,2,3,4- tetrahydro -1- oxo- β - carboline (135) was obtained as a yellowish amorphous solid. The mass spectrum revealed a pseudo-molecular ion peak at m/z 187.1271 $[M+H]^+$ corresponding to the molecular formula of $C_{11}H_{10}N_2O$. The UV spectrum the absorption bonds at 245, 285 and 336 nm implied the presence of a β - carboline chromophore (Koike *et al.*, 1990). The IR spectrum showed a band of NH at 3411 cm^{-1} . In addition, a peak was observed at 1665 cm^{-1} which indicated the presence of a conjugated ketone function. The ^1H NMR data (Figure 4.56) showed resonances attributed to an unsubstituted aromatic ring at δ (7.51, *dd*, 8.2, 2.1 Hz, H-9), (7.15, *t*, 7.9, 2.2 Hz, H-10), (7.31, *t*, 7.9, 2.1 Hz, H-11) and δ (7.44, *dd*, 8.2, 2.2 Hz, H-12). In addition, two NH proton signals at δ 5.73 (*s*), 9.25 (*s*) and four signals at δ (3.85, *m*, 3.69, *m*, H-5), δ (3.08, *m*, 3.04, *m*, H-6) were also shown. The ^{13}C NMR (Figure 4.57) and DEPT 135 NMR spectra indicated the presence of 11 carbon signals, including four sp^2 methines, five sp^2 quaternary carbons and two sp^3 methylenes.

Application of C-H correlations from HSQC and HMBC (Scheme 4.16) allowed the complete assignment of all signals (Table 4.17). In conclusion, data comparison with the

literature confirmed the isolation of 1, 2, 3, 4- tetrahydro -1- oxo- β - carboline (**135**). (Zhang & Yan, 2012), (Fadaeinasab *et al.*, 2013).

Table 4.17: ^1H NMR (400 MHz) and ^{13}C NMR (100 MHz) spectral data of β - carboline (**135**) in CDCl_3 (δ in ppm, J in Hz).

Position	^1H -NMR (δ ppm)	^{13}C -NMR (δ ppm)	^{13}C -NMR (δ ppm) (Zhang et al, 2012)
NH- 1	9.26 (1H, br s)		
2	-	126.2	127.2
3	-	163.1	163.1
NH- 4	5.76 (1H, br s)	153.0	153.0
5	3.69 (2H, <i>m</i>)	42.3	42.30
6	3.08 (2H, <i>m</i>)	20.9	21.11
7	-	120.0	120.1
8	-	126.2	126.2
9	7.51 (1H, <i>dd</i> , $J= 8.2, 2.1$)	120.4	120.4
10	7.15 (1H, <i>t</i> , $J= 7.9, 2.2$)	120.4	120.4
11	7.31 (1H, <i>t</i> , $J= 7.9, 2.1$)	125.3	125.3
12	7.44 (1H, <i>dd</i> , $J= 8.2, 2.2$)	112.5	112.5
13	-	137.2	137.2

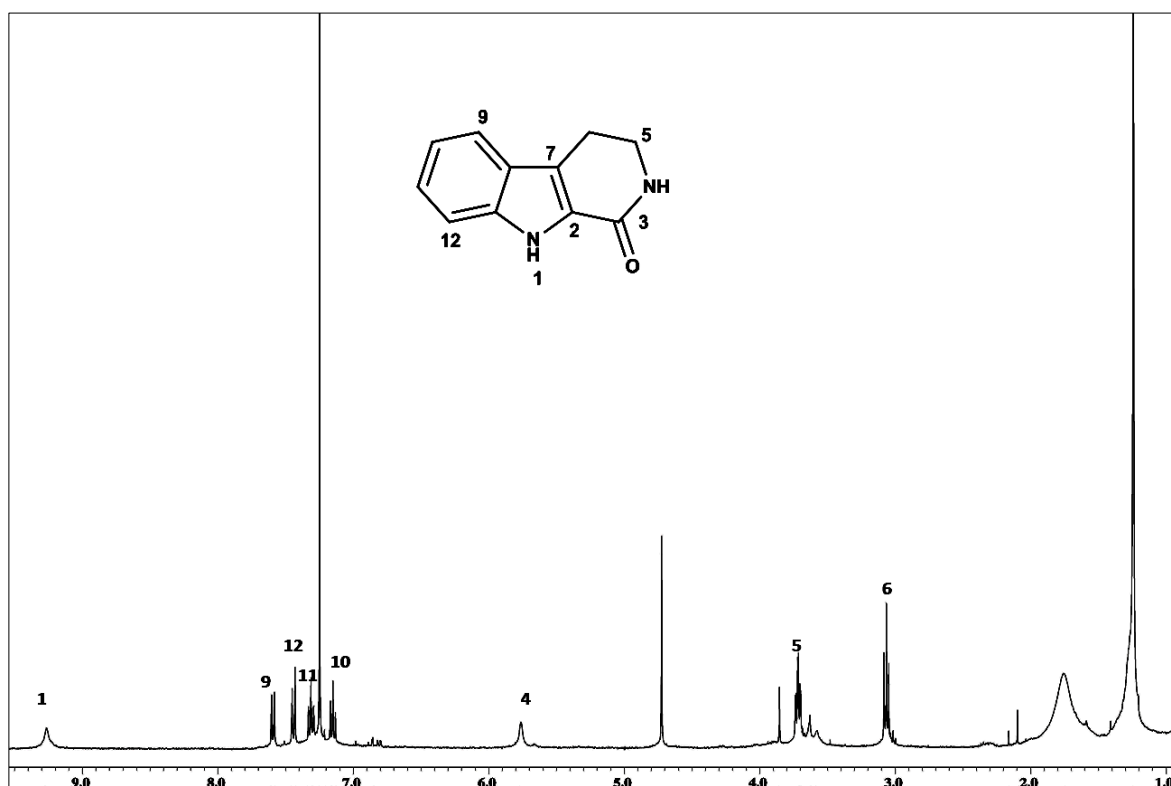


Fig. 4.56: ¹H NMR Spectrum of β- carboline (135)

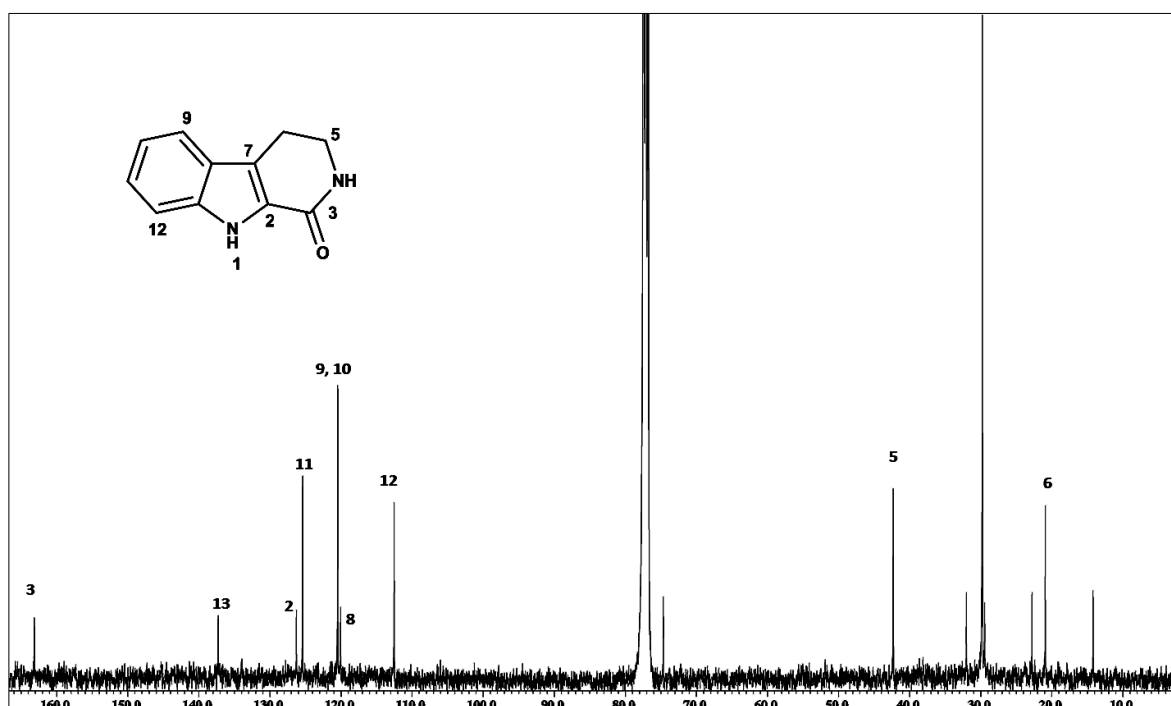


Fig. 4.57: ¹³C NMR Spectrum of β- carboline (135)

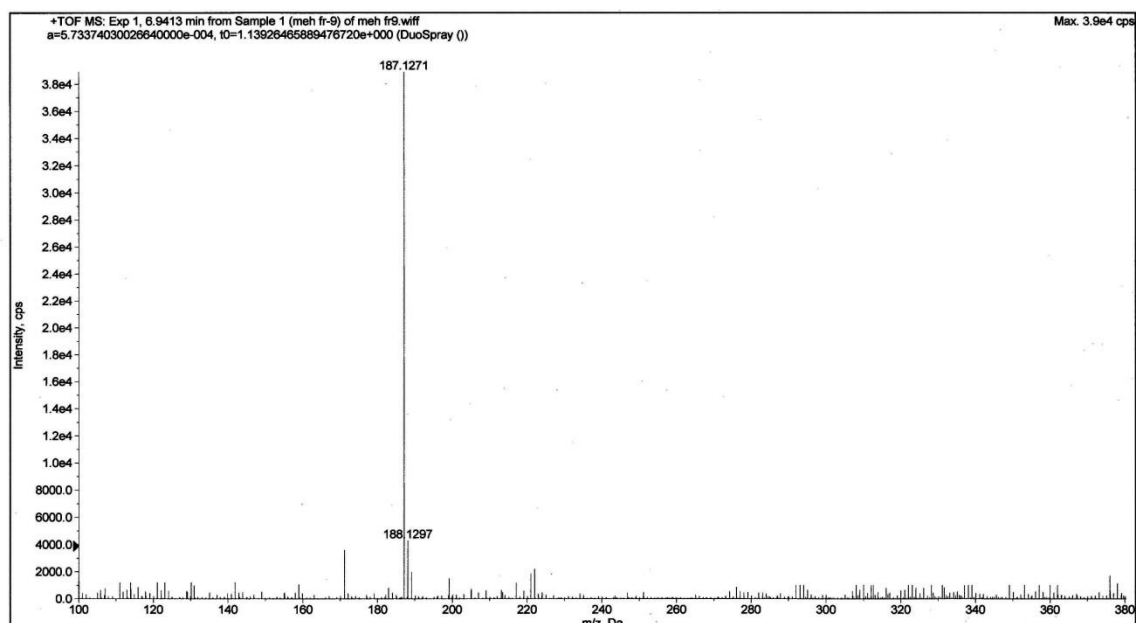
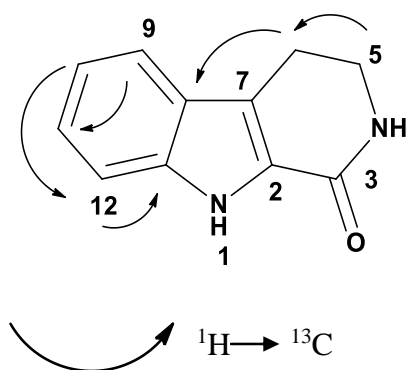
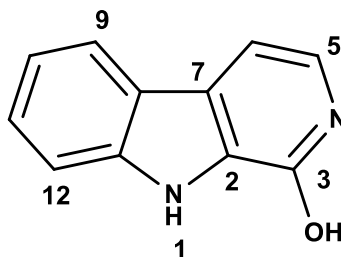


Fig. 4.58: LC-MS Spectrum of β - carboline (**135**)



Scheme 4.16: The HMBC Correlations of β - carboline (**135**)

4.2.2.5 3- Hydroxy- β - carboline (136)



136

3- hydroxy- β - carboline (**136**) was obtained as a yellowish amorphous solid. The mass spectrum revealed a pseudo-molecular ion peak at m/z 185.0711 $[M+H]^+$ corresponding to the molecular formula of $C_{11}H_8N_2O$. The UV spectrum the absorption bonds at 248, 283 and 335 nm indicating the existence of β - carboline chromophore. The IR spectrum showed a band of NH at 3389 cm^{-1} overlapped with an OH group.

The ^1H NMR data (Figure 4.59) showed resonances attributed to an unsubstituted aromatic ring at δ (7.91, *dd*, $J= 8.0, 2.1$ Hz, H-9), (7.36, *t*, $J= 7.6, 2.0$ Hz, H-10), (7.12, *t*, $J= 7.6, 2.0$ Hz, H-11) and δ (7.48, *dd*, $J=8.0, 2.1$ Hz, H-12). In addition, one NH proton signals at δ 5.73 (*s*) and two overlapping signals at δ (7.06 *dd*, $J= 1.64, 6.2$ Hz, H-5, H-6) were also shown.

The ^{13}C NMR (Figure 4.60) spectra indicated the presence of six sp^2 methines, and five sp^2 quaternary carbons. Two of the sp^2 quaternary carbons δ (C-2, C-13) were attached to the nitrogen atom in the indole ring (N-1). Another nitrogen atom (N-4) was attached to one sp^2 quaternary carbon (C-3) and one of the sp^2 methines (C-5).

Complete assignment of ^1H and ^{13}C signals (Table 4.18) established by HMBC (Scheme 4.17) correlations spectra proved (**136**) is 3- hydroxy- β - carboline (**136**) was isolated previously from *Picrasma quassioides* (Wei- Hua *et al.*, 2010).

Table 4.18: ^1H NMR (400 MHz) and ^{13}C NMR (100 MHz) spectral data β - carboline (**136**) in CDCl_3 (δ in ppm, J in Hz).

Position	^1H -NMR (δ ppm)	^{13}C -NMR (δ ppm)	^{13}C -NMR (δ ppm) (Wei-Hua et al, 2010)
2	-	128.8	129.0
3	-	157.9	157.9
5	7.06 (1H, <i>dd</i> , J = 1.64, 6.2)	125.0	125.1
6	7.06 (1H, <i>dd</i> , J = 1.64, 6.2)	102.8	102.8
7	-	123.5	123.5
8	-	127.9	127.9
9	7.91 (1H, <i>dd</i> , J = 8.0, 2.1)	128.2	128.3
10	7.36 (1H, <i>t</i> , J = 7.6, 2.0)	121.1	121.2
11	7.12 (1H, <i>t</i> , J = 7.6, 2.0)	122.3	122.2
12	7.48 (1H, <i>dd</i> , J = 8.0, 2.1)	113.4	113.4
13	-	141.2	142.1
NH	7.35 (1H, <i>s</i>)	-	-

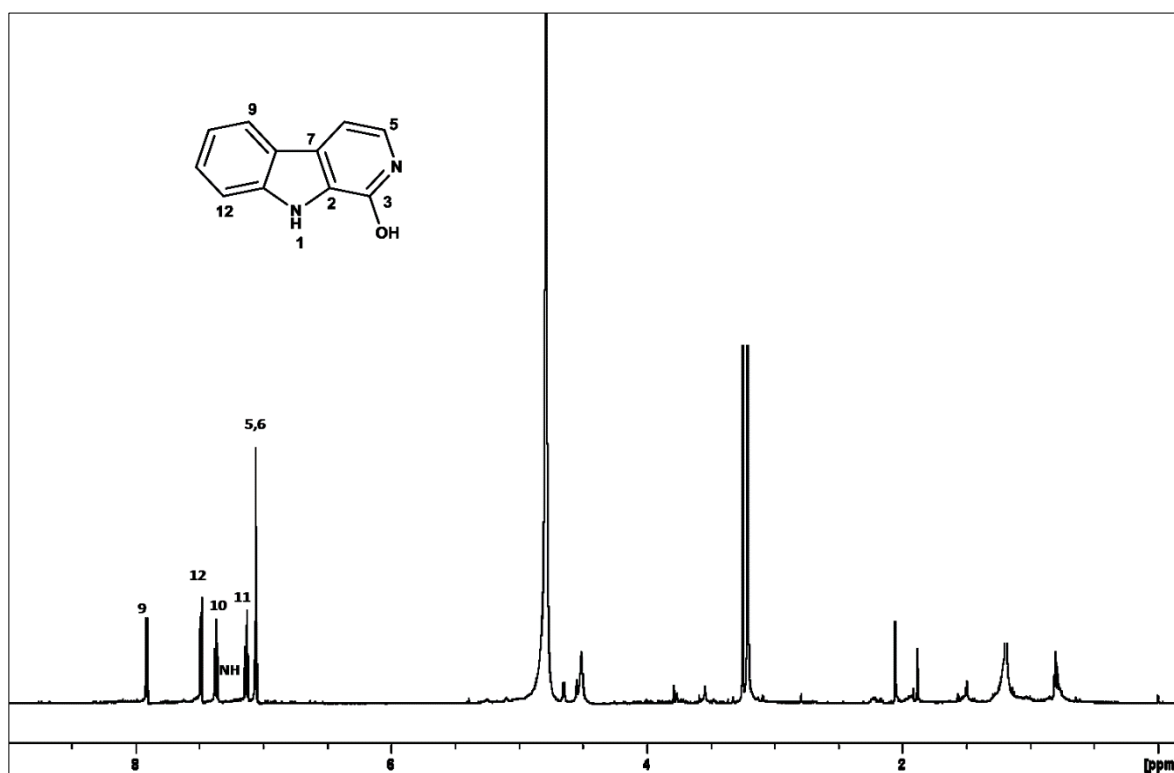


Fig. 4.59: ^1H NMR Spectrum of β - carboline (136)

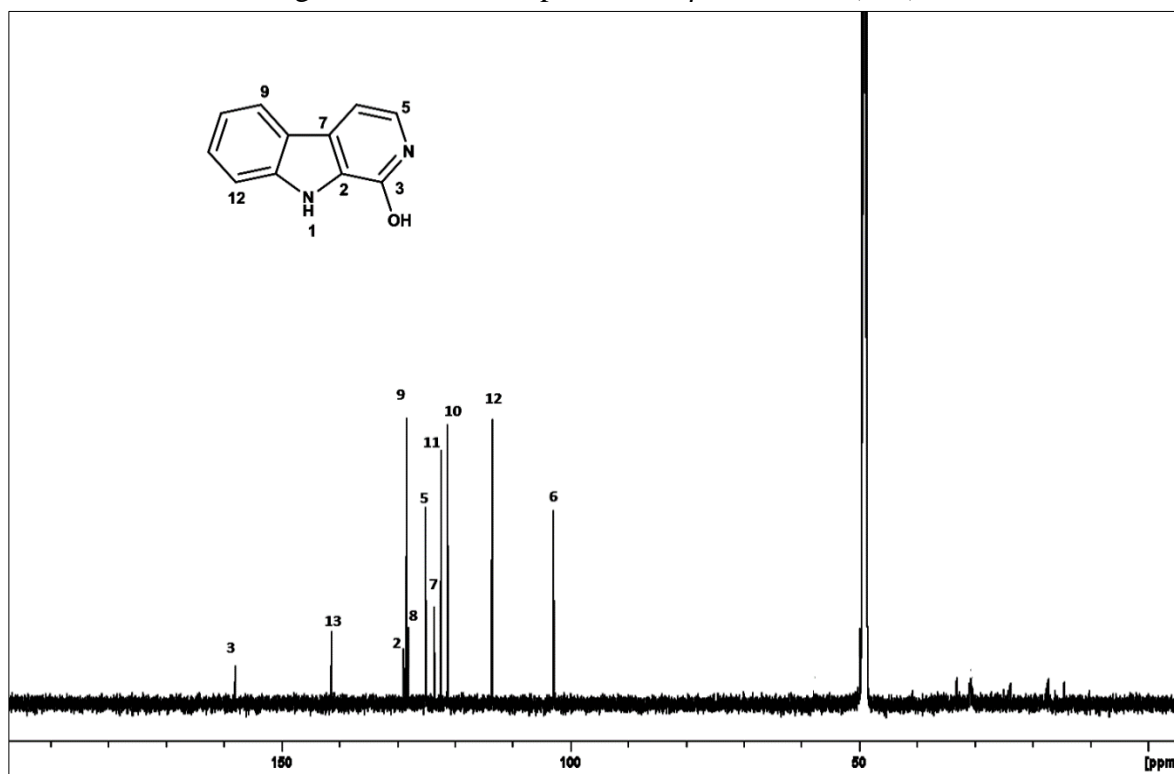


Fig. 4.60: ^{13}C NMR Spectrum of β - carboline (136)

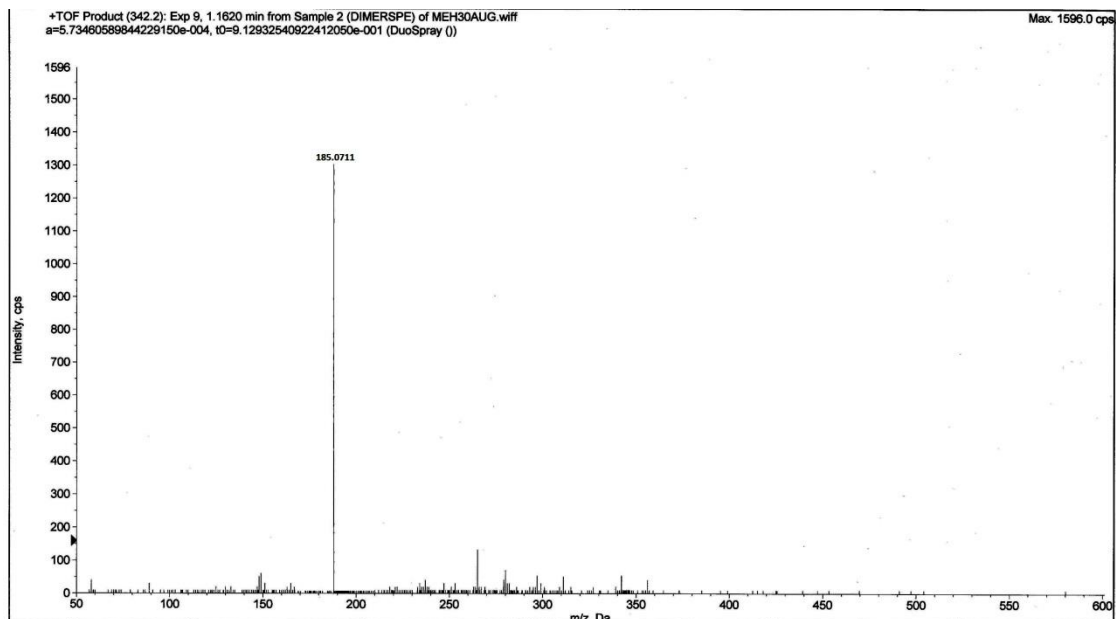
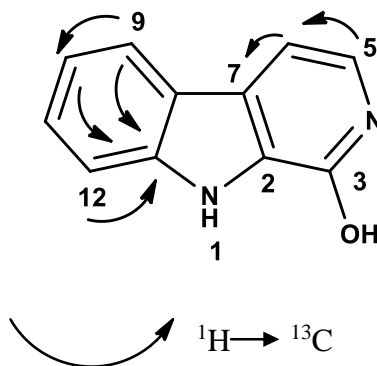
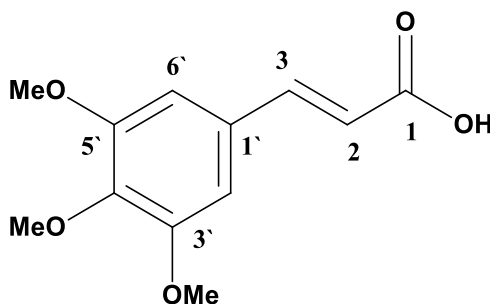


Fig. 4.61: LC-MS Spectrum of β - carboline (**136**)



Scheme 4.17: The HMBC Correlations of β - carboline (**136**)

4.2.2.6 (*E*)-3-(3,4,5-Trimethoxyphenyl) acrylic acid (**137**)



137

(*E*)-3-(3,4,5-trimethoxyphenyl)acrylic acid (**137**) was isolated as a whitish amorphous solid. The mass spectrum revealed a pseudo-molecular ion peak at m/z 239.04 $[M+H]^+$ corresponding to the molecular formula of $C_{12}H_{14}O_5$. The UV spectrum revealed maximum at 225 and 307 nm. The IR spectrum showed a band of OH at 3401 cm^{-1} . In addition, a peak was observed at 1704 cm^{-1} which indicated the presence of the conjugated carbonyl. The ^1H NMR spectrum (Figure 4.62) showed two overlapping aromatic protons at δ 6.75 attributed to H-6' and H-2' respectively. In the up field region, one singlet appeared at δ 3.90 attributed to three overlapping methoxy groups attached to C-3', C-4' and C-5'. The hypothesis was also supported further by the cross peaks of COSY experiment that showed existence of two sets of doublet ($J = 16.0\text{ Hz}$) in the ^1H NMR at δ 6.36 and 7.56 which corresponded to the resonances of H-2 and H-3. The ^{13}C NMR (Figure 4.63) and DEPT 135 showed the presence of 12 carbon atoms, four quaternary carbons, four methines, three methoxy. One peak appeared in δ 167.5 which is carbonyl of (C-1). The cross peak between H-3 and C-1 as observed from the HMBC spectrum (Scheme 4.18) indicated that C-1 is vicinal to the olefinic carbon, C-3.

The comprising of ^1H and ^{13}C data (Table 4.19), DEPT, HSQC and HMBC established the identify of (*E*)-3-(3,4,5-trimethoxyphenyl) acrylic acid (**137**). (Cotinguiba *et al.*, 2009)

Table 4.19: ^1H NMR (400 MHz) and ^{13}C NMR (100 MHz) spectral data of acrylic acid (**137**) in CDCl_3 (δ in ppm, J in Hz).

Position	^1H -NMR (δ ppm)	^{13}C -NMR (δ ppm)	^{13}C -NMR (δ ppm) (Cotinguiba et al, 2009)
1	-	167.5	168.1
2	6.36 (1H, <i>d</i> , J = 16.0)	118.6	118.6
3	7.56 (1H, <i>d</i> , J = 16.0)	153.4	154.1
1'	-	122.8	122.8
2'	6.75 (1H, <i>d</i> , J = 2.0)	105.1	105.1
3'	-	142.6	142.6
4'	-	131.2	131.2
5'	-	142.6	142.6
6'	6.75 (1H, <i>d</i> , J = 2.0)	105.1	105.1
OMe 3'	3.90 (3H, <i>s</i>)	56.1	56.2
OMe 4'	3.90 (3H, <i>s</i>)	60.9	60.2
OMe 5'	3.90 (3H, <i>s</i>)	56.1	56.1
OH	5.60 (1H, <i>s</i>)	-	-

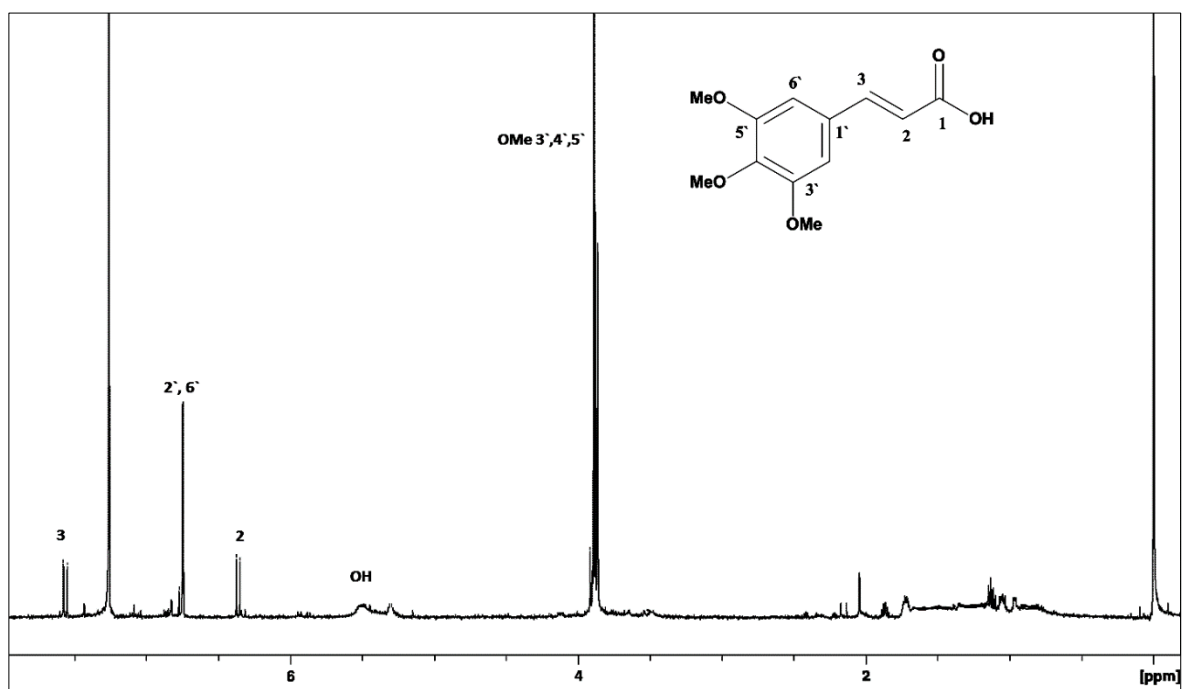


Fig. 4.62: ^1H NMR Spectrum of Acrylic Acid (137)

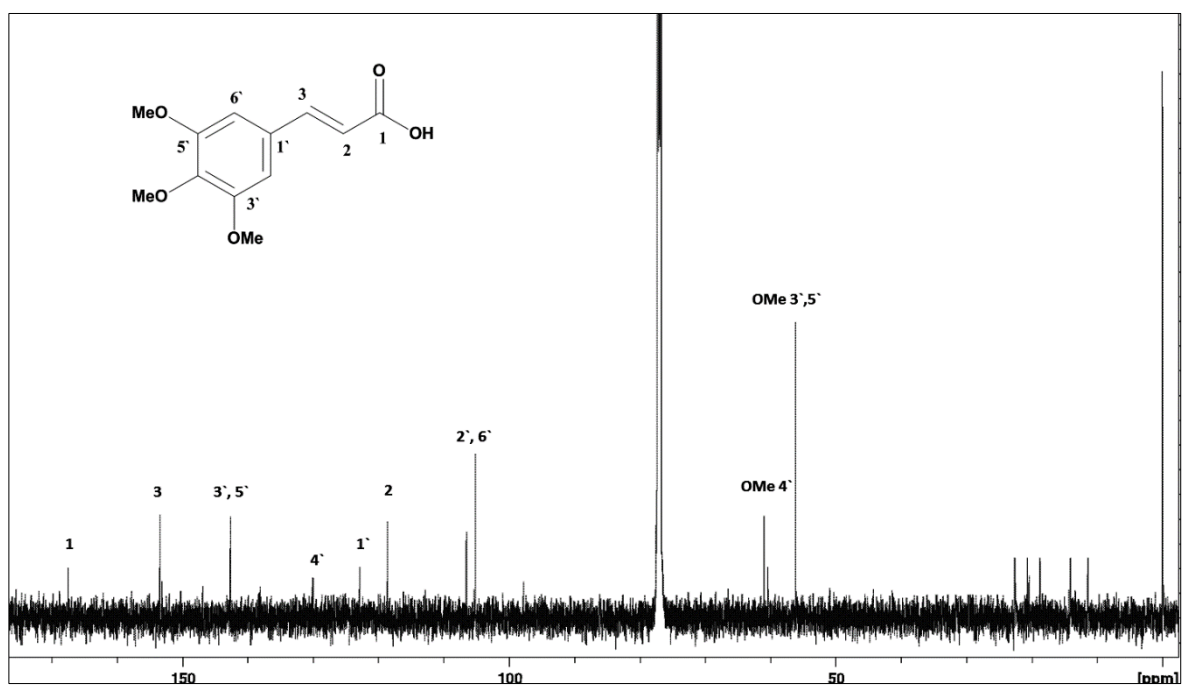


Fig. 4.63: ^{13}C NMR spectrum of Acrylic Acid (137)

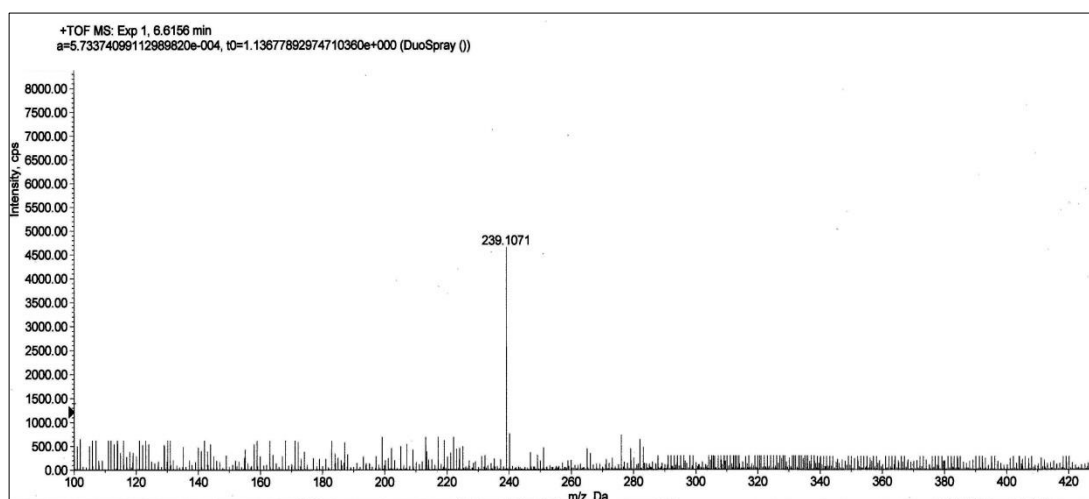
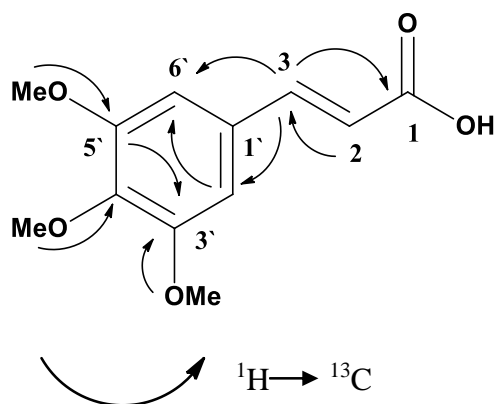
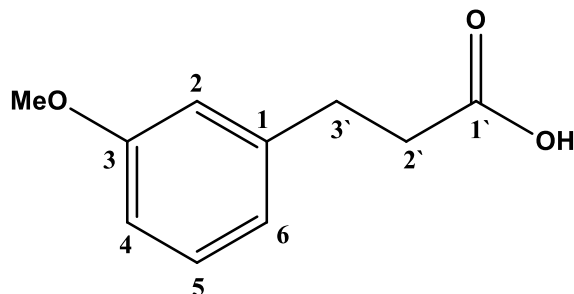


Fig. 4.64: LC-MS spectrum of Acrylic Acid (**137**)



Scheme 4.18: The HMBC Correlations of Acrylic Acid (**137**)

4.2.2.7 3- Methoxy, Benzenepropanoic acid (138)



138

3- methoxy, Benzenepropanoic acid (**138**) was isolated as a whitish amorphous solid. The mass spectrum revealed a pseudo-molecular ion peak at m/z 181.1020 $[M+H]^+$ corresponding to the molecular formula of $C_{10}H_{12}O_3$. The UV spectrum revealed maximum at 225 and 302 nm. The IR spectrum showed a band of OH at 3400 cm^{-1} . In addition, a peak was observed at 1704 cm^{-1} which indicated the presence of a carbonyl group.

The ^1H NMR spectrum (Figure 4.65) showed four aromatic protons at δ 6.26 attributed to H-2, δ 6.83, H-6, δ 7.15, H-4 and δ 7.28, H-5 respectively. In the up field region, one singlet appeared at δ 3.78 attributed to one methoxy group, and two methylenes at δ 3.08 corresponding to H-2' and 3' respectively.

The hypothesis was also supported further by the cross peaks of COSY experiment that showed existence of two sets of multiplet in the ^1H NMR which corresponded to the resonances of H-2' and H-3'.

The ^{13}C NMR (Figure 4.66) and DEPT 135 showed the presence of 10 carbon atoms, three sp^2 quaternary carbons, four sp^2 methines, one methoxy group and two sp^3 methylene. The cross peak between H-3' and C-1' was observed from the HMBC spectrum (Scheme 4.19)

The comprising of ^1H and ^{13}C data (Table 4.20), DEPT, HSQC and HMBC established the structure of 3- methoxy, benzenepropanoic acid (**138**). (Dippy & Page, 1998).

Table 4.20: ^1H NMR (400 MHz) and ^{13}C NMR (100 MHz) spectral data of benzenepropanoic acid (**138**) in CDCl_3 (δ in ppm, J in Hz).

Position	^1H -NMR (δ ppm)	^{13}C -NMR (δ ppm)	^{13}C -NMR (δ ppm) (Dippy et al, 1998)
1	-	132.3	133.2
2	6.36 (1H, <i>d</i> , $J= 2.2$)	114.1	114.1
3	-	158.3	158.3
4	7.15 (1H, <i>dd</i> , $J= 8.7, 2.1$)	113.2	113.2
5	7.28 (1H, <i>d</i> , $J= 8.2$)	129.4	129.4
6	6.82 (1H, <i>dd</i> , $J= 8.0, 2.1$)	119.0	120.0
1'	-	169.6	169.7
2'	3.09 (2H, <i>m</i>)	36.7	36.7
3'	3.05 (2H, <i>m</i>)	29.6	29.6
OMe- 3	3.90 (3H, <i>s</i>)	55.3	55.3

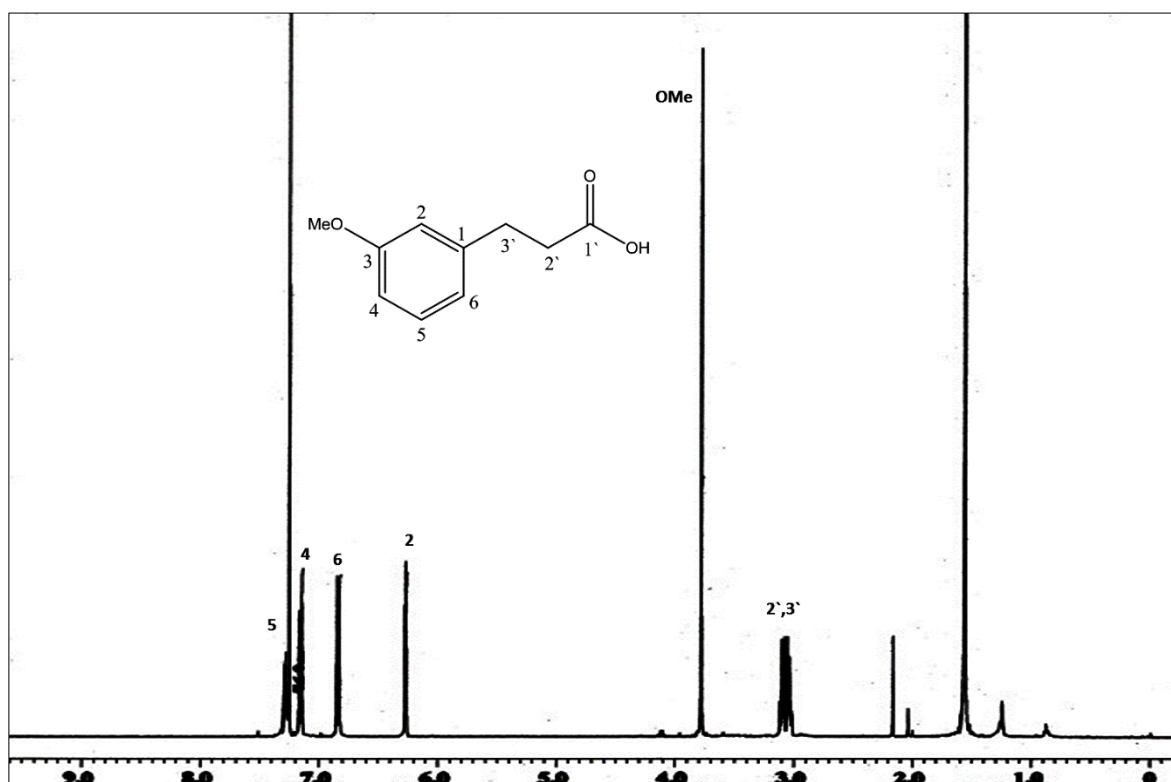


Fig. 4.65: ^1H NMR Spectrum of Benzenepropanoic Acid (138)

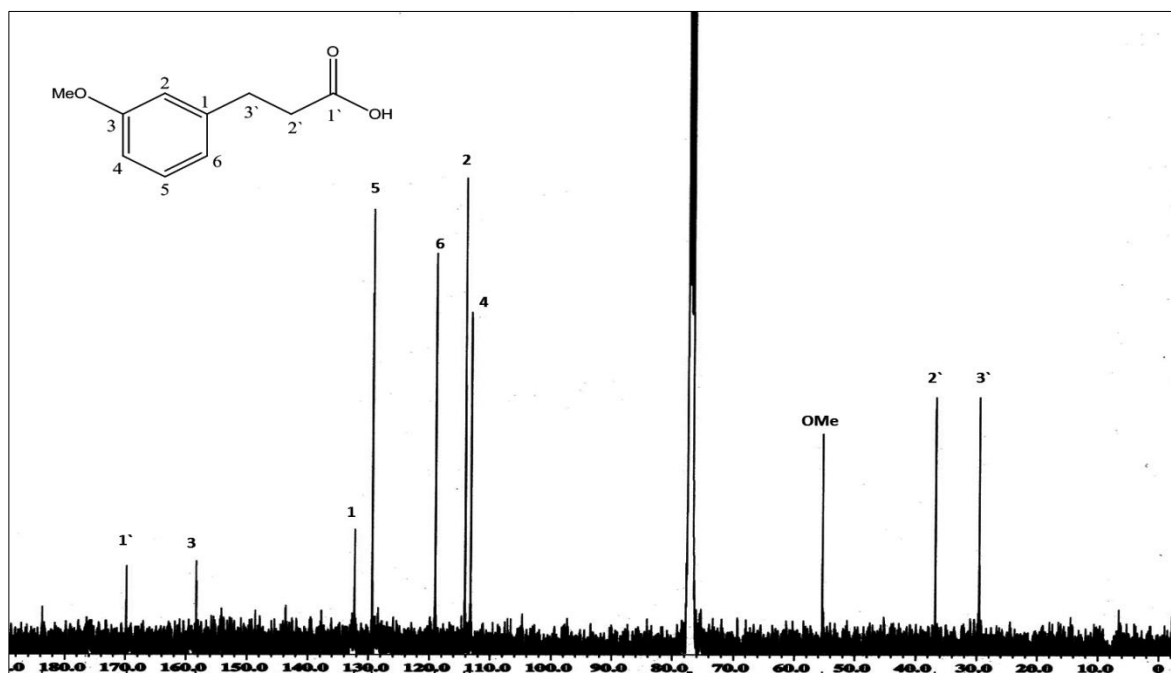


Fig. 4.66: ^{13}C NMR Spectrum of Benzenepropanoic Acid (138)

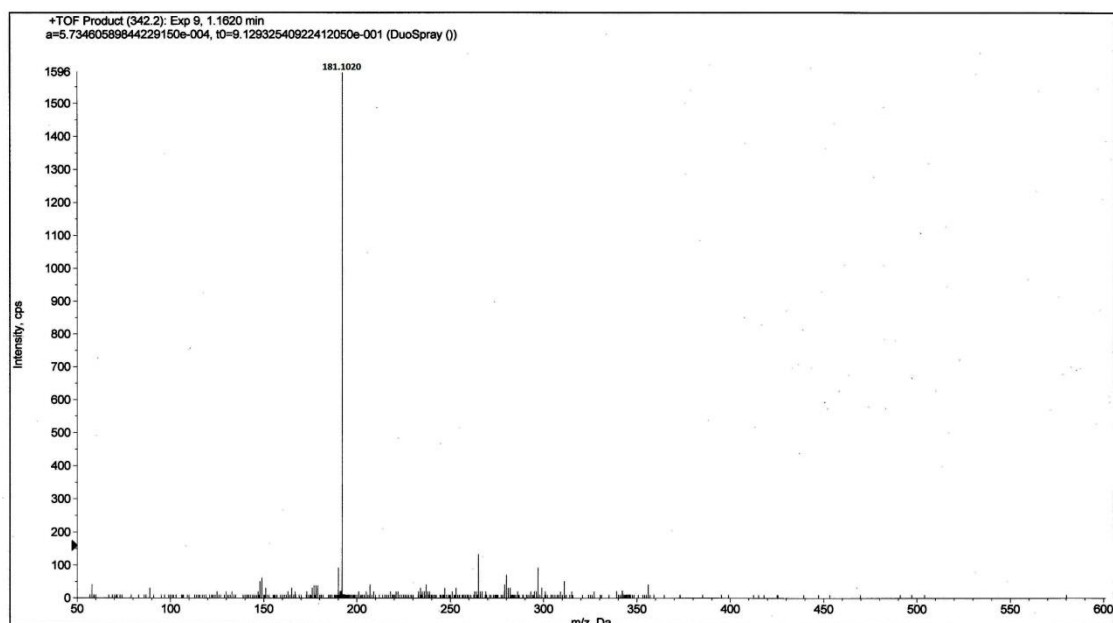
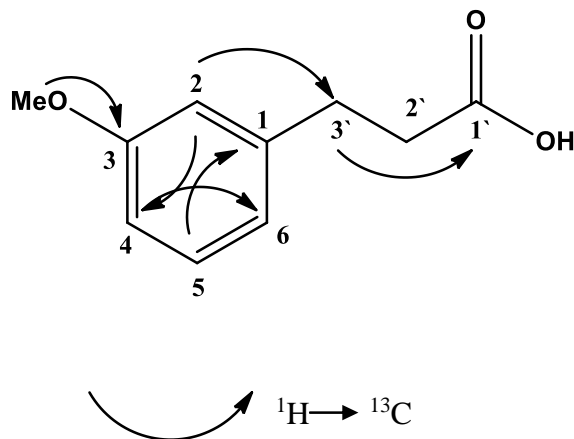


Fig. 4.67: LC-MS Spectrum of Benzenepropanoic Acid (**138**)

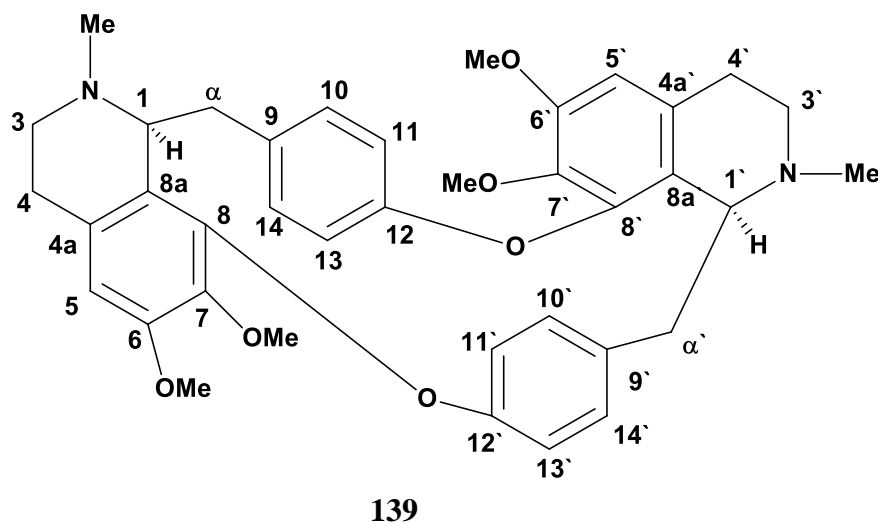


Scheme 4.19: The HMBC Correlations of Benzenepropanoic Acid (**138**)

4.3 Isolation and Structural Elucidation of Compounds from the Bark of *Actinodaphne macrophylla*

Bark of *Actinodaphne macrophylla* has afforded eight isoquinoline alkaloids. There were cycleanine (**139**), (-)-10-demethylxylopinine (**140**), reticuline (**141**), (+) laurotetanine (**142**), (+) bicuculine (**143**), (-) α -hydrastine (**144**), (+) parafumine (**145**) and (+) anolobine (**146**).

4.3.1 Cycleanine (**139**)



Cycleanine (**139**) was obtained as a brownish amorphous with $[\alpha]_D^{24} -16$ (c 0.05, CHCl_3). The UV spectrum revealed absorbance band at 238 nm, while the IR spectrum exhibited absorption for aromatic ring and diphenyl ether at 1500 and 1220 cm^{-1} respectively (Williams *et al.*, 1989). The mass spectrum revealed the $[\text{M}+\text{H}]^+$ peak at m/z 623.4118 thus suggesting a molecular formula of $\text{C}_{38}\text{H}_{42}\text{N}_2\text{O}_6$.

Although cycleanine (**139**) possesses two basic nitrogen atoms in the molecule, only two mono-*N*-oxides are theoretically possible, inasmuch as cycleanine (**139**) is a symmetrical molecule consisting of the same two benzylisoquinoline moieties. The ^1H NMR spectrum (Figure 4.68) particularly revealed one *N*-methyl singlet signal, at δ 2.45 corresponding to

N-2 methyl proton. It's also showed two singlet signals attributed to two methoxy groups appeared at δ 3.83 and 3.42 which were attached to C-6 and C-7, respectively. The absence of signals positioned between δ 3.30 to δ 3.85 characteristic of a C-8 methoxy indicated that C-8 was phenyl ether linkage (C-8-O-C-12') instead substituted with hydroxyl or methoxy group. The spectrum also showed one singlet signal at δ 6.42 which was assigned as H-5. The spectrum also displayed four doublet of doublet attributed to H-10, H-11, H-13 and H-14 were present at δ 6.14 (J = 8.2 and 2.1 Hz), δ 5.68 (J = 8.2 and 2.1 Hz), δ 6.46 (J = 8.3 and 2.1 Hz) and 6.89 (J = 8.4 and 2.1 Hz), respectively. A doublet (J = 10.4 Hz) signal corresponding to one proton, H-1 was observed at δ 4.11. In aliphatic region the multiplet signals appeared at δ (3.85 and 3.29, H-3), δ (2.74 and 2.83, H-4) and δ (2.34 and 3.09, H- α).

The ^{13}C NMR spectrum (Figure 4.69) and DEPT 135 (Figure 4.70) revealed nineteen carbons in a dimeric system. There were seven quaternary carbons, two methoxy groups, six methines, three methylenes, and one *N*-methyl. The complete 1D (^1H and ^{13}C) and 2D (COSY, HSQC), and HMBC (Scheme 4.20) NMR assignment and compare with the literature review confirmed the isolation of cycleanine (**139**) (de Wet *et al.*, 2005).

Complete assignments of cycleanine (**139**) were listed in table 4.21.

Table 4.21: ^1H NMR (400 MHz) and ^{13}C NMR (100 MHz) spectral data of cycleanine (**139**) in CDCl_3 (δ in ppm, J in Hz).

Position	^1H -NMR (δ ppm)	^{13}C -NMR (δ ppm)	^{13}C -NMR (δ ppm) (de Wet et al, 2005)
1	4.11 (1H, <i>d</i> , $J= 10.4$)	167.5	168.1
3	3.85 (1H, <i>m</i>)	44.7	44.7
	3.29 (1H, <i>m</i>)	-	-
4	2.74 (1H, <i>m</i>)	24.8	24.6
	2.83 (1H, <i>m</i>)	-	-
4a	-	129.7	129.8
5	6.42 (1H, <i>s</i>)	109.2	109.3
6	-	151.9	151.9
7	-	138.9	138.9
8	-	143.7	143.7
8a	-	125.5	125.5
α	2.34 (1H, <i>m</i>)	37.9	37.9
	3.09 (1H, <i>m</i>)	-	-
9	-	130.5	130.5
10	6.14 (1H, <i>dd</i> , $J= 8.2, 2.1$)	128.8	128.8
11	5.68 (1H, <i>dd</i> , $J= 8.2, 2.8$)	114.1	114.1
12	-	154.2	154.2
13	6.46 (1H, <i>dd</i> , $J= 8.5, 2.7$)	117.5	117.4
14	6.89 (1H, <i>dd</i> , $J= 8.4, 2.1$)	128.2	128.2
OMe- 6	3.83 (3H, <i>s</i>)	56.2	56.2
OMe- 7	3.42 (3H, <i>s</i>)	60.1	60.1
<i>N</i> - Me	2.45 (3H, <i>s</i>)	42.6	42.6

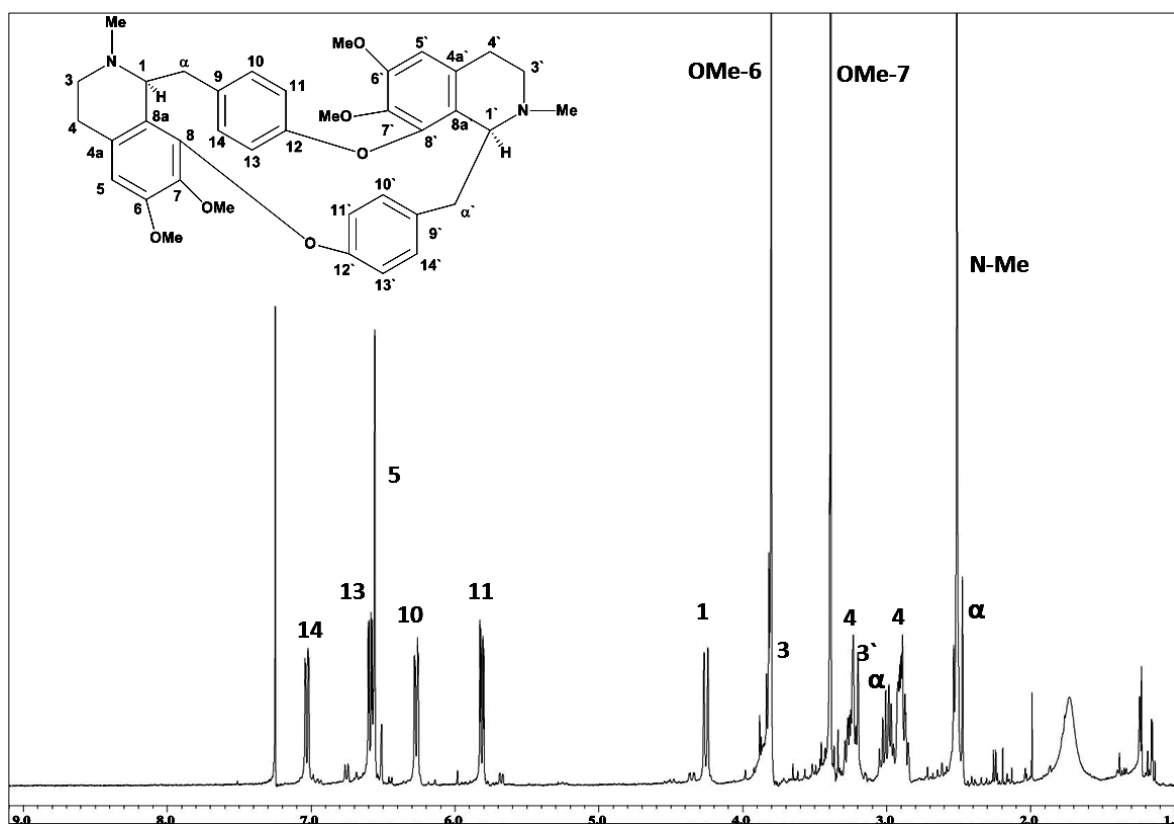


Fig. 4.68: ^1H NMR Spectrum of Cycleanine (139)

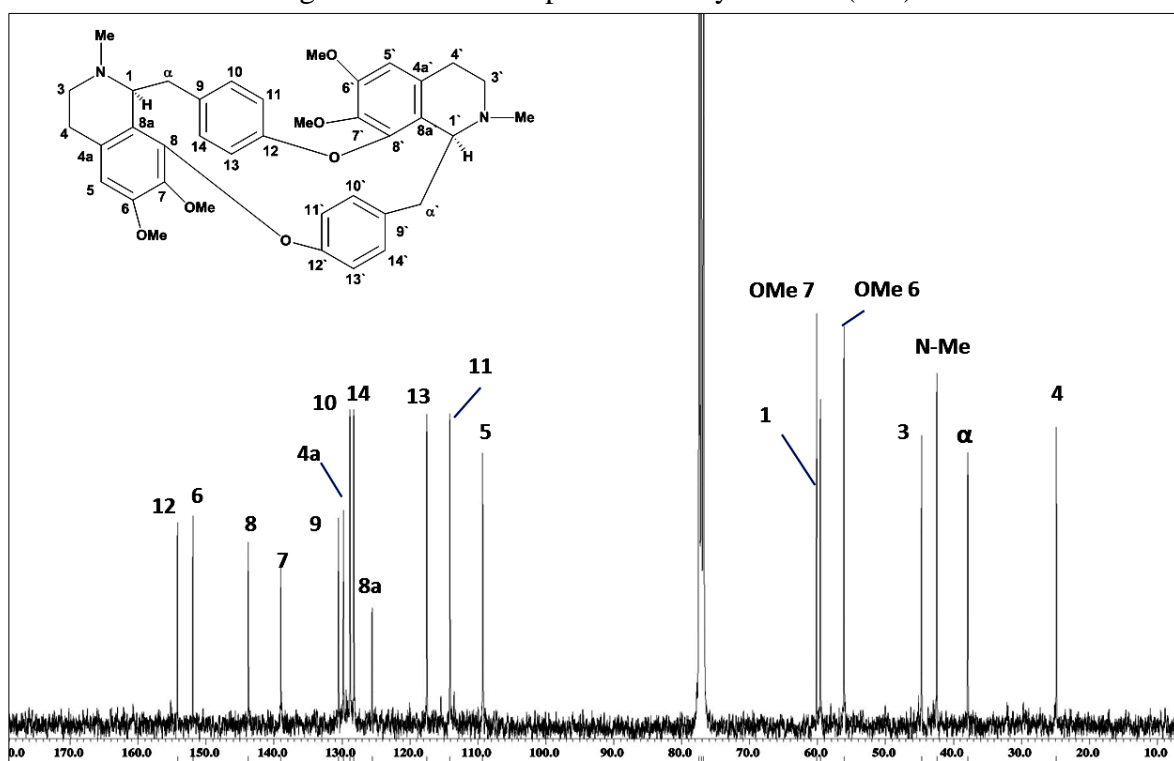


Fig. 4.69: ^{13}C NMR Spectrum of Cycleanine (139)

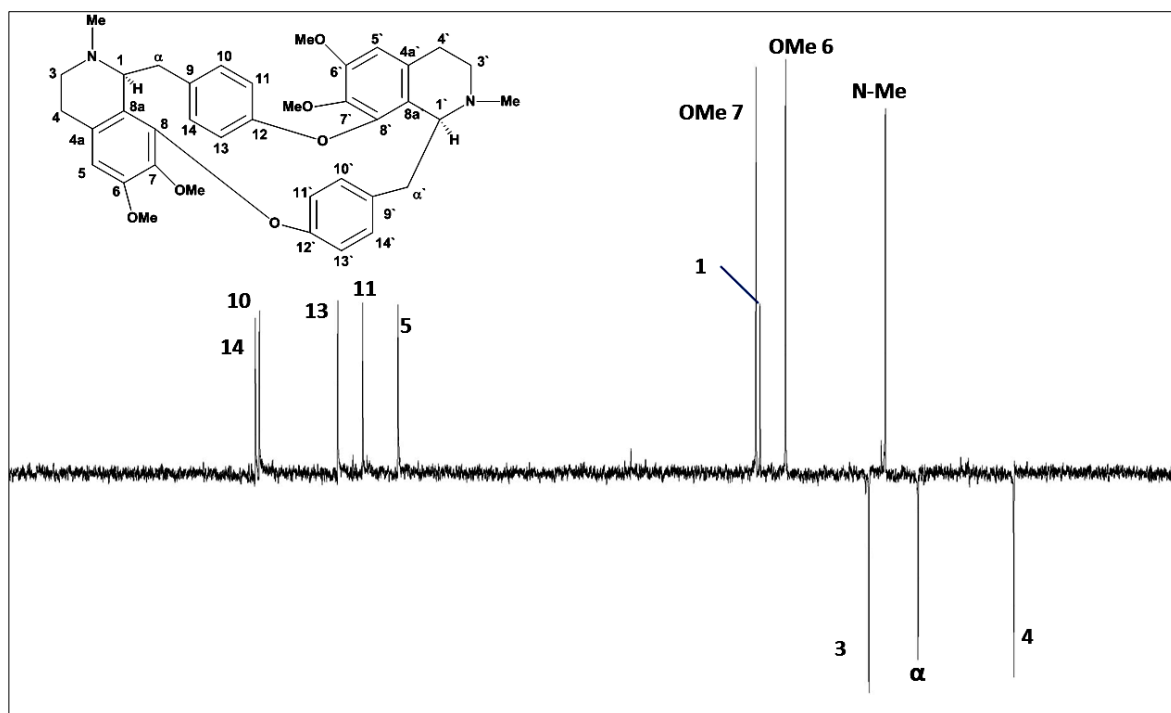


Fig. 4.70: DEPT 135 Spectrum of Cycleanine (139)

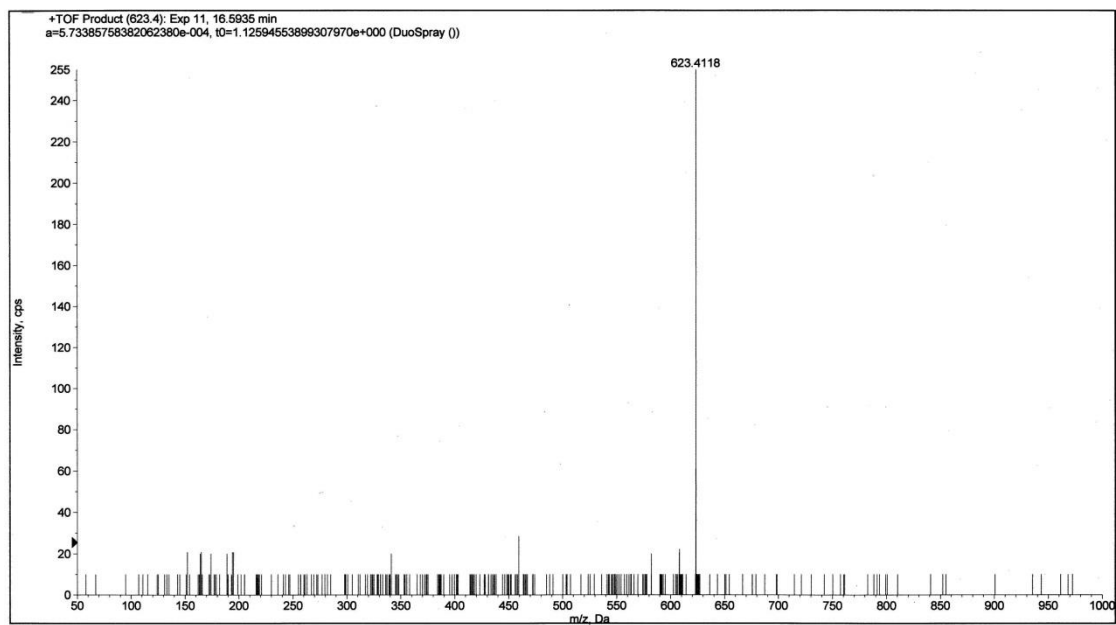
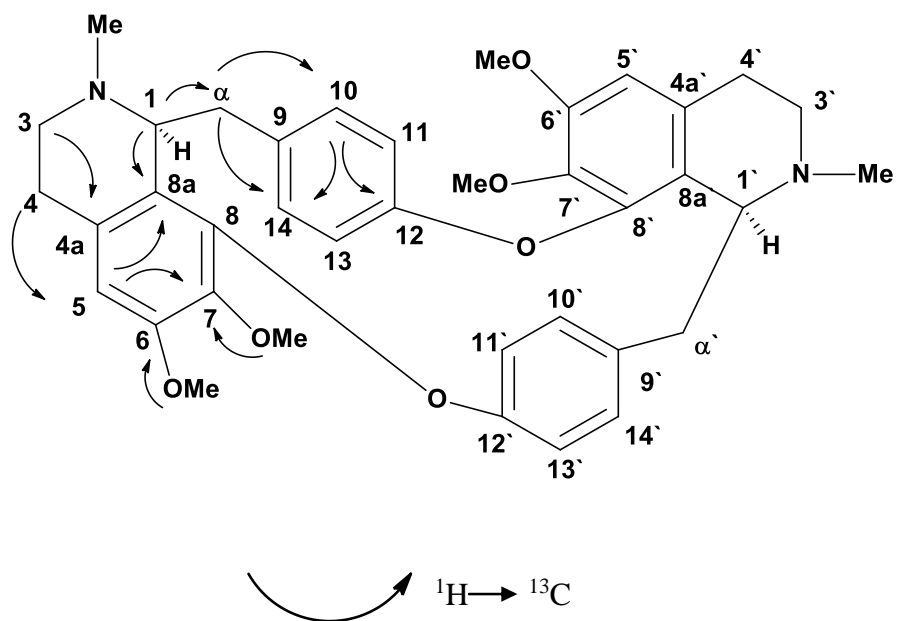
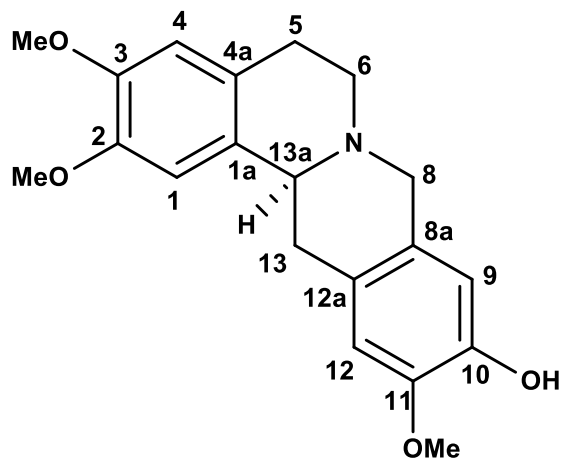


Fig. 4.71: LC-MS Spectrum of Cycleanine (139)



Scheme 4.20: The HMBC Correlations of Cycleanine (**139**)

4.3.2 (-)-10-Demethylxylopinine (**140**)



140

(-)-10-demethylxylopinine (**140**) was isolated as a brownish amorphous solid. $[\alpha]_{\text{D}}^{24} -227$ (c 0.06, CHCl_3). The mass spectrum revealed a pseudo-molecular ion peak at m/z 342.2540 $[\text{M}+\text{H}]^+$ corresponding to the molecular formula of $\text{C}_{20}\text{H}_{23}\text{NO}_4$. The UV spectrum revealed maximum at 301 nm which is characteristic of berbine type of alkaloids (Grycova et al., 2007). The IR spectrum showed band of OH at 3382 cm^{-1} .

The ^1H MNR spectrum (Figure 4.72) showed two tetra substituted aromatic rings including four singlet proton signals at δ (6.56, H-1), (6.64, H-4), (6.70, H-9) and (6.66, H-12). Another singlet peak appeared at δ 3.85 corresponding for three methoxy groups.

Due to existing an electron withdrawing group (N -7), protons H-6, H-8 and H-13a appeared at δ (2.84, m , 3.24, m), (3.69, m , 3.95, m) and δ (3.559, dd , $J= 4.1, 11.4\text{ Hz}$) respectively. Other aliphatic protons were appeared at δ (2.60, m , 3.11, m , H-5) and δ (2.63, m , 3.13, m , H-13).

The ^{13}C NMR (Figure 4.73) indicated the presence of four sp^2 methines, eight sp^2 quaternary carbons, four sp^3 methylenes, one sp^3 methine, and three methoxy groups. In addition, the HMBC spectrum revealed correlations of H- 4 to C-5, C- 2 and C-1a, H-1 to C- 4a and C-13a, H-13a to C-8 and C- 12a, H-9 to C-12a and C-11 and H-12 to C-10 and C-8a (Scheme 4.22). Through examination of ^1H , ^{13}C , (Table 4.21), DEPT, COSY, HSQC and HMBC spectra has made possible the complete assignments. In conclusion, data comparison with the literature confirmed thae isolation of (-)-10- demethylxylopinine (**140**) (Perez *et al.*, 2010).

Table 4.22: ^1H NMR (400 MHz) and ^{13}C NMR (100 MHz) spectral data of (-)-10-demethylxylopinine (**140**) in CDCl_3 (δ in ppm, J in Hz).

Position	^1H -NMR (δ ppm)	^{13}C -NMR (δ ppm)	^{13}C -NMR (δ ppm) (Perez et al, 2010)
1	6.56 (1H, <i>s</i>)	107.7	108.1
1a	-	126.2	126.2
2	-	147.6	147.7
3	-	147.6	147.2
4	6.64 (1H, <i>s</i>)	109.0	109.1
4a	-	126.3	126.3
5	2.60 (1H, <i>m</i>)	28.8	28.8
	3.11 (1H, <i>m</i>)	-	-
6	2.84 (1H, <i>m</i>)	51.3	51.3
	3.24 (1H, <i>m</i>)	-	-
8	3.69 (1H, <i>m</i>)	58.2	58.3
	3.95 (1H, <i>m</i>)	-	-
8a	-	127.5	127.5
9	6.70 (1H, <i>s</i>)	114.3	114.3
10	-	144.0	144.1
11	-	145.2	145.2
12	6.66 (1H, <i>s</i>)	111.4	111.3
12a	-	129.2	129.2
13	2.63 (1H, <i>m</i>)	36.5	36.51
	3.13 (1H, <i>m</i>)	-	-
13a	3.59 (1H, <i>dd</i> , $J= 4.1, 11.4$)	59.7	59.7
OMe 2,3,11	3.85 (9H, <i>s</i>)	56.0	56.1

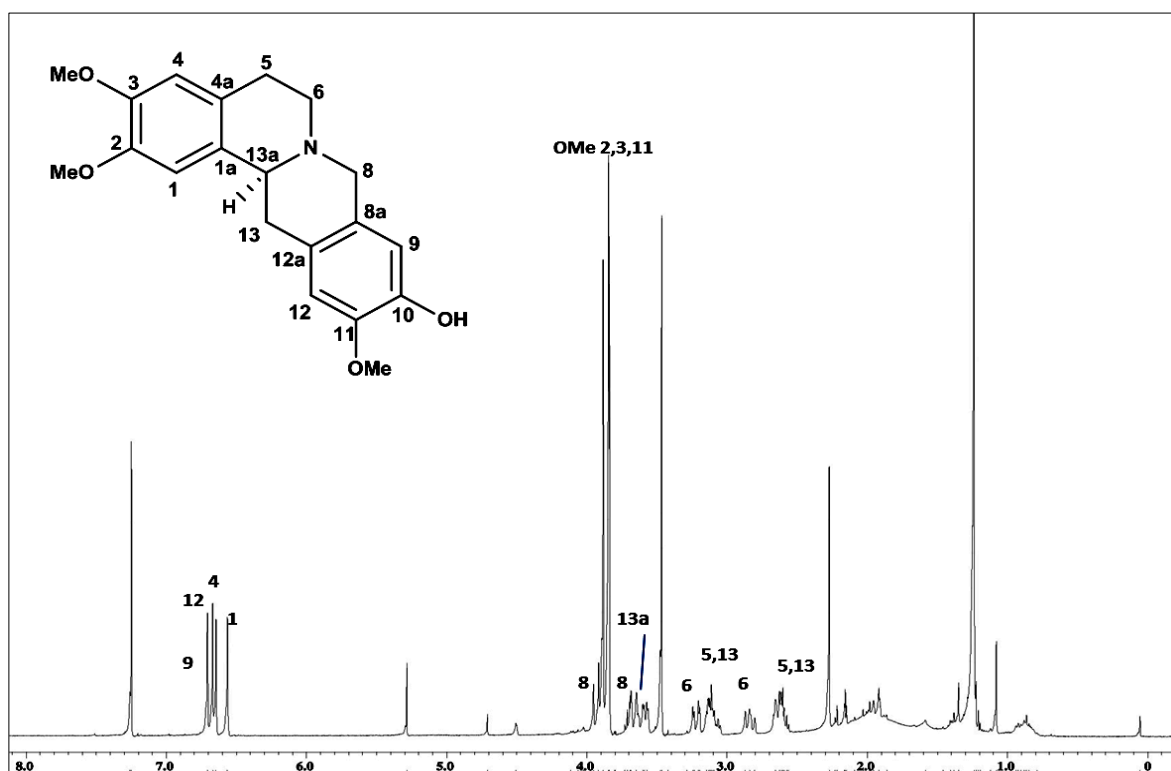


Fig. 4.72: ^1H NMR Spectrum of (-)-10- Demethylxylopinine (140)

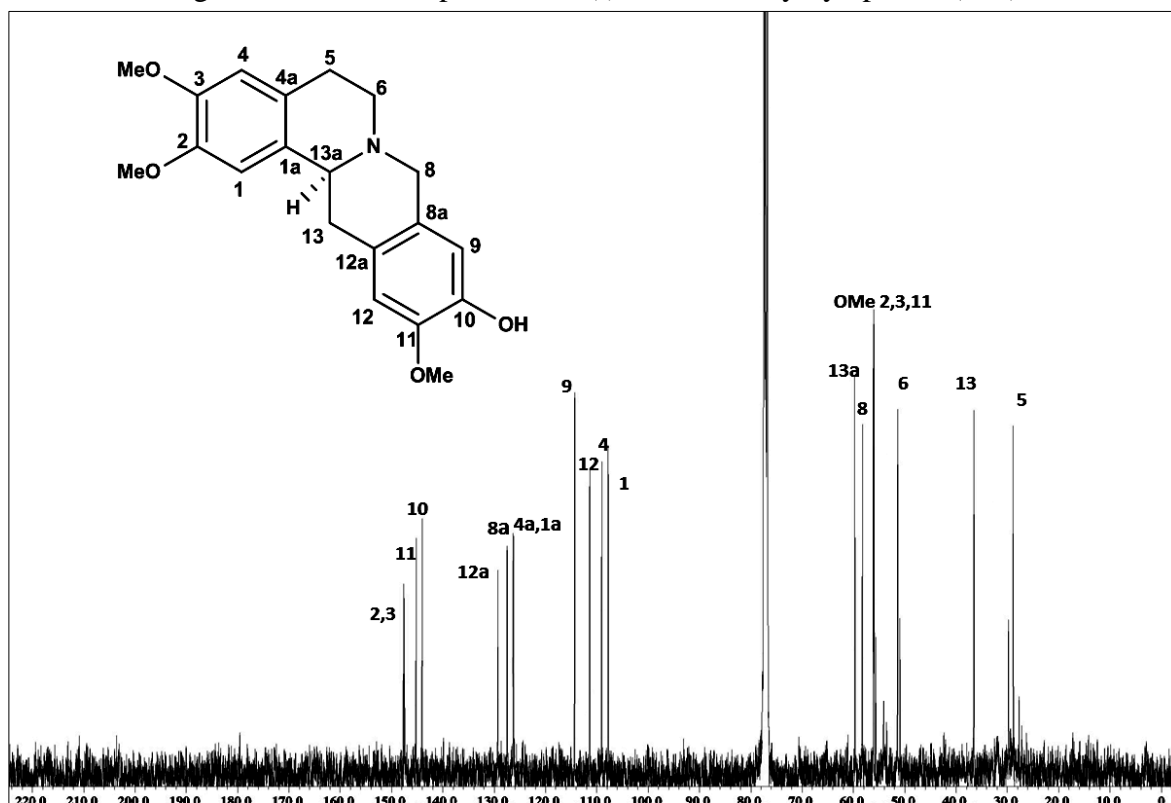
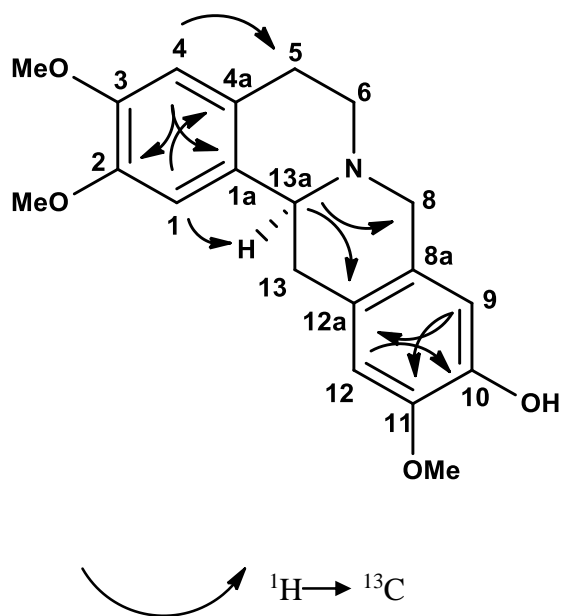
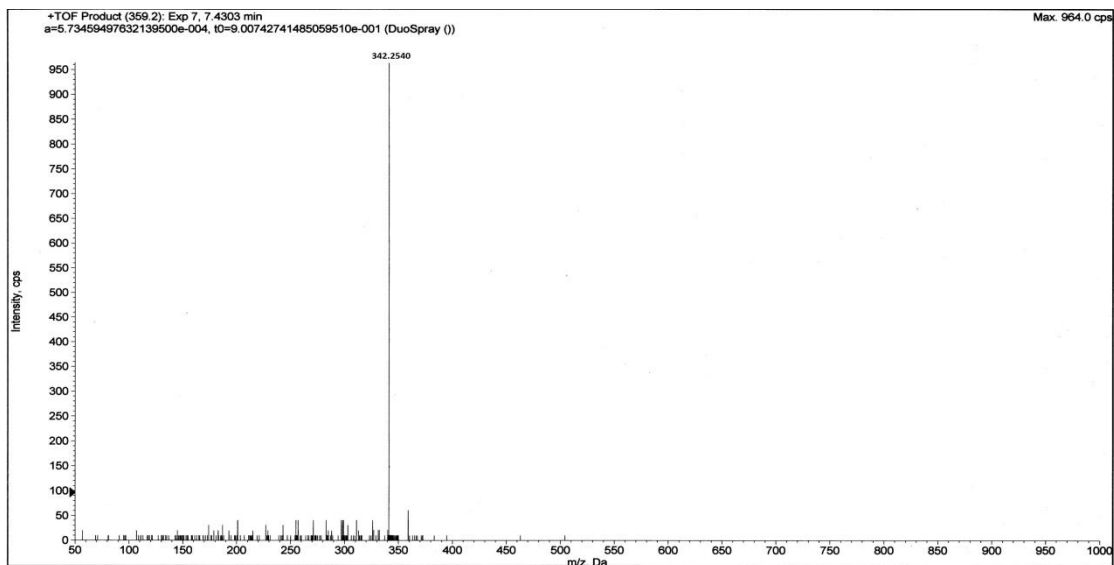
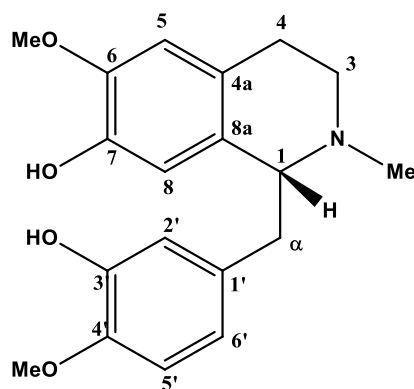


Fig. 4.73: ^{13}C NMR Spectrum of (-)-10- Demethylxylopinine (140)

Scheme 4.21: The HMBC Correlations of (-)-10- Demethylxylopinine (**140**)

4.3.3 Reticuline (141)



141

Reticuline (**141**) was afforded as a brownish amorphous solid, $[\alpha]_D^{24} -55$ (c 0.05, CHCl_3).

The UV spectrum showed absorption band at 235 and 283 nm which were a characteristic of a benzyloisoquinoline alkaloid (Kanyinda *et al.*, 1995). The IR spectrum showed absorption at 3447 cm^{-1} indicated the stretching of hydroxyl group in the structure. The LC-MS spectrum gave a pseudomolecular ion peak, $[\text{M}+\text{H}]^+$ at m/z 330.1331 consistent with the molecular formula of $\text{C}_{19}\text{H}_{23}\text{NO}_4$.

The ^1H -NMR spectrum (Figure 4.75) showed two overlapped methoxyl groups at δ 3.82, corresponding to OMe-6 and OMe-4' . In addition, there are five aromatic protons appeared at δ 6.74 (d , $J = 2.2\text{ Hz}$, 1H, H-2'), δ 6.71 (d , $J = 8.2\text{ Hz}$, 1H, H-5'), δ 6.56 (dd , $J = 1.8, 8.2$, 1H, H-6'), δ 6.51 (s , 1H, H-5) and δ 6.35 (s , 1H, H-8). One *N*-methyl proton resonated as a singlet at δ 2.43. The aliphatic protons appeared as multiplets at the region of δ 2.59-3.17. The complete assignments for the proton signals were tabulated in Table 4.23.

The ^{13}C -NMR (Figure 4.76) spectrum established the presence of 19 carbons which is in agreement with the molecular formula of reticuline. The ^{13}C -NMR experiment showed

three methyls, three methylenes, six methines and seven quaternary carbons in the molecule skeleton.

The cross peaks observed in the HMBC spectrum (Scheme 4.22) showed that the proton at δ 6.51 (H-5) correlated with δ 25.0 (C-4), δ 125.3 (C-8a) and δ 143.4 (C-7) while the proton at δ 6.35 (H-8) correlated with δ 64.5 (C-1), δ 143.4 (C-6) and 130.3 (C-4a). The carbon-bearing hydroxyl groups (δ 143.4 and δ 145.3) were placed at C-7 and C-3' respectively because of the connectivity of H-5 (δ 6.51) to C-7 (δ 143.4) and H-5' (δ 6.71) to C-3' (δ 145.3).

Finally, unambiguous assignment of all proton and carbon signals using HSQC and COSY and by comparison with literature data confirmed the isolation of reticuline (**141**). (Hughes *et al.*, 1968).

Table 4.23: ^1H NMR (400 MHz) and ^{13}C NMR (100 MHz) spectral data of reticuline (**141**) in CDCl_3 (δ in ppm, J in Hz).

Position	^1H -NMR (δ ppm)	^{13}C -NMR (δ ppm)	^{13}C -NMR (δ ppm) (Hughes et al, 1968)
1	3.69 (1H, <i>m</i>)	64.5	65.2
3	2.78 (1H, <i>m</i>)	46.8	46.1
	3.14 (1H, <i>m</i>)	-	-
4	2.52 (1H, <i>m</i>)	25.0	25.1
	2.72 (1H, <i>m</i>)	-	-
4a	-	130.3	130.3
5	6.51 (1H, <i>s</i>)	110.6	111.0
6	-	143.4	144.2
7	-	143.4	143.2
8	6.35 (1H, <i>s</i>)	113.7	113.7
8a	-	125.3	125.3
α	2.70 (1H, <i>m</i>)	41.0	41.1
	2.99 (1H, <i>m</i>)	-	-
1'	-	133.3	133.2
2'	6.74 (1H, <i>d</i> , $J=2.2$)	115.7	115.7
3'	-	145.3	145.4
4'	-	145.0	145.1
5'	6.71 (1H, <i>d</i> , $J=8.2$)	110.6	110.6
6'	6.56 (1H, <i>dd</i> , $J=1.8, 8.2$)	120.9	120.9
OMe-6	3.82 (3H, <i>s</i>)	55.9	55.9
OMe-4'	3.82 (3H, <i>s</i>)	55.9	55.9
N-Me	2.43 (3H, <i>s</i>)	42.5	42.3

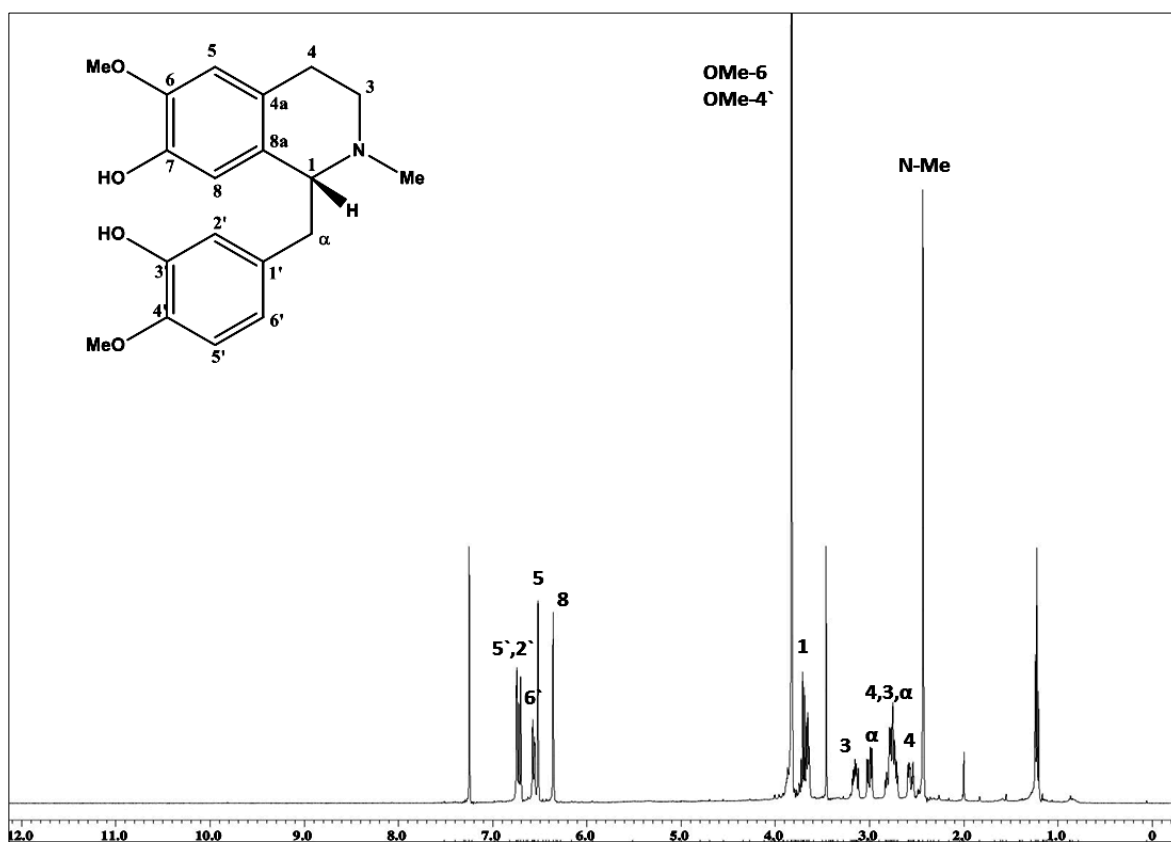


Fig. 4.75: ¹H NMR Spectrum of Reticuline (141)

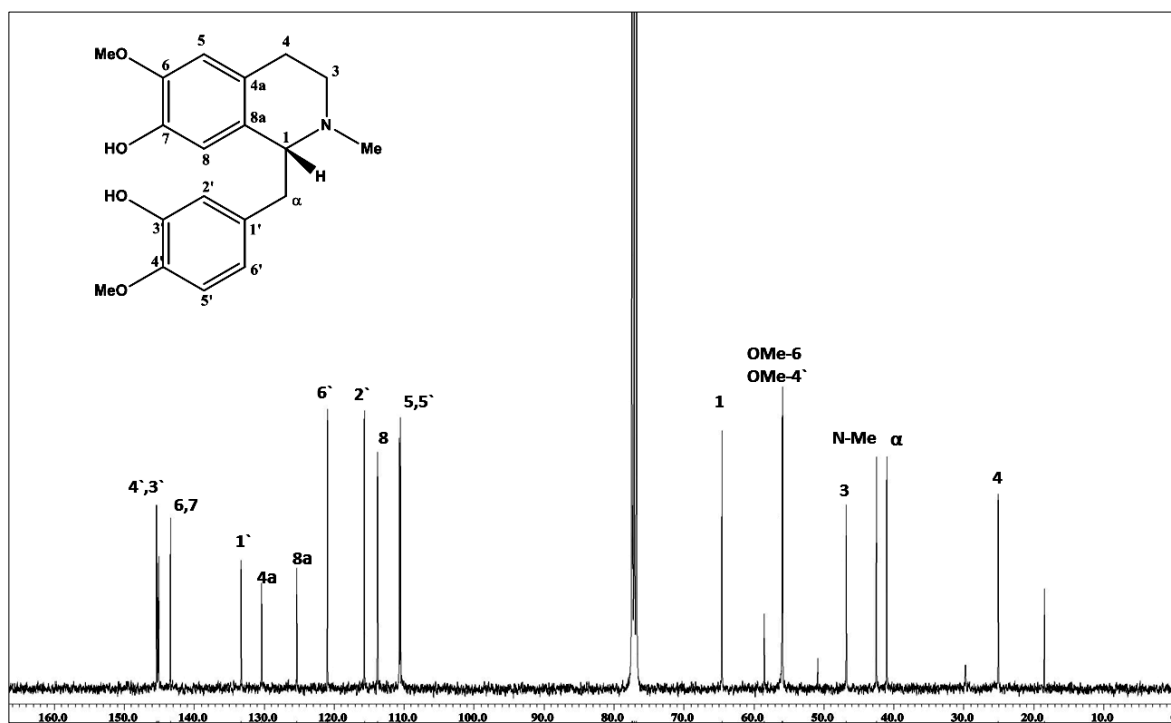


Fig. 4.76: ¹³C NMR Spectrum of Reticuline (141)

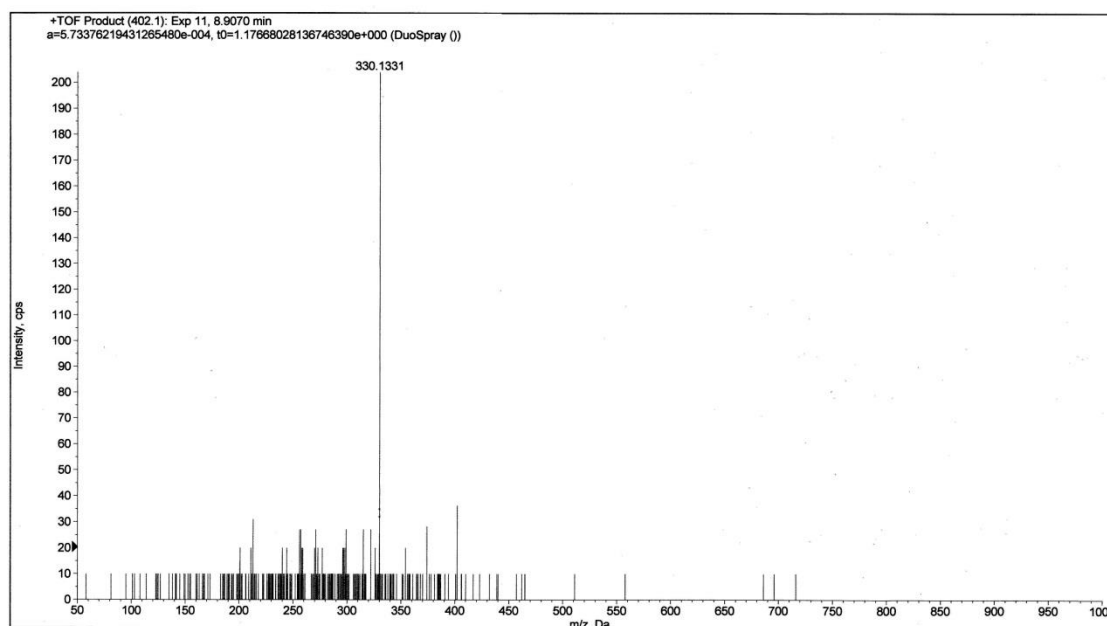
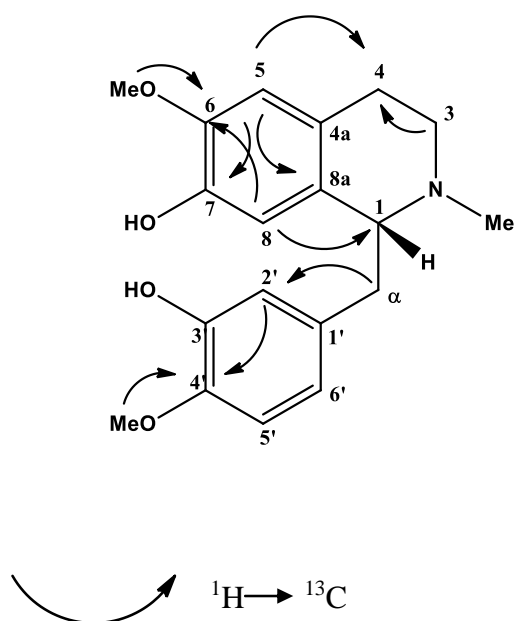
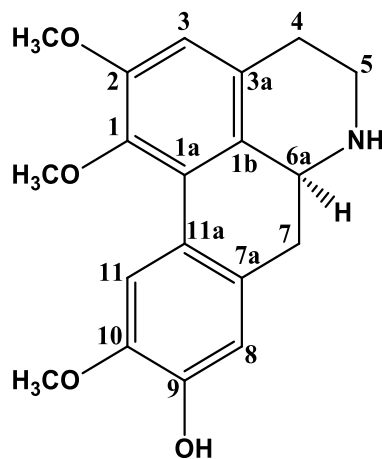


Fig. 4.77: LC-MS Spectrum of Reticuline (**141**)



Scheme 4.22: The HMBC Correlations of Reticuline (**141**)

4.3.4 (+) - Laurotetanine (142)



(+) - Laurotetanine (**142**) was isolated as a dark brown amorphous solid $[\alpha]_D^{24} +111$ (c 0.05, CHCl_3). The UV spectrum showed absorptions at 217 and 242 nm, characteristic values for 1, 2, 9, 10-tetradisubstituted aporphine (Israilov *et al.*, 1980). The IR spectrum showed absorption peak at 3385 cm^{-1} indicated the presence of hydroxyl group in the structure.

The LC-MS spectrum showed an intense pseudomolecular ion peak, $[\text{M}+\text{H}]^+$ at m/z 328.3761 corresponding to the molecular formula of $\text{C}_{19}\text{H}_{21}\text{NO}_4$.

The ^1H -NMR spectrum of (+) laurotetanine (**142**) (Table 4.23 and Figure 4.78) exhibited three distinct methoxyl signals at δ 3.63 and 3.87 which were most probably positioned at C-1, C-2 and C-10. The former is assigned to the methoxyl at C-1 since the protons were shielded by the anisotropic effect caused by ring D. A one singlet aromatic proton at δ (6.58, s, H-3) was observed in the spectrum, confirming that C-1 and C-2 are substituted. Furthermore, the singlet at δ 6.77 can be attributed to H-8. This value is typical of a 9, 10-substitution pattern. Down field signal of H-11 at δ 8.04 suggested that C-10 was

substituted by a methoxyl group. The aliphatic protons gave a multiplet signal between δ 3.80-2.64. The above observations were reinforced by HMBC experiment which displayed some correlations.

The ^{13}C -NMR spectrum (Figure 4.79) established the resonances of nineteen carbons while DEPT experiment showed three methyls, three methylenes, four methines and nine quaternary carbon signals in the molecule, consistent with the structure proposed. In the HMBC spectrum (Scheme 4.23), the cross-peaks were observed between H-8/C-10, C-7/C-11a; 10-OCH₃/C-10 suggesting that a methoxyl group attached to C-10 instead of C-9. The structural elucidation was completed by the help of the 2D experiments (HSQC and HMBC).

Finally, comparison of the spectroscopic data obtained with the literature values was deduced the isolation of (+) - laurotetanine (**142**). (Nafiah, 2009). Complete assignments were listed in table 4.24.

Table 4.24: ^1H NMR (400 MHz) and ^{13}C NMR (100 MHz) spectral data of (+) - laurotetanine (**142**) in CDCl_3 (δ in ppm, J in Hz).

Position	^1H -NMR (δ ppm)	^{13}C -NMR (δ ppm)	^{13}C -NMR (δ ppm) (Nafiah et al, 2009)
1	-	145.5	145.6
1a	-	126.8	126.8
1b	-	128.2	128.2
2	-	152.4	152.4
3	6.58 (1H, <i>s</i>)	110.6	110.6
3a	-	128.2	128.2
4	2.57 (1H, <i>m</i>)	29.4	29.4
	2.83 (1H, <i>m</i>)	-	-
5	2.76 (1H, <i>m</i>)	42.5	42.5
	3.06 (1H, <i>m</i>)	-	-
6a	3.71 (1H, <i>m</i>)	53.4	53.4
7	2.52 (2H, <i>m</i>)	34.9	34.9
7a	-	129.0	129.1
8	6.77 (1H, <i>s</i>)	114.0	114.1
9	-	144.4	144.5
10	-	145.1	145.1
11	8.04 (1H, <i>s</i>)	111.3	111.3
11a	-	123.4	123.4
OMe-1	3.63 (3H, <i>s</i>)	60.2	60.2
OMe-2	3.87 (3H, <i>s</i>)	55.9	55.9
OMe-10	3.87 (3H, <i>s</i>)	55.9	55.9

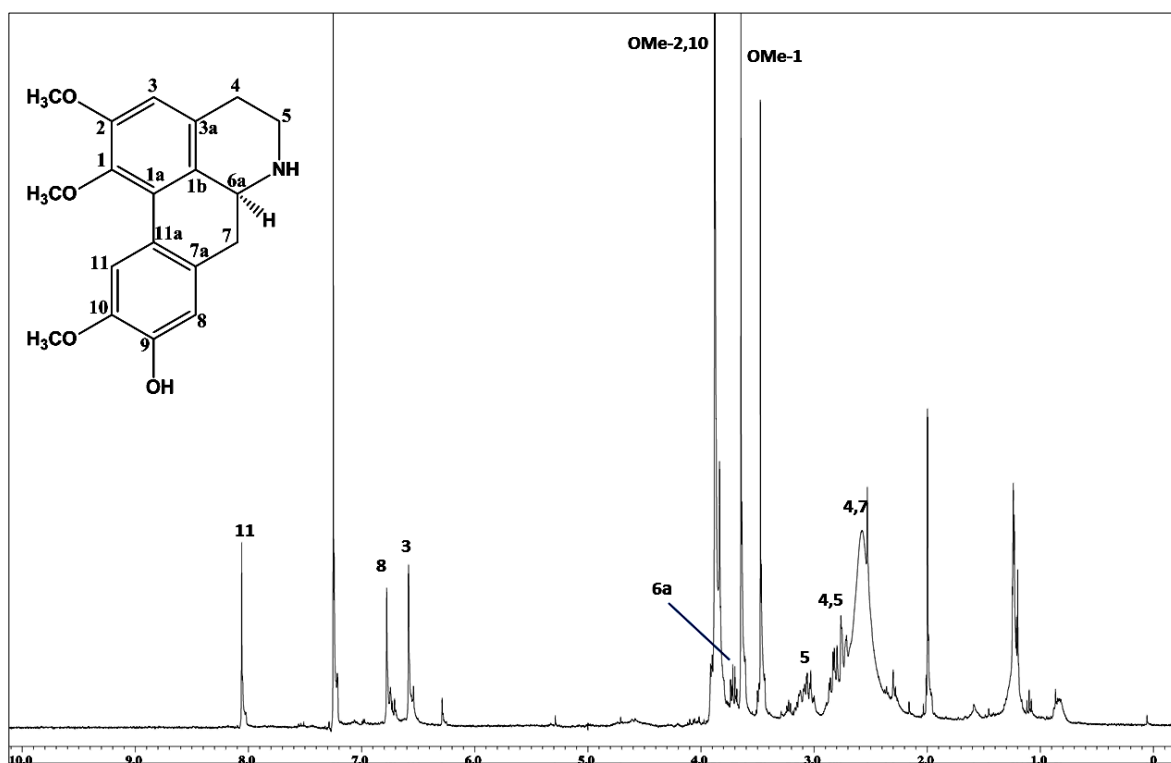


Fig. 4.78: ^1H NMR Spectrum of (+) - Laurotetanine (142)

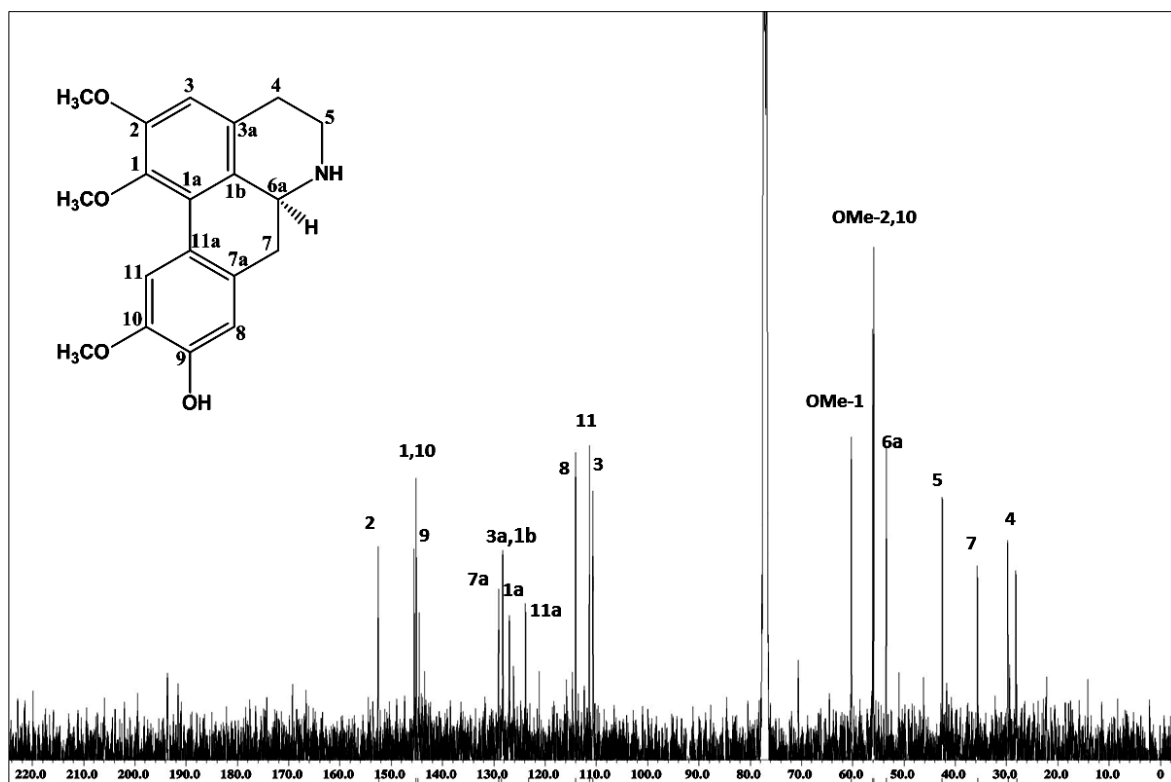


Fig. 4.79: ^{13}C NMR Spectrum of (+) - Laurotetanine (142)

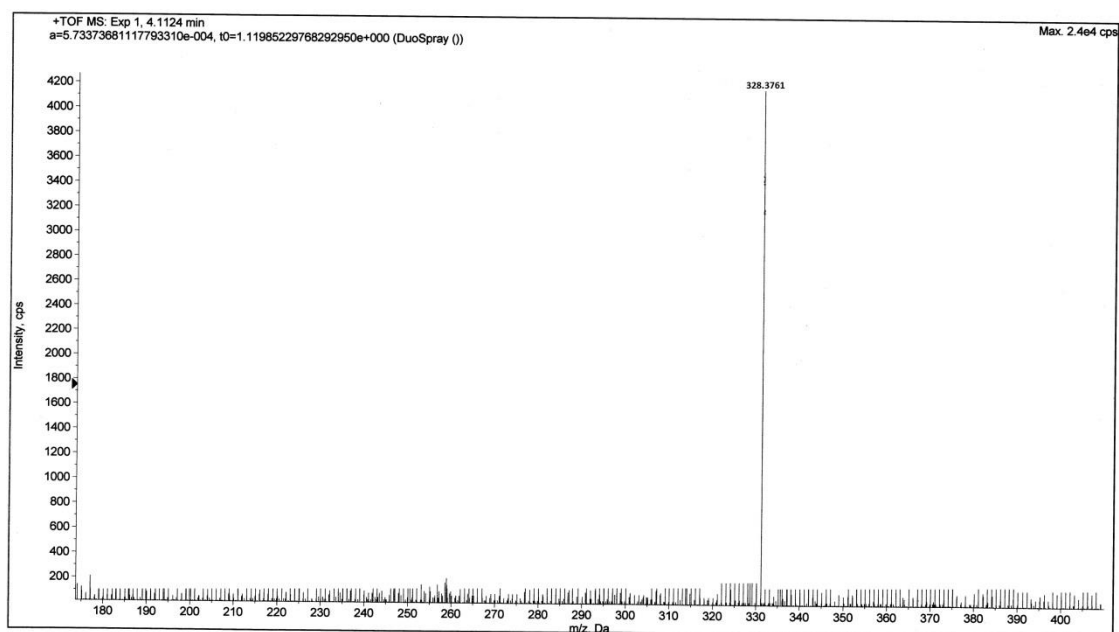
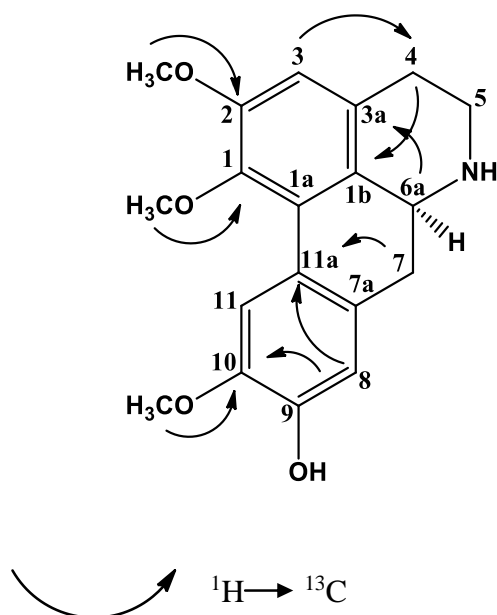
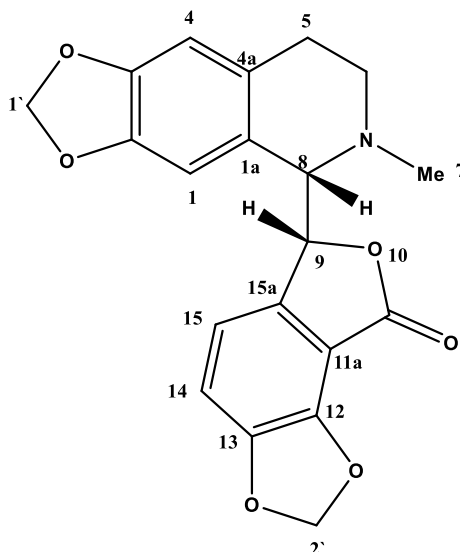


Fig. 4.80: LC-MS Spectrum of (+) - Laurotetanine (**142**)



Scheme 4.23: The HMBC Correlations of (+) - Laurotetanine (**142**)

4.3.5 (+) - Bicuculine (143)



(+) - Bicuculine (**143**) was afforded as a brownish amorphous solid, $[\alpha]_{\text{D}}^{24} -32$ (c 0.05, CHCl_3). The UV spectrum showed absorption band at 217 and 288 nm which were a characteristic of isoquinoline type of alkaloids (Menachery *et al.*, 1986). The IR spectrum showed absorption at 1692 cm^{-1} indicated the stretching of a conjugated carbonyl group in the structure. The LC-MS spectrum gave a pseudomolecular ion peak, $[\text{M}+\text{H}]^+$ at m/z 368.1132 consistent with the molecular formula of $\text{C}_{20}\text{H}_{17}\text{NO}_6$.

The ^1H -NMR spectrum (Figure 4.81) showed four aromatic proton signals at δ 6.40 (s , H-1), 6.64 (s , H-4), 7.09 (d , $J = 8.2$, H-14), 6.92 (d , $J = 8.2$, H-15) and two singlet peaks at δ 5.84 and δ 6.09 indicated of two methylenedioxy groups (H-1' and H-2') respectively. Due to neighboring with two electron withdrawing group (N - Me and oxygen) H-8 and H-9 appeared at δ 4.02 (d , $J = 2.3$, H-8) and 5.62 (d , $J = 2.3$, H-9). In the up field region one N - Me group at δ 2.56 (s) and two methylene groups at δ (2.72, m , 2.04, m , H-5) and (3.07, m ,

2.45, m, H-6) were observed corresponding to a tetrahydro isoquinoline ((El-Shazly *et al.*,1996).

The ^{13}C NMR (Figure 4.82) indicated the presence of four sp^2 methines, nine sp^2 quaternary carbons, four sp^3 methylenes, two sp^3 methines, and *N*- Me group. In addition, the HMBC spectrum revealed correlations of H- 4 to C-5, C- 2 and C-1a, H-1 to C- 4a and C-8, H-8 to C-4a and C- 6, H-9 to C-1a and C-11a and H-15 to C-9 and C-12 (Scheme 3.24). The hypothesis was also supported further by the cross peaks of COSY experiment that showed existence of two sets of doublet in the ^1H NMR at δ 4.02 and 5.62 which corresponded to the resonances of H-8 and H-9.

Through examination of ^1H , ^{13}C , (Table 4.25), DEPT, COSY, HSQC and HMBC (Scheme 4.24) spectra has made possible the complete assignments. In conclusion, data comparison with the literature confirmed the isolation of (+) - bicuculine (**143**). (Wangchuk *et al.*, 2010).

Table 4.25: ^1H NMR (400 MHz) and ^{13}C NMR (100 MHz) spectral data of (+) - bicuculine (**143**) in CDCl_3 (δ in ppm, J in Hz).

Position	^1H -NMR (δ ppm)	^{13}C -NMR (δ ppm)	^{13}C -NMR (δ ppm) (Wangchuk et al, 2010)
1	6.40 (1H, <i>s</i>)	101.2	102.0
1a	-	129.4	129.3
2	-	146.1	146.1
3	-	148.4	148.4
4	6.64 (1H, <i>s</i>)	101.2	101.2
4a	-	129.4	130.1
5	2.72 (1H, <i>m</i>)	29.8	29.8
	2.04 (1H, <i>m</i>)	-	-
6	3.07 (1H, <i>m</i>)	50.8	50.8
	2.45 (1H, <i>m</i>)	-	-
8	4.02 (1H, <i>d</i> , $J= 2.3$)	66.2	66.2
9	5.62 (1H, <i>d</i> , $J= 2.3$)	82.8	82.8
11	-	168.7	168.7
11a	-	124.8	124.8
12	-	146.1	146.1
13	-	148.4	148.4
14	7.09 (1H, <i>d</i> , $J= 8.2$)	116.0	116.1
15	6.92 (1H, <i>d</i> , $J= 8.2$)	113.0	113.2
15a	-	140.4	140.4
1`	5.84 (2H, <i>s</i>)	102.1	102.1
2`	6.09 (2H, <i>s</i>)	100.9	100.9
N-Me	2.56 (3H, <i>s</i>)	45.0	45.1

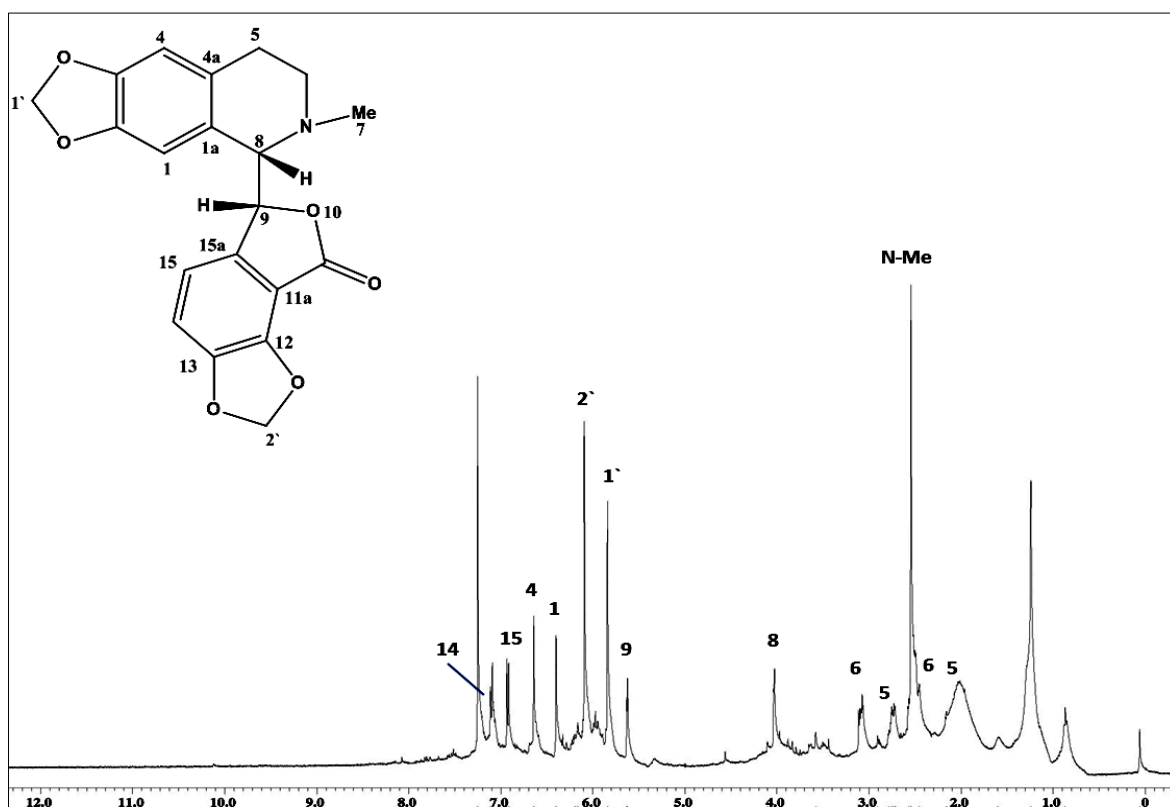


Fig. 4.81: ^1H NMR Spectrum of (+) - Bicuculine (143)

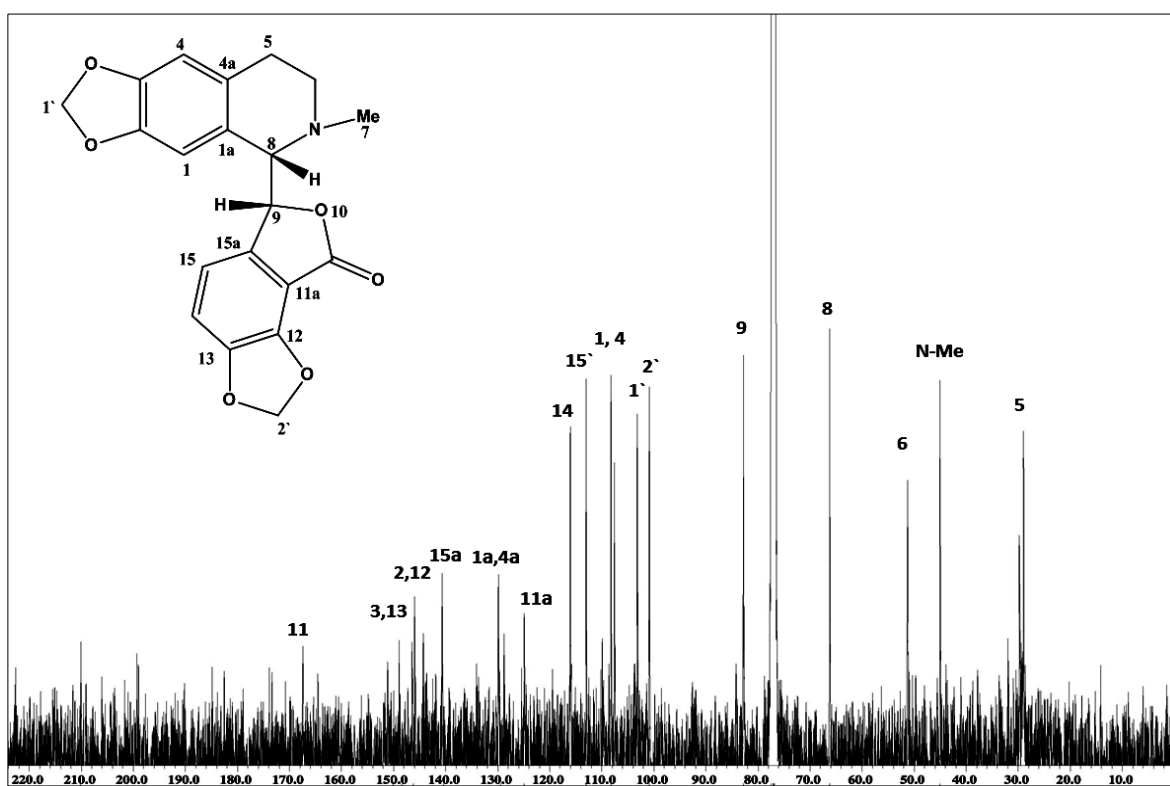
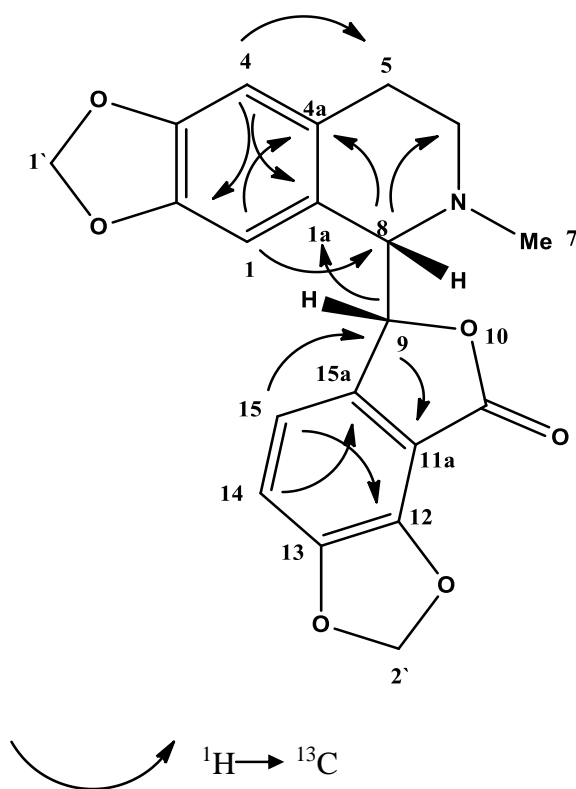
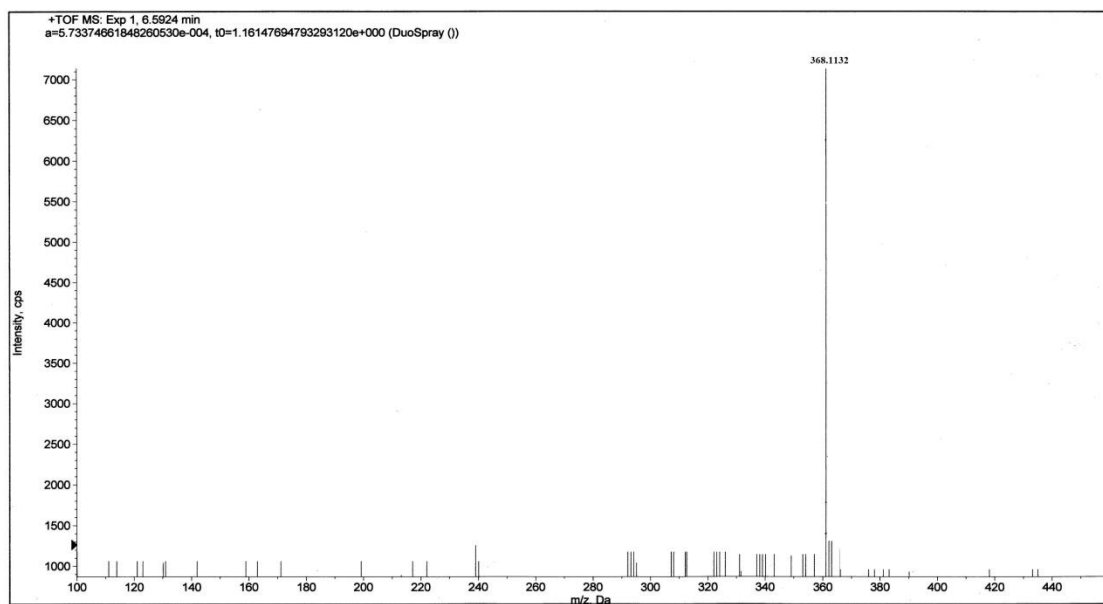
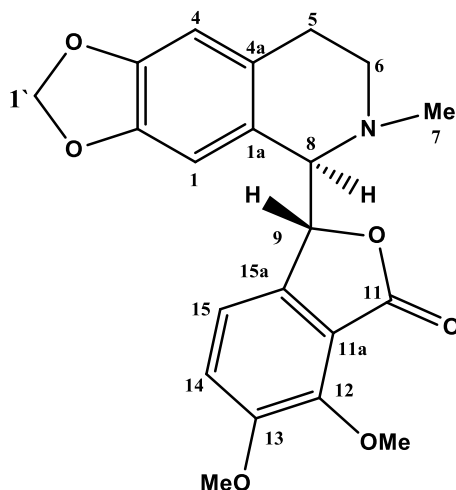


Fig. 4.82: ^{13}C NMR Spectrum of (+) - Bicuculine (143)

Scheme 4.24: The HMBC Correlations of (+) - Bicuculine (**143**)

4.3.6 (-) - α - Hydrastine (**144**)



144

(-) - α - Hydrastine (**144**) was obtained as a brownish amorphous solid, $[\alpha]_D^{24} -18$ (c 0.05, CHCl_3). The UV spectrum showed absorption band at 217 and 288 nm. The IR spectrum showed absorption at 1692 cm^{-1} indicated the stretching of a conjugated carbonyl group in the structure. The LC-MS spectrum showed a pseudomolecular ion peak, $[\text{M}+\text{H}]^+$ at m/z 384.1599 consistent with the molecular formula of $\text{C}_{21}\text{H}_{21}\text{NO}_6$.

(-) - α - Hydrastine (**144**) is reminiscent of (+) – bicuculine (**143**). The difference between (+)- bicuculine (**143**) and (-) - α - Hydrastine (**144**) is the existence of two methoxy groups instead of a methylenedioxy group attached to the C-12 and C-13 in the (-) - α - Hydrastine.

The ^1H NMR spectrum (Figure 4.84) showed four aromatic proton signals, one methylenedioxy, one *N*-Me, two protons bearing *N*- Me (H-8) and oxygen (H-9) and two methylenes. Two singlet peaks appeared at δ 3.75 and δ 3.98 corresponding to OMe-12 and OMe-13 respectively.

The ^{13}C NMR (Figure 4.85) indicated the presence of four sp^2 methines, nine sp^2 quaternary carbons, three sp^3 methylenes, two sp^3 methines, one *N*-Me group and two methoxy groups.

The absolute configuration of (-) - α - Hydrastine (**144**) is (C-8, *R* and C-9, *S*) while for the (+) – bicuculine (**143**) is (C-8, *S* and C-9, *S*) (Ohta *et al.*, 1964).

The complete assignments of all carbons and protons (Table 4.26) were confirmed with DEPT, HSQC and HMBC spectra. Analysis of all spectral data obtained and comparison with literature led to the isolation of (-) - α - hydrastine (**144**). (Jha *et al.*, 2009).

Table 4.26: ^1H NMR (400 MHz) and ^{13}C NMR (100 MHz) spectral data of (-) - α -hydrastine (**144**) in CDCl_3 (δ in ppm, J in Hz).

Position	^1H -NMR (δ ppm)	^{13}C -NMR (δ ppm)	^{13}C -NMR (δ ppm) (Jha et al, 2009)
1	6.72 (1H, <i>s</i>)	108.8	108.8
1a	-	130.1	130.1
2	-	146.1	146.1
3	-	147.4	147.4
4	6.34 (1H, <i>s</i>)	107.8	107.8
4a	-	130.1	130.1
5	2.68 (1H, <i>m</i>)	29.8	29.8
	2.14 (1H, <i>m</i>)	-	-
6	3.29 (1H, <i>m</i>)	50.4	50.4
	2.47 (1H, <i>m</i>)	-	-
8	4.02 (1H, <i>d</i> , $J= 2.3$)	66.2	66.2
9	5.62 (1H, <i>d</i> , $J= 2.3$)	82.8	82.8
11	-	168.7	168.7
11a	-	125.4	125.4
12	-	147.4	147.4
13	-	152.3	152.3
14	7.46 (1H, <i>d</i> , $J= 8.0$)	118.4	118.4
15	7.23 (1H, <i>d</i> , $J= 8.0$)	118.4	118.4
15a	-	140.4	140.4
1'	5.92 (2H, <i>s</i>)	100.1	100.1
N-Me	2.50 (3H, <i>s</i>)	44.6	44.6
OMe-12	3.75 (3H, <i>s</i>)	62.1	62.1
OMe-13	3.98 (3H, <i>s</i>)	56.4	56.3

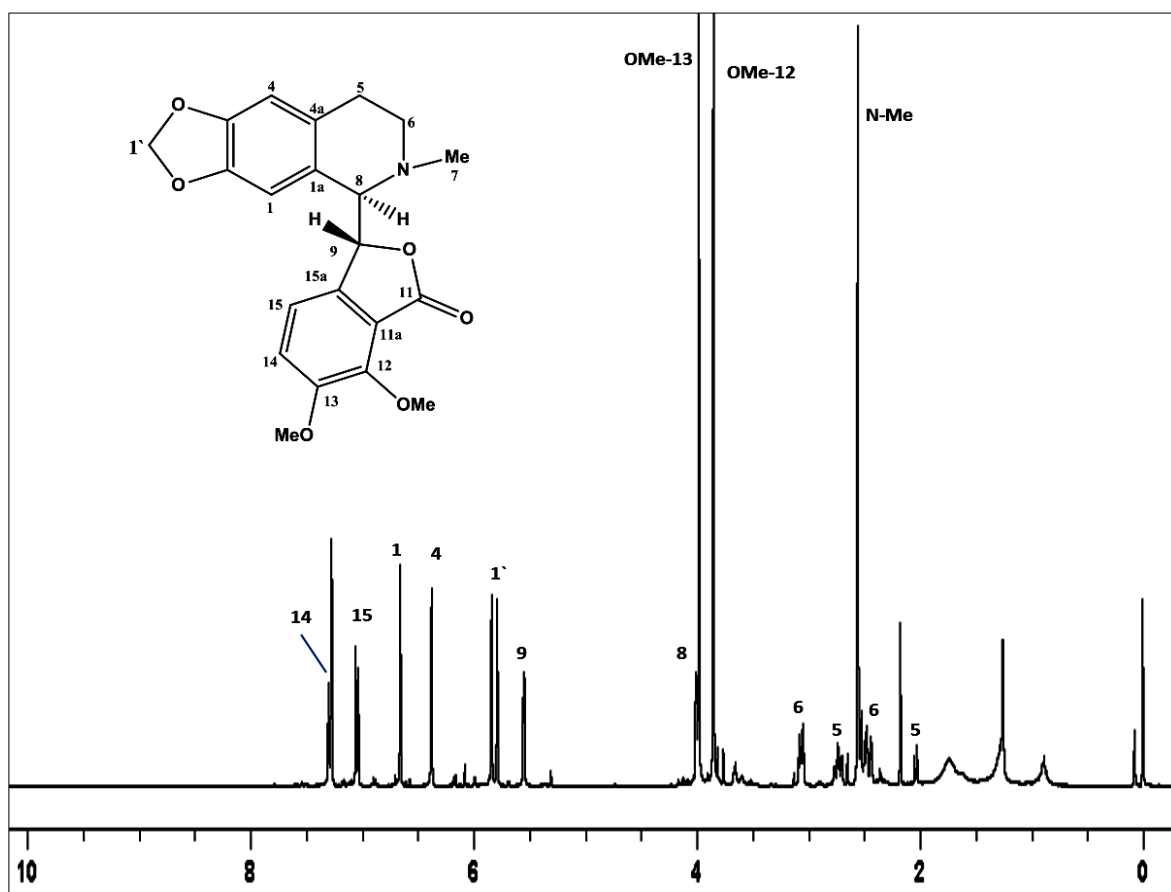


Fig. 4.84: ¹H NMR Spectrum of (-) - α- Hydrastine (**144**)

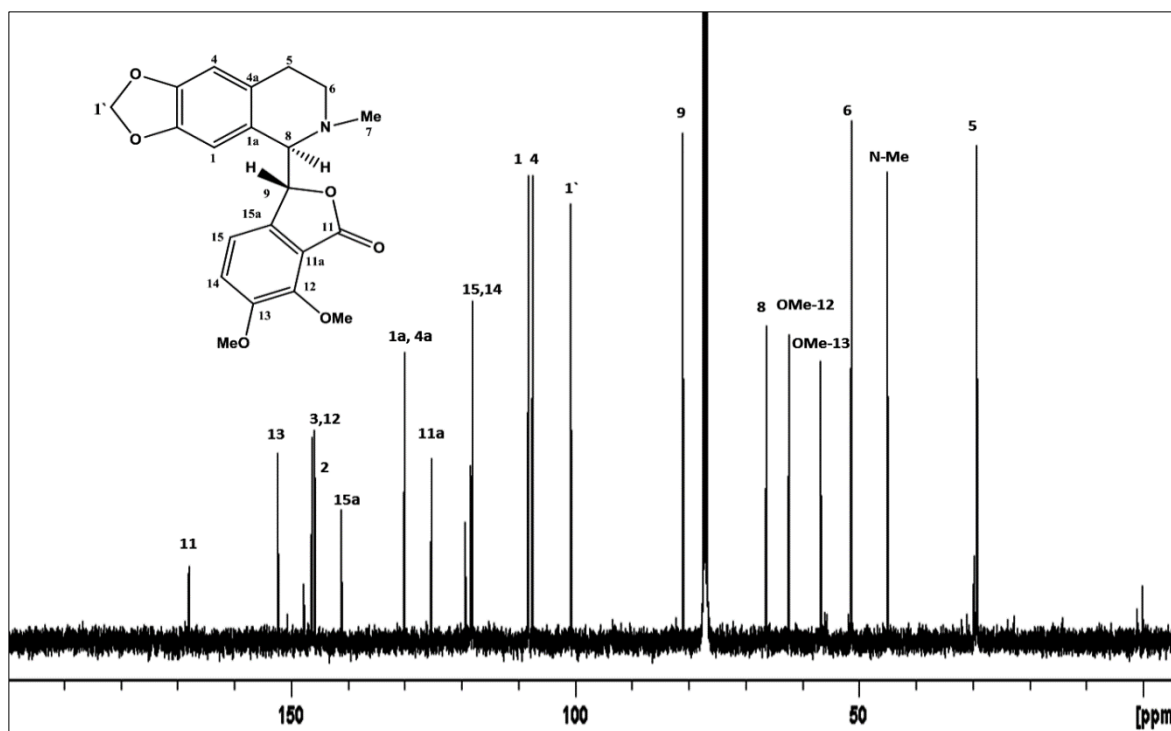


Fig. 4.85: ¹³C NMR Spectrum of (-) - α- Hydrastine (**144**)

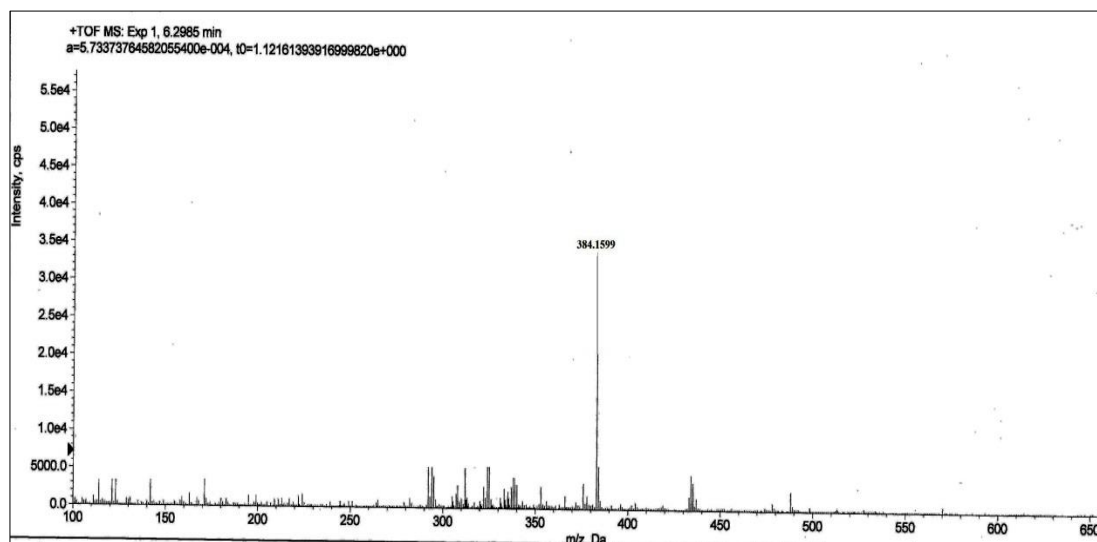
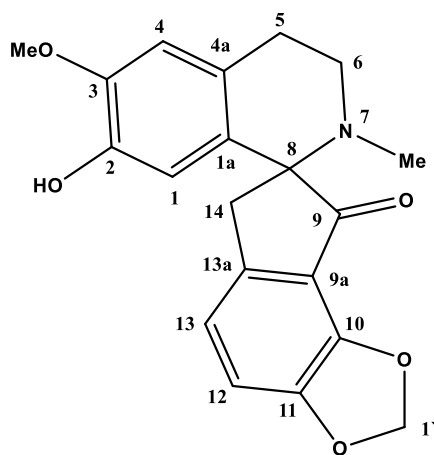


Fig. 4.86: LC-MS Spectrum of (-) - α - Hydrastine (**144**)

4.3.7 (+) - Parfumine (**145**)



145

(+) - Parfumine (**145**) was isolated as a brownish amorphous solid. $[\alpha]_{\text{D}}^{24} -28$ (c 0.05, CHCl_3). The mass spectrum revealed a pseudo-molecular ion peak at m/z 354.1336

[M+H]⁺ corresponding to the molecular formula of C₂₀H₁₉NO₅. The UV spectrum revealed maximum at 218 and 288 nm. The IR spectrum showed a band of OH at 3431 cm⁻¹ and absorption at 1692 cm⁻¹ indicated the stretching of a conjugated carbonyl group.

The ¹H NMR spectrum (Figure 4.87) showed four aromatic proton signals including two overlapped singlet signals (6.34, H-1 and H-4) and two doublet signals (7.34, *d*, *J*= 8.4 Hz, H-12 and 6.89, *d*, *J*= 8.4 Hz, H-13). A singlet peak appeared at δ 6.25 corresponding to a methylenedioxy group. There were two singlet peaks at δ 2.43 and δ 3.88 consistent to one *N*-Me and one methoxy group respectively. Three methylenes appeared at δ (2.42, *m*, 2.63, *m*, H-5) δ (2.98, *m*, 3.02, *m*, H-6) and δ (3.42, *d*, *J*= 9.8 Hz, 3.53, *d*, *J*= 9.8 Hz, H-14).

The ¹³C NMR spectrum (Figure 4.88) showed 20 signals corresponding to four sp² methines, nine sp² quaternary carbons, four sp³ methylenes, one sp³ quaternary carbon, one *N*-Me and one methoxy group. Application of ¹H-¹H COSY and C-H correlations from HSQC and HMBC (Scheme 4.25) allowed the complete assignment of all signals (Table 4.27). In conclusion, data comparison with the literature confirmed the isolation of (+) - parfumine (**145**). (Israilov, *et al.*, 1970).

Table 4.27: ^1H NMR (400 MHz) and ^{13}C NMR (100 MHz) spectral data of (+) - parfumine (**145**) in CDCl_3 (δ in ppm, J in Hz).

Position	^1H -NMR (δ ppm)	^{13}C -NMR (δ ppm)	^{13}C -NMR (δ ppm) (Israilov, et al, 1970)
1	6.34 (1H, <i>s</i>)	111.8	111.2
1a	-	127.3	127.3
2	-	142.5	142.1
3	-	142.8	143.2
4	6.34 (1H, <i>s</i>)	111.8	112.1
4a	-	127.3	128.5
5	2.93 (2H, <i>m</i>)	28.8	29.1
6	2.78 (2H, <i>m</i>)	53.3	53.8
8	-	70.0	70.1
9	-	208.7	202.1
9a	-	121.5	122.1
10	-	148.7	149.2
11	-	142.8	142.9
12	7.34 (1H, <i>d</i> , $J= 8.4$)	118.6	119.7
13	6.89 (1H, <i>d</i> , $J= 8.4$)	119.4	119.4
13a	-	143.2	143.2
14	3.42 (1H, <i>d</i> , $J= 9.8$)	37.3	37.2
	3.53 (1H, <i>d</i> , $J= 9.8$)	-	-
1'	6.25 (2H, <i>s</i>)	102.1	102.1
N-Me	2.43 (3H, <i>s</i>)	45.6	45.5
OMe-3	3.88 (3H, <i>s</i>)	53.3	53.6

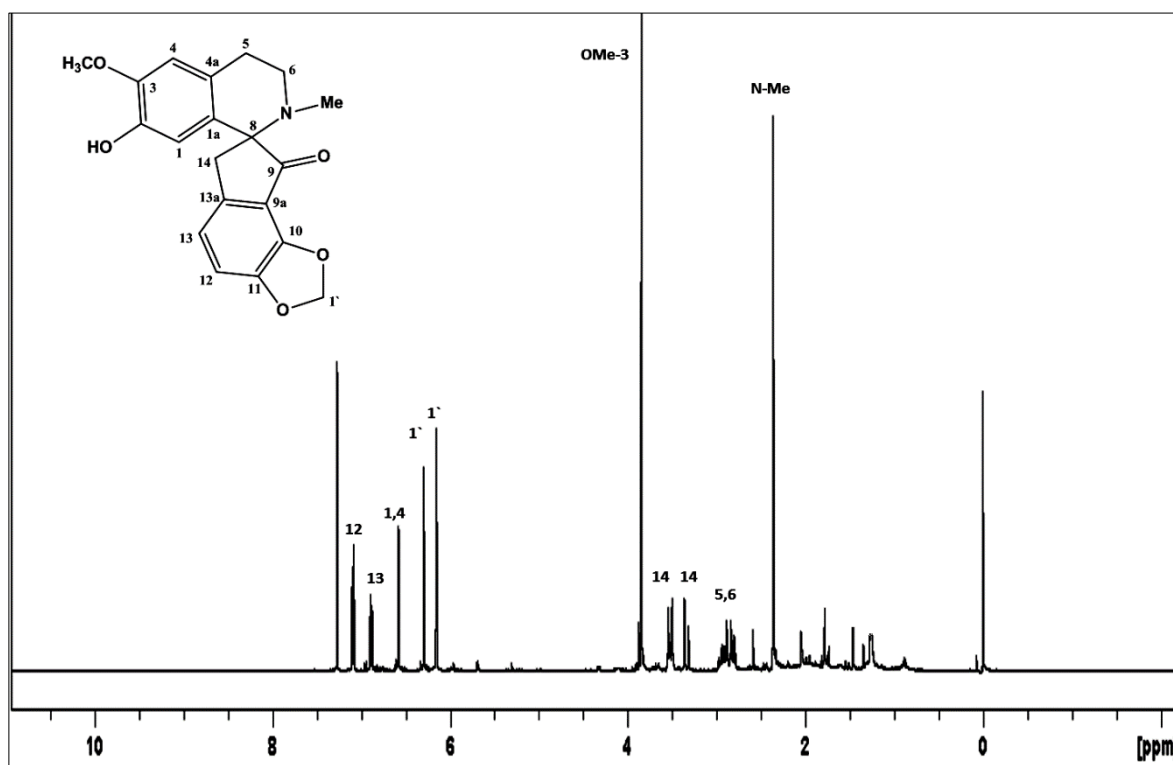


Fig. 4.87: ^1H NMR Spectrum of (+) - Parfumine (145)

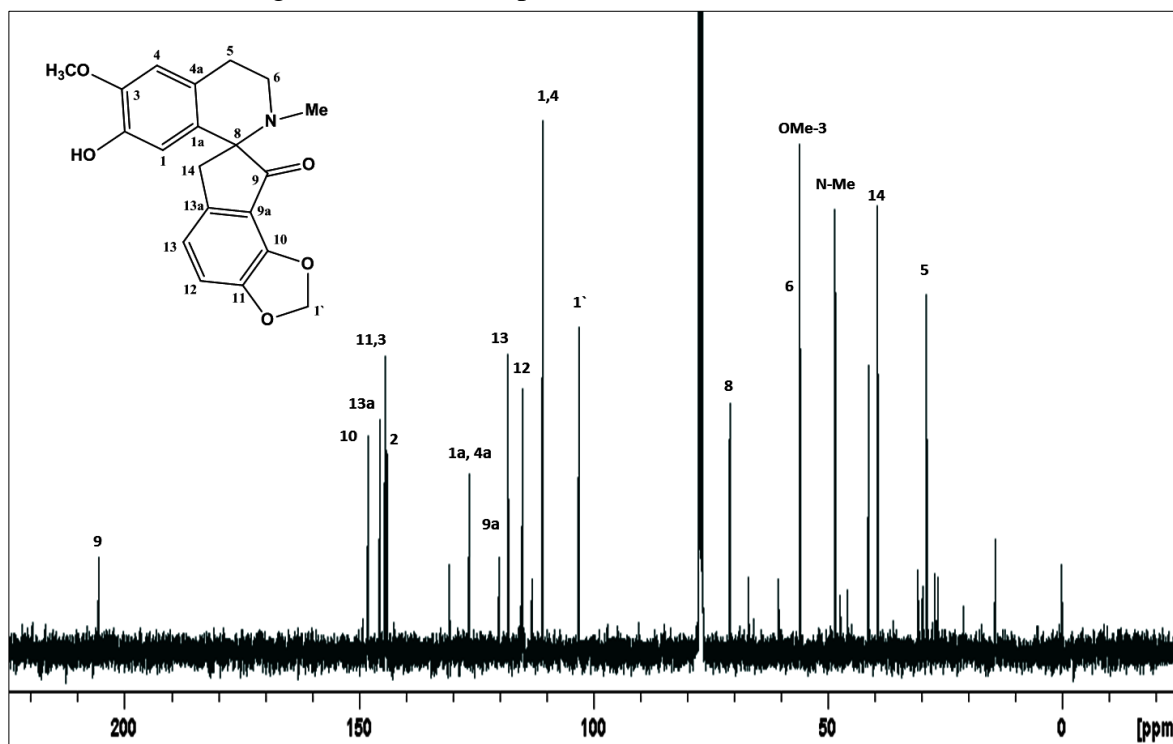


Fig. 4.88: ^{13}C NMR Spectrum of (+) - Parfumine (145)

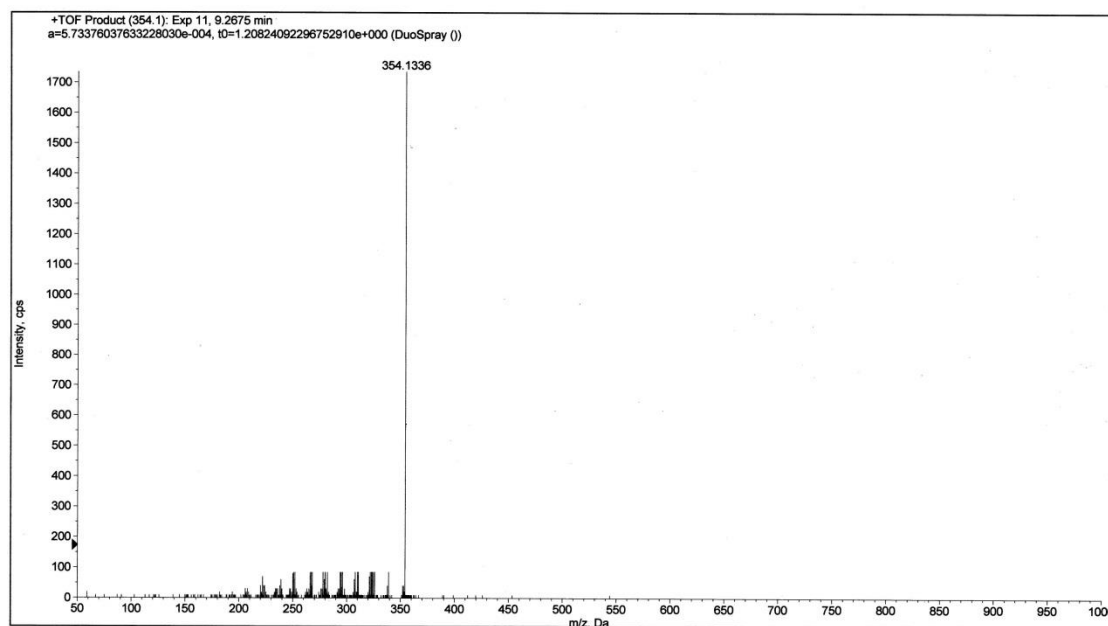
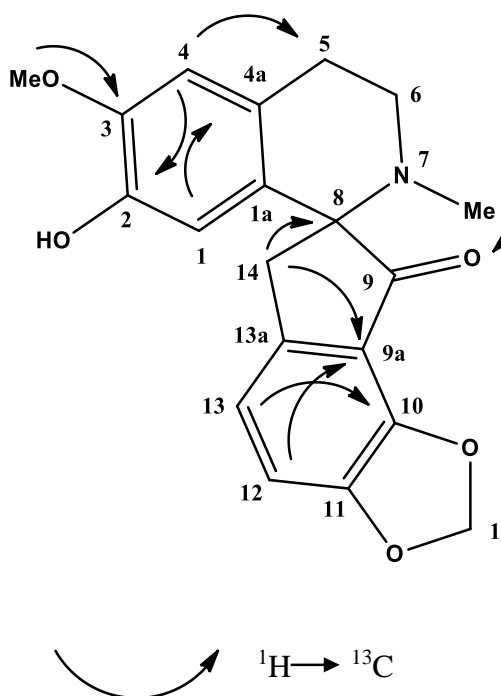
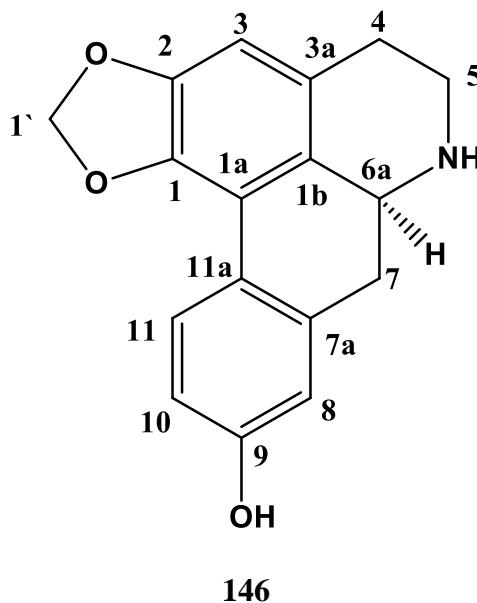


Fig. 4.89: LC-MS Spectrum of (+) - Parfumine (**145**)



Scheme 4.25: The HMBC Correlations of (+) - Parfumine (**145**)

4.3.8 (+) – Anolobine (**146**)



(+)- Anolobine (**146**) was isolated as a brown amorphous solid $[\alpha]_{\text{D}}^{24} +87$ (c 0.05, CHCl_3).

The UV spectrum showed absorptions at 219 and 246 nm, a characteristic values for an Aporphine type of isoquinoline alkaloids (Israilov *et al.*, 1980). The IR spectrum showed absorption peak at 3420 cm^{-1} indicated the presence of hydroxyl group in the structure. The LC-MS spectrum showed an intense pseudomolecular ion peak, $[\text{M}+\text{H}]^+$ at m/z 282.1119 corresponding to the molecular formula of $\text{C}_{17}\text{H}_{15}\text{NO}_3$.

The ^1H -NMR spectrum (Table 4.28 and Figure 4.90) showed methylenedioxy group peaks appeared at δ (5.90, d , 1.3 Hz, $\text{H}_{1-1'}$) and δ (6.03, d , 1.3 Hz, $\text{H}_{2-1'}$). There are four aromatic protons were observed; δ (6.47, s , H-3), δ (6.75, d , 1.6 Hz, H-8), δ (6.79, d , 7.6 Hz, H-10) and δ (7.89, d , 7.6 Hz, H-11). Furthermore, in up field signals of aliphatic protons appeared at δ 2.59 till 3.89 ppm. The above observations were reinforced by HMBC experiment which displayed long range H-C correlations.

The ^{13}C -NMR spectrum (Figure 4.91) established the resonances of seventeen carbons; one methylene dioxy, three methylenes, five methines and eight quaternary carbon signals in the molecule, consistent with the structure proposed. In the HMBC spectrum (Scheme 4.26), the cross-peaks were observed between H-4/C-4, 1a, H-5/C-6a; H-7/C-11a; H-8/ C-10, H-11/ C-7a, 9; H-1'/ C-1, 2. The structural elucidation was completed by the help of the 2D experiments (HSQC and HMBC).

Finally, comparison of the spectroscopic data obtained with the literature (+) - anolobine (**146**) was identified (Kablan *et al.*, 2013).

Table 4.28: ^1H NMR (400 MHz) and ^{13}C NMR (100 MHz) spectral data of (+) - anolobine (**146**) in CDCl_3 (δ in ppm, J in Hz).

Position	^1H -NMR (δ ppm)	^{13}C -NMR (δ ppm)	^{13}C -NMR (δ ppm) (Kablan et al, 2013)
1	-	144.8	145.8
1'	5.90 (2H, <i>d</i> , $J= 1.3$)	100.7	100.7
1a	-	117.8	117.8
1b	-	126.3	126.3
2	-	146.7	146.7
3	6.47 (1H, <i>s</i>)	106.5	106.5
3a	-	126.3	126.3
4	2.59 (1H, <i>m</i>)	29.3	29.3
	3.09 (1H, <i>m</i>)	-	-
5	2.73 (1H, <i>m</i>)	48.7	48.7
	3.29 (1H, <i>m</i>)	-	-
6a	3.87 (1H, <i>m</i>)	55.3	55.3
7	3.52 (2H, <i>m</i>)	34.2	34.1
7a	-	137.2	137.3
8	6.75 (1H, <i>d</i> , $J= 1.6$)	115.3	115.2
9	-	155.7	155.2
10	6.79 (1H, <i>d</i> , $J= 7.6$)	114.2	114.1
11	7.89 (1H, <i>d</i> , $J= 7.6$)	128.4	128.3
11a	-	123.8	123.8

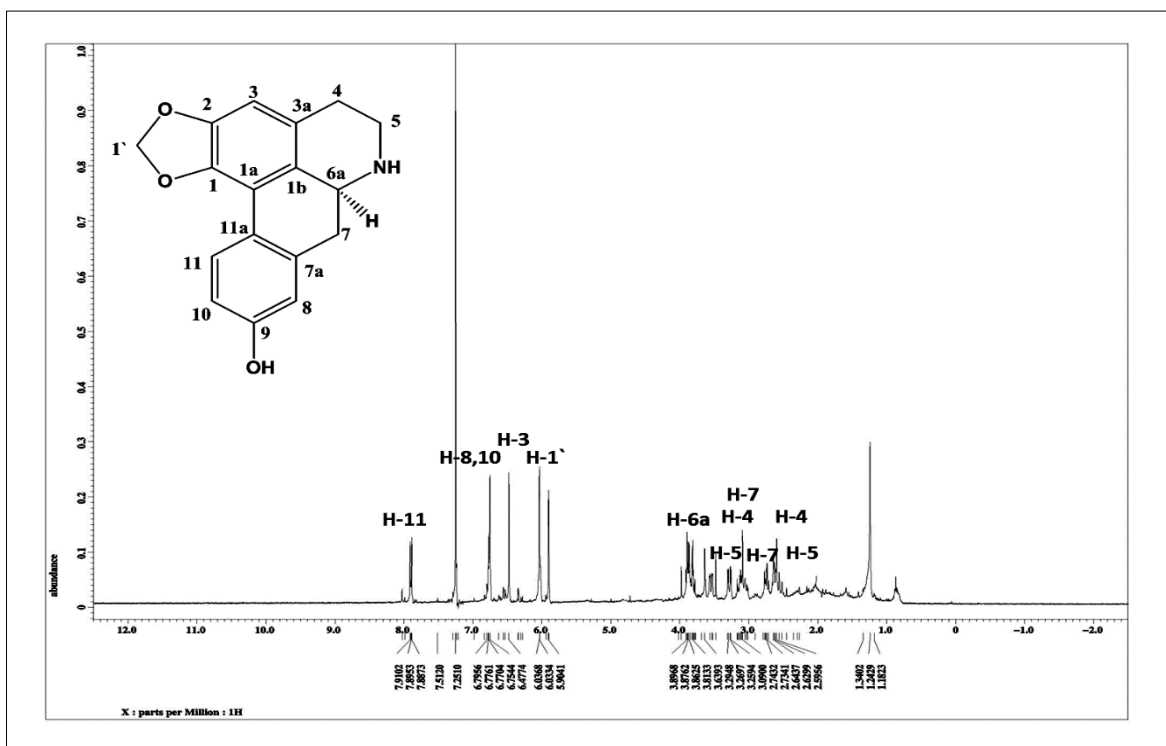


Fig. 4.90: ¹H NMR Spectrum of (+) - Anolobine (**146**)

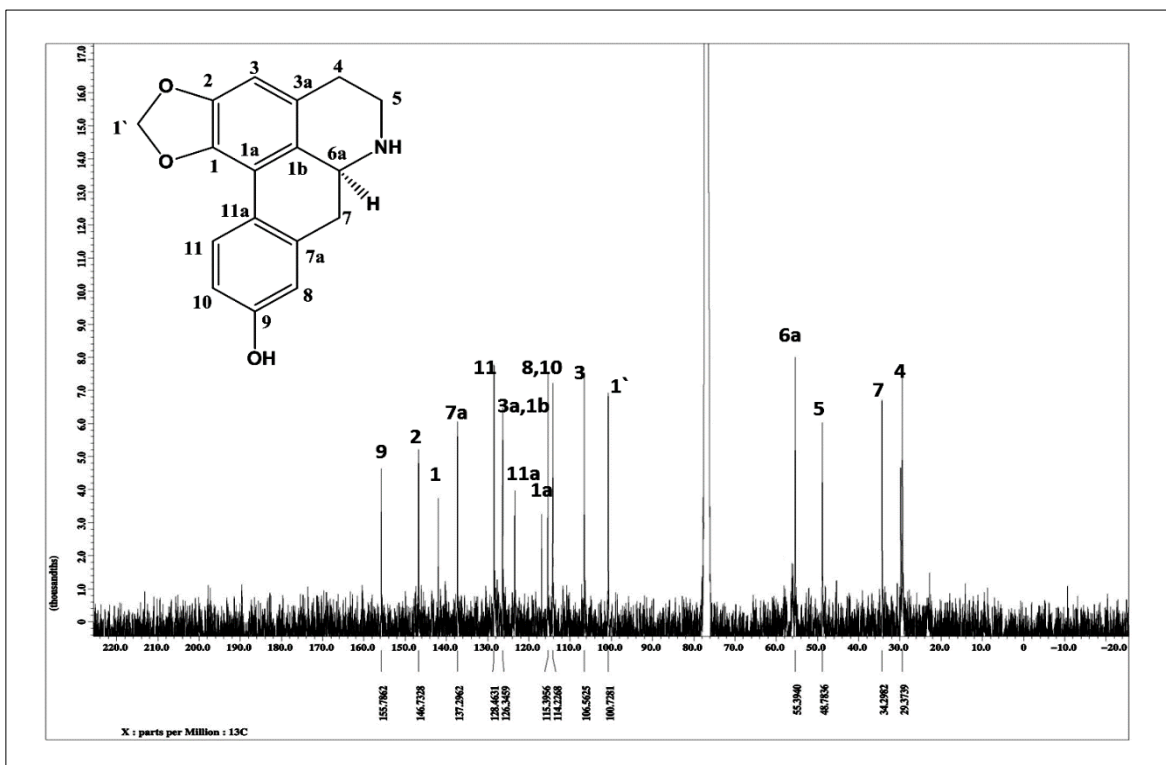


Fig. 4.91: ¹³C NMR Spectrum of (+) - Anolobine (**146**)

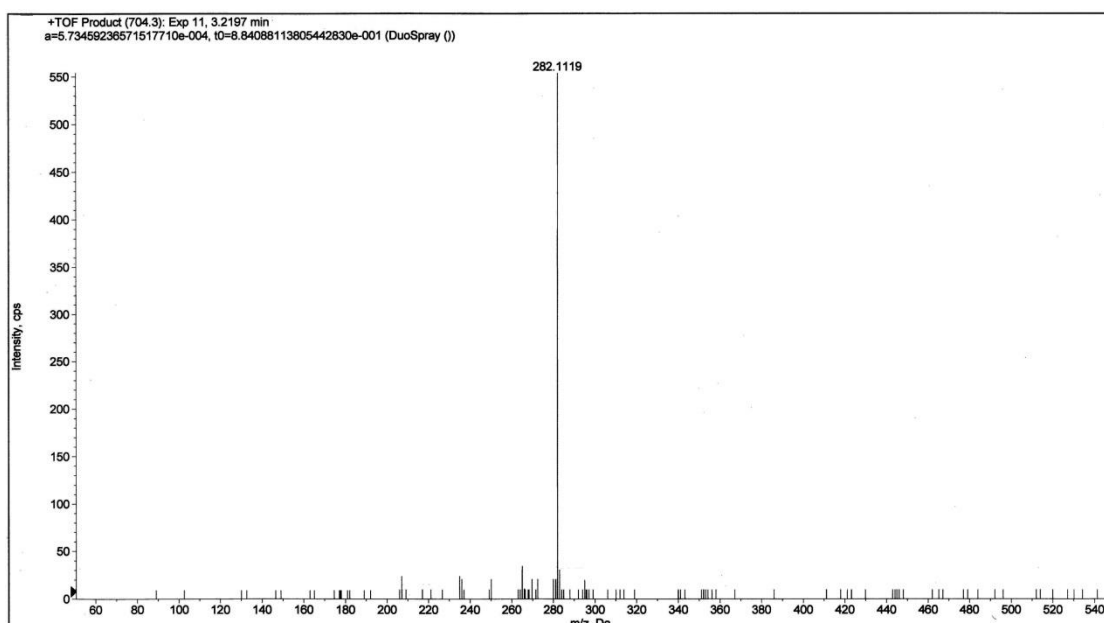
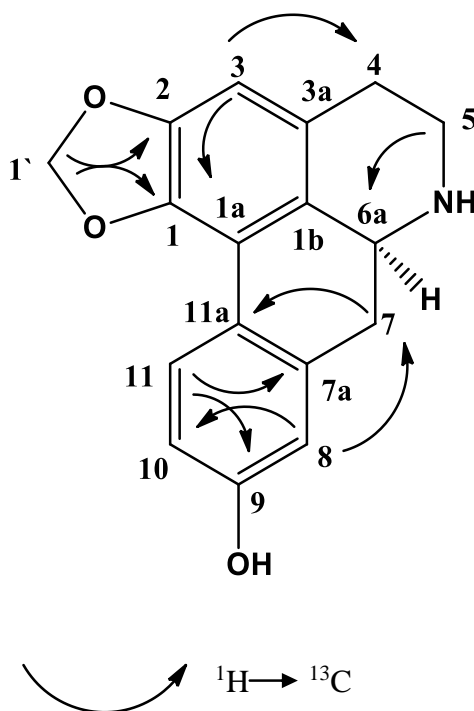


Fig. 4.92: LC-MS Spectrum of (+) - Anolobine (**146**)



Scheme 4.26: The HMBC Correlations of (+) - Anolobine (**146**)

4.4 Biological Activities

4.4.1 Introduction

Screening carried out to date has revealed several substances active in vitro under the micro molar range and with a good selectivity index, and nevertheless, *in vivo* activity has been confirmed only in a small number of cases. In this study the anti plasmodial, anti alzheimer and anti cancer activities of the crude extracts and pure compounds of *Ochrosia oppositifolia*, *Rauvolfia reflexa* and *Actinodaphne macrophylla* were investigated.

4.4.2 Antiplasmodial Activity

Six samples from the bark and leaves of *ochrosia oppositifolia* including three crude extracts and three indole alkaloids and eight isoquinoline alkaloids from the bark of *Actinodaphne macrophylla* have been tested for their *in-vitro* inhibitory activity against *P. falciparum* 3D7. Among the crude extracts of *Ochrosia oppositifolia* dichloromethane crude extract of bark showed the most potent inhibitory activity, with the IC₅₀ value of 0.05051 µg/mL (Table 4.28), the other crude extracts and compounds showed weak or no inhibitory activity against *P. falsiparum* as compare as standard which is chloroquine.

Three indole alkaloids isolated from the bark of *Ochrosia oppositifolia* and eight isoquinoline alkaloids isolated from the bark of *Actinodaphne macrophylla* showed moderate *in vitro* antiplasmodial activities against *Plasmodium falciparum* 3D7 with the IC₅₀ of 0.29 µM, 0.75 µM and 1.13 µM for isoreserpiline (**120**), neisosposinine (**121**), reserpine (**122**) (Table 4.29) (Fadaeinasab *et al.*, 2013), and 0.08 µM, 1.18

μM, 3.11 μM, 0.65 μM, 0.26 μM, 3.99 μM and 1.38 μM for cycleanine (**139**), (-)-10-demethylxylopinine (**140**), reticuline (**141**), (+) laurotetanine (**142**), (+) – bicuculine (**143**), (-) - a- hydrastine (**144**), (+) - parfumine (**145**) and (+) - anolobine (**146**) respectively which are comparable with chloroquine (Table 4.30).

Table 4.29: Inhibition growth percentage of *Plasmodium falciparum* and probit analysis with SPSS 11.5 (crude extracts of *Ochrosia oppositifolia*)

Crude extracts	% Inhibition at concentration (μg/mL)					IC ₅₀ (μg/mL)
	100	10	1	0.1	0.01	
DCM crude of Leaves	100	68.24	39.54	30.12	16.20	1.61338
Hexane crude of Bark	100	71.26	54.45	39.07	34.61	0.46951
DCM crude of Bark	100	91.78	69.73	63.65	22.04	0.05051
Chloroquine	87.32	76.43	54.45	31.09	19.23	0.002

Table 4.30: Inhibition growth percentage of *Plasmodium falciparum* and probit analysis with SPSS 11.5 (alkaloids of *Ochrosia oppositifolia*)

Alkaloids	% Inhibition at concentration (μg/mL)					IC ₅₀ (μmol L ⁻¹)
	10	1	0.1	0.01	0.001	
Reserpinine (122)	58.84	53.83	49.15	38.14	22.92	1.13
Neisosposinine (121)	55.13	54.43	51.55	41.88	31.37	0.75
Isoreserpiline (120)	76.31	64.4	40.59	33.33	29.25	0.29
Chloroquine	87.32	76.43	54.45	31.09	19.23	0.002

Table 4.31: Inhibition growth percentage of *Plasmodium falciparum* and probit analysis with SPSS 11.5 (alkaloids of *Actinodaphne macrophylla*)

Alkaloids	% Inhibition at concentration ($\mu\text{g/mL}$)					IC ₅₀ ($\mu\text{mol L}^{-1}$)
	10	1	0.1	0.01	0.001	
Cycleanine (139)	100	100	98.84	51.89	27.04	0.08
Demethylxylopinin (140)	98.98	96.08	89.97	60.76	45.64	0.05
Reticuline (141)	94.77	85.03	52.76	35.76	17.15	1.18
Laurotetanine (142)	99.27	65.12	40.70	29.80	11.92	3.11
Bicuculine (143)	98.34	70.84	61.73	43.96	25.22	0.65
α - Hydrastine (144)	98.42	93.08	77.85	50.53	22.07	0.26
Parfumine (145)	97.37	74.61	31.52	20.23	8.93	3.99
Anolobine (146)	96.95	91.28	55.66	28.49	14.54	1.38
Chloroquine	87.32	76.43	54.45	31.09	19.23	0.002

4.4.3 Anti Alzheimer Activity

The dichloromethane, ethanol and methanol extracts from the leaves and methanol crude extract from the bark of *Rauvolfia reflexa* showed potential acetylcholinesterase (AChE) and butyrylcholinesterase (BChE) inhibitory activities, with IC₅₀ values between 8.49 to 52.23 g/mL (Table 4.31). The compounds isolated from the bark and leaves of *Rauvolfia reflexa* showed moderate cholinesterase inhibitory activity compared to the reference standard, physostigmine. (Table 4.32)

Table 4.32: The IC₅₀ values of *Rauvolfia reflexa* extracts (leaves and bark) for inhibitory activities on cholinesterase enzymes.

Extract	AChE inhibition, IC ₅₀ (µg/mL)	BChE inhibition, IC ₅₀ (µg/mL)
Dichloromethane (leaves)	14.65 ± 0.32	8.49 ± 0.92
Ethanol (leaves)	38.40 ± 0.15	26.47 ± 2.05
Methanol (leaves)	52.23 ± 4.02	ND
Methanol (bark)	11.04 ± 0.14	6.28 ± 0.18

Data presented as Mean ± SD (n = 3); ^a Selectivity for AChE is defined as IC₅₀(BChE)/IC₅₀(AChE);

^b Selectivity for BChE is defined as IC₅₀(AChE)/IC₅₀(BChE).

Table 4.33: The IC₅₀ values of *Rauvolfia reflexa* compounds for inhibitory activities on cholinesterase enzymes.

Compounds	AChE inhibition, IC ₅₀		BChE inhibition, IC ₅₀	
	µg/mL	µM	µg/mL	µM
Acrylate (134)	14.32 ± 0.82	60.17	ND	-
Acrylic acid (137)	37.63 ± 1.42	158.06	14.69 ± 1.22	61.72
Cinnamate (132)	48.99 ± 2.86	97.37	ND	-
β- carboline (135)	15.52 ± 0.68	83.38	ND	-
Rauvolfine C (124)	-	-	23.74±0.23	73.23
β- carboline (133)	19.63±0.27	65.44	6.45±0.11	21.52
Macusine B (130)	14.91±0.21	48.39	12.52±0.15	40.63
Vinorine (125)	11.71±0.16	35.06	12.16±0.16	36.40
Undolifoline (129)	18.62±0.22	54.76	9.69±0.23	28.51
Isoreserpiline (120)	11.31±0.12	31.96	8.46±0.18	23.91
Rescinnamine (126)	6.98±0.11	11.01	5.11±0.16	8.06
Physostigmine	0.046	0.17	0.162	0.59

Data presented as Mean ± SD (n = 3); ^a Selectivity for AChE is defined as IC₅₀(BChE)/IC₅₀(AChE);

^b Selectivity for BChE is defined as IC₅₀(AChE)/IC₅₀(BChE).

4.4.4 Anti Cancer Activity

4.4.4.1 Effects of Isolated Compounds on Cell Proliferation of Different Cell Lines

Cytotoxic effects of rauvolfine B (**123**), macusine B (**130**) and isoreserpiline (**120**) against different cancer and normal cell lines were determined. As shown in Table 4.33, the indole alkaloids exhibited various cytotoxic effects against the cell lines. At the tested concentrations (1.5 – 250 μ M), macusine B (**130**) and isoreserpiline (**120**) did not effectively suppress the cell proliferations of cancer cells. Rauvolfine B (**123**) revealed moderate cytotoxic effects against two breast cancer cells (MCF-7 and MDA-MB-231) and colon cancer HT-29 cells. However, in HCT-116, rauvolfine B (**123**) elicited the strongest cytotoxic effect with IC₅₀ values of 46.86, 39.93 and 33.38 μ M after 24, 48 and 72 h of treatment. It is worth noting that normal human cancer CCD-841 cells and hepatic WRL-68 cells were not distinctly affected with rauvolfine B (**123**). The MTT result suggests that rauvolfine B (**123**) suppressive effect is selective for HCT-116 cancer cells. As rauvolfine B (**123**) demonstrated the most potent cytotoxic effects amongst the three isolated compounds against HCT-116.

Table 4.34: The IC₅₀ values of the isolated compounds on eight different cell lines after 24h treatment.

Cell Lines	IC ₅₀ (μM)		
	rauvolfine B (123)	macusine B (130)	isoreserpiline (120)
HCT-116	46.86	>100	>100
MCF-7	85.75	>100	>100
HT-29	107.05	>100	>100
MDA-MB-231	146.59	>100	>100
HepG2	206.98	>100	>100
A549	232.18	>100	>100
WRL-68	>100	>100	>100
CCD-841	>100	>100	>100

4.4.4.2 Quantification of Apoptosis Using Fluorescent Microscopy and AO/PI Double-Staining

Rauvolfine B (**123**) was selected for further study on the possible mechanism as it shown potential activity against HCT-116 cell line. Morphological changes in the treated HCT-116 cells with rauvolfine B (**123**) were observed under fluorescent microscope. After 24 h, apparent marks of apoptosis, such as membrane blebbing and cytoplasmic shrinkage were noted at IC₅₀ dose of rauvolfine B (**123**). Furthermore, small apoptotic bodies were discernible at 48 and 72 h. The observation of apoptosis was evidenced by fluorescent microscopy analysis in order to quantify viability, early apoptosis, late apoptosis and secondary necrosis. Early apoptosis was observed using intervening AO within the fragmented DNA under bright green fluorescence (Ocker & Hopfner, 2012). At the same time, the green intact nuclear structure confirmed the presence of control cells. After 24 h of treatment with rauvolfine B (**123**), moderate apoptosis was noted in the form of nuclear chromatin condensation and blebbing. After 48 and 72 h, changes such as presence of the reddish-orange colour due to binding of AO to denatured DNA were evidenced the late

stage of apoptosis. The results revealed induced morphological features of apoptosis by rauvolfine B (**123**) in a time-dependent manner (Zhang *et al.*, 1997). (Figure 4.93).

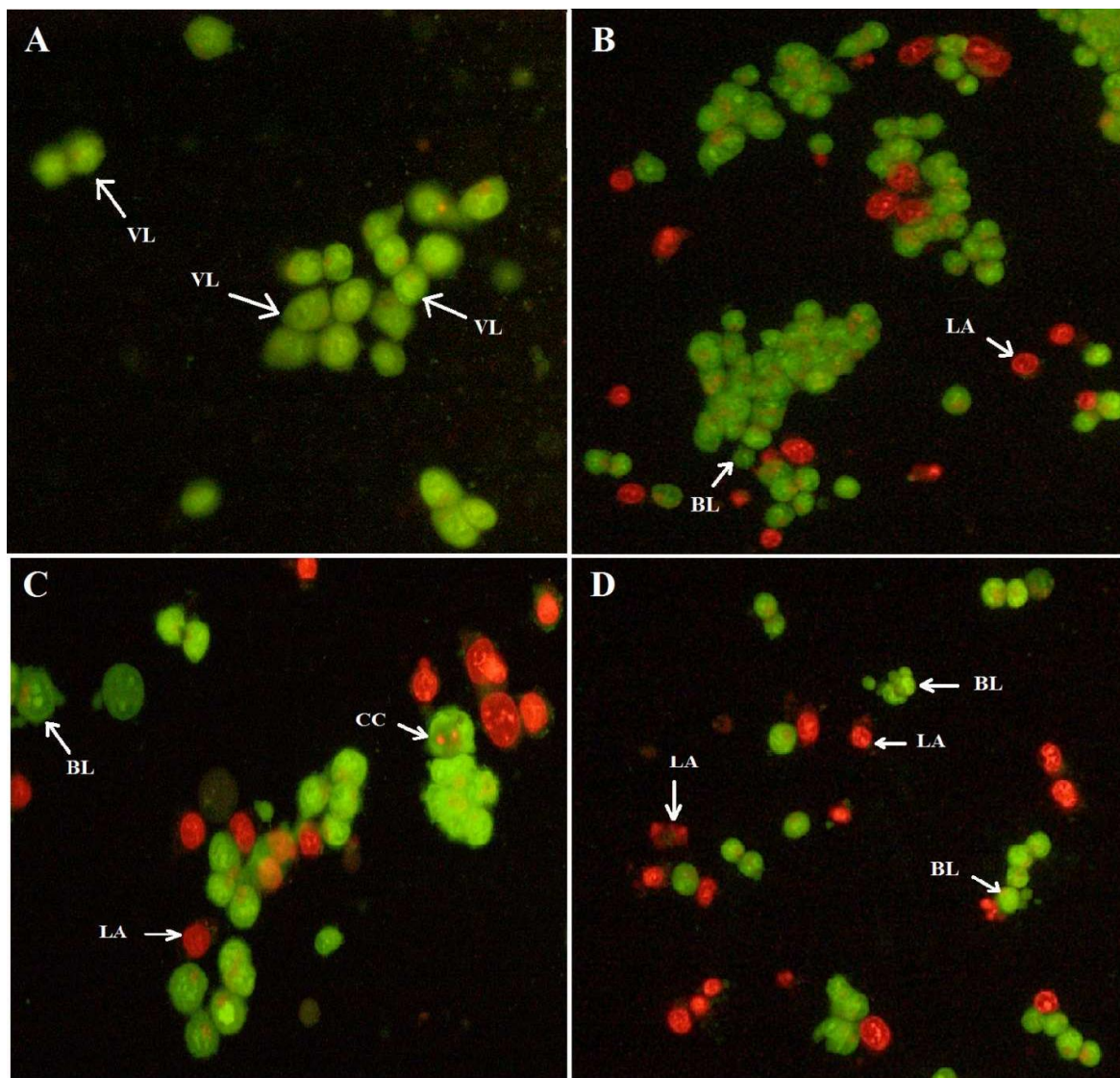


Figure 4.93. Fluorescent micrographs of AO/PI double stained HCT-116 cells. (A) Untreated HCT-116 cells after 72 h exhibit normal structures. Early apoptosis features, namely blebbing and chromatin condensation and late apoptosis were detected after (B) 24, (C) 48 h and (D) 72 h of treatment with rauvolfine B (**123**) (magnification: 200 \times). VI: Viable cells; CC: Chromatin condensation; BL: Blebbing of the cell membrane; LA: Late apoptosis.

CHAPTER 5

CONCLUSION

CONCLUSION

The first part of the study was dedicated to the investigation of the components of *Ochrosia oppositifolia* (KL 5349) and *Rauvolfia reflexa* (KL 4900) from Apocynaceae family, collected from Pangkor Island (Perak) and Kelantan respectively. A plant from Lauraceae family namely; *Actinodaphne macrophylla* (KL 4940) collected from Johor also was studied. The Apocynaceae plants produced alkaloids and phenolic compounds while Lauraceae family was rich in isoquinoline type of alkaloids. Three indole alkaloids were isolated from the bark of *Ochrosia oppositifolia* namely; isoreserpiline (**120**), neisosposinine (**121**), and reserpine (**122**). Seventeen compounds have been isolated from the *Rauvolfia reflexa* including ten alkaloids from the bark namely rauvolfine B (**123**), rauvolfine C (**124**), vinorine (**125**), rescinnamine (**126**), cantleyine (**127**), akuammilan-17-oic acid, 1,2-dihydro-3-hydroxy-1-methyl-, methyl ester (**128**), undulifoline (**129**), macusine B (**130**), isoreserpiline (**120**), akuammilan-17-oic acid, 12-hydroxy-, methyl ester (**131**). Leaves of *Rauvolfia reflexa* has afforded seven compounds, 17-methoxy-carbonyl-14-heptadecaenyl-4-hydroxy-3-methoxy cinnamate (**132**), 3-methyl-10,11-dimethoxyl-6-methoxycarbonyl- β -carboline (**133**), (*E*)-methyl 3-(4-hydroxy-3,5-dimethoxyphenyl)acrylate (**134**), 1,2,3,4-tetrahydro-1-oxo- β -carboline (**135**), 3-hydroxy- β -carboline (**136**), (*E*)-3-(3,4,5-trimethoxyphenyl) acrylic acid (**137**), and benzenepropanoic acid, 3-methoxy (**138**).

Bark of *Actinodaphne macrophylla* yielded eight alkaloids. There were cycleanine (**139**), (-)-10-demethylxylopinine (**140**), reticuline (**141**), (+)-laurotetanine (**142**), (+)-bicuculine (**143**), (-)- α -hydrastine (**144**), (+)-parafumine (**145**) and (+)-anolobine (**146**).

Structural elucidations were established through several spectroscopic methods, notably UV, IR, MS (HRESIMS and LC-MS), 1D and 2D NMR (^1H , ^{13}C , COSY, DEPT, HSQC, HMBC and NOESY).

The second part discussed the antiplasmodial activity of the crude extracts and isolated compounds from *Ochrosia oppositifolia* and *Actinodaphne macrophylla*. In antiplasmodial assay, dichloromethane crude extract of bark of *Ochrosia oppositifolia* showed most potent inhibitory activity, with IC_{50} 0.05051 $\mu\text{g/mL}$ against *P.falsiparum* while dichloromethane crude of leaves displayed very weak inhibitory activity against *P.falsiparum*.

Three indole alkaloids isolated from the bark of *Ochrosia oppositifolia* and eight isoquinoline alkaloids isolated from the bark of *Actinodaphne macrophylla* showed moderate *in vitro* antiplasmodial activities against *Plasmodium falciparum* 3D7 with the IC_{50} of 0.29 μM , 0.75 μM and 1.13 μM for isoreserpiline (**120**), neisosposinine (**121**), reserpine (**122**) (Table 4.29) (Fadaeinasab et al, 2013), and 0.08 μM , 1.18 μM , 3.11 μM , 0.65 μM , 0.26 μM , 3.99 μM and 1.38 μM for cycleanine (**139**), (-)-10-Demethylxylopinine (**140**), reticuline (**141**), (+) - laurotetanine (**142**), (+) – bicuculine (**143**), (-) - a- hydrastine (**144**), (+) - parfumine (**145**) and (+) - anolobine (**146**) respectively which are comparable with reference standard, chloroquine (Table 4.30).

The dichloromethane, ethanol and methanol extracts from the leaves and methanol crude extract from the bark of *Rauvolfia reflexa* showed potential acetylcholinesterase (AChE) and butyrylcholinesterase (BChE) inhibitory activities, with IC_{50} values between 8.49 to 52.23 g/mL (Table 4.31). The compounds isolated from the bark and leaves of *Rauvolfia reflexa* showed moderate cholinesterase inhibitory activity compared to the reference standard,

physostigmine. (Table 4.32) Cytotoxic effects of rauvolfine B (**123**), macusine B (**130**) and isoreserpiline (**120**) against different cancer and normal cell lines were determined. At the tested concentrations (1.5 – 250 μ M), macusine B (**130**) and isoreserpiline (**120**) did not effectively suppress the cell proliferations of cancer cells. Rauvolfine B (**123**) revealed moderate cytotoxic effects against two breast cancer cells (MCF-7 and MDA-MB-231) and colon cancer HT-29 cells. However, in HCT-116, rauvolfine B (**123**) elicited the strongest cytotoxic effect with IC_{50} value of 46.86, 39.93 and 33.38 μ M after 24, 48 and 72 h of treatment. Rauvolfine B (**123**) was selected for further study on the possible mechanism as it shown potential activity activity against HCT-116 cell line. Morphological changes in the treated HCT-116 cells with rauvolfine B (**123**) were observed under fluorescent microscope. After 24 h, apparent marks of apoptosis, such as membrane blebbing and cytoplasmic shrinkage were noted at IC_{50} dose of rauvolfine B (**123**). (Figure 4.93).

REFERENCES

- Ahmed, T., & Gilani, A. H. (2009). Inhibitory effect of curcuminoids on acetylcholinesterase activity and attenuation of scopolamine-induced amnesia may explain medicinal use of turmeric in Alzheimer's disease. *Pharmacology Biochemistry*, 91, 554-559.
- Ajay, S. P. (2010). *Pharmacognostical, Phytochemical and Hepatoprotective activity studies on the root of Capparis sepiaria L.* (Master Dissertation.). Ramaiah College of Pharmacy, India.
- Aly, Y., Galal, A., Wong, L. K., & Fu, E. W. (1989). A revision of the structure of the isoquinolone alkaloid thalflavine. *Phytochemistry*, 28(7), 1967-1971.
- Angerhofer, C. K., Guinaudeau, H., & Wongpanich, V., (1999). Antiplasmodial and cytotoxic activity of natural bisbenzylisoquinoline alkaloids. *Journal of Natural Products*, 62(1), 59-66.
- Arbain, D. A., Adek, Z., Birkbeck, A. A., Byrne, L. T., Harahap, A. K., & Sargent, M. V. (1991). Methyl 12-hydroxyakuammilan-17-oate: a new indolenine alkaloid from *Rauwolfia sumatrana*. *Australian Journal of Chemistry*, 44(7), 1007-1011.
- Arvind, M. K. B., Upadhyay, A. K., Anupa, T., & Bikram, D. O. (2011). Quantitative determination of Yohimbine alkaloid in the different part of the *Rauwolfia tetraphylla*. *Journal of Chemistry Pharmacology Research*, 3(2), 907-910.
- Barbosa-Filho, J., Vasconcelos, E., Leitão da, C., & Gray, A.I., (2000). Alkaloids of the *Menispermaceae*. *The Alkaloids: Chemistry and Biology*, 54,185-190.
- Benn, M., & Mitchell, R.(1972). The alkaloids of *Argemone grandiflora*. *Phytochemistry*, 11(1), 461-464.
- Biemann, K. (1962). *Mass Spectroscopy, Organic Chemical Applications* (pp. 297- 333). New York: McGraw Hill.
- Bingtao, L., & David, J. (1998). *Flora of China*. (pp. 189) Science Press.
- Boeder, E., (1999). *Analysis of pyrrolizidine alkaloids*. *Current Organic Chemistry*, 3(6): pp. 557-576).
- Bost, J.B, (2009)., *Edible plants of the Chinantla, Oaxaca, Mexico with an emphasis on the participatory domestication prospects of persea schiedeana*. (Master Dissertation.). University of Florida, USA.
- Bruneton, J., (1995). *Pharmacognosy, Phytochemistry, Medicinal Plants*. (pp. 101-132). Hampshire: USA.

Bruneton, J., (1995). *Pharmacognosy, Phytochemistry, Medicinal Plants*. (pp. 629) Hampshire: USA.

Bruneton, J., (1995). *Pharmacognosy, Phytochemistry, Medicinal plants*. (pp. 722- 723). Publishing Inc: London- Paris- New York.

Cancelieri, N.M., Curcino, V.I.J., & Schripsema, J., (2002). Darcyrine, a novel pentacyclic indole alkaloid from *Rauwolfia grandiflora* Mart. *Tetrahedron letters*, 43(10), 1783-1787.

Cavé, A., (1989). *The Alkaloids: Chemistry and Pharmacology*. (pp. 118-119). Academic Press, Inc.: USA.

Chatterjee, A., Pakrashi, S.C., & Werner, G., (1956). *Recent developments in the chemistry and pharmacology of Rauwolfia alkaloids*. (pp. 346-443). Springer.

Chen, C.Y., Chang, F.R., Pan, W.B., & (2001). Four alkaloids from *Annona cherimola*. *Phytochemistry*, 56(7), 753-757.

Clemens, H.M., Richard, L.B., (1995). Minimal variation in the transmission blocking vaccine candidate Pfs48/45 of the human malaria parasite *Plasmodium falciparum*. *Molecular and Biochemical. Parasitology*, 69, 115-118.

Cotinguiba, F., Regasini, L. O., & Deboni, H. M. (2009). Piperamides and their derivatives as potential anti-trypanosomal agents. *Medicinal Chemistry Research*, 18(9), 703-711.

Cordell, G.A., (1981). *Introduction to alkaloids (A Biogenetic Approach)*. (pp. 317-328). John Wiley and Sons Inc.: USA.

Cordell, G.A., Beattie, M.L., & Fransworth, N.R., (2001). The Potential of alkaloids in drug discovery. *Phytotherapy Research*, 15(3), 183-205.

Corner, E.J.H., (1988). *Wayside trees of Malaya*. (pp. 672).

da Silva, T.M., da Silva, B.A., & Mukherjee, R., (1999). The monoterpene alkaloid cantleyine from *Strychnos trinervis* root and its spasmolytic properties. *Phytomedicine*, 6(3), 169-176.

da Silva, V.C., de Carvalho, M.G., & Alves, A.N., (2008). Chemical constituents from leaves of *Palicourea coriacea* (Rubiaceae). *Journal of natural medicines*, 62(3), 356-357.

de Lira, G.A., de Andrade, L.M., & Brabosa, F.J.M., (2002). Roraimine: a bisbenzylisoquinoline alkaloid from *Cissampelos sympodialis* roots. *Fitoterapia*, 73(4), 356-358.

de Souza, J.J., Mathias, L., & Vieira, I.J.C., (2010). Two new indole alkaloids from *Tabernaemontana hystrix* Steud. (Apocynaceae). *Helvetica Chimica Acta*, 93(3), 422-429.

- de Wet, H., Heerden, F.R., & Wyk, B.E., (2005). Alkaloids of *Antizoma miersiana* (Menispermaceae). *Biochemical systematics and ecology*, 33(8), 799-807.
- Desjardins, R.E., Haynes, C.J., & Chulay, J.D., (1979). Malarone treatment failure and *In vitro* confirmation of resistance of *Plasmodium falciparum* isolate from Lagos, Nigeria. *Antimicrobial. Agents and Chemotherapy*. 16, 708-710.
- Dippy, J.F.J., & Page, J.E., (1998). Chemical constitution and the dissociation constants of monocarboxylic acids. Part IX. Monosubstituted β -phenylpropionic and cinnamic acids. *Journal of the Chemical Society*, 6(13), 357-363.
- El-Sayed, M., & Verpoorte R., (2007). Catharanthus terpenoid indole alkaloids: biosynthesis and regulation. *Phytochemistry Reviews*, 6(3), 277-305.
- El-Sebakhy, N., & Waterman, P.G., (1984). Methylcuspidaline from the leaves of *Aristolochia elegans*. *Phytochemistry*, 23(11), 2706-2707.
- El-Shazly, A., Sarg, T., & Ateya, A., (1996). Pyrrolizidine and tetrahydroisoquinoline alkaloids from *Echium humile*. *Phytochemistry*, 42(1), 225-230.
- Landry, K., Joel, D., Timothee, O., & Pierre, C., (2013). Alkaloids from the leaves of *Monodora crispate* and *Mondora. brevipes* Benth (Annonaceae). *Biochemical Systematics and Ecology*, 46, 162-165.
- Essam, A.S., Fathall, M.H., & Hiroaki, K., (2009). Antiplasmodial and Antitrypanosomal Activity of Plants from the Kingdom of Saudi Arabia. *Journal of Natural Medicines*, 63, 232-239.
- Facchini, P.J., (2001). Alkaloid biosynthesis in plants: biochemistry, cell biology, molecular regulation, and metabolic engineering applications. *Annual review of plant biology*, 52(1), 29-66.
- Fadaeinasab, M., Hamid, H., & Kia, Y., (2013). Cholinesterase Enzymes Inhibitors from the Leaves of *Rauvolfia Reflexa* and Their Molecular Docking Study. *Molecules*, 18(4), 3779-3788.
- Fadaeinasab, M., Hamid. H., Aty, W., Alfarius, E. N., & Hiroshi, M., (2013). Indole Alkaloids from the stem bark of *Ochrosia oppositifolia* (Apocynaceae) with Antiplasmodial Activity. *Journal of Natural Medicines Note*, 67(2), 65-66.
- Ferrigni, N.R., Sweetana, S.A., & Singleton, K.E., (1984). Identification of new cactus alkaloids in *Backebergia militaris* by tandem mass spectrometry. *Journal of Natural Products*, 47(5), 839-845.
- Fidock, D.A., Nomura, T., & Wellems, T.E., (1998). Antimalaria activity and metabolism of biguanides. *Molecular Pharmacology*, 54, 1140-1147.

- Frappier, F., Jossang, A., Soudon, J., & Schrevel, J., (1996). Bisbenzylisoquinolines as modulators of chloroquine resistance in *Plasmodium falciparum* and multidrug resistance in tumor cells. *Antimicrobial agents and chemotherapy*, 40(6), 1476-1481.
- Fujii, T., & Ohaba, M., (1998). Racemic and chiral synthesis of some indole. *Heterocycles*, 47, 525- 539.
- Garcia, M.T., Plumb, G.W., Waldron, K.W., Ralph, J., Williamson, G., (1997). Ferulic acid dehydro dimers from wheat bran: isolation, purification and antioxidant properties. *Europe PubMed*, 3(5), 319-323.
- Galinis, D.L., Wiemer, D.F., & Cazin J. J., (1993). Cissampentin: A new bisbenzylisoquinoline alkaloid from *Cissampelos fasciculata*. *Tetrahedron*, 49(7), 1337-1342.
- Gower, A.E., Pereira, B.D.S., & Marsaioli A.J., (1986). Indole alkaloids from *Peschiera campestris*. *Phytochemistry*, 25(12), 2908-2910.
- Grey, F.A., *Organic Chemistry*. (1999). (pp.954.2006). New York: McGraw Hill.
- Grycová, L., Dostál, J., & Marek, R., 2007. Quaternary protoberberine alkaloids. *Phytochemistry*, 68(2), 150-175.
- Guanatilaka, A.A.L., (1998). The Alkaloids. *Chemistry & Biology*, 52, 98- 101.
- Guha, K., & Mukherjee, B., (1979). Bisbenzylisoquinoline alkaloids--a review. *Journal of Natural Products*, 42(1), 1-84.
- Guinaudeau, H., Leboeuf, M., & Cavé, A., (1979). Aporphine alkaloids. II. *Journal of Natural Products*, 42(4), 325-360.
- Guinaudeau, H., Leboeuf, M., & Cavé, A., (1983). Aporphinoid alkaloids, III. *Journal of Natural Products*, 46(6), 761-835.
- Guinaudeau, H., Leboeuf, M., & Cavé, A., (1988). Aporphinoid alkaloids, IV. *Journal of Natural Products*, 51(3), 389-474.
- Gurib-Fakim, A., (2006). Medicinal plants: traditions of yesterday and drugs of tomorrow. *Molecular Aspects of Medicines*, 27(1), 60-65.
- Haslam, E., (1986) Secondary metabolism--fact and fiction. *Natural Product Reports*, 3, 217-249.
- Hendrian, M., (2004). *Revision of Ochrosia (Apocynaceae) in Malaysia*. (pp. 101-128) National Herbarium Netherland.
- Hughes, D., Genest, K., & Skakum, W., (1968). Alkaloids of *Peumus boldus*. Isolation of (+) reticuline and isoboldine. *Journal of Pharmaceutical Sciences*, 57(6), 1023-1025.

- Hussain, S.F., Minard, R.D., & Freyer, A.J., (1981). New alkaloids from *Fumaria parviflora*. *Journal of Natural Products*, 44(2), 169-178.
- Israilov, I., Karimova, S.U., & Yunusov, M.S., (1980). Aporphine alkaloids. *Chemistry of Natural Compounds*, 16(3), 197-225.
- Israilov, I., Yunusov, M., & Yunusov, S.Y., (1970). Structure of parfimidine. *Chemistry of Natural Compounds*, 6(4), 518-518.
- Jacqueline, G., & Culvenor, J.G., (2000). Targeted mutagenesis of *Plasmodium falciparum* erythrocyte membrane protein 3 (PfEMP3) disrupts cytoadherence of malaria infected red blood cells. *The EMBO Journal*. 19, 2813-2823.
- Jha, R., Pandey, M.B., & Singh, A.K., (2009). New alkaloids from *Corydalis* species. *Natural Product Research*, 23(3), 250-255.
- Jia, Z.T.K., Leeuwenberg, M., David, J., & Middleton, A., (1995). revision of *Epigynum* (Apocynaceae). *Harvard Herbaria*,. 63, 143-188.
- Jonathan, R., Joseph, F., & David, F., (1992). *Plasmodium falciparum*: In vitro characterization and human infectivity of a cloned line. *Experimental. Parasitology*. 74, 159-168.
- Jordan, W., & Scheuer, P. J., (1965). Hawaiian plant studies, XIV alkaloids of *Ochrosia sandwicensis* A.Gray. *Tetrahedron letters*, 21(12), 3731-3740.
- Joy, D.A., (2003). Early origin and recent expansion of *Plasmodium falciparum*. *Science*, 300, 318-321.
- Kablan, L., Dade, J., & Okpekon, T., (2013). Alkaloids from the leaves of *Monodora crispate*. *Plantes Medicinales et Phytoterapie*, 23(14), 142-143.
- Kam, T.S., & Choo, Y.M., (2004). Venalstonine and dioxokopsan derivatives from *Kopsia fruticosa*. *Phytochemistry*, 65(14), 2119-2122.
- Kanyinda, B., R. Vanhaelen-Fastre., Vanhaelen, M., (1995). Benzyloisoquinoline alkaloids from *Anisocycla jollyana* leaves. *Journal of Natural Products*, 58(10), 1587-1589.
- Kato, L., Marques B.R., & Koch, I. (2002). Indole alkaloids from *Rauwolfia bahiensis* A. DC.(Apocynaceae). *Phytochemistry*, 60(3), 315-320.
- Kisakurek, M.V., Leeuwenberg, A., & Hesse, M., (1983). A Chemotaxonomic Investigation of the Plant Families of Apocynaceae, Loganiaceae, and Rubiaceae by their Indole Alkaloid. *Content. Hobsons*, 1, 211-376.
- Klohs, M., Draper, M., & Keller, F., (1954). Alkaloids of *Rauwolfia serpentina* benth. iii. 1 rescinnamine, a new hypotensive and sedative principle. *Journal of the American Chemical Society*, 76(10), 2843-2843.

- Kochummen, K.M., (1972). *Tree Flora of Malaya*. (pp. 105).
- Kochummen, K.M., (1972). *Tree Flora of Malaya*. (pp. 102-103).
- Koehn, F. E. & Carter G. T., (2005). *Natural Revision and Drug Discovery* (pp. 206-220)
- Koike, K., Ohmoto, T., & Ikeda, K., (1990). β -Carboline alkaloids from *Picrasma quassioides*. *Phytochemistry*, 29(9), 3060-3061.
- Krane, B.D., Shamma, M., (1982). The isoquinolone alkaloids. *Journal of Natural Products*, 45(4), 377-384.
- Krunczynski, A. J., & Jean, M.B., (1998). Antimitotic and Tubulin Interacting Properties of Vinflunine. *Biochemical Pharmacology*, 55, 635- 648.
- Ku, W.F., Tan, S.J., & Low, Y.Y., (2011). Angustilobine and andranginine type indole alkaloids and an uleine vallesamine bisindole alkaloid from *Alstonia angustiloba*. *Phytochemistry*, 72(17), 2212-2218.
- Kutchan, T., Dittrich, H., & Bracher, D., (1991). Enzymology and molecular biology of alkaloid biosynthesis. *Tetrahedron*, 47(31), 5945-5954.
- Lamberton, J., & Vashist, V., (2011). Alkaloids of *Litsea leefeana* and *Cryptocarya foveolata* (Lauraceae). *Australian Journal of Chemistry*. 25(12), 2737-2738.
- Lee, S.S., Chen, C.H, & Liu, Y.C., (2003). Additional alkaloids from *Cryptocarya chinensis*. *Journal of Natural Products*, 56(2), 227-232.
- Lee, S.S., Lin, Y.J., & Chen, C.K, (1993). Quaternary alkaloids from *Litsea cubeba* and *Cryptocarya konishii*. *Journal of Natural Products*, 56(11), 1971-1976.
- Leslie, G.A.A., Chandasiri, F.H., & Munawer, Q., (1989). Neisosposinine: a new oxindole alkaloid from *Neisosperma oppositifolia* (Apocynaceae). *Heterocycles*, 28(2), 999-1005.
- Lim, T., (2013). *Papaver somniferum*, in *Edible Medicinal And Non-Medicinal Plants*., (pp. 202-217. Springer.
- Little, S.A., Stockey, R.A., Penner, B., (2009). Anatomy and development of fruits of Lauraceae from the *Middle Eocene Princeton Chert*. *American Journal of Botany*, 96(3), 637-651.
- Liu Ching, Y., & Knochel, P., (2007). A new synthesis of *Ellipticine*. *Journal of Organic Chemistry*, 72, 7106- 7115.
- Lucilia K., & Raquel, M.B., (2002). Indole alkaloids from *Rauvolfia bahiensis* (Apocynaceae). *Phytochemistry*, 60, 315- 320.

- Massiot, G.L., Catherine, V., Joseph, L.M., Levy, J., Giulhem, J., & Pascard, C., (1983). Rearrangement of two indole alkaloids in trifluoroacetic acid: desformocorymine and dihydrocorymine. *Helvetica Chimica Acta*, 66(8), 2414-30
- Matsuo, H., Okamoto, R., & Zaima, K., (2011). New vasorelaxant indole alkaloids, villocarines A–D from *Uncaria villosa*. *Bioorganic and medicinal chemistry*, 19(13), 4075-4079.
- Meissner, C.D., & Friedrich., (1964). Flora of Hawaiian Islands. *Lauraceae in A.L.P.P. de Candolle*. 15(1), 249.
- Menachery, M.D., Lavanier, G. L., & Wetherly, M. L., (1986). Simple isoquinoline alkaloids. *Journal of Natural Products*, 49(5), 745-778.
- Mia, M.M.K., Kadir, M.F., & Hossan, M.S., (2009). Medicinal plants of the Garo tribe inhabiting the Madhupur forest region of Bangladesh. *American Eurasian Journal of Sustainable Agriculture*, 3(2), 165-171.
- Montagnac, A., Hamid, H., & Remy, F., (1995). Isoquinoline alkaloids from *Ancistrocladus tectorius*. *Phytochemistry*, 39(3), 701-704.
- Morikawa, T., Sun, B., Matsuda, H., & Wu, L. J., (2004). Bioactive constituents from Chinese natural medicines. XIV. new glycosides of. Beta.-carboline-type alkaloid, neolignan, and phenylpropanoid from *Stellaria dichotoma* L. var. *lanceolata* and their antiallergic activities. *Chemical and Pharmaceutical Bulletin*, 52(10), 1194-1199.
- Mosmann, T., (1983). Rapid colorimetric assay for cellular growth and survival: application to proliferation and cytotoxicity assays. *Journal of Immunology Methods*, 16(65), 1-2.
- Mukherjee, P.K., Kumar, V., & Mal, M., (2007). Acetylcholinesterase inhibitors from plants. *Phytomedicine*, 14(4), 289-300.
- Nafiah, M.A., (2009). *Alkaloids isolated from Alseodaphne species (Lauraceae) and their bioactivities*. (PhD Dissertation). University of Malaya, Malaysia.
- Nafiah, M.A., Mat Ropi, M., Morita, H., Ahmad, K., Awang, K., & Hadi, Hamid, A. A., (2010). Alkaloids from roots of *Alseodaphne corneri* kosterm. *Malaysian Journal of Science*, 29(3), 281-284.
- Noedl, H.C., Woongsrichanalai. & Wernsdorfer, W.H., (2003). A new double-antibody sandwich elisa targeting Plasmodium falciparum addolase to evaluate anti Malaria drug sensitivity. *Trends Parasitology*. 19, 175-181.
- Obregon, A.D.C., Schetinger, M.R.C., Correa, M.M., Morsch, V.M., Da Silva, J.E.P., Martins M.A.P., Bonacorso, H.G., & Zanatta, N., (2005). Effects per se of organic solvents in the cerebral acetylcholinesterase of rats. *Neurochemical Research*, 30, 379–384.

- Ocker, M., & Höpfner, M., (2012). Apoptosis-modulating drugs for improved cancer therapy. *European Surgical Research*, 48(3), 111-120.
- Oduola, A.M., Weatherly, N.F., Bowdre, J.H., & Desjardins, R.E., (1988). *Plasmodium falciparum*: cloning by signal erythrocyte micromanipulation and heterogeneity *in vitro*. *Experimental Parasitology*, 66, 86-95.
- Ohta, M., Hideo, V., & Deng, S., (1964). The stereochemistry of hydrastine, narcotine, ophiocarpine, and their derivatives. ii. absolute configuration of narcotine and their derivatives. *Chemical and pharmaceutical bulletin*, 12, 1080.
- Pérez, E.G., & Cassels, B.K., (2010). *The Alkaloids: Chemistry and Biology*, (pp. 83-101), Elsevier 68.
- Peube, L.N., & Koch, M., (1972). Alcaloides des Ecorces d *Ochrosia oppositifolia*. *Phytochemistry*, 11, 2109- 2111.
- Phillipson, J.D., (2001). Phytochemistry and medicinal plants. *Phytochemistry*, 56(3), 237-243.
- Phillipson, J.D., & Zenk, M.H., (1980). Indole and Biogenetically Related Alkaloids. *Academic Press*, 7-10.
- Plummer, A.J., Earl, A., Schneider, J.A., & Trapold, J., (1954). Pharmacology of *Rauwolfia alkaloids*, including reserpine. *Annals of the New York Academy of Sciences*, 59(1), 8-21.
- Rashid, N.A., (2008). *Chemical constituents of Actinodaphne macrophylla (BL.) Nees* (Master Dissertation). University of Malaya, Malaysia.
- Rasoanaivo, P., Ratsimamanga-Urverg, S., & Rakoto-Ratsimamanga, A., (1995). Isoquinoline alkaloid constituents of *Spirospermum penduliflorum* and *Strychnopsis thouarsii* (Menispermaceae). *Biochemical systematics and ecology*, 23, 67-69.
- Raven, P.H., Evert, R.F., & Eichhorn, S.E., (2005). *Biology of plants*. (pp. 168) WH Freeman & Company.
- Ridley, H.N., (1924). *Flora of the Malay peninsula*. 3 (pp. 37).
- Roberts, M.F., (1998). *Alkaloids: biochemistry, ecology, and medicinal applications*. (pp. 189-198) Plenum Publishing Corporation: New York.
- Schmidt, L.H., Harrison, J., Rossan, R.N., Vaughan, D., & Crosby, R., (1977). Funsidar resistant falciparum malaria in Papua New Guinea. *American Society of Tropical Medicine and Hygiene*, 26, 837-849.
- Scholz, U., & Winterfeldt, E., (2000). Biomimetic synthesis of alkaloids. *Natural product reports*, 17(4), 349-366.

- Schütte, H.R., (1986). *Secondary plant substances: monoterpene indole alkaloids*, (pp.151-166). in *Progress in botany*, Springer.
- Shamma, M., & Moniot, J.L., (1987). *Isoquinoline alkaloids research*. (pp. 386-398). Plenum Press- New York and London.
- Sheludko, Y., Gerasimenko, I., & Kolshorn, H., (2002). New alkaloids of the sarpagine group from *Rauvolfia serpentina* Hairy Root Culture. *Journal of Natural Products*, 65(7), 1006-1010.
- Slater, L.M., Sweet, P., & Stupecky, M., (1986). Cyclosporin A reverses vincristine and daunorubicin resistance in acute lymphatic leukemia *in vitro*. *Journal of Clinical Investigation*, 77(4), 1405.
- Stöckigt, J., & Zenk, M.H., (1977). Strictosidine (isovincoside): the key intermediate in the biosynthesis of monoterpene indole alkaloids. *Journal of the Chemical Society, Chemical Communications*, 18, 646-648.
- Suau, R., Rico, R., & Lopez- Romero, J.M., (1994). Benzyloisoquinoline alkaloids from *Ceratopogon heterocarpus*. *Phytochemistry*, 36(1), 241-243.
- Suau, R., Rico, R., & Nájera, F., (1998). Isoquinoline alkaloids from *Berberis vulgaris* subsp. *australis*. *Phytochemistry*, 49(8), 2545-2549.
- Swan, G.A., (1967). *An introduction to the alkaloids*. (pp. 200-219). St Paul's Press LTD.: Oxford.
- Tanahashi, T., & Zenk, M., (1985). Isoquinoline alkaloids from cell suspension cultures of *Fumaria capreolata*. *Plant Cell Reports*, 4(2), 96-99.
- Trease, G., & Evans, W., (1989). *A textbook of Pharmacognosy*, (pp.314). Bailliere Tindall Ltd, London.
- Valencia, E., Weiss, I., & Firdous, S., (1984). The isoindolobenzazepine alkaloids. *Tetrahedron*, 40(20), 3957-3962.
- Verpoorte, R.J., (1986). Annual review of plant physiology and plant molecular biology. *Natural. Product. Reports*, 49, 1-25.
- Victor, M.L., & Roberto, K.C., (2007). *Catharanthus* biosynthetic enzymes: the road ahead. *Phytochemistry. Reviews.*, 6, 307-339.
- Walliker, D., (1987). Genetic analysis of the human malaria parasite *Plasmodium falciparum*. *Science*, 236, 1661-1666.
- Wangchuk, P., Bremner, J. B., & Rattanajak, R., (2010). Antiplasmodial agents from the Bhutanese medicinal plant *Corydalis calliantha*. *Phytotherapy Research*, 24(4), 481-485.

Waterman, P.G., (1998). The new chemosystematics: Phylogeny and phytochemistry. *Phytochemistry*, 68(22), 2904-2908.

Wei-Hua Jiao, H.G., Chen- Yang Li., Guang- Xiong, Z., Susumu, K., Atsuko, O., & Xin-Sheng Yao., (2010). β - carboline alkaloids from the stems of *Picrasma quassioides*. *Magnetic Resonance in Chemistry*, 48, 490-495.

Wellems, T., & Tinsley, H., (1990). Potential for human Exposure. *Nature*, 345, 253-255.

Whitmore, T.C., (1989). *Tree Flora of Malaya*. 4 (pp.3-8).

Wu, W.N., Beal, J.L., & Doskotch, R.W., (1980). Alkaloids of *Thalictrum* . Eleven minor alkaloids from *Thalictrum rugosum*. *Journal of Natural Products*, 43(1), 143-150.

Wu, W.N., Beal, J.L., & Doskotch, R.W., (1980). Alkaloids of *Thalictrum*. Isolation and characterization of alkaloids from the root of *Thalictrum alpinum*. *Journal of Natural Products*, 43(3), 372-381.

Xie, C., Veitch, N., & Houghton, P., (2004). Flavonoid glycosides and isoquinolinone alkaloids from *Corydalis bungeana*. *Phytochemistry*, 65(22), 3041-3047.

Zabel, V., Watson, W.H., & Knapp, J.E., (1982). Melosmine and melosmidine 7, 7-dimethyltetrahydroaporphine alkaloids from *Guatteria melosma*. *Journal of Natural Products*, 45(1), 94-101.

Zawawi, N.A., Ahmat, N., & Ghani, N.A., (2012). Oxoaporphine alkaloids and flavonols from *Xylopia ferruginea* (Annonaceae). *Biochemical Systematics and Ecology*, 43, 7-9.

Zhang, G., Gurtu, V., Kain, S.R., & Yan, G., (1997). Early detection of apoptosis using a fluorescent conjugate of annexin V. *Biotechniques*, 23, 525-531.

Zhang, L.S.F., & Yan, L.K., (2012). β -carboline alkaloids from the leaves of *Trigonostemon lii* Y.T. Chang. *Bioorganic.and Medicinal. Chemistry. Letters.*, 22, 2296–2299.

Zhang, X., Ye, W., Zhao, S., (2004). Isoquinoline and isoindole alkaloids from *Menispermum dauricum*. *Phytochemistry*, 65(7), 929-932.

APPENDICES

PUBLICATIONS AND CONTRIBUTIONS:

1. Cholinesterase Enzymes Inhibitors from the Leaves of *Rauvolfia Reflexa* and Their Molecular Docking Study (**Molecules** 2013, 18, 3779-3788).

Authors	Authors Contributions
1. Mehran Fadaeinasab	Isolate the compounds, identify their structures and write the chemistry part
2. A. Hamid A. Hadi	PhD supervisor
3. Yalda Kia	Ran the Antialzheimer test
4. Alireza Basiri	Ran the molecular docking
5. Vikneswaran Murugaiyah	Write the biology part

2. Indole Alkaloids from the stem bark of *Ochrosia oppositifolia* (Apocynaceae) with Antiplasmodial Activity (**Journal of Natural Medicines Note** 2013, 67 (2), 65-66).

Authors	Authors Contributions
1. Mehran Fadaeinasab	Isolate the compounds, identify their structures and write the chemistry part
2. A. Hamid A. Hadi	PhD supervisor
3. Aty Widyawaruyanti	Ran the Antiplasmodial test
4. Alfarius Eko Nugroho	Revise the paper
5. Hiroshi Morita	Write the biology part

3. Evaluation of green corrosion inhibition by alkaloid extracts of *Ochrosia oppositifolia* and isoreserpiline against mild steel in 1M HCl medium (**Ind. Eng. Chem. Res.** 2013).

Authors	Authors Contributions
1. Pandian Bothi Raja	Ran the anti corrosion activity
2. Mehran Fadaeinasab	Isolate the compounds, identify their structures and write the chemistry part
3. Ahmad Kaleem Qureshi	Ran the anti corrosion activity
4. Afidah Abdul Rahim	Head of anti corrosion group
5. Hasna Osman	Revise the paper
6. Marc Litaudon	Revise the paper
7. Khalijah Awang	Revise the paper

4. Flavonoids and Linderone from *Lindera oxyphylla* and their Bioactivities. **Combinatorial Chemistry & High Throughput Screening**, 2013,16.

Authors	Authors Contributions
1. Masoumeh Hosseinzadeh	Isolate the compounds, identify their structures
2. A. Hamid A. Hadi	PhD supervisor
3. Jamaludin Mohamad	PhD co-supervisor, write the biology part
4. Mohammad A. Khalilzadeh	PhD co-supervisor, revise the paper
5. Shiau-Cheahd	Ran the antioxidant and anti cancer activities
6. Mehran Fadaeinasab	Write the chemistry part

5. In Vitro Plant Regeneration, Antioxidant and Antibacterial Studies on Broccoli, *Brassica oleracea* var. *italic*. **Pakistan Journal of Botany** 44 (6),2117-2122 (2012).

Authors	Authors Contributions
1. Reza Farzinebrahimi	Ran the antioxidant and antibacterial tests and write the Paper
2. Rosna Mat Taha	PhD supervisor
3. Mehran Fadaeinasab	Extract the plant material
4. Solmaz Mokhtari	Revise the paper

6. Tanacetum polycephalum (L.) Schultz-Bip. Induces Bax/Bcl-2 Mediated Apoptosis through Mitochondrial Pathway in Human Breast Cancer Cells. **Molecules**. 19, 9478- 9501 (2014).

Authors	Authors Contributions
1. Hamed Karimian	Ran the anti cancer assay and write the biology part
2. Syam Mohan	PhD supervisor
3. Soheil Zorofchian	Revise the paper
4. Mehran Fadaeinasab	Chemical analysis of the extract by using GC-MS and write the chemistry part
5. Hapipah Mohd Ali	PhD supervisor
6. Mohamad Ibrahim Noordin	PhD supervisor

7. *Ferulago angulata* activates intrinsic pathway of apoptosis in MCF7 cells associated with G1 cell cycle arrest via involvement of p21/p27. **Drug Design, Development and Therapy**. Accepted.

Authors	Authors Contributions
1. Hamed Karimian	Ran the anti cancer assay and write the biology part
2. Mehran Fadaeinasab	Chemical analysis of the extract by using GC-MS and write the chemistry part
3. Soheil Zorofchian	Revise the paper
4. Syam Mohan	PhD supervisor
5. Aditya Arya	Revise the paper
6. Najihah Mohd Hashim	PhD co- supervisor
7. Mohamad Ibrahim Noordin	PhD supervisor
8. Hapipah Mohd Ali	PhD supervisor

8. *Annona muricata* leaves induces G1 cell cycle arrest and apoptosis through mitochondria-mediated pathway in human HCT-116 and HT-29 colon cancer cells. **Journal of Ethnopharmacology**. Accepted.

Authors	Authors Contributions
1. Soheil Zorofchian	Ran the anti cancer assay and write the biology part
2. Habsah Abdul Kadir	PhD supervisor
3. Hamed Karimian	Revise the paper
4. Elham Rouhollahi	PhD supervisor
5. Mohammadjavad Paydar	Revise the paper
6. Mehran Fadaeinasab	Chemical analysis of the extract by using GC-MS and write the chemistry part

9. New Indole Alkaloid from *Rauvolfia reflexa* Bark Exerts Cytotoxic and Apoptotic Effects on Colon Cancer HCT-116 Cells. **Journal of Natural Product**. Submitted.

Authors	Authors Contributions
1. Mehran Fadaeinasab	Isolate the compounds, identify their structures and write the paper
2. Hesham El- Seedi	Revise the paper
3. Najihah Mohd Hashim	PhD co- supervisor
4. Hamed Karimian	Ran the anti cancer assay
5. Hapipah Mohd Ali	PhD supervisor

